UNIVERSITÉ DU QUÉBEC À TROIS-RIVIÈRES

AMÉLIORATION DE LA PERFORMANCE DES VÉHICULES À PILE À COMBUSTIBLE MULTI-PILES PAR LA CONCEPTION D'UNE STRATÉGIE DE GESTION DE L'ÉNERGIE ET D'UNE GESTION DU SYSTÈME DE PILES À COMBUSTIBLE

THÈSE PRÉSENTÉE
COMME EXIGENCE PARTIELLE DU

DOCTORAT EN GÉNIE ÉLECTRIQUE

PAR
MOHAMMADREZA MOGHADARI

MARS 2025

UNIVERSITÉ DU QUÉBEC À TROIS-RIVIÈRES

ENHANCING THE PERFORMANCE OF MULTI-STACK FUEL CELL VEHICLES THROUGH THE DESIGN OF ENERGY MANAGEMENT STRATEGY AND FUEL CELL SYSTEM MANAGEMENT

A THESIS PRESENTED
IN PARTIAL FULFILLMENT OF
THE REQUIREMENTS FOR THE DEGREE
DOCTOR OF PHILOSOPHY IN ELECTRICAL ENGINEERING

BY
MOHAMMADREZA MOGHADARI

MARCH 2025

Université du Québec à Trois-Rivières

Service de la bibliothèque

Avertissement

L'auteur de ce mémoire, de cette thèse ou de cet essai a autorisé l'Université du Québec à Trois-Rivières à diffuser, à des fins non lucratives, une copie de son mémoire, de sa thèse ou de son essai.

Cette diffusion n'entraîne pas une renonciation de la part de l'auteur à ses droits de propriété intellectuelle, incluant le droit d'auteur, sur ce mémoire, cette thèse ou cet essai. Notamment, la reproduction ou la publication de la totalité ou d'une partie importante de ce mémoire, de cette thèse et de son essai requiert son autorisation.

UNIVERSITÉ DU QUÉBEC À TROIS-RIVIÈRES

DOCTORAT EN GÉNIE ÉLECTRIQUE (PH.D.)

Direction de recherche:

Loïc Boulon Université du Québec à Trois-Rivières	directeur de recherche
Hicham Chaoui Carleton University	codirecteur de recherche

Jury d'évaluation:

Loïc Boulon Université du Québec à Trois-Rivières	directeur de recherche
Hicham Chaoui Carleton University	codirecteur de recherche
Michel Lemaire Université du Québec à Trois-Rivières	président du jury
Alexandre Ravey Université de Technologie de Belfort-Montbéliard	évaluateur externe
Hazzab Abdeldjebar École de Technologie Supérieure	évaluateur externe

Thèse soutenue le 28 Mars 2025

UNIVERSITÉ DU QUÉBEC À TROIS-RIVIÈRES

DOCTOR OF PHILOSOPHY IN ELECTRICAL ENGINEERING (PH.D.)

Research Supervision:

Loïc Boulon — research director
Université du Québec à Trois-Rivières

Hicham Chaoui — research co-director
Carleton University

Evaluation jury:

Loïc Boulon — research director
Université du Québec à Trois-Rivières

Hicham Chaoui — research co-director
Carleton University

Michel Lemaire — jury president
Université du Québec à Trois-Rivières

Alexandre Ravey — external evaluator
Université de Technologie de Belfort-Montbéliard

Hazzab Abdeldjebar — external evaluator
École de Technologie Supérieure

Thesis defended on 28 March 2025

Abstract

Using low-power fuel cell (FC) stacks instead of a single high-power FC stack, known as a multi-stack FC system, can potentially address technical challenges in FC technology, including limitations in efficiency, durability, and reliability. Modularity, redundancy, and access to several optimal operating points are the main advantages of a multi-stack FC system compared to a single-stack FC system. To operationalize these potentials and distribute optimal power between sub-stacks, an energy management strategy (EMS) as a software component is vital. Designing an EMS plays an undeniable role in reducing the operating cost of a multi-stack system, which is an open issue and one of the main concerns in such systems. However, while the EMS is responsible for distributing optimal power, it cannot ensure that sub-stacks operate properly. Therefore, alongside the EMS's role in the performance of the multi-stack FC system, FC operating parameters play a crucial role. One of the most important operating parameters is voltage, which is recognized as an indicator of FC performance. The FC voltage level directly impacts efficiency, which is one of the most important criteria for FC performance. In this regard, voltage stability plays an essential role in voltage performance at each level and can influence FC efficiency and overall performance. On the other hand, Stable voltage helps the EMS control the output power of sub-stacks more easily and improves the efficiency of the power electronics. FC voltage performance is highly dependent on the water content in the FC membrane, which is regulated by the water management system. In this regard, to enhance the performance of the multi-stack FC system, this thesis aims to integrate water management into the EMS.

This thesis consists of three phases. The first phase analyzes the impact of multi-stack advantages on the operating cost and performance of a fuel cell hybrid electric vehicle (FC-HEV) and conducts an analytical performance comparison between multi-stack and single-stack FC systems using an EMS.

The second phase is dedicated to designing an advanced EMS for the multi-stack FC system to enhance its performance, reduce operating cost, and increase the lifespan and reliability of the sub-stacks. The designed EMS is a multiple time-point strategy that utilizes prediction to improve its results. The proposed EMS, utilizing a finite prediction

horizon, eliminates the need to know the entire driving cycle in advance, making it a suitable and promising approach for real-time applications. Additionally, incorporating prediction improves the EMS performance compared to single time-point strategies, bringing its results closer to those achieved by global optimization approaches.

In the third phase, water management is integrated into the EMS using an adaptive efficient purge strategy. The purpose of this phase is to enhance sub-stacks performance by increasing voltage stability during operation through effective water management. The results demonstrate that improving sub-stacks voltage stability enhances the overall performance of the multi-stack FC system and reduces its operating cost.

Résumé

L'utilisation d'empilements de piles à combustible (PC) de faible puissance au lieu d'un seul empilement de PC de forte puissance, connu sous le nom de système de PC multi-piles, peut potentiellement relever les défis techniques de la technologie des PC, y compris les limitations en matière d'efficacité, de durabilité et de fiabilité. La modularité, la redondance et l'accès à plusieurs points de fonctionnement optimaux sont les principaux avantages d'un système PC multi-piles par rapport à un système de PC seule-pile. Pour exploiter ces potentiels et distribuer la puissance optimale entre les sous-piles, une stratégie de gestion de l'énergie (SGE) en tant que composant logiciel est vitale. La conception d'une SGE joue un rôle indéniable dans la réduction de coût d'exploitation d'un système multi-piles, qui est une question ouverte et l'une des principales préoccupations de ces systèmes. Toutefois, si le SGE est responsable de la distribution optimale de l'énergie, il ne peut pas garantir le bon fonctionnement des sous-piles. C'est pourquoi, parallèlement au rôle de la SGE dans les performances du système PC multi-piles, les paramètres de fonctionnement du PC jouent un rôle crucial. L'un des paramètres de fonctionnement les plus importants est la tension, qui est reconnue comme un indicateur des performances du système PC. Le niveau de tension de la PC a un impact direct sur l'efficacité, qui est l'un des critères les plus importants pour la performance de la PC. À cet égard, la stabilité de la tension joue un rôle essentiel dans la performance de la tension à chaque niveau et peut influencer l'efficacité et la performance globale de la PC. D'autre part, une tension stable permet à la SGE de contrôler plus facilement la puissance de sortie des sous-piles et d'améliorer l'efficacité de l'électronique de puissance. La performance de la tension de la PC dépend fortement de la teneur en eau de la membrane de la PC, qui est régulée par le système de gestion de l'eau. À cet égard, pour améliorer les performances du système PC multi-piles, cette thèse vise à intégrer la gestion de l'eau dans la SGE.

Cette thèse comporte trois phases. La première phase analyse l'impact des avantages du système PC multi-piles sur le coût d'exploitation et les performances d'un véhicule électrique hybride à PC et effectue une comparaison analytique des performances entre les systèmes multi-piles et seule-pile à l'aide d'une SGE.

La deuxième phase est consacrée à la conception d'une SGE avancé pour le système PC multi-piles afin d'améliorer ses performances, de réduire les coûts d'exploitation et d'augmenter la durée de vie et la fiabilité des sous-piles. La SGE conçu est une stratégie à points temporels multiples qui utilise la prédiction pour améliorer ses résultats. La SGE proposé, qui utilise un horizon de prédiction fini, élimine la nécessité de connaître à l'avance l'ensemble du cycle de conduite, ce qui en fait une approche appropriée et prometteuse pour les applications en temps réel. En outre, l'intégration de la prédiction améliore les performances de la SGE par rapport aux stratégies à un seul point temporel, ce qui rapproche ses résultats de ceux obtenus par les approches d'optimisation globale.

Au cours de la troisième phase, la gestion de l'eau est intégrée à la SGE à l'aide d'une stratégie de purge adaptative et efficace. L'objectif de cette phase est d'améliorer les performances des sous-piles en augmentant la stabilité de la tension pendant le fonctionnement grâce à une gestion efficace de l'eau. Les résultats démontrent que l'amélioration de la stabilité de la tension des sous-piles améliore les performances globales du système PC multi-piles et réduit son coût d'exploitation.

Acknowledgement

I would like to express my gratitude to Université du Québec à Trois-Rivières and the Institut de recherche sur l'hydrogène (IRH), one of the most prestigious research institutes in hydrogen and clean energy, for granting me the opportunity to pursue my education and broaden my knowledge as a PhD student.

Before anything else, I want to express my appreciation to my supervisor, Prof. Loïc Boulon, for his motivation, professional treatment, and helpful criticism. His support has been crucial in my PhD, and he played a significant role in helping me develop a clear perspective on my research topic by providing an equipped test center and experimental environment. Furthermore, I would like to extend my gratitude to my co-supervisor, Prof. Hicham Chaoui, for his guidance and insightful comments, which have been invaluable in writing my papers and thesis. It is my great fortune to have such professional and top-ranked academic supervisors.

Besides my supervisors, I would like to extend my heartfelt thanks to Prof. Mohsen Kandidayeni. Without his assistance and encouragement, accomplishing my PhD would have been difficult.

During this four-year journey, many people have helped me achieve my goals and navigate this academic path. I would like to sincerely thank my teammates for their collaboration, support, and valuable contributions throughout this journey.

Finally, and most importantly, I would like to express my deepest gratitude to my beloved family. Their unconditional love, unwavering support, and endless encouragement have been the foundation of my progress. Their patience, understanding, and constant belief in me gave me the strength to overcome every challenge and reach this important milestone.

Table of Contents

List of Tables

List of Figures

List of Symbols

AFC	Alkaline fuel cell
AIWM-EMS	Adaptive integrated water management into the energy management strategy
BEV	Battery electric vehicle
BLSTM	Bidirectional long short-term memory
$C_{bat,deg}$	Cost of battery degradation
$C_{FC,deg}$	Cost of fuel cell degradation
C_{H_2}	Cost of hydrogen consumption
DEA	Dead-end anode
DMFC	Direct methanol fuel cell
DP	Dynamic programming
ECMS	Equivalent consumption minimization strategy
EEA	European environment agency
EKF	Extended Kalman filter
EMS	Energy management strategy
ESS	Energy storage system
EV	Electric vehicle
F	Faraday's constant
FC	Fuel cell
FCEV	Fuel cell electric vehicle
FC-HEV	Fuel cell hybrid electric vehicle
F_{in}	Fuel input
GDL	Gas diffusion layer
GHG	Greenhouse gas
HEV	Hybrid electric vehicles

HHV	High heating value
HIL	Hardware-in-the-loop
HPEMS	Hierarchical predictive energy management strategy
ICE	Internal combustion engines
IEA	International energy agency
I_{FC}	Fuel cell current
IWM-EMS	Integrated water management into the energy management strategy
KF	Kalman filter
LDV	Light-duty vehicle
m	Molecular weight
MCFC	Molten carbonate fuel cell
MEA	Membrane electrode assembly
MHDV	Medium and heavy-duty vehicle
MPC	Model predictive control
n	Number of electrons
NAIWM-EMS	Non-adaptive integrated water management into the energy management strategy
OPI	Online parameter identification
PAFC	Phosphoric acid fuel cell
PEMFC	Proton exchange membrane fuel cell
PEMS	Predictive energy management strategy
PHE-EMS	Predictive health-conscious energy management strategy
PHEV	Plug-in hybrid electric vehicle
P_{FC}	Fuel cell power
q_{H_2}	Hydrogen consumption rate
RLS	Recursive least square
RNN	Recurrent neural network
RUL	Remaining useful life
SBLSTM	Stacked bidirectional long short-term memory
SC	Supercapacitor
SOC	State of charge

SOFC	Solid oxide fuel cell
SRUKF	Square root unscented Kalman filter
V_{FC}	Fuel cell voltage
VM	Voltage monitoring
ΔH	Enthalpy
η_{FC}	Fuel cell efficiency

Chapter 1 - Introduction

1.1 Motivation

1.1.1 The Demand for Eco-Friendly Energy in Transportation

Since the industrial revolution, fossil fuels have been widely used, leading to CO_2 and other gas emissions that contribute to global warming [1]. According to the International Energy Agency (IEA) and the European Environment Agency (EEA), global energy consumption in transport and industry sectors is nearly equal. In recent decades, greenhouse gas (GHG) emissions from transportation have increased significantly. For instance, EU27 road transport emissions in 2018 were 26.8% higher than in the 1990s. To address transportation's impact on pollution, governments aim to reduce CO_2 emissions by 60% by 2050 [2], [3].

The transportation sector is shifting from fossil fuels to renewable energy, spurring academic research and innovative green energy solutions [4]. Electrifying vehicle traction systems is a key strategy. Various vehicles, ranging from light-duty vehicles (LDVs) such as passenger cars to medium and heavy-duty vehicles (MHDVs) such as buses, trucks, and trains, are now undergoing electrification [5], [6]. Electric Vehicle (EV) types include Battery Electric Vehicles (BEVs), Hybrid Electric Vehicles (HEVs), Plug-in Hybrid Electric Vehicles (PHEVs), Fuel Cell Electric Vehicles (FCEVs), and Fuel Cell Hybrid Electric Vehicles (FC-HEVs) [7]. Major manufacturers like Daimler, General Motors,

Toyota, and Ford are advancing EV technologies using fuel cells (FCs) or batteries for power generation [8], [9].

1.1.2 Fuel Cell Electric Vehicles (FCEVs)

Despite manufacturers' advancements, BEVs have a range of less than 400 km per charge and a recharge time of 1–3 hours. HEVs and PHEVs are considered transition models, as they still rely on fossil fuels and emit pollution [10]. FC is well-suited for various vehicular applications, including LDVs and MHDVs. It is a suitable option for long-distance vehicle applications due to its higher energy density compared to other energy sources. Additionally, FCEVs have an energy efficiency of 40–60%, significantly higher than conventional internal combustion engines (ICEs). These advantages have spurred further research and development of FC-powered vehicles, making the market for FCEVs appealing and important. FCEVs have been commercially shown as innovative, promising, and environmentally friendly vehicles [5], [11]. FCs can be used in various applications, such as vehicular, stationary, and portable applications. Based on their chemical and operational characteristics, FCs can be categorized into six common types: Proton Exchange Membrane Fuel Cells (PEMFCs), Solid Oxide Fuel Cells (SOFCs), Direct Methanol Fuel Cells (DMFCs), Alkaline Fuel Cells (AFCs), Molten Carbonate Fuel Cells (MCFCs), and Phosphoric Acid Fuel Cells (PAFCs) [12]. Figure 1-1 shows the applications, operating temperatures, and power ranges of different types of FCs. Among the different types of FCs, PEMFCs have gained significant attention for use in vehicular applications [13].

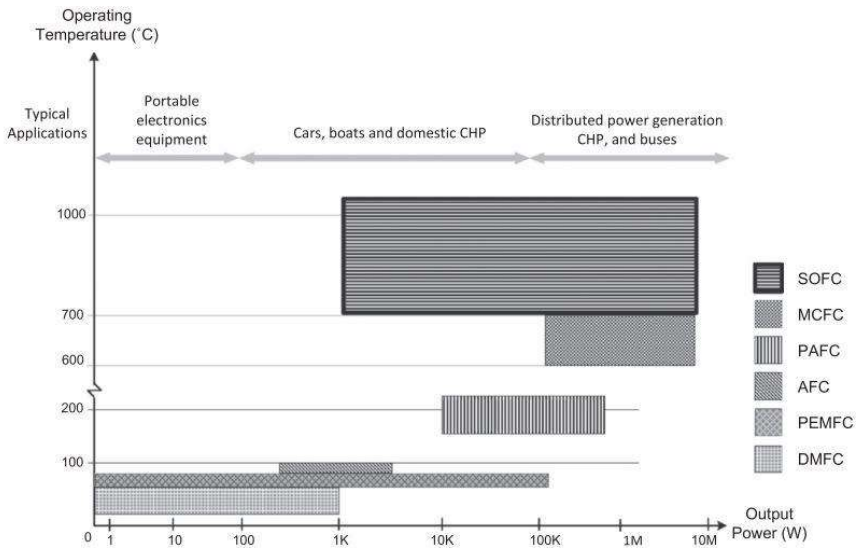

Figure 1-1- Applications, operating temperature and power range of various FC types [14].

The high-power density of PEMFCs (0.3-0.8 W/cm^2) makes them more appealing for vehicular applications compared to other types of FCs. PEMFCs also have the advantages of appropriate weight and size, operating at a low temperature between 60-80 ℃, and minimal corrosion risk [6].

Despite of remarkable advantages of FCEV, some challenges still hinder their commercialization and mass production. Table 1-1 compares the main advantages and challenges of FCEVs.

Table 1-1- Main advantages and challenges of FCEVs.

Advantages	Challenges
zero emission (locally)	Hydrogen storage and distribution
Reduction of dependency on fossil fuels	Insufficient hydrogen supply facilities
Short refueling time	High operating cost (H_2 fuel, degradation, and maintenance)
Short refueling time	FC confined lifetime
High efficiency	FC poor dynamic response
High driving range	Insufficient reliability and safety concerns

1.1.3 Energy Storage System (ESS) as a Secondary Power Source

FC systems cannot fully meet vehicle power requirements due to their inherent limitations. Pure FC systems have a slow dynamic response, making them unsuitable for handling power peaks during start-up and acceleration. Additionally, they cannot recover energy during braking. Integrating an energy storage system (ESS) into the FCEV powertrain creates the FC-HEV, addressing these challenges. The ESS supports fast dynamic load response, reduces PEMFC degradation, lowers fuel consumption, and enables energy recovery during braking. Batteries or supercapacitors (SCs) are commonly used as ESSs due to their charge-discharge capabilities [12], [15]. SCs offer high-power density and rapid transient response, making them ideal for quick recharging, though their low energy density limits broader application [16]. Research highlights that combining a FC with a battery enhances FC-HEV performance by (I) compensating for FC power output, (II) recovering energy during braking, and (III) reducing voltage fluctuations in the power systems. Li-ion batteries are widely adopted for their high energy density, extended lifespan, low self-discharge, and fast charging [17]. FC-HEVs powered by FC and battery are more appealing for automakers due to their less complexity, lower powertrain cost, and more compact volume. On the other hand, FC-battery hybrid systems can adapt to different types of vehicle thanks to their adaptability and various configurations. Hyundai Nexo, Toyota Mirai, Mercedes-Benz F-Cell, and Honda FCX Clarity are examples of FC-HEVs equipped with a FC and a battery [12], [18].

1.1.4 Multi-Stack FC System

The single-stack FC system may fail to meet the increasing demands for high-power generation and faces challenges such as low fault tolerance, low reliability, limited

durability, and high operating cost. To extend the power range of single-stack FC system, manufacturers have tried using larger membrane electrode assemblies (MEA) and higher-power FCs. However, longer and wider stacks take up too much space and are not practical for all applications, especially in vehicles [19], [20]. Moreover, manufacturers face technical and material challenges in producing a single high-power FC stack. Key challenges include the need for advanced catalysts, durable materials like bipolar plates, and structural integrity to withstand high-power demands. Complex manufacturing processes, such as precise stacking and material bonding, add costs and limit scalability. Additionally, designing FC stacks for high-power applications requires innovative solutions to address weight constraints [21], [22]. Using several low-power FC stacks, known as a multi-stack FC system, instead of a single high-power FC stack, can be a suitable solution to deliver higher output power and overcome single-stack challenges such as high operating cost, limited lifespan, and low reliability [23], [24]. The multi-stack FC has potential technical advantages, such as access to an broader efficient operating range, higher output power, and longer longevity over the single-stack FC [25].

As mentioned before, one of the main benefits of multi-stack FC systems is their ability to operate within a wider efficient range compared to single-stack FC systems. As shown in Figure 1-2, single-stack FC systems have only one peak efficiency point, whereas the multi-stack FC system provides multiple optimal operating points, which allow the system to access a broader efficient operating range and enable more flexible power distribution [19], [23], [25]. It should be noted that, according to Figure 1-2(b), the multi-stack FC system has the potential to increase system efficiency by accessing several optimal operating points. However, this does not mean that efficiency overlap across the power

range is automatically guaranteed by having identical sub-stacks. Operationalizing this potential depends on several factors, including multi-stack FC architectures, the energy management strategy (EMS) serving as the power controller, and the requested power.

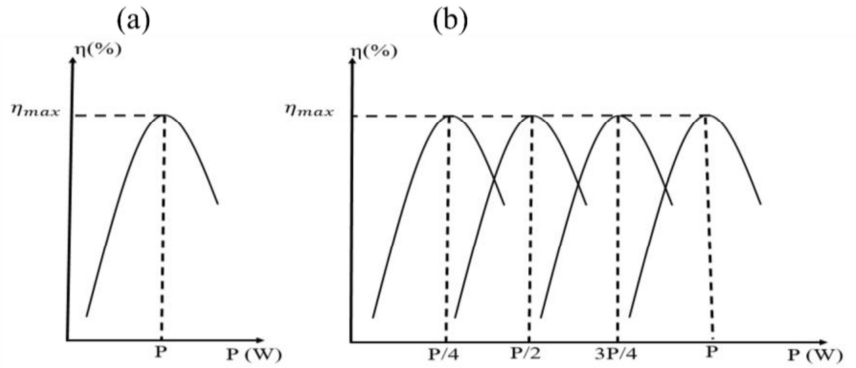

Figure 1-2- Overall system efficiency comparison between: (a) Single-stack FC system; (b) Multi-stack FC system [23].

The EMS plays a key role in operating the sub-stacks near their maximum efficiency points by activating the required number of sub-stacks and optimally distributing power among them. In other words, Figure 1-2(a) illustrates that a single-stack FC system is forced to supply the entire requested power, which can result in operation far from the maximum efficiency point. Figure 1-2(b) shows that, based on the requested power and with a suitable and advanced EMS, a multi-stack FC system composed of identical sub-stacks enables some sub-stacks to operate close to their maximum efficiency point. For example, at low requested power levels, a single-stack FC system must operate at low power, which is far from its maximum efficiency point. In contrast, a multi-stack FC system allows the EMS to activate only the minimum number of sub-stacks needed, enabling them to operate near their maximum efficiency point and meet the requested power. On the other hand, when the requested power is high, a single-stack FC system must operate in a high-power zone, which is far from its maximum efficiency point. In such

high-power situations, it may not be possible for each sub-stack in a multi-stack FC system to operate at its maximum efficiency. However, by using a suitable EMS, the multi-stack FC system can manage the sub-stacks in a way that allows some to operate at high power while others operate near their maximum efficiency. This approach demonstrates the flexibility of the multi-stack system to activate and manage sub-stacks, which can result in higher overall system efficiency compared to a single-stack FC system.

In a single-stack FC system, a FC stack failure will affect the entire performance. Due to its modularity, a multi-stack FC can manage this issue. The modular architecture improves the FC system's survivability, allowing failing stacks to be replaced individually, with only simple reconfiguration or component replacement needed to continue normal operation [25]. The modularity feature provides more degree of freedom by adjusting the number of sub-stacks in a multi-stack FC system and reduces system cost through convenient component replacement.

One of the most important aspects of multi-stack FC is redundancy. This feature improves system fault tolerance and enables the system to function in a degraded mode by stopping power generation from malfunctioning sub-stacks. When the malfunctioning stacks recover from unfavorable performance, such as flooding and drying out, they rejoin the system and start functioning again. The redundancy characteristic in a multi-stack FC system enhances overall stability, increases reliability, and reduces individual stack degradation [26]–[28].

The commercialization of FC technology in various vehicular applications, such as LDVs and MHDVs, is still constrained by technical and scientific obstacles, as mentioned in Table 1-1, including high operating cost, limited lifespan, low durability, and reliability.

To take effective steps in developing the commercialization and performance of FC-HEVs, a multi-stack FC system could be a promising choice. The multi-stack FC system is a mandatory option for high-power applications like MHDVs including trucks and buses. However, due to the significant potential and advantages of multi-stack FC systems, they can also be applied in LDVs, such as passenger cars [25], [29]–[31]. Mercedes buses, space exploration spacecraft power systems, and submarine airless propulsion are examples that have all adopted the multi-stack FC system [32]. Different designs, such as parallel-connected and series-connected architectures, can be used to link sub-stacks. Marx et al. conducted a comparative simulation examination of parallel and series architectures in [33]. The results show that the parallel design is a good way to slow down the rate of multi-stack FC degradation [34]. In the parallel architecture, each PEMFC stack is connected to the DC bus through a unidirectional DC-DC power converter, while the battery is directly connected to the DC bus to maintain the bus voltage. This architecture provides redundancy and enables the independent management of each FC stack [20], [23], [34].

1.1.5 The Significance of an Energy Management Strategy (EMS)

Efficient power distribution in powertrain systems with multiple power sources relies on a well-designed EMS as the core of power control. EMS is crucial for advancing clean vehicle technology by optimizing power distribution among components through appropriate operating modes. Its objectives include improving fuel economy, extending power source lifespan, and maintaining the state of charge (SOC) of the ESS while meeting constraints. Designing an effective EMS is challenging due to the distinct characteristics of multiple power sources and the need for real-time implementation with low computational demands [35]–[37].

EMSs are categorized into rule-based (RB), optimization-based (OB), and learning-based (LB) approaches. RB methods distribute power based on predefined rules, often derived from intuition or experience. They are simple and feasible for real-time applications but lack optimality and require significant calibration for each driving cycle. Common types include fuzzy logic and deterministic RB-EMSs [36], [38].

OB-EMS minimizes a cost function while satisfying constraints. These strategies are divided into offline and online approaches. Offline methods, such as dynamic programming (DP), rely on prior knowledge of driving cycles and serve as benchmarks but are unsuitable for real-time control. Online methods, like the equivalent consumption minimization strategy (ECMS) and model predictive control (MPC), use instantaneous cost functions and are designed for real-time application with minimal computational requirements [35], [36], [38], [39].

LB-EMS leverages advanced data mining to extract optimal control laws from historical and real-time data. These methods do not require precise model information but depend on creating a structured, well-sized database, which is time-consuming and complex. LB approaches include reinforcement learning, neural network learning, and classification techniques [36], [37], [40].

1.1.6 The Important Role of Voltage in PEMFC Performance

FC output voltage is a critical parameter that reflects the operational state of a FC system. Output voltage directly impacts the FC system's output power, efficiency, and hydrogen consumption, all of which are important indicators of FC performance [41]. Figure 1-3 illustrates the characteristic curves of a 500-W PEMFC, including polarization,

hydrogen consumption, power, and efficiency. It should be mentioned that the PEMFC characteristic curves were extracted experimentally at the Hydrogen Research Institute of the University of Quebec at Trois-Rivières (UQTR). The electrical power output of a FC is simply the product of voltage and current, as shown in (1-1).

$$P_{FC} = V_{FC}.I_{FC} \tag{1-1}$$

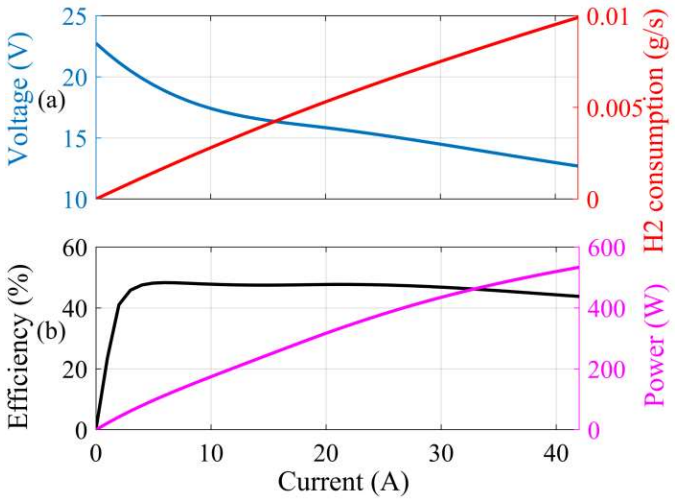

Figure 1-3- Characteristic curves of a 500-W PEMFC: (a) Polarization and hydrogen consumption; (b) Power and efficiency.

According to Figure 1-3(b), although FC output power increases with current, voltage plays a highly important role in supplying the requested power for real-world applications like FCEVs. According to (1-1) and Figure 1-3, for a given power, if the FC output voltage drops or is low, the FC must operate at a higher current to meet the requested power. This forces the FC to function in the concentration loss zone, leading to increased hydrogen consumption and reduced efficiency [42], [43].

Fuel input (W) is calculated as the product of the hydrogen consumption rate (g/s) and its energy content, typically expressed as enthalpy (ΔH) or high heating value (HHV). The

HHV of hydrogen is 142000 J/g. The hydrogen consumption rate during the electrochemical reaction is determined by Faraday's law, as shown in (1-2) [44].

$$q_{H_2} = \frac{mI}{nF} \tag{1-2}$$

where m represents the molecular weight of hydrogen (2.016 g/mol), I is the current (A), n is the number of electrons involved in the reaction, and F is Faraday's constant (96450 C/mol). Therefore, the fuel input is calculated as:

$$F_{in} = q_{H_2}.\Delta H = \frac{m\Delta H}{nF} I \tag{1-3}$$

According to (1-3) and Figure 1-3(a), FC hydrogen consumption increases with current. As mentioned earlier, for a constant power, if the voltage drops, the FC must operate at a higher current to meet the requested power. This results in increased fuel input and higher hydrogen consumption.

The efficiency of a FC is defined as the ratio of the electrical power output to the fuel input, with both expressed in the same units (W) [44], [45]:

$$\eta_{FC} = \frac{\text{Electrical power output } (P_{FC})}{\text{Fuel input } (F_{in})} = \frac{V_{FC}\, I_{FC}}{q_{H_2}.\Delta H} \tag{1-4}$$

According to (1-1), (1-2), and (1-4), when the FC voltage is stable, the FC output power, hydrogen consumption, and efficiency primarily depend on the current drawn from the FC, as illustrated in Figure 1-3. A stable voltage ensures that variations in output power are solely influenced by changes in current, simplifying the power control strategy. The EMS can directly calculate the required current for optimal power distribution without the need to account for voltage fluctuations. Stable voltage enables predictable efficiency at a given current, as the hydrogen flow rate is a function of the current [46]. Voltage instability disrupts this relationship, resulting in energy losses and challenges in maintaining optimal

operating conditions. When voltage is stable, the FC can consistently operate near its maximum efficiency, thereby reducing hydrogen consumption and minimizing energy losses [47]. On the other hand, voltage instability can cause inefficiencies in power electronics, such as DC-DC converters, as they must continuously adapt to fluctuating input voltages [48]. Components like switches and inductors operate less efficiently when the voltage deviates from the optimal range, resulting in increased energy losses and reduced overall system performance [49].

Alongside its role in FC performance, output voltage is a reliable indicator for monitoring the health and proper functioning of the FC. Voltage drops, which can result in unstable voltage, can negatively affect FC health, and increase the risk of malfunctions. In real-world applications, the FC operates under various dynamic conditions, which can increase voltage drops and fluctuations [50], [51]. Voltage drops negatively affect system performance and occur over short and long-term periods [52]. Short-term drops are temporary and result from transient conditions, such as water management issues (flooding or drying out) or reactant starvation. These are typically reversible with appropriate remedial actions, restoring stable voltage [53], [54]. Long-term drops occur gradually due to irreversible degradation, such as catalyst degradation, membrane deterioration, or electrode corrosion. These indicate aging and lead to a permanent decline in performance [55]–[57]. It is worth noting that if short-term malfunctions are not addressed and resolved, and the FC continues to operate under such conditions, it can accelerate degradation, contribute to long-term voltage drops, and damage FC components [58].

In summary, FC performance is highly dependent on voltage, a key output of the FC system. As discussed, voltage drops and fluctuations can negatively impact FC health, causing degradation, while also increasing operating current and hydrogen consumption,

ultimately reducing FC efficiency. Therefore, reducing voltage drops and fluctuations, which define stable voltage, can enhance FC performance, and minimize the risk of FC malfunctions. A stable voltage indicates proper FC operation, ensuring that electrochemical reactions proceed as expected.

1.1.7 The Impact of Water Management on PEMFC Voltage

PEMFC malfunctions and faults are major contributors to short-term voltage drops and unstable voltage [52]. In real-world applications, water management faults are among the most common issues that affect PEMFC voltage and performance. The operation of PEMFCs depends on the complex interplay of interconnected physicochemical and electrochemical processes, and cell performance is heavily influenced by effective water management [59]. Water management in PEMFCs is particularly sensitive to the hydration (flooding) and dehydration (drying out) of membranes, which are directly associated with protonic resistance [60]. Flooding refers to the accumulation of liquid water in gas channels or electrodes, hindering the access of reactive gases to the active layers and lowering the reaction rate. Drying out occurs when the membrane is insufficiently hydrated, leading to an increase in membrane resistance [61]. Flooding and drying out can reduce the PEMFC system's output voltage in the short term, and if not addressed promptly, they may result in long-term issues such as corrosion of the catalyst's carbon substrate and membrane degradation, ultimately leading to PEMFC failure [8]. Therefore, efficient water management is essential for maintaining the voltage stability, overall functionality, and durability of PEMFC systems. In summary, improving the performance, durability, and reliability of PEMFC systems is challenging and largely depends on FC voltage. Water

management is a key factor that significantly affects FC voltage, and inefficient water management can cause short-term voltage drops and compromise voltage stability [62].

1.2 Literature Review

In real-world applications of FCs, two levels of management are necessary to ensure proper operation. The first level is FC system management, which manages operating parameters such as water content, temperature, and reactants pressure, essential for the proper functioning of the FC. By maintaining these parameters within their optimal ranges, this level ensures reliable and efficient operation while preventing FC faults and malfunctions. The second level is vehicle energy management, which focuses on distributing optimal power between the FC and the battery or SC to meet the requested power. This level aims to improve FC performance, reduce fuel consumption, and prolong the system's lifespan by optimizing energy flow. As a result, these two management levels enable reliable and sustainable FC operation.

The first part of this section is dedicated to a literature review on the FC system management level, while the second part focuses on a literature review of EMSs for multi-stack FC-HEVs.

1.2.1 FC System Management Level

FC proper operation is critical in real-time applications like FC-HEVs to ensure the FC can meet the requested power without malfunctions. In this regard, monitoring and controlling FC operating parameters such as water content, temperature, and reactants pressure can enhance FC performance, reliability, and durability, which is achieved through FC system management. Thermal management, pressure management, and water

management are key aspects of FC system management, each contributing to improving FC performance under various dynamic conditions.

Some studies focus on thermal management, which involves maintaining the FC temperature within an optimal range. The goal of thermal management is to ensure efficient electrochemical reactions by preventing overheating or excessive cooling. Effective thermal regulation reduces energy losses, minimizes thermal stress on components, and extends the lifespan of the FC [63]–[66].

Other works focus on pressure management, which involves regulating the supply of reactants, such as hydrogen and oxygen, at appropriate pressure levels. The purpose of pressure management is to maintain consistent and uniform reactant distribution across the FC membrane. This enhances fuel utilization efficiency, ensures stable power output, and prevents issues such as reactant starvation or uneven reactions, which could negatively affect performance or reliability [67]–[70].

As discussed earlier, voltage, as the output of the PEMFC, is one of the most important operating parameters and has a significant impact on PEMFC performance and efficiency [71]. Voltage is a key indicator of PEMFC performance and is highly sensitive to water content. Improper hydration levels can cause issues such as flooding or drying out, leading to voltage drops and PEMFC malfunctions. In real-time applications, stable voltage is essential to ensure the FC meets the requested power. Short-term voltage drops compromise stability and negatively affect FC performance and efficiency. PEMFC voltage performance depends heavily on water content, which is controlled through water management. As a result, while thermal and pressure management are important for FC performance, due to the direct and undeniable impact of water management on PEMFC

voltage behavior, this section focuses on water management as a key aspect of FC system management. In this regard, various studies aim to improve water management in PEMFCs to mitigate the risks of water management faults, particularly flooding, which is frequent in real-world applications, and to enhance PEMFC performance.

Some studies aim to address water management faults in PEMFCs by improving water transfer through optimizing flow fields, gas diffusion layers (GDLs), and materials [72]–[76]. However, these methods are complex and cannot adapt to real-time operating conditions, making PEMFCs prone to water management faults during transient states. This limitation increases the risk of flooding in real-world dynamic conditions.

A feasible and economical solution to improve water management is the use of a purge valve, particularly in dead-end anode (DEA) PEMFCs. The purge valve controls water management on the anode side by promptly removing accumulated water, mitigating flooding, and restoring PEMFC voltage stability [62]. The timing of the purge valve is critical, as it directly affects water management and voltage stability. This timing, referred to as the purge strategy, involves adjusting the purge interval (time the valve remains closed) and purge duration (time it remains open). A short purge time fails to remove excess water, causing flooding and voltage drop. Conversely, an excessively long purge time dehydrates the membrane, leading to drying out and voltage drop [77]–[79]. Therefore, designing an appropriate purge strategy is crucial for PEMFCs to improve water management and performance. Figure 1-4 illustrates the effect of the purge strategy on water management and voltage stability. The desired voltage under normal PEMFC conditions is shown by a dashed red line, while the blue line represents experimental data from the Hydrogen Research Institute at the University of Quebec in Trois-Rivières. For a

20 s purge interval, a 100 ms purge duration (Figure 1-4(a)) fails to remove water, resulting in voltage instability and flooding. However, a 600 ms purge duration (Figure 1-4(b)) maintains voltage stability and prevents water management faults. This example illustrates that effective water management and voltage stability in PEMFCs are closely tied to the purge strategy.

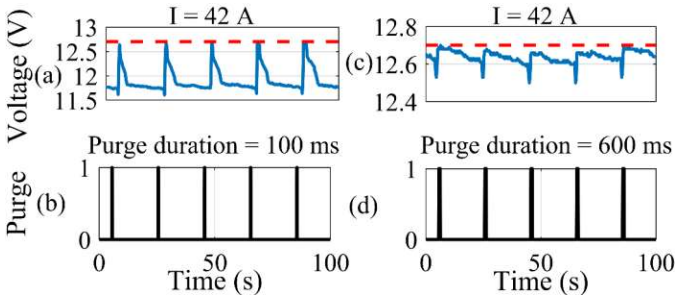

Figure 1-4- Voltage behavior under two different purge strategies for 42 A current level.

Some studies focus on analyzing the impact of various purge strategies on the water content inside the PEMFC [80]–[82]. However, this approach relies on a precise model to estimate the water content, which is challenging due to the complexity and multi-physics nature of PEMFCs. Consequently, it may not effectively enhance water management.

Voltage, as the output of a FC system, is a vital parameter with a significant impact on FC performance. It serves as a straightforward indicator of the electrochemical behavior of PEMFCs, effectively reflecting their performance under varying operating conditions, where any drop indicates a malfunction in the FC. Voltage is among the most accessible parameters of FC, measurable directly without requiring complex sensors [83]. Therefore, voltage monitoring (VM) is a reliable and widely used method for detecting FC malfunctions in real-world applications [61]. As unstable voltage is a consequence of water management faults, maintaining voltage stability through an appropriate purge strategy

ensures effective water management in the PEMFC. In this regard, many studies on purge strategies focus on voltage behavior as the output of the PEMFC system to improve water management. These studies primarily aim to design the suitable purge strategies to maintain PEMFC voltage stability and mitigate water management faults. In [84], experiments identify suitable purge intervals and durations to enhance cell voltage stability and stack power output, recommending a 10 s interval and 90 ms duration for stable PEMFC performance. In [85], a 3D model for gas purging in DEA-PEMFC shows that purge durations of 1–1.5 s improve water removal and voltage stability, particularly at high current densities. The paper in [86] proposes a dynamic purge strategy under varying load conditions, activating the purge valve when the cell current density ratio drops below 0.8, with a 3 s purge duration to maintain stable performance.

Another category of studies focuses on the impact of various parameters, such as PEMFC temperature, anode pressure, relative humidity, and air stoichiometry, on purge strategies by analyzing voltage behavior to improve water management. [77], [79], [87], [88].

In the purge process, a pressure difference between the inside and outside of the anode generates a hydrogen flow that expels accumulated water to recover FC performance by reducing water management faults. In fact, when the purge valve opens, a portion of hydrogen is discharged as part of the purge process. Despite the effectiveness of the purge method in PEMFCs, a significant issue with this approach is the loss of hydrogen during the purge. Since hydrogen is an expensive fuel and a crucial component of PEMFCs, considering wasted hydrogen when designing a suitable purge strategy is essential, especially in real-time applications like vehicular systems, as it significantly impacts

system efficiency and FC operating cost [62], [89]. As a result, an efficient purge strategy should reduce water management faults to achieve voltage stability while also minimizing wasted hydrogen during the purge to enhance PEMFC efficiency and lower operating cost.

Few studies focus on designing efficient purge strategies that maintain voltage stability while minimizing hydrogen consumption. In [90], optimal purge strategies for PEMFCs with DEA suggest intervals of 400–500 s and durations of 5–20 ms, effectively maintaining voltage stability and reducing hydrogen consumption. In [78], experimental results of the purge process in DEA-PEMFCs identify a 14.86 s interval and 0.44 s duration as optimal. This approach balances hydrogen consumption and voltage stability, significantly improving PEMFC stack performance. The study in [91] uses a numerical model to optimize purge strategies, showing that intervals of 15–30 s and durations of 0.25–0.5 s effectively maintain voltage stability and reduce hydrogen consumption. The study of [92] experimentally determines a 0.2 s purge duration as optimal for balancing hydrogen consumption and performance recovery in DEA-PEMFCs. In [93], a mathematical model identifies a 260 s purge interval and 25 ms duration as ideal for minimizing wasted energy, improving voltage stability, and reducing hydrogen consumption under varying conditions. The paper of [94], develops a mathematical model indicating that durations of 0.2–0.4 s maximize energy efficiency, balancing hydrogen consumption and reducing voltage drops.

1.2.2 Energy Management Level of FC in Vehicle

After highlighting the importance of FC system management in controlling operating parameters, this section aims to investigate the role of EMS in enhancing FC performance in vehicular applications, with a focus on the multi-stack FC system configuration.

Due to the mentioned benefits of multi-stack FC systems, researchers in recent years have focused on developing the use of multi-stack systems in FC-HEVs. A multi-stack FC-HEV requires a mature EMS to manage power distribution, which is crucial for reducing fuel consumption and improving system efficiency, FC lifespan, and reliability. In this regard, improving the EMS in multi-stack FC-HEVs, as the software component, is a critical priority and a significant topic of discussion. Consequently, the following section provides a brief summary of recent EMSs in multi-stack FC-HEVs.

1.2.2.1 RB-EMS in the Multi-Stack FC-HEVs

The study of [95] presents a power system model for FC-HEVs, validated using Hardware-in-the-Loop (HIL) emulation. A multi-stack FC system with a RB-EMS maintains battery SOC targets and optimizes FC operation in high-efficiency regions. In [96], a RB strategy distributes demand across three FC stacks to reduce individual stack usage and extend lifespan in vehicles like the Toyota Mirai. Economic analysis shows improved FC lifespan and lower costs per mile compared to single-stack systems. In [28], proposes an online EMS for multi-stack FC-HEVs, improving fuel economy and FC lifespan. A two-layer strategy uses a Kalman filter to assess stack efficiency and allocates power among components. HIL tests confirm enhanced system performance.

1.2.2.2 OB-EMS in the Multi-Stack FC-HEVs

Various studies focus on designing OB-EMSs for multi-stack FC systems to optimize power distribution among FC system, battery, or SC. The objectives include minimizing hydrogen consumption, extending FC lifespan, and enhancing system efficiency. OB-EMSs for multi-stack systems are divided into offline and online categories.

Offline OB-EMSs

Offline OB-EMSs aim to find the global optimal power distribution trajectory to reduce hydrogen consumption, minimize FC degradation, and increase system efficiency. However, they are typically benchmarks due to high computational burden, making them unsuitable for real-time applications. In [97] a constrained exploration method optimizes EMS in multi-stack FC-HEVs, improving fuel economy and FC durability, surpassing traditional methods like DP in cost-effectiveness. In [98], a multi-objective hierarchical EMS balances FC aging and battery SOC, closely aligning with DP performance while extending FC lifespan. The paper of [99] proposes a bi-level EMS for multi-stack FC-battery hybrids. The first level smooths power demands, and the second allocates power to enhance efficiency, extend remaining useful life (RUL), and reduce lifecycle costs, outperforming equal allocation methods.

Online OB-EMSs

The focus of online OB-EMSs is to develop EMSs suitable for real-time applications, such as FC-HEVs, emphasizing low computational burden and real-world implementation. The proposed EMSs are often compared with benchmarks like DP to assess their effectiveness.

Most studies in this category aim to improve multi-stack FC system performance by applying optimization algorithms. Objectives include reducing hydrogen consumption, increasing FC efficiency, decreasing degradation, and lowering operating cost. The study of [100] introduces a dual FC powertrain with an optimal EMS, enhancing efficiency and reducing fuel consumption. It outperforms single-stack configurations in performance and

operating cost for FC-HEVs. In [101], an optimal coordination method derives efficiency distribution functions from stack energy consumption models, enabling real-time control through power allocation matrices. Tests with 100-kW stacks validate its effectiveness. The paper of [30] compares decentralized convex optimization frameworks using alternating direction method of multipliers for a modular FC-HEV with two FC stacks and a battery. Results highlight improved modularity and flexibility in power allocation. In [102], an EMS is proposed to reduce operating cost and extend system lifespan. RT-LAB tests demonstrate its effectiveness, showing increases in efficiency and reductions in operating cost by 15.85% and 9.75%, respectively. The study of [103] proposes a downgrade power allocation strategy for multi-stack FCs, activating only necessary stacks to minimize hydrogen consumption. This approach reduces auxiliary losses, extends FC lifespan, and improves efficiency.

Another group of online OB-EMSs employs hierarchical strategies to enhance multi-stack FC system performance. These approaches use a two-layer EMS, combining methods like RB-EMS with OB-EMS, two OB-EMSs, or offline and online OB-EMSs. In [104], a hierarchical EMS compares single-stack and multi-stack configurations for a FC-HEV. The multi-stack system demonstrates lower hydrogen consumption, reduced FC degradation, and decreased operating cost, making it more efficient than the single-stack setup. In [105], a two-layer EMS for a hybrid electric ship with multi-stack FC and battery optimizes real-time power distribution, improving fuel efficiency by 28% and reducing computation time by 99.9%, making it suitable for maritime applications.

Another group of online OB-EMS focuses on multi-stack FC system sizing and stack allocation to extend FC lifespan, reduce start-stop cycles, increase RUL, and lower

hydrogen consumption and system costs. In [106], the study optimizes multi-stack FC systems for efficiency and durability with a fault-tolerant power management system, achieving 34% lifetime cost savings and a 30% lifespan increase across various FC technologies. The paper of [107] uses a multi-objective cost function to optimize stack allocation, targeting minimum life-cycle cost. For a 240 kW multi-stack FC, this approach achieves 0.06 kg/100 km hydrogen savings compared to traditional equal allocation methods.

1.2.2.3 LB-EMS in the Multi-Stack FC-HEVs

The paper of [29] presents a Q-learning-based EMS for multi-stack FC-HEVs, aiming to minimize hydrogen consumption and power sources degradation. A three-layer online EMS adapts dynamically, achieving up to 13.08% cost savings under real driving conditions. In [31], an independent Q-learning-based EMS for multi-stack FC-HEVs maintains battery SOC, reduces hydrogen consumption, and improves generalization and fault tolerance. Experimental results show the proposed EMS outperforms equi-distribution and daisy chain methods in fuel economy. The study of [108] proposes a decentralized reinforcement learning EMS for FC-HEVs with two parallel FC systems and a battery. This multi-agent framework enhances convergence speed and optimization through modular, interconnected learning strategies.

To summarize the literature study on FC system management and EMS in FC-HEVs, the following sections provide a conclusion of the reviewed studies, highlighting the research gaps in developing and improving FC performance in vehicular applications.

In real-world applications like FC-HEVs, an advanced EMS is essential for optimizing power distribution and reducing operating cost. On the other hand, a suitable EMS for real-

time applications should have a reasonable computational burden. RB-EMS is suitable for real-time applications but depends on precise parameter calibration, limiting its adaptability and ability to ensure optimal performance under dynamic conditions. As a result, RB-EMS is less commonly used in multi-stack FC-HEVs. LB-EMS has gained attention due to its nonlinear modeling capabilities, flexibility, and independence from physical formulations. However, LB-EMS faces challenges, including complex data requirements, dependence on large datasets, dimensionality issues, and limited hardware testing. In multi-stack FC systems, the presence of multiple FCs increases the computational burden, making LB-EMS implementation more challenging. Consequently, only 12% of EMSs in multi-stack FC-HEVs use LB-EMS approaches.

A review of EMSs in multi-stack FC-HEVs from 2017 to the present shows that 76% of studies focus on OB-EMS approaches, as illustrated in Figure 1-5. Offline OB-EMS, which requires prior knowledge of driving cycles to achieve global optimization, is unsuitable for real-time applications due to its impracticality in real-world scenarios. In contrast, online OB-EMS has gained significant attention for its low computational burden, simple implementation, and suitability for real-time use without needing prior driving cycle data, making it a promising option for FC-HEVs. Among OB-EMS studies, 84% of studies focus on online OB-EMS due to these advantages. These studies aim to improve EMS performance, achieving results close to global optimization and enhancing multi-stack FC-HEV efficiency. Additionally, research on online OB-EMS addresses challenges like reducing operating cost, increasing reliability, and supporting commercialization efforts for FC-HEVs.

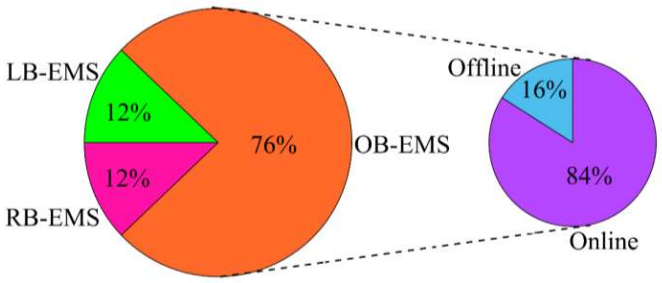

Figure 1-5- Contributions of different EMS approaches in multi-stack FC systems.

In light of studies on FC-HEVs, the literature reveals that most papers focus solely on designing an EMS to distribute optimal power between sub-stacks and the battery, aiming to reduce hydrogen consumption, increase system efficiency, and extend the lifespan of power sources, without addressing PEMFC operating parameters. According to the literature on EMSs in FC-HEVs, despite the importance of operating parameters for real-time PEMFC performance, the integration of FC system management into EMSs has received limited attention. Few studies attempt to incorporate FC temperature into the EMS by controlling the thermal management system's fan to enhance PEMFC performance, improve efficiency, and reduce degradation [109], [110]. However, despite the significance of water management and its substantial impact on PEMFC output voltage, to the best of the author’s knowledge, integrating water management into EMS design has not yet been addressed.

1.3 Thesis Problem Statement and Conceptual Framework

According to the literature review, a multi-stack FC system is a mandatory option for MHDVs. However, due to its notable advantages, such as modularity, operation in degraded mode, higher reliability and durability, and improved efficiency compared to a single-stack FC system, it can also be utilized in LDVs. Despite these benefits, it is not

considered a mandatory option for LDVs. In fact, using a multi-stack FC system instead of a single-stack in LDVs may increase the initial investment cost of these vehicles. However, the impact of the multi-stack system on operating cost and FC performance is determinant and can make it a feasible solution for LDVs compared to a single-stack system. As previously mentioned, one of the primary concerns regarding the commercialization of FC-HEVs is the operating cost, along with reliability and durability. The literature review emphasizes that the impact of the advantages of a multi-stack FC system on the operating cost and performance of LDVs, compared to a single-stack system, has not been thoroughly explored.

According to the literature, the implementation of multi-stack FC systems in various applications, especially in vehicular applications such as FC-HEVs, is growing and advancing. Despite the significant potential and advantages of the multi-stack FC system, a software part is required to operationalize these capabilities, and the EMS is responsible for this task. Additionally, in a multi-stack FC system, operating cost, FC lifespan and reliability are challenging factors that can be greatly improved with an advanced EMS. Alongside reducing hydrogen consumption, which is a major factor in the operating cost of a multi-stack FC system, FC degradation plays a critical role in FC reliability and durability, with an undeniable impact on operating cost. The presence of multiple power sources makes controlling FC degradation challenging, requiring an advanced EMS to monitor and manage sub-stack health. Maintaining similar degradation rates across all FCs is crucial, as uneven degradation leads to imbalanced performance, reduced reliability, and higher operating cost. As a result, in multi-stack FC-HEVs, a mature EMS is essential to fully utilize the system's potential, optimize power distribution between FCs and the

battery, lower operating cost, and enhance FC lifespan and system efficiency. However, developing a dependable EMS for multi-stack FC-HEVs remains a key area for further research and innovation.

In this regard, most studies focus on designing an OB-EMS to distribute optimal power between the FCs and the battery. In online OB-EMSs, single time-point strategies, like ECMS, consider only the current dynamic conditions and requested power to reduce operating cost and improve FC performance. However, they lack adaptability to future load variations, which limits their ability to optimize performance in real-world applications [111], [112]. In real-world applications, FCs experience varying dynamic conditions, and a lack of awareness of future dynamics can lead to suboptimal performance of FC-HEVs, limiting the effectiveness of cost reduction. Offline OB-EMSs like DP consider the entire driving cycle, achieving globally optimal results and improving performance. However, they are unsuitable for real-time use due to their need for complete driving cycle data and high computational requirements. Multiple time-point strategies could be a reasonable compromise between single time-point strategies and offline strategies methods like DP. By incorporating prediction, multiple time-point strategy that considers a finite prediction horizon, producing results close to global optimization. As shown in Figure 1-6, multiple time-point EMS serves as a bridge between single time-point and offline EMSs by using prediction and a finite horizon. It addresses the shortcomings of offline EMSs, such as inapplicability for real-time performance and high computational burden, by applying a finite horizon.

As a result, a multiple time-point EMS improves EMS performance by predicting load variations and dynamic situations, achieving better results than a single time-point EMS

[113]–[116]. Additionally, by utilizing a finite prediction horizon, it overcomes the need to know the entire driving cycle in advance, making it a promising approach for real-time applications. In a multi-stack FC system with several sub-stacks, distributing optimal power among FCs is crucial for reducing operating cost and increasing FC lifespan and reliability. In this regard, using a multiple time-point strategy as a predictive EMS (PEMS) that can anticipate future dynamic situations and requested powers can enhance multi-stack FC system performance, improve efficiency, and, as a final goal, effectively reduce operating cost.

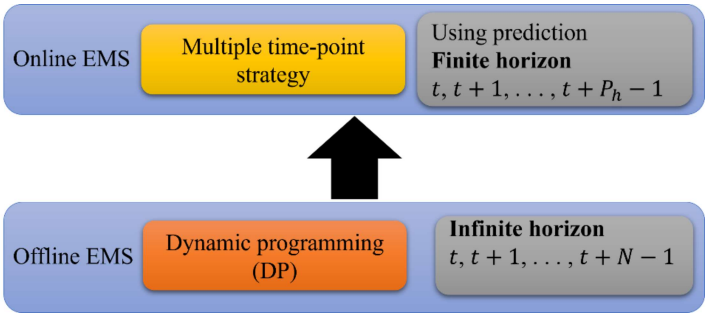

Figure 1-6- Concept of multiple time-point EMS framework [36].

The literature review reveals that 76% of EMSs for multi-stack FC-HEVs focus on OB-EMS, with 84% of these studies concentrating online OB-EMS due to their applicability for real-world scenarios. However, according to Table 1-2, the literature review indicates that among the online OB-EMSs developed for multi-stack FC-HEVs, the majority focus on single time-point EMSs. As shown in Table 1-2, among online OB-EMSs, only 9.5% of EMS studies in multi-stack FC-HEVs employ a multiple time-point strategy that incorporates prediction. According to the literature review on multi-stack FC-HEVs, the multiple time-point strategy as a PEMS has not been well-researched or widely utilized.

Therefore, addressing this research gap in multi-stack FC systems could lead to a more developed and reliable EMS.

Table 1-2- Online OB-EMSs in multi-stack FC-HEVs.

Application	Single time-point EMS	Multiple time-point EMS
MHDVs	[100], [101], [122], [102], [106], [107], [117]–[121]	[25], [105]
LDVs	[27], [30], [103], [104], [123]–[126]	

In a FC, voltage, as the system's output, plays a crucial role in determining the FC performance and efficiency. Moreover, voltage serves as an indicator, with any drops or fluctuations signaling potential malfunctions in the FC. In real-world applications, especially in vehicular systems, achieving stable voltage is crucial to meet the requested power, ensure the proper functioning of power electronics, and enable effective control of the power supplied by the FC. However, in real-world applications, FCs experience various dynamic conditions that can threaten voltage stability and increase voltage fluctuations. One of the main contributors to voltage drops and instability is the occurrence of faults. Among various faults, water management faults are the most common in vehicular applications. Water management faults can lead to voltage drops and, if not corrected, may result in long-term effects such as FC degradation and failure. Flooding is the most common water management fault in PEMFCs, linked to water content, which can cause short-term voltage drops and, if not removed, can result in long-term voltage drops and degradation. To mitigate water management faults and control water content in PEMFCs, using a purge valve is considered an effective and economical solution. In the purge process, timing is crucial to minimize the risk of water management faults and maintain

voltage stability. Therefore, the purge strategy, defined by the purge interval and duration, is essential for controlling water levels and maintaining voltage stability in the PEMFC.

According to the literature review, output current is a critical parameter that affects PEMFC performance during operation. Increasing PEMFC current intensifies water flooding, a water management fault that is a primary cause of PEMFC voltage decline and can potentially lead to reduced power and efficiency [127]. Some studies have shown that changes in output current significantly affect water management and the short-term performance of PEMFC voltage [128]–[130]. According to the literature review in the previous section, most studies focus on improving water management and achieving stable voltage by designing a constant, non-adaptive purge strategy for all current levels. The purge strategies in these studies cannot adjust to different current levels, increasing the risk of water management faults like flooding, affecting PEMFC voltage stability, and reducing PEMFC efficiency. Due to current variations in real-world applications and the sensitivity of water management and PEMFC performance to output current, designing an adaptive purge strategy capable of adjusting to different current levels can minimize the risk of water management faults and enhance PEMFC voltage stability and performance. However, despite the critical role of current in PEMFC performance, considering current variations when designing an effective purge strategy has been escaped attention and represents a research gap.

An EMS is responsible for distributing optimal power between power sources to achieve objectives such as reducing the total operating cost. It sends a reference power to the FC to meet the requested power, but it cannot, by itself, ensure that the FC operates properly without malfunctions. As mentioned earlier, in real-world applications, voltage

has a significant impact on FC performance, and stable voltage is essential to ensure that the PEMFC meets the requested power and supports the proper functioning of power electronics. According to the above explanations, water management has a significant impact on PEMFC voltage, and water management faults directly influence PEMFC performance. In this context, water management is a critical factor that plays a key role in minimizing the risk of faults and helps the FC maintain stable voltage through the regulation of the purge strategy. Integrating water management into the EMS allows for active monitoring and adjustments to address voltage drops, ensuring voltage stability and reliable power output. This approach prevents situations where the PEMFC stack may fail to meet requested power, reducing risks of shutdowns or performance issues. On the other hand, integrating water management into the EMS can reduce voltage instability and its negative effects, such as accelerated PEMFC degradation, increased operating cost, and a shortened PEMFC lifespan. To the best of the author's knowledge, despite the importance of water management and its impact on FC voltage, integrating it into the EMS for FC-HEVs has not yet been explored. This research gap can be addressed by integrating water management into the EMS through the design of a suitable purge strategy that distributes optimal power while mitigating water management faults, thereby enhancing voltage stability.

1.4 Aims and Objectives

As mentioned earlier, challenges in FC-HEVs, such as operating cost, limited FC lifespan, and low reliability, hinder the commercialization of FC technology in vehicular applications. A suitable EMS, as a software part, can significantly mitigate and overcome these challenges by optimally distributing power. However, designing an advanced EMS

that can distribute optimal power to reduce system operating cost and increase FC lifespan and reliability remains an open issue and requires further investigation. Designing such an EMS in a multi-stack FC-HEV is more challenging due to the presence of multiple sub-stacks. In a multi-stack FC system, an EMS should not only distribute power between the FCs and ESS but also allocate optimal power to each sub-stack to enhance FC lifespan and efficiency. In this regard, the primary aim of this thesis is to design an advanced EMS for a multi-stack FC-HEV to reduce system operating cost, extend sub-stack lifespan, and enhance system reliability. After developing an advanced and reliable EMS, this study aims to enhance FC performance and efficiency by integrating water management into the EMS. To achieve this, the thesis focuses on mitigating water management faults and improving voltage stability through the design of an effective purge strategy.

To address the research gaps mentioned in the previous section, the objectives of this thesis consists of three main stages.

- Operating cost comparison between multi-stack and single-stack FC systems:

As mentioned before, multi-stack FC systems have significant advantages over single-stack FCs, including redundancy, modularity, and access to a wider range of optimal operating points, making them a promising option for real-world applications. However, a suitable EMS is needed to operationalize these advantages and fully realize the potential of multi-stack systems. Despite the potential and advantages of multi-stack FC systems, the literature reveals a lack of investigation into the impact of these advantages on multi-stack performance and operating cost, which are main concerns in FC-HEVs. Therefore, the first objective of this thesis is to design a suitable EMS to analyze the impact of multi-stack FC

system advantages on operating cost, hydrogen consumption, FC efficiency, and FC durability, and to compare the results with a single-stack FC system.

- Designing a mature and advanced EMS for a multi-stack FC-HEV:

As mentioned before, on the hardware side, the multi-stack FC system presents significant potential and advantages. However, to operationalize this potential and fully leverage these advantages, designing a suitable EMS as the software side is crucial. On the other hand, in multi-stack FC-HEVs, distributing power among sub-stacks, optimizing hydrogen consumption, and extending FC lifespan are challenging due to the use of multiple FC stacks, and require an advanced and dependable EMS. Therefore, the second objective of this project is to design an advanced EMS for the multi-stack FC-HEV. To improve EMS performance and bring its results closer to the benchmark, this thesis incorporates prediction into the EMS. Literature consideration shows that among various works on multi-stack FC-HEVs, using prediction in EMS has been far from the center of attention. As a result, this thesis utilizes a PEMS to make optimal decisions based on vehicle speed predictions and improve power distribution. In addition, the proposed EMS not only distributes optimal power but also aims to improve the reliability and lifespan of sub-stacks by supervising and managing the degradation rate of each FC. The EMS uses a hierarchical PEMS (HPEMS) to mitigate further degradation of sub-stacks, which is a critical concern in multi-stack FC systems.

- Integrating water management into the EMS by designing an adaptive purge strategy:

As mentioned earlier, voltage, as the output of the FC system, significantly impacts FC performance and serves as a health indicator for the FC, where any drops or fluctuations in voltage indicate a fault in operation and can reduce performance and efficiency. In real-

world applications like FC-HEVs, mitigating voltage drops and achieving stable voltage are crucial for FC performance. Maintaining voltage stability improves performance and reduces stress on power electronics, such as DC-DC converters. Furthermore, stable voltage facilitates easier and more efficient control of FC output power and performance, as it allows FC performance to depend primarily on current. However, due to the various dynamic conditions in real-world applications, the FC is always prone to voltage instability and fluctuations. One of the main contributors to voltage drops and instability is related to water management faults. In this regard, the third stage of this thesis aims to mitigate water management faults, particularly flooding, by designing an adaptive purge strategy to improve FC voltage stability. Although water management in PEMFCs depends on fluidic architecture and is inherently a complex problem, this stage of the thesis aims to simplify the issue by controlling water management through a purge strategy. In other words, as a proof of concept, this stage of the thesis demonstrates the critical role of water management in FC voltage and performance. For this purpose, the study defines a simple indicator based on voltage to ensure effective purge management. In the voltage behavior analysis, a threshold of 100 mV is selected for unstable voltage based on the literature review, as exceeding this value can result in water management faults [77], [84], [131], [132].

Increasing FC operating current can elevate the risks of water management faults and negatively impact FC performance. However, despite the importance of FC current in water management, a review of the literature reveals that most studies on water management through purge strategies focus on developing static, non-adaptive strategies for varying FC current levels. Although a static purge strategy is convenient and straightforward, it fails to achieve efficient water management or guarantee voltage stability. Therefore, this study

aims to conduct comprehensive experimental tests and analyses to develop an adaptive purge strategy for different current levels, mitigating water management faults and maintaining voltage stability.

After designing the proposed purge strategy to improve water management and FC voltage stability, the final step in the third stage of this thesis involves integrating water management into the EMS. The main purpose of this step is to enhance the real-time performance of the FC by mitigating the risk of water management faults and increasing voltage stability using the proposed purge strategy. In other words, the third step of this thesis aims to enhance the performance of FCs in a multi-stack FC-HEV by integrating the effects of water management, without requiring a redesign of the EMS.

1.5 Contribution of the Research

A comprehensive literature study shows that the development and commercialization of multi-stack FC system in vehicular applications, alongside hardware advancements, require an advanced and mature EMS as a software component. Based on the literature, multi-stack FC-HEVs have been evolving in recent years, but the need for a proper and reliable EMS is still evident. On the other hand, FC voltage has an undeniable impact on FC performance, as voltage drops and fluctuations can disrupt its operation. Therefore, maintaining stable voltage is crucial in real-world applications to ensure the FC meets the requested power and enables the EMS to control FC output power more effectively. One of the main issues that directly affects FC output voltage is water management, which plays a crucial role in ensuring FC voltage stability. However, a literature review reveals that most studies on multi-stack FC-HEVs focus solely on designing an EMS to distribute optimal power among power sources, without considering the effect of water management on voltage stability.

The contributions of this research can be divided into three parts:

1) According to the literature, while many studies emphasize the benefits and practicality of multi-stack FC systems, the impact of multi-stack advantages on performance and operating cost, which are important and challenging issues for FC-HEVs, has not been thoroughly addressed. Therefore, the first contribution of this thesis is to conduct an analytical comparison between multi-stack and single-stack FC systems through an online EMS to evaluate the effects of multi-stack FC system advantages on operating cost, efficiency, and durability. For this purpose, the performance of a single-stack FC system with one 2000-W PEMFC is compared to that of a multi-stack FC system with four 500-W PEMFCs in a FC-HEV.

2) According to the literature review, most multi-stack FC-HEV research focuses on reducing operating cost by managing and optimizing each FC's hydrogen consumption and power distribution without considering future vehicle speeds and FC dynamic behavior. In other words, a comprehensive literature study on multi-stack FC-HEVs highlights the lack of using a PEMS. In optimal control problems, it has been proven that awareness of future events leads to decisions that approach global optimization results. Therefore, this study aims to employ a predictive OB-EMS, utilizing a novel prediction method based on a deep neural network to forecast future vehicle speed. In addition to hydrogen consumption, the degradation of FCs and the battery is considered in the proposed EMS's objective function to reduce system total operating cost. As discussed earlier, power distribution among sub-stacks in a multi-stack FC system is a crucial and challenging issue that plays a key role in operating cost and FC lifespan. In other words, an EMS in a multi-stack FC system consists of two parts: a) distributing power between sub-stacks and the battery, and b) distributing

power among the sub-stacks. To mitigate the degradation rate and increase the lifespan of sub-stacks in a multi-stack FC system, this study employs a HPEMS. In the upper layer, an RB-EMS is used in this study to distribute power between each FC, from the least degraded to the most degraded, based on the requested power, battery SOC, and FC degradation rates. The goals of the upper layer are:

a) Preventing further degradation of the most degraded FCs and ensuring that all FCs have a close degradation rate.

b) Deactivating unnecessary FCs to reduce hydrogen consumption.

In the lower layer, a predictive real-time OB-EMS combined with vehicle speed prediction is employed to make optimal control decisions between the FCs and the battery.

3) In the previous sections, it has been shown that FC output voltage is sensitive to water management, and water management faults can lead to voltage drops and unstable voltage. Therefore, the third contribution of this study is to integrate water management into the EMS to analyze the effects of voltage stability on FC performance in a multi-stack FC-HEV. In this regard, this stage aims to improve water management and FC voltage stability through the implementation of an efficient adaptive purge strategy. Most existing studies on purge strategy design employ static, non-adaptive approaches that fail to adjust to varying PEMFC current levels, potentially reducing voltage stability and FC efficiency. Due to the importance of FC current and its impact on water management, this study designs an adaptive purge strategy that can adjust to different current levels.

Regarding water management, when the purge valve opens to expel accumulated water, some hydrogen is wasted due to the pressure difference between the inside and outside of

the anode. In designing a purge strategy to improve water management, this wasted hydrogen is a critical factor that increases fuel consumption and impacts FC operating cost and efficiency. Therefore, this study proposes an efficient purge strategy that, alongside improving water management and voltage stability, aims to minimize hydrogen consumption during the purge process.

In the final step, water management through the proposed purge strategy is integrated into the EMS developed in the second stage of this thesis. In other words, the contribution of this integration is to distribute optimal power between the sub-stacks and the battery while accounting for water management and its impact on FC voltage through the proposed purge strategy. Integrating water management into the EMS improves FC voltage stability and prevents FCs from operating at higher currents to compensate for voltage drops. This reduces operating cost and enhances FC performance.

In summary, the third stage of the thesis consist of two contributions:

a) Designing an adaptive efficient purge strategy that aims to improve water management and voltage stability while minimizing hydrogen consumption during the purge process.

b) Improving the performance of FCs in a multi-stack FC-HEV by integrating water management into the EMS without the need to redesign the existing EMS.

1.6 Methodology

The first stage of this thesis aims to analyze the effect of multi-stack FC system advantage on its performance by comparing the operating cost, efficiency, and FC lifespan of a multi-stack FC system (four 500-W PEMFCs) with a single-stack FC system (a 2000-

W PEMFC). To ensure a fair comparison, it is crucial to use the same FC technology. This stage employs an online OB-EMS capable of conducting real-time applications. The ECMS, an online single time-point EMS, is a reliable strategy for reducing energy consumption in real-time applications. Additionally, this stage includes an experimental part to validate the FC model. Alongside simulation, PEMFC experimental data is used to avoid common inaccuracies of numerical models and make the results more realistic. FC polarization, hydrogen consumption, power, and efficiency curves are extracted from a developed PEMFC test bench at the Hydrogen Research Institute of Université du Québec à Trois-Rivières (UQTR). In the software part, the proposed strategy is implemented in MATLAB, while LabVIEW is used to extract the characteristic curves of the FC. The hardware part consists of a developed PEMFC test bench.

The second stage focuses on designing an advanced EMS for multi-stack FC-HEVs. For this purpose, a HPEMS is designed. Power allocation in multi-stack FC-HEVs involves two steps: 1) between sub-stacks, and 2) between the FCs and the battery. The proposed EMS uses a two-layer structure. In the first layer, a RB-EMS employs a rotary state machine approach to determine how many sub-stacks should be activated based on requested power, battery SOC, and FC degradation. At each time step, the upper layer selects the minimum number of FCs needed based on their degradation rates. For example, if two FCs are required, it chooses those with the lowest degradation. In other words, FCs with higher output power and lower voltage degradation are considered younger and are given the highest priority for participation in the lower layer. As a result, the upper layer aims to keep all sub-stacks at a similar degradation rate, which is crucial in a multi-stack FC system. On the other hand, another goal of the upper layer is to activate the minimum

number of FCs to lower hydrogen consumption, which significantly impacts operating cost. By determining when to activate or deactivate FCs, the upper layer aims to turn off unnecessary FCs and minimize hydrogen consumption. These sub-stacks then participate in the predictive OB-EMS. In the second layer, MPC is used as a multiple time-point strategy for optimal power distribution. MPC makes optimal control decisions based on future events like vehicle speed. To achieve accurate speed forecasting, a novel prediction method using a deep neural network approach, called stacked bidirectional long short-term memory (SBLSTM), is implemented. The results are compared with ECMS (as a single time-point strategy) and DP (as a benchmark) to validate and assess the performance of the proposed strategy. The first phase in designing the EMS involves using a trustworthy FC model to simulate its behavior. This study uses experimental FC data to generate polarization, hydrogen consumption, power, and efficiency curves, reducing inaccuracies commonly found in numerical models and improving the accuracy of FC outputs. MATLAB is used to implement the designed EMS, while LabVIEW is employed to collect and analyze the FC experimental data. The hardware component includes a developed PEMFC test bench.

The third stage of this thesis focuses on improving PEMFC water management and the resulting voltage stability by designing an adaptive efficient purge strategy and subsequently integrating water management into the EMS. This stage utilizes the air-cooled open cathode H-500 DEA-PEMFC for experiments conducted at the Hydrogen Research Institute’s test center at Université du Québec à Trois-Rivières (UQTR). During the purge process, when the purge valve opens to expel accumulated water, hydrogen is wasted due to the pressure difference between the anode's interior and exterior. This hydrogen loss increases fuel consumption and decreases the FC system's efficiency. Therefore, this stage

aims to develop an efficient purge strategy for each current level to improve water management while minimizing hydrogen consumption, ultimately enhancing PEMFC operating cost and efficiency. Because the proposed purge strategy adjusts to different current levels, it is called an adaptive efficient purge strategy. In this regard, the proposed purge strategy consists of two steps: 1) The first step involves analyzing various combinations of purge intervals and durations for each current level to identify which combinations achieve effective water management, resulting in stable voltage (voltage drop below 100 mV). 2) The second step is to examine hydrogen consumption. Among the combinations that ensure FC performance without water management faults (stable voltage), the one with the lowest hydrogen consumption is selected.

The final step of the third stage of this thesis integrates water management into the EMS proposed in the second stage. This integration comprises two main levels. The first level is the HPEMS from the second stage, responsible for distributing optimal power between the FCs and the battery. The second level is the water management system, which includes the adaptive efficient purge strategy developed in the third stage through extensive experiments and analyses. The procedure for integrating water management into the EMS involves the HPEMS determining the optimal power for the FCs. Based on this optimal power, the reference current for each sub-stack is sent to the water management level. At the water management level, the proposed purge strategy determines the efficient strategy to mitigate water management faults, enhance voltage stability, and minimize hydrogen consumption based on the reference currents. The proposed integrated water management into the EMS is implemented in a HIL setup to evaluate its effectiveness. The results are compared with a water management approach that employs a non-adaptive purge strategy

recommended by the FC manufacturer for all current levels. This comparison aims to demonstrate the impact of integrating the proposed water management into the EMS on real FC performance, focusing on voltage stability, hydrogen consumption, and efficiency.

Chapter 2 - Importance of Multi-Stack FC System Operating Cost and Performance Comparison Between Single-Stack and Multi-Stack FC Systems

2.1 Introduction

The literature review in the previous section highlights the increasing use of multi-stack FC systems across various domains, such as vehicular applications. Despite the advantages of multi-stack FC systems, operating cost, as well as distributing optimal power between sub-stacks to increase FC longevity and reduce hydrogen consumption, remain key challenges in their commercialization. Therefore, the first objective of this stage is to design a reliable EMS consisting of a two-layer structure to control power distribution among sub-stacks and allocate optimal power between the FCs and the battery, with the aim of reducing total operating cost and increasing the longevity of the sub-stacks in the multi-stack system. On the other hand, many studies emphasize the potential and valuable advantages of multi-stack FC systems compared to single-stack systems, such as the ability to operate in degraded mode, high reliability and durability, and increased system efficiency. However, the literature reveals a lack of analysis on the impact of multi-stack FC system advantages on FC performance and operating cost. Therefore, the second objective of this stage is to evaluate the impact of multi-stack FC system advantages on FC performance and compare it with a single-stack FC system.

2.2 Paper 1: Operating Cost Comparison of a Single-Stack and a Multi-Stack Hybrid Fuel Cell Vehicle through an Online Hierarchical Strategy

Authors: Mohammadreza Moghadari, Mohsen Kandidayeni, Loïc Boulon, and Hicham Chaoui.

Journal: IEEE Transactions on Vehicular Technology.

Publication status: Published (12/09/2022).

2.2.1 Methodology

In the first step, this paper aims to design a reliable EMS for a multi-stack system to manage power distribution between sub-stacks and the battery, with the goal of reducing total operating cost. The second objective is to compare the multi-stack FC system (four Horizon 500-W FCs) with a single-stack FC system (Horizon 2000-W FC) in terms of hydrogen cost, FC degradation cost, system efficiency, and total cost. To achieve this, a hierarchical EMS, as shown in Figure 2-1, is developed for the multi-stack system. In the first layer, a rule-based strategy determines how many FCs should be activated based on requested power, SOC, and FC degradation rates. The purpose of the first layer is to activate the minimum number of FCs needed to meet the requested power, to reduce hydrogen consumption and minimize FC degradation. The FC or FCs with the lowest degradation rate are considered the youngest and are given the highest priority to participate in the second layer at each time step. The second layer employs ECMS to allocate optimal power between the FCs and the battery, meeting the requested power while minimizing the cost function. ECMS, as an OB-EMS, serves two key purposes: reducing total hydrogen consumption (FC and battery equivalent consumption) and minimizing FC

degradation. As this is a multi-objective problem, there is always a trade-off between different objectives. Since ECMS is a local optimization strategy, this paper uses DP as a global optimization strategy to validate the results. For the single-stack FC system, ECMS is also used to manage power distribution between the FC and the battery pack.

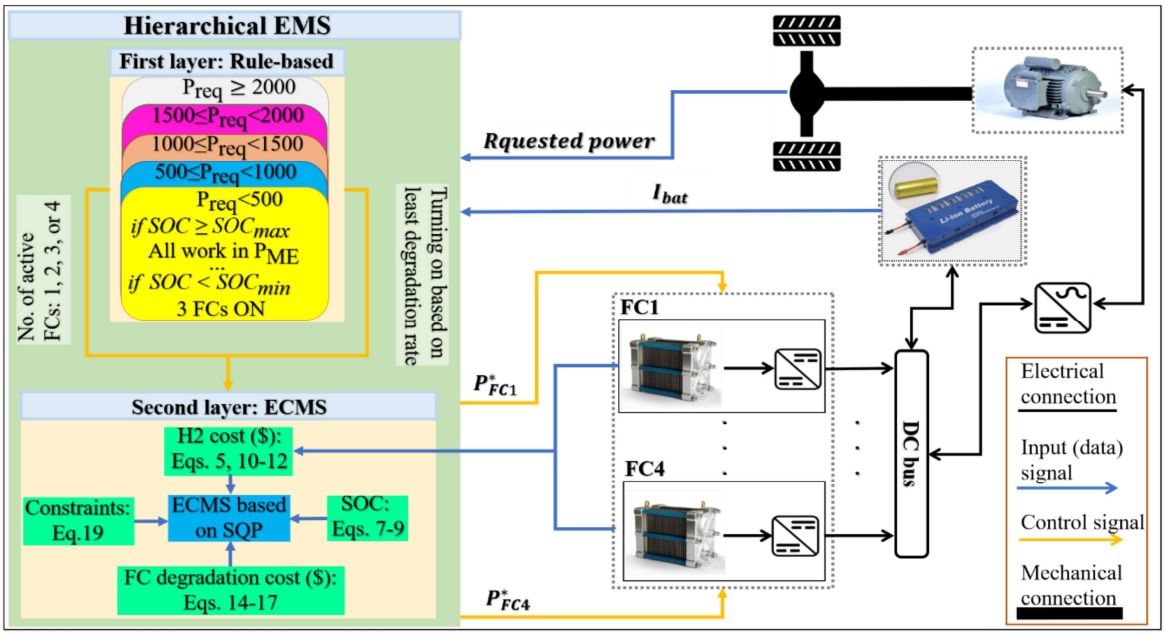

Figure 2-1- The proposed Hierarchical EMS conceptual framework.

2.2.2 Summary of the Results Analysis

The results of the single-stack and multi-stack FC systems are compared to determine which has a lower operating cost and is more suitable for real-world FC-HEV applications. Two different driving cycles, WLTC-class 3 and FTP-75 are used to test each system's performance in terms of hydrogen consumption, degradation, efficiency, and total operating cost. The results of both FC configurations under each driving cycle are compared with DP.

Figure 2-2 shows the operation of the single-stack and multi-stack FC systems in the safe zone under WLTC-class3 driving cycle, which is defined as the area between

maximum efficiency power and high load ($0.8\,P_{max}$) zones [28]. This figure clearly illustrates why the multi-stack FC system is more efficient than the single-stack FC system. As seen in Fig. Figure 2-2(a), 99.4% of the FC power in the multi-stack system operates within the safe zone throughout the driving cycle, while in the single-stack FC system (Figure 2-2(b)), this amount drops to 97%. The multi-stack FC system operates 2.4% more in the safe zone compared to the single-stack FC system, leading to lower operating cost.

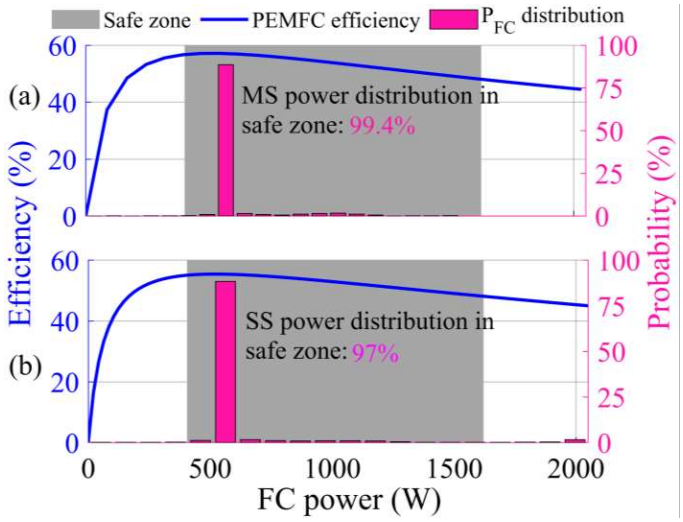

Figure 2-2- FC operating in the safe zone for the WLTC-class3 driving cycle: (a) Multi-stack; (b) Single-stack.

Figure 2-3 shows the operation of the single-stack and multi-stack FC systems in the safe zone under the FTP-75 driving cycle. As observed in the multi-stack FC system (Figure 2-3(a)), 97% of the FC power operates within the safe zone throughout the entire driving cycle, while in the single-stack FC system (Figure 2-3(b)), this amount decreases to 95.4%. The multi-stack FC system operates 1.6% more in the safe zone compared to the single-stack.

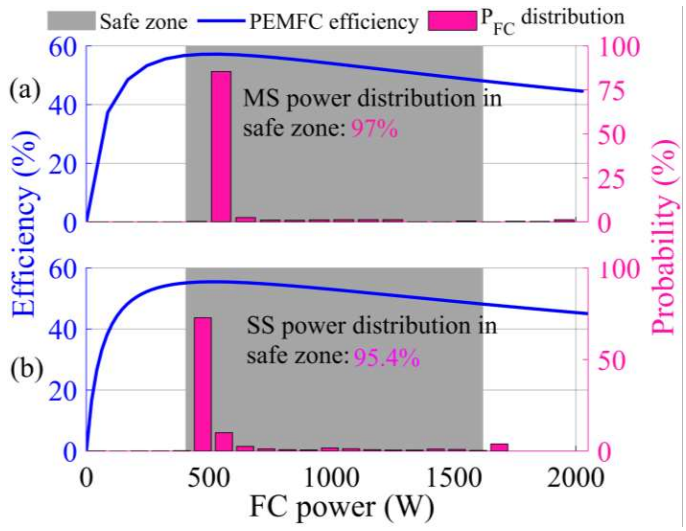

Figure 2-3- FC operating in the safe zone for the FTP-75 driving cycle: (a) Multi-stack; (b) Single-stack.

Table 2-1 presents a comprehensive comparison between the single-stack and multi-stack FC systems, evaluating hydrogen cost, degradation cost, and total operating cost under ECMS and DP. The results indicate that the multi-stack FC system is more efficient and economical than the single-stack FC system.

Table 2-1- Operating costs comparison.

Driving cycle	WLTC-class3				FTP-75			
EMS	DP		ECMS		DP		ECMS	
Configuration	SS	MS	SS	MS	SS	MS	SS	MS
H_2 cost (Cent)	5.860	5.673	6.400	6.153	6.716	6.514	7.040	6.850
Degradation cost (Cent)	0.011	0.006	0.046	0.010	0.019	0.012	0.074	0.051
Total cost (Cent)	5.870	5.680	6.445	6.163	6.735	6.530	7.114	6.900
	MS 3.2% less than SS		MS 4.4% less than SS		MS 3.0% less than SS		MS 3.0% less than SS	

Operating Cost Comparison of a Single-Stack and a Multi-Stack Hybrid Fuel Cell Vehicle Through an Online Hierarchical Strategy

Mohammadreza Moghadari, Mohsen Kandidayeni, *Member, IEEE*, Loïc Boulon, *Senior Member, IEEE*, and Hicham Chaoui, *Senior Member, IEEE*

***Abstract*—One of the recently suggested solutions for enhancing the fuel economy and lifetime in a fuel cell (FC) hybrid electric vehicle (HEV) is the use of a multi-stack (MS) structure for the FC system. However, to fully realize the potential of this structure, the design of an appropriate energy management strategy (EMS) is necessary. This paper aims to compare the operating cost, including hydrogen consumption and degradation of the FC, between a single-stack (SS) and an MSFC-HEV. To do so, a hierarchical EMS, composed of two layers, is devised for the MS system. In the first layer, a rule-based strategy determines how many FCs should be ON according to the requested power, battery state of charge (SOC), and FCs degradations. In the second layer, an equivalent consumption minimization strategy (ECMS) is developed to determine the output power of each activated FC according to the cost function and constraints. Regarding the SS structure, ECMS is employed for power distribution. The purpose of this strategy is to decrease fuel consumption and FC system degradation costs in both structures. The performance of the ECMS is compared with dynamic programming (DP) as a global optimization strategy for validation purposes. The obtained results using experimental data show that an FC-HEV with an MS structure reaches less hydrogen and degradation costs than an SS one.**

***Index Terms*—Energy management strategy, equivalent consumption minimization strategy, fuel cell degradation, fuel cell hybrid electric vehicle, multi-stack configuration.**

NOMENCLATURE

Symbols	*Definition*
P_{req}	Requested power.
F_r	Rolling friction of the tires.
F_{ad}	Force of aerodynamic resistance.
F_a	Acceleration force.
v	Vehicle velocity.
M	Total mass of the vehicle.
g	Gravitational acceleration.
θ	Slope of the road.
ρ_{air}	Air density.
c_d	Aerodynamic drag coefficient.
A_{ad}	Contact area of the vehicle's front surface.
η_{drive}	Efficiency of the driving line.
η_{em}	Efficiency of the electric motor.
η_{DC-AC}	Efficiency of the DC-AC inverter.
η_{DC-DC}	Efficiency of the DC-DC converter.
V	FC voltage.
I	FC current.
H_2	FC hydrogen consumption.
P_{FC}	FC power.
$b_1, b_2, b_3, b_4, b_5, a_1, a_1, a_3$	Fitting coefficients.
ΔV_{cell}	FC voltage degradation.
$\beta_{on/off}$	FC degradation rate of start-stop cycle.
β_{high}	FC degradation rate of High load.
β_{low}	FC degradation rate of low load.
β_{tran}	FC degradation rate of transition load.
$N_{on/off}$	Number of the start-stop cycle.
T_{high}	Duration of FC working under high load.
T_{low}	Duration of FC working under low load.
N_{tran}	Amount of load change.
I_{bat}	Battery current.
V_{oc}	Open-circuit voltage.
SOC	Battery state of charge.
R_{bat}	Battery internal resistance.
P_{bat}	Battery output power.
V_{bus}	Bus voltage.
η_{bat}	Coulombic efficiency.
Q_{bat}	Nominal battery capacity.
P_{ME}	FC power at maximum efficiency.
SOC_{max}	SOC maximum value.
SOC_{min}	SOC minimum value.
k	Time step.

Manuscript received 2 December 2021; revised 11 April 2022 and 19 July 2022; accepted 19 August 2022. Date of publication 12 September 2022; date of current version 16 January 2023. The review of this article was coordinated by Prof. Saeed Manshadi. *(Corresponding author: Mohammadreza Moghadari.)*

Mohammadreza Moghadari and Loïc Boulon are with the Hydrogen Research Institute, Electrical and Computer Engineering Department, Université du Québec à Trois-Rivières, Trois-Rivières, QC G8Z 4M3, Canada (e-mail: mohammadreza.moghadari@uqtr.ca; loic.boulon@uqtr.ca).

Mohsen Kandidayeni is with the e-TESC and IRH labs, Department of Electrical Engineering and Computer Engineering, University of Sherbrooke, Sherbrooke, QC J1K 2R1, Canada (e-mail: mohsen.kandidayeni@usherbrooke.ca).

Hicham Chaoui is with the Intelligent Robotic and Energy Systems (IRES) Research Group, Department of Electronics, Carleton University, Ottawa, ON K1S 5B6, Canada (e-mail: hicham.chaoui@carleton.ca).

Digital Object Identifier 10.1109/TVT.2022.3205879

0018-9545 © 2022 IEEE. Personal use is permitted, but republication/redistribution requires IEEE permission.
See https://www.ieee.org/publications/rights/index.html for more information.

Authorized licensed use limited to: Universite du Quebec a Trois-Rivieres. Downloaded on January 08,2025 at 21:44:39 UTC from IEEE Xplore. Restrictions apply.

C_{H_2}	Total hydrogen consumption.
$C_{H_2,FC}$	FC hydrogen consumption.
$C_{H_2,bat}$	Battery equivalent consumption.
α_{H_2}	Hydrogen price per kilogram.
$C_{H_2,FC,avg}$	Average FC hydrogen consumption.
$P_{FC,avg}$	Average FC power.
η_{chg}	Battery charging efficiency.
η_{dis}	Battery discharge efficiency.
$\eta_{chg,avg}$	Average charging efficiency of the battery.
$\eta_{dis,avg}$	Average discharge efficiency of the battery.
η_{bat}	Battery efficiency.
R_{dis}	Battery discharging resistance.
R_{chg}	Battery charging resistance.
C_{deg}	Cost of FC degradation.
$C_{on/off}$	Cost of start-stop cycle degradation.
C_{high}	Cost of high load degradation.
C_{low}	Cost of high load degradation.
C_{tran}	Cost of transition load degradation.
V_{EOL}	FC end of life voltage.
ζ_{stack}	Unit of FC stack price.
P_{rated}	FC rated power in kW.
N_{cell}	Number of cells in an FC stack.
Δt	Sampling period.
J_k	Total cost function.
$P_{FC,max}$	FC maximum power.
$P_{FC,min}$	FC minimum power.
$\Delta P_{FC,max}$	FC maximum fluctuation.
$\Delta P_{FC,min}$	FC minimum fluctuation.
$P_{bat,max}$	Battery maximum power.
$P_{bat,min}$	Battery minimum power.
x_k	State variable.
u_k	Control signal.
t_f	Final time of the driving cycle.
t_s	Sampling time.

I. Introduction

PROTON exchange membrane (PEM) fuel cell (FC) has been increasingly used in FC-hybrid electric vehicles (HEV) due to its high-power density, high efficiency, less noise, low operating pressure and temperature, and local-zero-emission [1]. Despite the valuable merits of an FC-HEV, some obstacles, such as hydrogen availability, the high price of components, and PEMFC reduced lifetime, have hindered its mass production compared with HEVs [2]. The US Department of Energy (DOE) has set a lifespan target of 5000 hours in a passenger vehicle for automotive PEMFCs [3]. Start-up/shutdown cycling, low-power operation, high-power operation, and fast load shifting cycles are all part of a typical automotive FC load profile. This kind of power demand on the FC stack might result in substantial reversible and permanent degradations, as well as hastened decay of the FC system [4]. As a result, it is critical to regulate the safe operation of the FC stack to a feasible extent. Using low-power FC stacks, known as a multi-stack (MS) FC system, instead of a single high-power FC stack can be considered a suitable solution to overcome some of the mentioned barriers [5], [6]. In comparison to the single-stack (SS) system, the MSFC performs well in terms of space flexibility, efficiency, and power level. In conventional FC-HEVs with one FC stack, the whole performance will change by a single FC failure. However, an MSFC can control this problem by its modularity [7], [8]. The modular design enables the failed stacks to be changed independently without affecting the overall electrical connection, hence enhancing the FC system's maintainability [9], [10]. Redundancy is one of the most important attributes of MSFC. This feature allows the whole system to continue working even in degraded mode by halting the power production of the faulty stacks. When the faulty stacks recover from unhealthy behavior, like flooding and drying out, they contribute to the overall system and begin to operate again [11]. Furthermore, the use of MSFC assists in the reduction of individual stack degradation as well as the system's overall stability [12]. The slow dynamic response is an intrinsic characteristic of an FC. To overcome this defect, using an energy storage system (ESS) like the battery alongside the FC is vital [13]. Besides, an ESS provides power peaks and regenerative energy, which helps the FC work in its efficiency range and decreases hydrogen consumption and degradation [14]. Efficient power distribution in a powertrain system with two or more power sources needs a suitable energy management strategy (EMS) as the heart of power control to ensure system drivability, fuel economy, emission reduction, and sustaining ESS state of charge (SOC) [15]. Generally, EMSs can be divided into rule-based and optimization-based approaches [16]. Optimization-based strategies are also divided into offline and online. One of the most well-known offline methods is dynamic programming (DP) which requires the driving cycle information in advance. DP is usually used as a benchmark for other optimization methods. Equivalent consumption minimization strategy (ECMS), model predictive control, and robust control are parts of online optimization strategies [17], [18], [19].

Due to the aforementioned benefits of the MSFC, the usage of such an architecture has been taken into consideration in different vehicular applications like passenger vehicles, heavy-duty, locomotives, and so forth, recently. On the other hand, the researchers endeavor to increase the potential, lifespan, and efficiency of the MSFC to exploit its advantages as much as possible. A hierarchical power distribution method for a dual-stack FC hybrid powertrain is suggested in [6]. This research also focuses on an online identification approach based on the forgetting factor recursive least square algorithm for updating the dual-PEMFC system's parameters in real-time. The experimental results show that the suggested strategy can improve the efficiency and performance of FC systems while lowering system fuel consumption. In [7], the authors introduce a self-adaptive EMS for an MSFC powertrain that takes into account the efficiency and health of dual-stack FC as well as overall trip costs to raise the FC's power level. The suggested EMS is projected to deal with the dynamic price fluctuations of different energy sources, lowering overall trip costs and

Authorized licensed use limited to: Universite du Quebec a Trois-Rivieres. Downloaded on January 08,2025 at 21:44:39 UTC from IEEE Xplore. Restrictions apply.

extending the dual-stack FC's lifespan. The "equivalent fitting circle" approach is presented as the control layer method in [8] for the system consisting of multiple FCs to tackle the energy distribution among sets of FCs with various characteristics. In comparison to other methods, the simulation results demonstrate good performance in terms of hydrogen consumption. To tackle a multi-objective power allocation strategy issue in MSFC, [9] introduces a novel decentralized convex optimization framework based on the auxiliary problem idea. To validate the benefits of the suggested method over existing centralized ones, various simulations and experimental validations are performed. In [10], a predictive soft loading approach with an enhanced overall efficiency maximization strategy is proposed for dual-stack FC systems to reduce the unfavorable loading situations that may degrade the sub-stacks. The authors of [11] suggest a bi-level optimization problem for the MSFC under constraints for stack allocation and power management. Finally, the solution findings are studied and assessed using different efficiency weights, application situations, efficiency, and Remaining Useful Life (RUL) features of accessible stacks as effect variables. In [12], an increment-oriented online power distribution strategy for MSFC is used to improve the collaboration between fuel economy and durability. In comparison to other advanced methodologies, the results show that the suggested approach can provide fault tolerance operation and collaborative performance improvement for MSFC. The authors of [20] design a power allocation method for the MSFC in order to lessen the performance gap between the FCs and prolong the system's lifespan. To execute the power distribution among four PEMFC stacks, the given approach uses the degree of performance degradation of stacks and the demand power. The results show that even if one of the stacks in the system fails unexpectedly, the MSFC can continue to function and allocate power. An online EMS for an MSFC hybrid electric vehicle is devised in [21] to improve fuel efficiency and the lifespan of the FC stacks. In this regard, a two-layer strategy for sharing power across four FCs and a battery pack is presented. The results of the proposed EMS point to a substantial increase in the system's overall performance. The study of [22] proposes a novel power distribution approach based on forgetting factor recursive least square online identification to fulfill the aim of minimizing the fuel consumption of an MSFC. The results show that the performance of the proposed power allocation strategy can be properly validated and it can provide satisfactory results.

According to the recent works on the MSFC system, one of the most significant issues in such systems is minimizing hydrogen consumption. In this respect, ECMS could be a practical choice among other online strategies since it has a viable ability to obtain optimal control quickly, which is necessary for real FC-HEVs [16], [18]. In recent years, many researchers have used ECMS to achieve the best fuel economy. In [23], ECMS is proposed for a hybrid tram where, compared to the operation mode switching method, it has saved hydrogen consumption up to 3.5%. The results indicate that the suggested EMS improves drivability and efficiency. In [24], the authors have shown that considering the maximum efficiency range in an ECMS can improve FC performance and fuel economy. In [25], an online adaptive ECMS based on power source degradation is proposed for a vehicle powered by an FC, battery, and supercapacitor. To achieve precise and reliable results of ECMS, the authors adjust the equivalent factor based on the state of health of FC and battery by using the degradation model. The authors in [26] employ SQP-based ECMS for a hybrid vehicle equipped with an FC, battery, and supercapacitor. This study shows that the proposed strategy can achieve better fuel economy compared with a rule-based control strategy.

Several advantages of MSFC systems have been documented in the literature, but the cost is still an open question. This cost could be divided between system cost and operating cost. This paper focuses on the operating cost. For this purpose, This paper puts forward a hierarchical EMS with two operating layers for an MSFC-HEV. The first layer of the strategy (rule-based) decides on the number of FCs that should be ON, and the second layer (optimization-based) is accountable for distributing the power among the active FCs and the battery pack by means of ECMS. The operating cost of the MS system, including hydrogen (FC and battery equivalent consumption), and FC degradation, is compared with an SS one. In this regard, DP is used as a benchmark to confirm the obtained results based on ECMS. From the conducted literature study, the novelties of this paper are:

1) Comparing the total operating cost (hydrogen and degradation costs) between an SS and an MSFC-HEV: prior research on MSFC lacks an analytical comparison of the operational costs between the two systems.
2) Designating the number of active FCs in the MS system by devising a hierarchical EMS: To achieve the lowest operational cost, this research proposes a hierarchical energy management strategy. Controlling hydrogen consumption and FC degradation in an MSFC system is largely reliant on how each FC operates. It is critical that FCs operate in a different way in order to reduce system operating costs. A rule-based layer is developed to decide how many FCs should participate in the multi-objective cost function at each time step depending on the requested power, battery SOC, and health state of each FC.
3) Taking into account FC degradation terms alongside hydrogen consumption for an MS configuration: The majority of ECMS articles concentrate on reducing hydrogen consumption without taking into account the cost of FC degradation.

The rest of this paper is organized as follows. Section II describes the vehicle modeling. EMS explanation is provided in Section III. Section IV discusses the achieved results, and the conclusion is given in Section V.

II. Modeling

A. Vehicle Structure and Powertrain Configuration

This paper investigates a hybrid powertrain with two different configurations: one is an SSFC, and another is an MSFC system. Fig. 1 displays the MS powertrain that utilizes four 500-W PEMFCs, as the primary power sources, with a battery pack. For the SS system, a 2000-W FC substitutes the four 500-W PEMFCs. Both configurations follow a semi-active principle where FCs are connected to the DC bus through unidirectional DC-DC

Authorized licensed use limited to: Universite du Quebec a Trois-Rivieres. Downloaded on January 08,2025 at 21:44:39 UTC from IEEE Xplore. Restrictions apply.

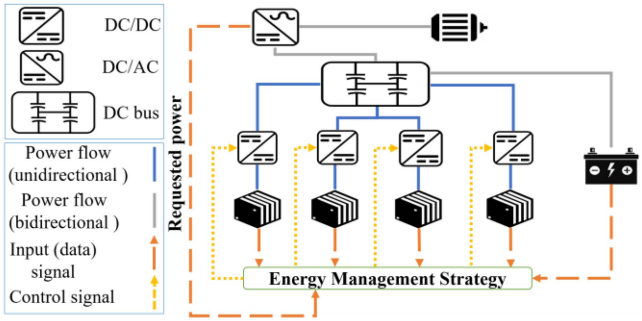

Fig. 1. Powertrain structure for the MS system.

TABLE I
VEHICLE SPECIFICATIONS

Parameters	Value
Coefficient of rolling friction c_r	0.015
The total mass of the vehicle M	896 kg
Gravitational acceleration g	9.81 m/s^2
The slope of the road θ	0°
Air density ρ_{air}	1.2 kg/m^3
Aerodynamic drag coefficient c_d	0.42
The contact area of the vehicle's front surface A_{ad}	4 m^2
Top speed	40 km/h

converters while the battery pack is linked to the bus directly without any converters [21], [24], [25], [26]. The requested power from the driving cycle (P_{req}) can be calculated by (1) based on longitudinal dynamics of a road vehicle:

$$P_{req} = v \;\; F_{req} = (F_r + F_{ad} + F_a)\, v \tag{1}$$

$$\begin{cases} F_r = c_r \; M \; g \; \cos(\theta) \\ F_{ad} = \frac{1}{2} \; \rho_{air} \; c_d A_{ad} \; v^2 \\ F_a = M \frac{dv(t)}{dt} \end{cases} \tag{2}$$

Where F_r is the rolling friction of the tires, F_{ad} is the force of aerodynamic resistance, F_a is the acceleration force, v is the vehicle speed . The FC-HEV that is employed in this paper is Nemo. Table I shows the vehicle's specifications [27].

The battery and the FC supply the requested power imposed by the driving cycle, and their power merge in the DC bus (P_{dc}) is given by (3).

$$\begin{aligned} P_{dc} &= P_{bat} + P_{FC} \; \eta_{DC-DC} \\ &= \begin{cases} \frac{P_{req}}{\eta_{drive} \; \eta_{em} \; \eta_{DC-AC}}, & P_{req} \geq 0 \\ P_{req}.(\eta_{drive} \; \eta_{em} \; \eta_{DC-AC}), & P_{req} < 0 \end{cases} \end{aligned} \tag{3}$$

Where $\eta_{drive}, \eta_{em}, \eta_{DC-AC}$ and, η_{DC-DC} are the efficiency of the driving line, electric motor, DC-AC inverter, and DC-DC converter, respectively.

B. Fuel Cell Model

As mentioned before, PEMFC is used as the primary power source. In this paper, two PEMFCs with different power rates but produced with the same technology are employed. As one of the goals of this study is to compare the operating cost of an SSFC-HEV with an MS one, it is vital to utilize the FCs with the same technology to avoid any confusion in the comprehension of the obtained results. The first FC is the Horizon 2000-W used in the SS configuration, and the second one is the Horizon 500-W employed in the MS structure. These FC technologies have been used in other studies as well [9], [21], [28], [29].

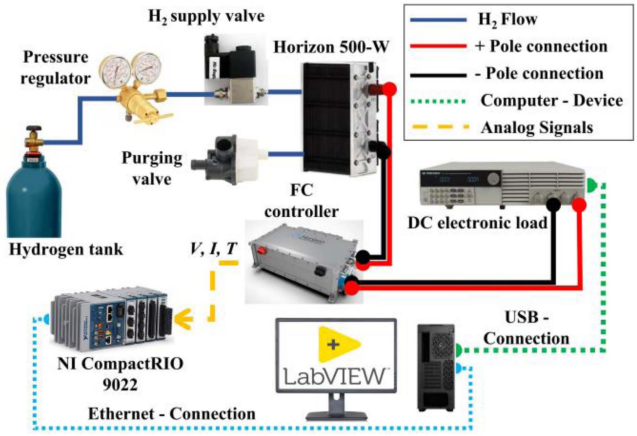

Fig. 2. The PEMFC test bench in the Hydrogen Research Institute of Université du Québec à Trois-Rivières (UQTR).

TABLE II
FUEL CELLS SPECIFICATION

FC technology / Characteristics	Horizon 2000-W (PEM)	Horizon 500-W (PEM)
Number of cells	48	24
Rated Power	2000 W	500 W
Voltage range	24-43 V	12-23 V
Maximum current	78 A	40 A
Weight (with fan & casing)	10 kg (±200grams)	2.52 kg (±50grams)

The curves of Horizon 2000-W and Horizon 500-W have been obtained from a developed test bench presented in Fig. 2. Both FCs are open cathode and air-cooled.

Due to the low-power nature of the application, the open cathode FC (air-cooled) is employed in this study. The vehicle under investigation is a low-speed vehicle with a maximum speed of 40 km/h. Open cathode FCs are suggested for this range of power applications [30].The main components of each FC include an FC stack and some auxiliaries, such as a cooling fan and hydrogen supply subsystem. Therefore, the net produced power of the FC system is equal to the difference between produced power from the stack (P_{stack}) and the used power from the auxiliary components (P_{aux}). The specification of each FC system is listed in Table II. The presented set-up in Fig. 2 has been developed in Hydrogen Research Institute of Université du Québec à Trois-Rivières (UQTR). This figure shows that a Horizon 500-W is connected to a National Instrument CompactRIO using the PEMFC controller. For an SS system, the Horizon 2000-W is substituted for 500-W in the test bench. The pressure of hydrogen is set between 0.5 and 0.6 bar. The hydrogen supply valve, located on the anode side, provides dry hydrogen for the PEMFC stack, and its flow rate is between 0 and 7 $\frac{l}{min}$ according to the drawn power from the stack. On the anode outlet, the purge valve is responsible for removing excess hydrogen, water, and

Authorized licensed use limited to: Universite du Quebec a Trois-Rivieres. Downloaded on January 08,2025 at 21:44:39 UTC from IEEE Xplore. Restrictions apply.

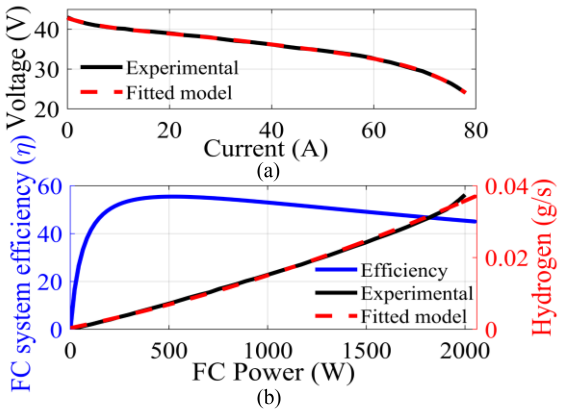

Fig. 3. The characteristic curves of the Horizon 2000-W: (a) polarization curve; (b) hydrogen consumption and efficiency curve.

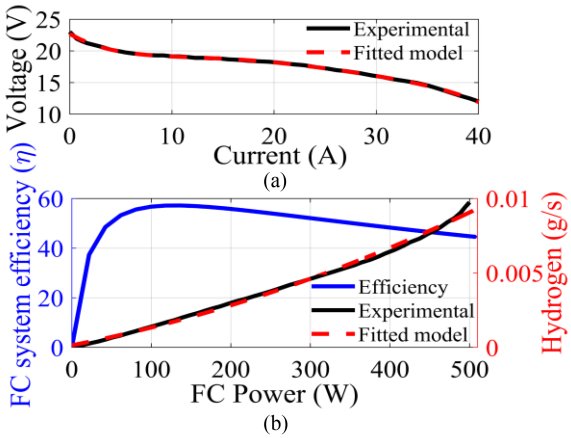

Fig. 4. The characteristic curves of the Horizon 500-W: (a) polarization curve; (b) hydrogen consumption and efficiency curve.

nitrogen every 10 s with a duration of 100 ms. An Ethernet connection transfers the data between the CompactRIO and the PC every 100 ms, then FC system voltage, current, and temperature are recorded. For requesting load profiles from the PEMFC, an 8514 BK Precision DC Electronic Load is utilized.

Fig. 3 shows the polarization, hydrogen consumption, and FC system efficiency curves of the Horizon 2000-W PEMFC, where the solid black lines are the experimental reference curves, and the red dashed lines illustrate the fitted models. Fig. 4 displays the polarization, hydrogen consumption, and FC system efficiency curves of Horizon 500-W.

The fitted polarization and hydrogen consumption models are a polynomial function of current and FC power, as shown in (4)-(5).

$$V\ (I) = b_1\ I^4 + b_2 I^3 + b_3 I^2 + b_4 I + b_5 \tag{4}$$

$$H_2\ (P_{FC}) = a_1\ P_{FC}^2 + a_2 P_{FC} + a_3 \tag{5}$$

The values of all the coefficients in (4)-(5) for Horizon 2000-W and Horizon 500-W are introduced in Table III.

FC degradation is a natural and inevitable phenomenon that can lead to voltage decrease and performance loss. Choosing and designing a suitable EMS has a crucial role in slowing down

TABLE III
COEFFICIENT VALUES OF (4)-(5)

Equation (4)		
Coefficients (unit)	Values	
$b_1(\frac{V}{A^4})$, $b_2(\frac{V}{A^3})$, $b_3(\frac{V}{A^2})$, $b_4(\frac{V}{A})$, $b_5(V)$	FC 2000-W	FC 500-W
	-7.8×10^{-7}, 4.934×10^{-5}, 5.832×10^{-4}, -0.207, 42.41	1.353×10^{-5}, -0.001, 0.046, -0.663, 22.390
Equation (5)		
Coefficients (unit)	Values	
	FC 2000-W	FC 500-W
$a_1(\frac{g}{W^2})$, $a_1(\frac{g}{W})$, $a_3(g)$	3.050×10^{-9}, 1.190×10^{-5}, 8.253×10^{-4}	1.470×10^{-8}, 1.080×10^{-5}, 2.450×10^{-4}

the FC degradation and increasing its lifetime by avoiding the operation in high and low power for an extended period and decreasing high and frequent transition loads [31]. Each component of a PEMFC has its degradation mechanism, so focusing on the degradation of the component level and its relation and effects on the other components cannot be covered and are hard to reach. Therefore, the FC degradation modeling is normally considered at the stack level [32]. The rate of degradation will change based on the FC technology used, as well as the operating conditions. In fact, developing a comprehensive degradation model for an FC system is still an area of investigation [32], [33].

According to the above descriptions, four operating conditions of PEMFC are known as primary degradation factors. These four operating conditions are start-stop cycle, high load, low load, and transition load [32], [34], [35]. The start-stop cycle, which is the FC on/off, has a predominant and adverse effect on voltage degradation, and it can decrease FC voltage enormously [34], [36]. For other factors of degradation, high loading is described as when $P_{FC} \geq 0.8\ P_{FC,max}$ and low loading is defined as when $P_{FC} \leq 0.2\ P_{FC,max}$. In Horizon 500-W and 2000-W, $P_{FC,max}$ are 500 W and 2000 W, respectively. The transition load is considered as the absolute value changes of the FC output power [34], [35], [36]. Equation (6) illustrates the total voltage degradation (μV) of a cell [34], [35], [36]:

$$\Delta\ V_{cell} = \beta_{on/off}\ N_{on/off} + \beta_{high}\ \frac{T_{high}}{3600} + \beta_{low}\ \frac{T_{low}}{3600} + \beta_{tran}\ N_{tran} \tag{6}$$

Where β_{high}, β_{low}, $\beta_{on/off}$, and β_{tran} are the degradation of voltage cell rate per hour $\left(\frac{\mu V}{h}\right)$, per cycle $\left(\frac{\mu V}{cycle}\right)$, and per kilowatt $\left(\frac{\mu V}{kW}\right)$ for each high load, low load, start-stop cycle, and transition load, respectively. The degradation rates are listed in Table IV. $N_{on/off}$ denotes the number of the start-stop cycle during a driving cycle, T_{high}, and T_{low} are the duration that FC works under high and low load (in second), and $N_{tran} = |\Delta P_{FC}| = P_{FC}\ (t) - P_{FC}(t-1)$ is the amount of load change. It is worth noting that $|\Delta P_{FC}|$ refers to the absolute change in FC power between two consequent points. To clarify, $|\Delta P_{FC}|$ is defined as the difference in the FC power of time steps *t* and *t-1* during the driving cycle. In each time step in the simulation, ΔV_{cell} is deducted from the FC voltage. The

Authorized licensed use limited to: Universite du Quebec a Trois-Rivieres. Downloaded on January 08,2025 at 21:44:39 UTC from IEEE Xplore. Restrictions apply.

TABLE IV
THE RATE OF PEMFC DEGRADATION (CELL LEVEL)

Operating condition	Degradation rate	Data reference
Strat-stop cycle ($\beta_{on/off}$)	13.79 $\frac{\mu V}{cycle}$	[34], [35], [37]
High load (β_{high})	10.00 $\frac{\mu V}{h}$	[34], [35], [37]
Low load (β_{low})	8.66 $\frac{\mu V}{h}$	[34], [35], [37]
Transition load (β_{tran})	0.0441 $\frac{\mu V}{kW}$	[34], [35], [37]

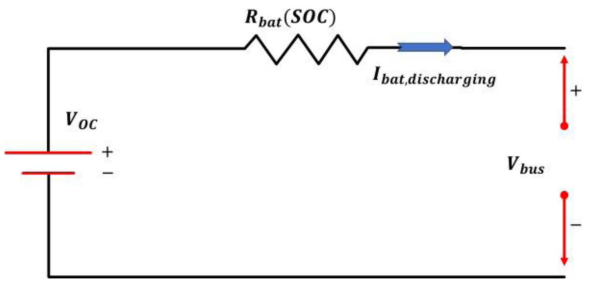

Fig. 5. Equivalent circuit of the battery model [29].

TABLE V
SPECIFICATION OF THE BATTERY

SAFT Rechargeable lithium-ion battery cell	
Capacity	6 Ah
Maximum current continuous	C/1 A
Nominal voltage	3.65 V
Number of cells in series	20
Coulombic efficiency	0.99
Cell mass	0.34 kg

accuracy of the degradation model is not the main focus of this study. The major emphasis is on the strategy's performance when the FCs degrade. The employed degradation model to evaluate the strategy's performance has been used in a number of papers [9], [34], [35], [37].

C. Battery Model

As mentioned earlier, an ESS in an FC-HEV is necessary to assist FC with operating in its efficient zone and decrease the degradation by absorbing peak powers and supplying low powers of the driving cycle [36]. Therefore, in this paper, a lithium-ion battery is employed as an ESS. For modeling the battery, this paper uses the internal resistance-based model [29]. Fig. 5 illustrates the equivalent circuit of the battery model. The features of the battery are listed in Table V.

It is important to note that the battery current (I_{bat}) flows in a positive direction while the battery is discharging and in a negative direction when it is charged. The relation of open-circuit voltage and internal resistance with battery SOC is presented in Fig. 6. The utilized battery data have been extracted from experimental tests performed by the National Renewable Energy Laboratory [29]. Equations (7), (8), and (9) show the battery

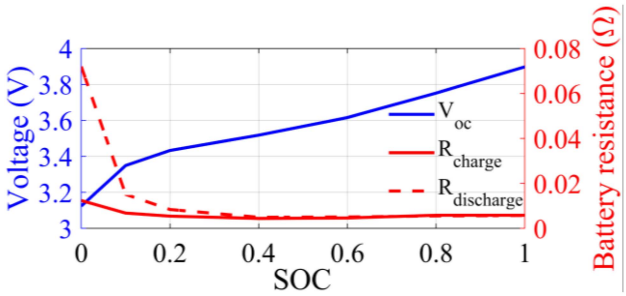

Fig. 6. The correlation of SOC with battery open-circuit voltage and resistance.

current (I_{bat}), bus voltage (V_{bus}), and SOC.

$$I_{bat} = \frac{V_{oc} - \sqrt{V_{oc}^2\,(SOC) - 4\,R_{bat}\,(SOC)\;P_{bat}}}{2\,R_{bat}\,(SOC)} \tag{7}$$

$$V_{bus} = V_{oc}\;(SOC) - I_{bat}\,R_{bat} \tag{8}$$

$$SOC\;(t) = SOC\,(t_0) - \eta_{bat}\,\frac{\int_{t_0}^{t} I_{bat}\,dt}{Q_{bat}} \tag{9}$$

Where $P_{bat} = I_{bat}\;\;V_{bus}$, V_{oc} and R_{bat} are the open-circuit voltage and battery internal resistance and can be expressed as a function of SOC. P_{bat} is the battery output power, Q_{bat} is the nominal battery capacity (Ah), and η_{bat} is the Coulombic efficiency.

III. ENERGY MANAGEMENT STRATEGY

The primary purpose of this paper is to compare operating costs, including hydrogen cost, FC degradation cost, and total cost between the SS (Horizon 2000-W) and the MSFC system (four Horizon 500-W). In this regard, a hierarchical EMS, as shown in Fig. 7, is developed for the MS system. In the first layer, a rule-based strategy is used to determine how many FCs should be ON according to the requested power, SOC, and FCs degradation rate. The second layer employs ECMS to determine the output power of each FC to satisfy the requested power while minimizing the defined cost function. ECMS as an optimization-based EMS is used for two principal purposes: reducing the total hydrogen consumption (FC and battery equivalent consumption) and FC degradation. Regarding the battery pack, the necessary constraints are considered to enhance its lifetime. Obviously, such problems are known as multi-objective problems, and there is always a trade-off between different purposes. Since ECMS is a local optimization strategy, this paper uses DP as a global optimization strategy to validate the achieved results. Regarding the SS configuration, ECMS is utilized to distribute the power between the FC and the battery pack.

A. First Layer: Rule-Based

In the first layer of this hierarchical EMS, a rule-based strategy determines the number of FCs that should participate in the

Authorized licensed use limited to: Universite du Quebec a Trois-Rivieres. Downloaded on January 08,2025 at 21:44:39 UTC from IEEE Xplore. Restrictions apply.

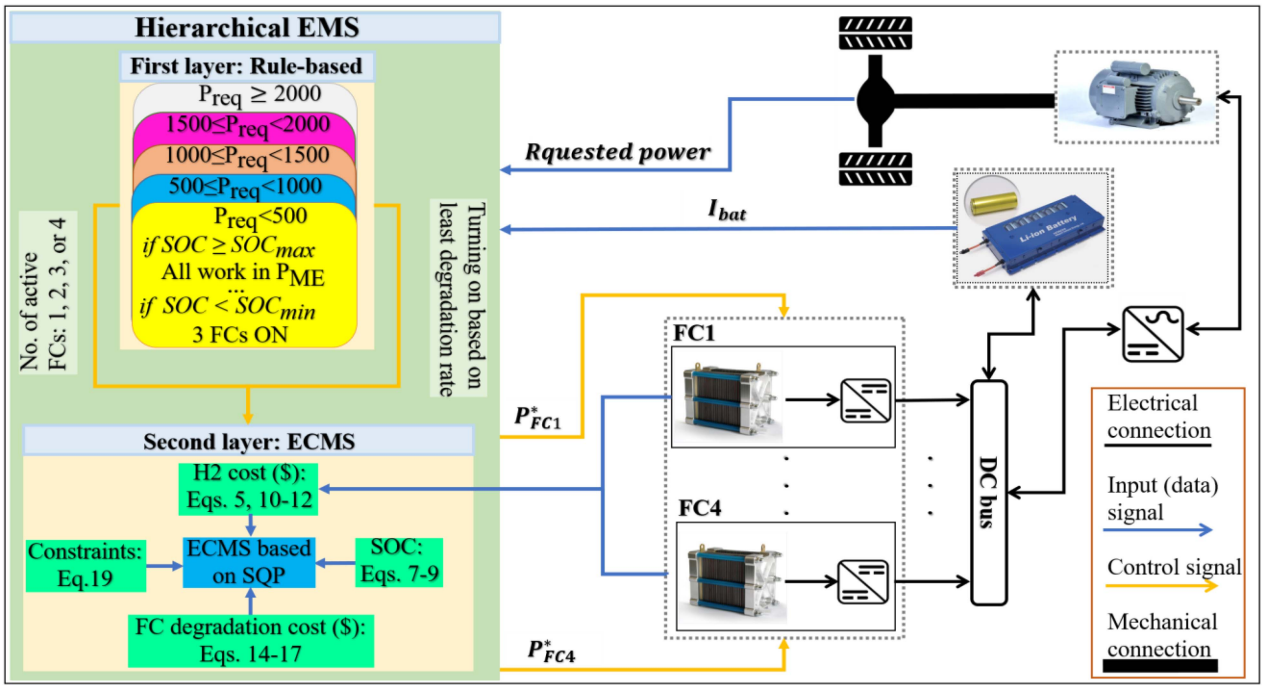

Fig. 7. The concept of the proposed hierarchical EMS.

optimization problem based on the requested power, SOC, and FCs degradation rate. The primary purpose of this strategy is to activate the minimum number of FCs to meet the requested power considering the age and other constraints. In each step, the voltage drop from previous times is collected until the current time step and then subtracted from the FC voltage (equation (4)). The output power of the FC is lowered by decreasing the voltage in each step according to the circumstances in which each FC operates. As a result, the FC or FCs with the lowest voltage drop or greatest maximum power are regarded the youngest FCs and have the highest priority to participate in the optimization algorithm at each time step. For instance, if two FCs are adequate to provide the requested power, the two least degraded FCs will be ON, and the other two that are most degraded operate at their maximum efficiency point (P_{ME}). FC ON means that it can operate between minimum power and maximum power in its whole domain. This strategy aims to prevent the most degraded FCs from more degradation. The most degraded FCs will not be OFF because start-stop cycles increase the degradation dramatically. The reason for working at the maximum efficiency point is that at this point, the hydrogen consumption is minimal, and the degradation rate is mild as it is between high load and low load limitation.

Table VI shows the rules of this strategy. The maximum and minimum values of SOC are 90% and 50%, respectively.

TABLE VI
RULE-BASED STRATEGY

Conditions \ P_{req}	Range of P_{req} (kW)				
	<0.5	0.5–1	1–1.5	1.5–2	>2
	Number of active FCs				
SOC≥SOC$_{max}$	All P_{ME}	All P_{ME}	1 FC	2 FCs	3 FCs
80%≤SOC<SOC$_{max}$	All P_{ME}	All P_{ME}	1 FC	2 FCs	3 FCs
70%≤SOC<80%	1 FC	1 FC	2 FCs	3 FCs	3 FCs
60%≤SOC<70%	2 FCs	2 FCs	3 FCs	3 FCs	4 FCs
SOC$_{min}$≤SOC<60%	2 FCs	3 FCs	4 FCs	4 FCs	4 FCs
SOC<SOC$_{min}$	3 FCs	4 FCs	4 FCs	4 FCs	4 FCs

B. Second Layer: Equivalent Consumption Minimization Strategy

In the second layer, ECMS is utilized as an optimization algorithm to designate the output power of each FC activated in the first layer.

The output power of each FC is determined so that the minimum value of the cost function is obtained. The concept of ECMS is to convert electrical energy from ESS to the equivalent hydrogen consumption to minimize the total hydrogen consumption of the system [23], [24], [25], [26], [38]. In this paper, alongside the cost of hydrogen consumption, FC degradation is added to the cost function. Indeed, in this problem, the optimization algorithm chooses its optimal control decision by minimizing the total cost of the cost function. Therefore, the cost function is introduced in two parts: the definition of hydrogen consumption cost and FC degradation. SQP algorithm is one of the powerful methods to solve constrained nonlinear optimization problems. SQP uses a series of quadratic programming sub-problems to reach a minimum value of a cost function [24], [25], [26], [34], [39]. Indeed, in this paper, SQP solves the ECMS by finding a suitable FC power as a control variable to minimize the cost function. The SQP is programmed in MATLAB to solve the ECMS problem in real-time.

1) Multi-Objective Cost Function: According to the concept of ECMS, the total hydrogen consumption is the sum of the

Authorized licensed use limited to: Universite du Quebec a Trois-Rivieres. Downloaded on January 08,2025 at 21:44:39 UTC from IEEE Xplore. Restrictions apply.

hydrogen consumption on the FC side and the equivalent hydrogen consumption on the battery side. Equation (10) describes the hydrogen consumption cost in the multi-objective cost function. The required units for the following equations are introduced in the parentheses.

$$C_{H_2,k} = \left(C_{H_2,FC,k} + C_{H_2,bat,k}\right) \alpha_{H_2} \ (\$) \tag{10}$$

Where $C_{H_2,FC,k}$ is the FC hydrogen consumption over the time step k that is a polynomial function of FC output power according to (5). The battery equivalent consumption is a function of FC average hydrogen consumption, FC average power, battery power, and battery charge and discharge efficiencies as explained in (11). α_{H_2} is the hydrogen price per kilogram, so the hydrogen consumption must be in kg.

$$C_{H_2,bat,k} = \begin{cases} \frac{P_{bat,k}}{\eta_{chg,avg}\ \eta_{dis}} \ \frac{C_{H_2,FC,avg}}{P_{FC,avg}} \ (g), & P_{bat} \geq 0 \\ P_{bat,k}\ \eta_{dis,avg}\ \eta_{chg} \ \frac{C_{H_2,FC,avg}}{P_{FC,avg}} \ (g), & P_{bat} < 0 \end{cases} \tag{11}$$

In the above equation, $C_{H_2,FC,avg}$ is the average FC hydrogen consumption, $P_{FC,avg}$ is the average FC power, $P_{bat,k}$ is the battery power over the time step k . η_{dis} is the battery discharge efficiency, $\eta_{chg,avg}$ is the average charging efficiency of the battery, η_{chg} is the charging efficiency of the battery, and $\eta_{dis,avg}$ is the battery average discharge efficiency. The battery charge and discharge efficiencies are derived from (12):

$$\eta_{bat} = \begin{cases} \frac{1}{2}\left(1 + \sqrt{1 - \frac{4\ R_{dis}\ P_{bat}}{V_{oc}^2}}\right), & P_{bat} \geq 0 \\ \frac{2}{\left(1 + \sqrt{1 - \frac{4\ R_{chg}\ P_{bat}}{V_{oc}^2}}\right)}, & P_{bat} < 0 \end{cases} \tag{12}$$

Where R_{dis} is the battery discharging resistance, and R_{chg} is the battery charging resistance, and V_{oc} is the battery open-circuit voltage. According to (11)-(12), in discharge mode, η_{dis} and the battery recharge efficiency by the FC system ($\eta_{chg,avg}$) are taken into consideration for calculating the battery power. However, in the charging mode, P_{bat} is weighted by η_{chg} and whether the battery has previously been discharged ($\eta_{dis,avg}$). Aside from the cost of hydrogen consumption, this paper considers the degradation cost consisting of start-stop, high load, low load, and transition load. Equation (13) shows the degradation cost.

$$C_{deg,k} = C_{on/off,k} + C_{high,k} + C_{low,k} + C_{tran,k} \tag{13}$$

Where $C_{on/off}$ is the cost of start-stop cycle degradation that can be calculated as the following equation:

$$C_{on/off,k} = \frac{\beta_{on/off}\ N_{on/off,k}}{V_{EOL}} \ \zeta_{stack}\ P_{rated} \ (\$) \tag{14}$$

Where $N_{on/off,k}$ is the number of start-stop cycles over the time step of k, V_{EOL} is the voltage drop until a single PEMFC end of life which is a 10% decrease in the FC voltage. A cell approaches the end of its life when the cell voltage of an FC decreases to 10% of its nominal voltage, according to the literature study [34], [35], [37]. ζ_{stack} is the unit of FC stack price, and P_{rated} is FC rated power (in kW). The degradation cost caused by the high and low load can be described in (15) and (16):

TABLE VII
OPERATING COST PARAMETERS

Parameter	Value	Unit	Data reference
PEMFC stack price (ζ_{stack})	93.00	\$/kW	[34], [35]
P_{rated}	2 and 0.5	kW	[34], [35]
Hydrogen price (α_{H_2})	4.00	\$/kg	[34], [35]
V_{EOL}	60000	μV	[34], [35]

$$C_{high,k} = \frac{\beta_{high}\frac{T_{high,k}}{3600}}{V_{EOL}} \ \zeta_{stack}\ P_{rated} \ (\$) \tag{15}$$

$$C_{low,k} = \frac{\beta_{low}\frac{T_{low,k}}{3600}}{V_{EOL}} \ \zeta_{stack}\ P_{rated} \ (\$) \tag{16}$$

Where $T_{high,k}$, and $T_{low,k}$ are the duration of the high and low load over the time step of k. The index k determines each time step, which lasts one second. To reduce FC degradation and overall operating cost, the optimization method seeks to prevent FCs from working at their high and low loads at each time step. The values of $T_{high,k}$, and $T_{low,k}$ will be 1 if FC operates in its high or low load, in time step k, since the FC works for one second in these loads. The last part of the degradation cost is related to the transition load cost shown in (17).

$$C_{tran,k} = \frac{\beta_{tran}\ \left(\left|P_{FC}\left(k\right) - P_{FC}\left(k-1\right)\right|\right)\ \Delta t}{V_{EOL}\ N_{cell}} \ \zeta_{stack}\ P_{rated} \ (\$) \tag{17}$$

Where N_{cell} is the number of cells in a stack, and Δt is the sampling period which equals 1 second.

Finally, the total cost function can be written as (18):

$$J_k = C_{H_2,k} + C_{deg,k} = \left(C_{H_2,FC,k} + C_{H_2,bat,k}\right) \alpha_{H_2} + C_{on/off,k} + C_{high,k} + C_{low,k} + C_{tran,k} \tag{18}$$

Regarding the cost function of the MS, each stack has a degradation cost and a hydrogen cost; therefore, the final operating cost will be the sum of the four FC stacks. The values of hydrogen consumption and unit of FC stack price are provided in Table VII.

2) Constraints: In an optimization problem, various constraints are vital to ensure that the powertrain components work in normal conditions and the optimal control decision is acceptable. Reactant flows, heat management, and water content in the streams and inside the FC all influence the PEMFC dynamic reaction, and they need to be controlled for the optimum operation of FCs when the system experiences varying load changes [40]. Generally, a dynamic load fluctuation cycle is defined by a sudden change from low current to maximum current in degradation tests [37]. However, in the energy management design, a conservative transition is usually considered. In this work, a dynamic limitation of 50 W/s and 200 W/s, which implies 10% of the maximum power per second is considered for the operation of the FCs [41], [42], [43]. For these reasons, several constraints must be applied to the FC and battery. Equation (19) shows these

Authorized licensed use limited to: Universite du Quebec a Trois-Rivieres. Downloaded on January 08,2025 at 21:44:39 UTC from IEEE Xplore. Restrictions apply.

TABLE VIII
VALUES OF CONSTRAINT PARAMETERS

Parameter	Value		Unit
	FC 2000-W	FC 500-W	
$P_{FC,min}$, $P_{FC,max}$	0, 2000	0, 500	Watt
$\Delta P_{FC,min}$, $\Delta P_{FC,max}$	-200, 200	-50, 50	Watt
SOC_{int}, SOC_{min}, SOC_{max}	70%, 50%, 90%		%
$P_{bat,min}$, $P_{bat,max}$	-1000, 1000		Watt

constraints.

$$\begin{cases} P_{FC,min} \le P_{FC,k} \le P_{FC,max} \\ \Delta P_{FC,min} \le P_{FC}(k) - P_{FC}(k-1) \le \Delta P_{FC,max} \\ SOC_{min} \le SOC(k) \le SOC_{max} \\ P_{bat,min} \le P_{bat,k} \le P_{bat,max} \end{cases} \tag{19}$$

All the parameters in the mentioned constraints are shown in Table VIII.

C. Dynamic Programming (DP)

As explained in the previous parts, DP is one of the most well-known benchmarks in optimization problems. The essence of DP is that it is aware of what happens in the future to choose the best optimal control decision. One of the weaknesses of DP is that it cannot be used in real-time problems because it needs complete driving cycle information in advance and is highly time-consuming. DP is a good choice for solving a wide range of optimization problems like nonlinear, constrained, time-variant, and discrete-time [44]. According to the pros and cons of DP, this method is a suitable criterion to validate the results of local optimization methods like ECMS. This paper utilizes the MATLAB function introduced in [44] to solve this problem with the DP algorithm. In the DP, the first step is to determine the state and control variables. In this paper, SOC is considered as the state variable (x_k) and FC power is considered as the control signal (u_k). The next step is to discretize the continuous-time model to the discrete-time model, as shown in (20).

$$\begin{cases} x_{k+1} = F(x_k, u_k) + x_k, \ k = 01, \ldots, N-1 \\ x_k = SOC \\ u_k = P_{FC} \\ N = \frac{t_f}{t_s} + 1 \end{cases} \tag{20}$$

Where t_f is the final time of the driving cycle and t_s is the sampling time. For the MS problem, DP has four control signals as four FCs exist in this configuration. A cost function like ECMS aims to minimize operating costs by reducing hydrogen consumption and degradation costs. Concerning the constraints, the same ones defined for ECMS are used in the DP problem. According to the following objective function, by the trade-off between hydrogen consumption and FC degradation, the best values of FC power as the control variable are chosen to minimize the total operating cost.

$$J = \min \sum_{k=0}^{N-1} \left(C_{H_2}(P_{FC,k}, k) + C_{deg}(P_{FC,k}, k) \right) \tag{21}$$

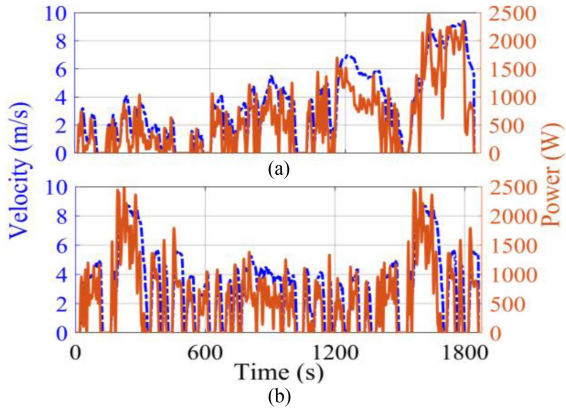

Fig. 8. Driving cycles: (a) WLTC-class3; (b) FTP-75.

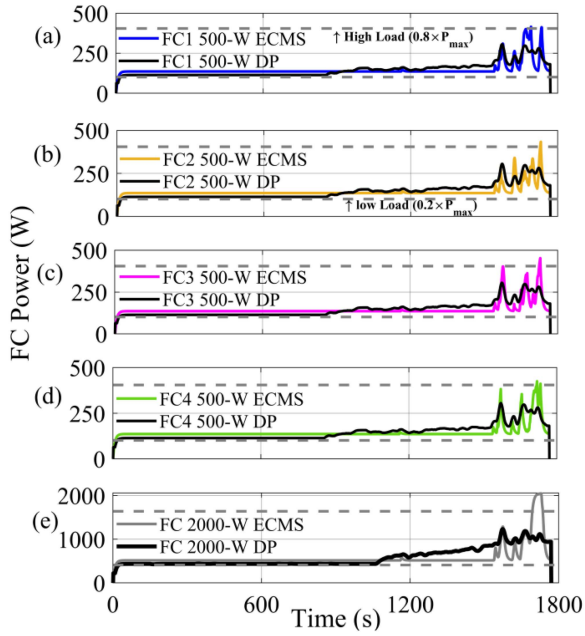

Fig. 9. Comparison of FCs power distribution for the WLTC-class3 driving cycle: (a-d) MS; (e) SS.

IV. RESULT AND DISCUSSION

In this section, the SS and the MS system results are compared to illustrate which one has a lower operating cost and is more reasonable to be used in a real FC-HEV. For this purpose, two different driving cycles, WLTC-class3 and FTP-75, are employed to test the performance of each case study in terms of hydrogen consumption, degradation, and total costs. The results of the two FC configurations under each driving cycle are compared with DP to illustrate the validation of the proposed EMS. The utilized driving cycles are shown in Fig. 8, where the right vertical axis shows the power (W), and the left one shows the velocity (m/s).

A. Obtained Results Under WLTC-Class3 Driving Cycle

Fig. 9 shows the comparison of FC power distribution between the SS and the MS for the WLTC-class3. Fig. 9(a-d) and Fig. 9(e) illustrate the FC power distribution of the MS and SS structures using DP and ECMS, where colored lines and black lines display

Authorized licensed use limited to: Universite du Quebec a Trois-Rivieres. Downloaded on January 08,2025 at 21:44:39 UTC from IEEE Xplore. Restrictions apply.

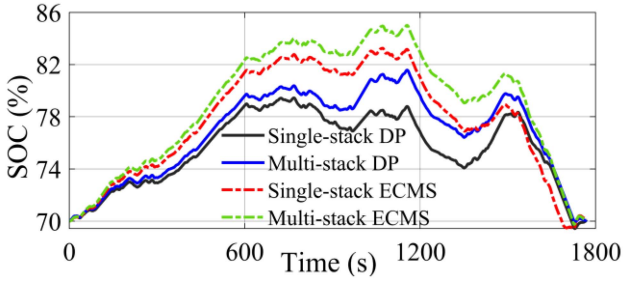

Fig. 10. Battery SOC comparison for the WLTC-class3 driving cycle.

the power distribution for ECMS and DP, respectively. As shown in Fig. 9(a)–(d), to lower the overall cost of the system, the optimization algorithm prefers to utilize the battery over FCs in the period 0–1550s. Due to the high cost of an ON/OFF cycle, the optimization algorithm prefers not to switch off FCs. Each ON/OFF cycle greatly raises the system's cost.

As a result, the ECMS algorithm selects the ideal operating point to decrease hydrogen consumption and FC degradation while lowering overall cost. The ECMS approach prefers that each FC operates at its maximum efficiency point between 0 and 1550 seconds since, during this period, each FC not only avoids the ON/OFF cycle but also has the best fuel economy.

DP shows the same tendency in the FC power distribution. The driving cycle has high velocities within 1551–1800s time range. Therefore, FCs should work at a higher power level during this time since the requested power has increased. Indeed, it is at this time that FCs begin to operate differently. Working differently allows each FC to consume less hydrogen and degrade less than the SS system.

The mentioned explanations are true for the SS system. As shown in Fig. 9(e), the SS system works more time in the high load zone because it does not have the modularity and flexibility of the MS system. According to the feature of DP that is aware of what happens in the future in advance, it reduces FC degradation cost more than ECMS, and FCs work less in the high load zone in the DP algorithm in comparison with ECMS.

Fig. 10 describes the battery SOC regarding the SS and the MS configurations using ECMS and DP algorithms. Although the EMS chooses to make the battery work harder than FC in the 0–1550s, SOC rises in certain time intervals since the driving cycle consists of low and medium velocities and the requested power is not high. Because the driving cycle throughout the 1551–1800s includes high velocities and high requested power, the battery should work harder alongside the FCs. As a result, the SOC drops more during this period. The most significant aspect is that the SOC in the MS system, SS system, and DP algorithm should all end at the same point in order to compare them fairly. To guarantee that all these algorithms achieve the same final SOC, the final SOC related to SS is imposed on the SOC of MS and the DP algorithm as a terminal SOC. Since DP tries to reach a minimum cost at the end of the cycle while ECMS minimizes the cost function at each time step, the SOC trend between DP and ECMS is different.

Fig. 11 represents the operation of the SS and MS systems in the safe zone. The safe zone is an area between the power of

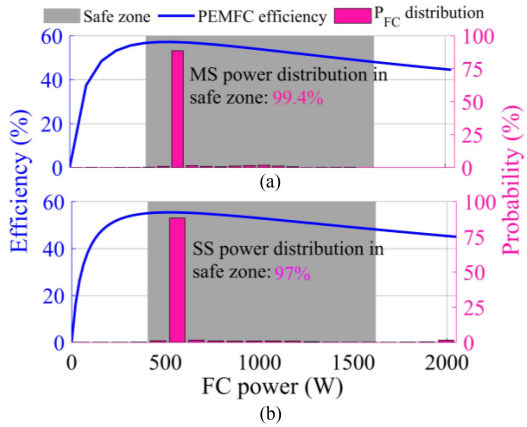

Fig. 11. FC operating in the safe zone for the WLTC-class3 driving cycle: (a) MS; (b) SS.

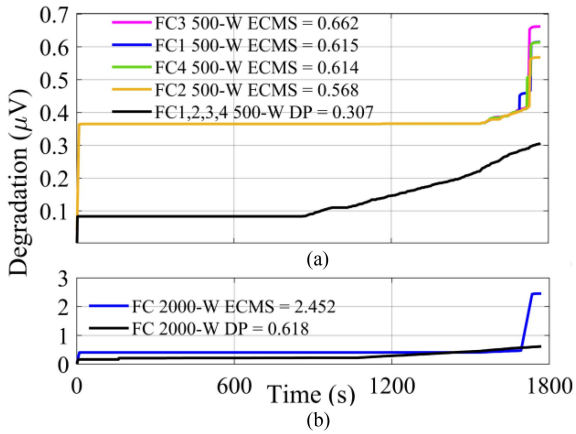

Fig. 12. FC voltage degradation for the WLTC-class3 driving cycle: (a) MS; (b) SS.

maximum efficiency and high load (0.8 P_{max}) zones [21]. This figure can illustrate clearly why an MS system is more efficient than an SS system. As is seen, in the MS system (Fig. 11(a)), 99.4% of the FCs power is in the safe zone in the total time of the driving cycle, while in the SS system (Fig. 11(b)), this amount decreases to 97%. In fact, the MS system works 2.4% more than the SS system in the safe zone. This difference in operation leads to fewer operating cost for the MS system.

According to Fig. 12, each FC in the MS system has a slower degradation rate than the utilized FC in the SS system. DP, as a benchmark, has fewer voltage drops for both 2000-W and 500-W FCs. When one FC degrades more than other FCs, the system uses the most degraded one less than others to avoid further degradation, thanks to the modularity and flexibility of the MS system. If an FC operates in a high load zone for a long time in the MS system, however, the system can reduce the power of the most degraded FC while boosting the usage of the other FCs. Because there is no other option or flexibility in an SS system, the high-power FC must continue to operate in the high load zone. Therefore, it is evident that an FC in the SS system has a faster degradation than that of the MS system. From Fig. 12(b), in the SS system, the difference in degradation of DP and ECMS

Authorized licensed use limited to: Universite du Quebec a Trois-Rivieres. Downloaded on January 08,2025 at 21:44:39 UTC from IEEE Xplore. Restrictions apply.

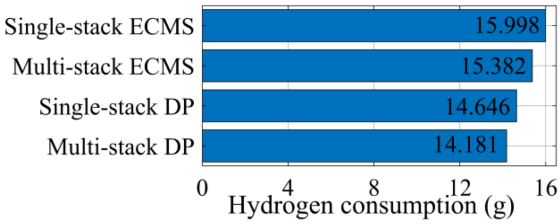

Fig. 13. Hydrogen consumption comparison between the MS and the SS for the WLTC-class3 driving cycle.

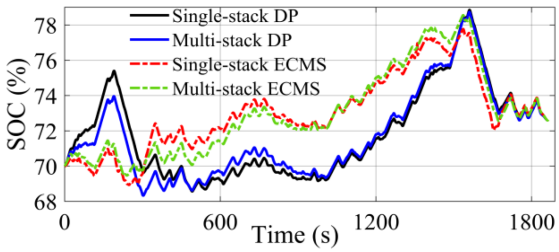

Fig. 14. Battery SOC comparison for the FTP-75 driving cycle.

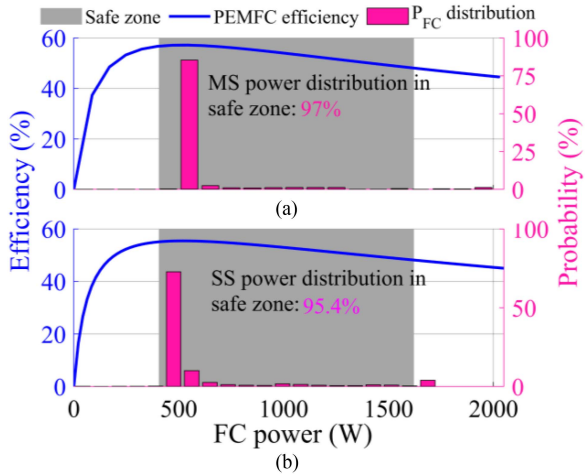

Fig. 15. FC operating in the safe zone for the FTP-75 driving cycle: (a) MS; (b) SS.

is more significant than the MS system. This stems from the fact that the FC in an SS system spends more time in the high load zone than the FCs in an MS system, as shown in Fig. 9(e). Working in the high load zone intensifies the FC's degradation and reduces its lifetime. As is seen in Fig. 9(e), ECMS, which is a real-time strategy, keeps working at maximum efficiency point until 1550 s. Then, the FC power experiences a striking increase and keeps working at the high load zone. However, in the case of DP which is aware of the whole driving cycle in advance, the FC operates at the maximum efficiency point for 1000s. After that, the FC power gradually increases to meet the requested power, and therefore it works in the high load zone less than the ECMS.

Fig. 13 shows the hydrogen consumption of the SS and MS systems. The results confirm that the MS configuration consumes less hydrogen than the SS system. According to the obtained results by DP and ECMS, the hydrogen consumption of the MS system is 3.173% and 3.852% less than the SS one, respectively. This lower hydrogen consumption is also in agreement with the presented results in Fig. 11, based on which the MS system works in the safe zone more than the SS.

B. FTP-75 Driving Cycle

Fig. 14 describes the battery SOC regarding the SS and the MS configurations using ECMS and DP algorithms. It should be said again that the most important thing about comparing MS systems, SS systems, and DP algorithms is that they all must finish in the same SOC.

It does not imply that the SOC must terminate in the initial SOC; rather, the final SOC in the SS system, MS system, and DP must be the same value.

Fig. 15 represents the operation of the SS and MS systems in the safe zone. As can be observed in the MS system (Fig. 15(a)), throughout the whole driving cycle, 97% of the FCs power is in the safe zone, while in the SS system (Fig. 15(b)), this amount decreases to 95.4%. The MS system works 1.6% more than the SS system in the safe zone. This difference of operation leads to less operating cost for the MS system. Table IX shows a comprehensive comparison between the SS system and the MS system. Hydrogen cost, degradation cost, and total cost are compared between ECMS and DP. The results show that the MS system is more efficient and economical than the SS system.

TABLE IX
OPERATING COSTS COMPARISON

Driving cycle	WLTC-class3				FTP-75			
EMS	DP		ECMS		DP		ECMS	
Configuration	SS	MS	SS	MS	SS	MS	SS	MS
H_2 cost (Cent)	5.860	5.673	6.400	6.153	6.716	6.514	7.040	6.850
Degradation cost (Cent)	0.011	0.006	0.046	0.010	0.019	0.012	0.074	0.051
Total cost (Cent)	5.870	5.680	6.445	6.163	6.735	6.530	7.114	6.900
	MS 3.2% less than SS		MS 4.4% less than SS		MS 3.0% less than SS		MS 3.0% less than SS	

V. CONCLUSION

This paper aims to compare the operating costs between the SS and the MSFC-HEV. The considered SSFC-HEV in this study is composed of a 2000-W Horizon FC, while the MS one utilizes four 500-W Horizon FCs. Both configurations utilize a battery pack as an ESS. The operating cost consists of hydrogen consumption and FC degradation costs. Indeed, the main objective of this optimization problem is to decide on a suitable FC power signal, as the control variable, to reach the minimum operating cost. To do so, this paper puts forward a hierarchical EMS for the MS system, and the obtained results are compared with those from DP, which is a well-accepted benchmark in this line of work. In the MS system, a rule-based strategy is used in the first layer of the EMS to determine the number of FCs that should participate in the optimization problem of the second layer, where ECMS is responsible for power distribution. The results of this study illustrate that the hydrogen consumption, degradation, and total costs of the MS system are lower than the SS system. Therefore, in terms of operating cost, the MS system can be a suitable choice for an FC-HEV.

Authorized licensed use limited to: Universite du Quebec a Trois-Rivieres. Downloaded on January 08,2025 at 21:44:39 UTC from IEEE Xplore. Restrictions apply.

REFERENCES

[1] X. Liu, K. Reddi, A. Elgowainy, H. Lohse-Busch, M. Wang, and N. Rustagi, "Comparison of well-to-wheels energy use and emissions of a hydrogen fuel cell electric vehicle relative to a conventional gasoline-powered internal combustion engine vehicle," *Int. J. Hydrogen Energy*, vol. 45, no. 1, pp. 972–983, 2020, doi: 10.1016/j.ijhydene.2019.10.192.

[2] E. Ogungbemi, T. Wilberforce, O. Ijaodola, J. Thompson, and A. G. Olabi, "Selection of proton exchange membrane fuel cell for transportation," *Int. J. Hydrogen Energy*, vol. 46, no. 59, pp. 30625–30640, 2021, doi: 10.1016/j.ijhydene.2020.06.147.

[3] S. Satyapal, "2017 Annual progress report: DOE hydrogen and fuel cells program," Nat. Renewable Energy Lab., Golden, CO, USA, Tech. Rep. NREL/BK-6A20-69077; DOE/GO-102017-5042, Jul. 2018.

[4] A. Jacome, D. Hissel, V. Heiries, M. Gerard, and S. Rosini, "Prognostic methods for proton exchange membrane fuel cell under automotive load cycling: A review," *IET Elect. Syst. Transp.*, vol. 10, no. 4, pp. 369–375, 2020, doi: 10.1049/iet-est.2020.0045.

[5] N. Marx, L. Boulon, F. Gustin, D. Hissel, and K. Agbossou, "A review of multi-stack and modular fuel cell systems: Interests, application areas and on-going research activities," *Int. J. Hydrogen Energy*, vol. 39, no. 23, pp. 12101–12111, 2014, doi: 10.1016/j.ijhydene.2014.05.187.

[6] T. Wang, Q. Li, L. Yin, W. Chen, E. Breaz, and F. Gao, "Hierarchical power allocation method based on online extremum seeking algorithm for dual-pemfc/battery hybrid locomotive," *IEEE Trans. Veh. Technol.*, vol. 70, no. 6, pp. 5679–5692, Jun. 2021, doi: 10.1109/TVT.2021.3078752.

[7] J. Zhou, J. Liu, Y. Xue, and Y. Liao, "Total travel costs minimization strategy of a dual-stack fuel cell logistics truck enhanced with artificial potential field and deep reinforcement learning," *Energy*, vol. 239, 2022, Art. no. 121866, doi: 10.1016/j.energy.2021.121866.

[8] Y. Yan, Q. Li, W. Chen, W. Huang, and J. Liu, "Hierarchical management control based on equivalent fitting circle and equivalent energy consumption method for multiple fuel cells hybrid power system," *IEEE Trans. Ind. Electron.*, vol. 67, no. 4, pp. 2786–2797, Apr. 2020, doi: 10.1109/TIE.2019.2908615.

[9] A. Khalatbarisoltani, M. Kandidayeni, L. Boulon, and X. Hu, "Power allocation strategy based on decentralized convex optimization in modular fuel cell systems for vehicular applications," *IEEE Trans. Veh. Technol.*, vol. 69, no. 12, pp. 14563–14574, Dec. 2020, doi: 10.1109/tvt.2020.3028089.

[10] C. Zhang, T. Zeng, Q. Wu, C. Deng, S. H. Chan, and Z. Liu, "Improved efficiency maximization strategy for vehicular dual-stack fuel cell system considering load state of sub-stacks through predictive soft-loading," *Renewable Energy*, vol. 179, pp. 929–944, 2021, doi: 10.1016/j.renene.2021.07.090.

[11] S. Zhou, G. Zhang, L. Fan, J. Gao, and F. Pei, "Scenario-oriented stacks allocation optimization for multi-stack fuel cell systems," *Appl. Energy*, vol. 308, no. 10, 2022, Art. no. 118328, doi: 10.1016/j.apenergy.2021.118328.

[12] X. Li, Z. Shang, F. Peng, L. Li, Y. Zhao, and Z. Liu, "Increment-oriented online power distribution strategy for multi-stack proton exchange membrane fuel cell systems aimed at collaborative performance enhancement," *J. Power Sources*, vol. 512, no. 8, 2021, Art. no. 230512, doi: 10.1016/j.jpowsour.2021.230512.

[13] J. Snoussi, S. B. Elghali, M. Benbouzid, and M. F. Mimouni, "Optimal sizing of energy storage systems using frequency-separation-based energy management for fuel cell hybrid electric vehicles," *IEEE Trans. Veh. Technol.*, vol. 67, no. 10, pp. 9337–9346, Oct. 2018, doi: 10.1109/TVT.2018.2863185.

[14] N. Mebarki, T. Rekioua, Z. Mokrani, D. Rekioua, and S. Bacha, "PEM fuel cell/battery storage system supplying electric vehicle," *Int. J. Hydrogen Energy*, vol. 41, no. 45, pp. 20993–21005, 2016, doi: 10.1016/j.ijhydene.2016.05.208.

[15] S. Zendegan, A. Ferrara, S. Jakubek, and C. Hametner, "Predictive battery state of charge reference generation using basic route information for optimal energy management of heavy-duty fuel cell vehicles," *IEEE Trans. Veh. Technol.*, vol. 70, no. 12, pp. 12517–12528, Dec. 2021, doi: 10.1109/TVT.2021.3121129.

[16] D. D. Tran, M. Vafaeipour, M. El Baghdadi, R. Barrero, J. Van Mierlo, and O. Hegazy, "Thorough state-of-the-art analysis of electric and hybrid vehicle powertrains: Topologies and integrated energy management strategies," *Renewable Sustain. Energy Rev.*, vol. 119, 2020, Art. no. 109596, doi: 10.1016/j.rser.2019.109596.

[17] Y. Huang et al., "A review of power management strategies and component sizing methods for hybrid vehicles," *Renewable Sustain. Energy Rev.*, vol. 96, no. 4, pp. 132–144, 2018, doi: 10.1016/j.rser.2018.07.020.

[18] T. Teng, X. Zhang, H. Dong, and Q. Xue, "A comprehensive review of energy management optimization strategies for fuel cell passenger vehicle," *Int. J. Hydrogen Energy*, vol. 45, no. 39, pp. 20293–20303, 2020, doi: 10.1016/j.ijhydene.2019.12.202.

[19] C. Zhang et al., "Real-Time optimization of energy management strategy for fuel cell vehicles using inflated 3D inception long short-term memory network-based speed prediction," *IEEE Trans. Veh. Technol.*, vol. 70, no. 2, pp. 1190–1199, Feb. 2021, doi: 10.1109/TVT.2021.3051201.

[20] T. Wang, Q. Li, X. Wang, W. Chen, E. Breaz, and F. Gao, "A power allocation method for multistack PEMFC system considering fuel cell performance consistency," *IEEE Trans. Ind. Appl.*, vol. 56, no. 5, pp. 5340–5351, Sep./Oct. 2020, doi: 10.1109/TIA.2020.3001254.

[21] A. M. I. Fernandez, M. Kandidayeni, L. Boulon, and H. Chaoui, "An adaptive state machine based energy management strategy for a multi-stack fuel cell hybrid electric vehicle," *IEEE Trans. Veh. Technol.*, vol. 69, no. 1, pp. 220–234, Jan. 2020, doi: 10.1109/TVT.2019.2950558.

[22] T. Wang, Q. Li, L. Yin, and W. Chen, "Hydrogen consumption minimization method based on the online identification for multi-stack PEMFCs system," *Int. J. Hydrogen Energy*, vol. 44, no. 11, pp. 5074–5081, 2019, doi: 10.1016/j.ijhydene.2018.09.181.

[23] W. Zhang, J. Li, L. Xu, and M. Ouyang, "Optimization for a fuel cell/battery/capacity tram with equivalent consumption minimization strategy," *Energy Convers. Manag.*, vol. 134, pp. 59–69, 2017, doi: 10.1016/j.enconman.2016.11.007.

[24] T. Wang et al., "An optimized energy management strategy for fuel cell hybrid power system based on maximum efficiency range identification," *J. Power Sources*, vol. 445, 2020, Art. no. 227333, doi: 10.1016/j.jpowsour.2019.227333.

[25] H. Li, A. Ravey, A. N'Diaye, and A. Djerdir, "Online adaptive equivalent consumption minimization strategy for fuel cell hybrid electric vehicle considering power sources degradation," *Energy Convers. Manag.*, vol. 192, no. 3, pp. 133–149, 2019, doi: 10.1016/j.enconman.2019.03.090.

[26] H. Li, A. Ravey, A. N'Diaye, and A. Djerdir, "A novel equivalent consumption minimization strategy for hybrid electric vehicle powered by fuel cell, battery and supercapacitor," *J. Power Sources*, vol. 395, no. 5, pp. 262–270, 2018, doi: 10.1016/j.jpowsour.2018.05.078.

[27] F. Martel, S. Kelouwani, Y. Dubé, and K. Agbossou, "Optimal economy-based battery degradation management dynamics for fuel-cell plug-in hybrid electric vehicles," *J. Power Sources*, vol. 274, pp. 367–381, 2015, doi: 10.1016/j.jpowsour.2014.10.011.

[28] M. Kandidayeni, A. O. M. Fernandez, A. Khalatbarisoltani, L. Boulon, S. Kelouwani, and H. Chaoui, "An online energy management strategy for a fuel cell/battery vehicle considering the driving pattern and performance drift impacts," *IEEE Trans. Veh. Technol.*, vol. 68, no. 12, pp. 11427–11438, Dec. 2019, doi: 10.1109/TVT.2019.2936713.

[29] M. Kandidayeni, A. Macias, L. Boulon, and S. Kelouwani, "Investigating the impact of ageing and thermal management of a fuel cell system on energy management strategies," *Appl. Energy*, vol. 274, no. 12, 2020, Art. no. 115293, doi: 10.1016/j.apenergy.2020.115293.

[30] "Proton-Exchange membrane fuel cells," in *Fuel Cell Systems Explained*. Hoboken, NJ, USA: Wiley, 2018, pp. 69–133.

[31] M. Kandidayeni, J. P. Trovão, M. Soleymani, and L. Boulon, "Towards health-aware energy management strategies in fuel cell hybrid electric vehicles: A review," *Int. J. Hydrogen Energy*, vol. 7, pp. 10021–10043, 2022, doi: 10.1016/j.ijhydene.2022.01.064.

[32] M. Yue, S. Jemei, R. Gouriveau, and N. Zerhouni, "Review on health-conscious energy management strategies for fuel cell hybrid electric vehicles: Degradation models and strategies," *Int. J. Hydrogen Energy*, vol. 44, no. 13, pp. 6844–6861, 2019, doi: 10.1016/j.ijhydene.2019.01.190.

[33] J. Zhao and X. Li, "A review of polymer electrolyte membrane fuel cell durability for vehicular applications: Degradation modes and experimental techniques," *Energy Convers. Manag.*, vol. 199, no. 8, 2019, Art. no. 112022, doi: 10.1016/j.enconman.2019.112022.

[34] X. Hu, C. Zou, X. Tang, T. Liu, and L. Hu, "Cost-optimal energy management of hybrid electric vehicles using fuel cell/battery health-aware predictive control," *IEEE Trans. Power Electron.*, vol. 35, no. 1, pp. 382–392, Jan. 2020, doi: 10.1109/TPEL.2019.2915675.

[35] Y. Zhou, A. Ravey, and M. C. Péra, "Real-time cost-minimization power-allocating strategy via model predictive control for fuel cell hybrid electric vehicles," *Energy Convers. Manag.*, vol. 229, 2021, Art. no. 113721, doi: 10.1016/j.enconman.2020.113721.

[36] T. Fletcher, R. Thring, and M. Watkinson, "An energy management strategy to concurrently optimise fuel consumption & PEM fuel cell lifetime in a hybrid vehicle," *Int. J. Hydrogen Energy*, vol. 41, no. 46, pp. 21503–21515, 2016, doi: 10.1016/j.ijhydene.2016.08.157.

Authorized licensed use limited to: Universite du Quebec a Trois-Rivieres. Downloaded on January 08,2025 at 21:44:39 UTC from IEEE Xplore. Restrictions apply.

[37] H. Chen, P. Pei, and M. Song, "Lifetime prediction and the economic lifetime of proton exchange membrane fuel cells," *Appl. Energy*, vol. 142, pp. 154–163, 2015, doi: 10.1016/j.apenergy.2014.12.062.
[38] Q. Li et al., "A state machine control based on equivalent consumption minimization for fuel cell/supercapacitor hybrid tramway," *IEEE Trans. Transp. Electrific.*, vol. 5, no. 2, pp. 552–564, Jun. 2019, doi: 10.1109/TTE.2019.2915689.
[39] X. Lin, Z. Wang, S. Zeng, and W. Huang, "Real-time optimization strategy by using sequence quadratic programming with multivariate nonlinear regression for a fuel cell electric vehicle," *Int. J. Hydrogen Energy*, vol. 46, no. 24, pp. 1–12, 2021, doi: 10.1016/j.ijhydene.2021.01.125.
[40] A. Rabbani and M. Rokni, "Dynamic characteristics of an automotive fuel cell system for transitory load changes," *Sustain. Energy Technol. Assessments*, vol. 1, no. 1, pp. 34–43, 2013, doi: 10.1016/j.seta.2012.12.003.
[41] K. Ettihir, L. Boulon, and K. Agbossou, "Optimization-based energy management strategy for a fuel cell/battery hybrid power system," *Appl. Energy*, vol. 163, pp. 142–153, 2016, doi: 10.1016/j.apenergy.2015.10.176.
[42] A. Macias, M. Kandidayeni, L. Boulon, and J. P. Trovão, "Fuel cell-supercapacitor topologies benchmark for a three-wheel electric vehicle powertrain," *Energy*, vol. 224, 2021, Art. no. 120234, doi: 10.1016/j.energy.2021.120234.
[43] P. Thounthong, S. Raël, and B. Davat, "Test of a PEM fuel cell with low voltage static converter," *J. Power Sources*, vol. 153, no. 1, pp. 145–150, 2006, doi: 10.1016/j.jpowsour.2005.01.025.
[44] W. Zhou, L. Yang, Y. Cai, and T. Ying, "Dynamic programming for new energy vehicles based on their work modes part II: Fuel cell electric vehicles," *J. Power Sources*, vol. 407, no. 10, pp. 92–104, 2018, doi: 10.1016/j.jpowsour.2018.10.048.

Mohammadreza Moghadari received the B.S. degree in mechanical engineering from Islamic Azad University Central Tehran Branch, Tehran, Iran, in 2015, the master's degree in automotive engineering with the Iran University of Science and Technology, Tehran, Iran, in 2018, and the Ph.D. degree from the Hydrogen Research Institute, University of Quebec, Trois-Rivières, QC, Canada, in 2020. He held the third rank among master's students in automotive engineering. He has been authored or coauthored several scientific papers in SCI journals since 2016. His research interests include PEMFC, water management in PEMFC, gas diffusion layer, CFD, optimal control, prediction, deep neural network, energy management strategy, and fault-tolerant control. In the capacity of a Reviewer, he has contributed to several scientific journals.

Mohsen Kandidayeni (Member, IEEE) was born in Tehran, Iran, in 1989. His educational journey has spanned through different paths. He received the B.S. degree in mechanical engineering in 2011, the master's degree in mechatronics with Arak University, Arak, Iran, in 2014, and the the Ph.D. degree in electrical engineering from the Hydrogen Research Institute of University of Quebec, Trois-Rivières (UQTR), Trois-Rivières, QC, Canada, in 2020. He joined the Hydrogen Research Institute of University of Quebec, in 2016. He is currently a Postdoctoral Researcher with electric-Transport Energy Storage and Conversion Lab with Université de Sherbrooke, Sherbrooke, QC, Canada and a Research Assistant Member with Hydrogen Research Institute, UQTR. He was a straight-A student during his master and Ph.D. Programs. Moreover, he has been the recipient of several awards/honors during his educational path, such as a Doctoral Scholarship from the Fonds de recherche du Québec–Nature et technologies(FRQNT), a Postdoctoral Scholarship from FRQNT, an Excellence Student Grant from UQTR, and the 3rd prize in Energy Research Challenge from the Quebec Ministry of Energy and Natural Resources. He has been actively involved in conducting research through authoring, coauthoring, and reviewing several papers in different prestigious scientific journals and also participating in various international conferences. His research interests include energy-related topics, such as hybrid electric vehicles, fuel cell systems, energy management, Multiphysics systems, modeling, and control.

Loïc Boulon (Senior Member, IEEE) received the master's degree in electrical and automatic control engineering from the University of Lille, Lille, France, in 2006, and the Ph.D. degree in electrical engineering from the University of Franche-Comté, Besançon, France. Since 2010, he has been a Professor with the University of Quebec, Trois-Rivières (UQTR), and a Full Professor since 2016. He has been with Hydrogen Research Institute as a Deputy Director since 2019. His work deals with modeling, control and energy management of multiphysics systems. He has authored or coauthored more than 120 scientific papers in peer-reviewed international journals and international conferences and given more than 35 invited conferences all over the world. His research interests include hybrid electric vehicles, energy and power sources (fuel cell systems, batteries, and ultracapacitors). In 2015, he was the General Chair of the IEEE-Vehicular Power and Propulsion Conference in Montréal, QC, Canada. Prof. Loïc Boulon is currently VP-Motor Vehicles of the IEEE Vehicular Technology Society and found the International Summer School on Energetic Efficiency of Connected Vehicles and the IEEE VTS Motor Vehicle Challenge. He is the Holder of the Canada Research Chair in Energy Sources for the Vehicles of the future.

Hicham Chaoui (Senior Member, IEEE) received the Ph.D. degree in electrical engineering (with Hons.) from the University of Quebec, Trois-Rivières, QC, Canada, in 2011. His career has spanned both academia and industry in the field of control and energy systems. From 2007 to 2014, he held various engineering and management positions with the Canadian industry. He is currently an Associate Professor with Texas Tech University, Lubbock, TX, USA, and Carleton University, Ottawa, ON, Canada. His research interests include adaptive and nonlinear control theory, intelligent control, robotics, electric motor drives, and energy conversion and storage systems. His scholarly work has resulted in more than 150 journal and conference publications. Dr. Chaoui is a registered Professional Engineer with the province of Ontario. He is also an Associate Editor for IEEE TRANSACTIONS ON POWER ELECTRONICS and several other IEEE journals. He was the recipient of the Best Thesis Award, the Governor General of Canada Gold Medal Award, the Carleton's Research Excellence Award, the Early Researcher Award from the Ministry of Colleges and Universities, and the Top Editor Recognition from IEEE Vehicular Technology Society.

Authorized licensed use limited to: Universite du Quebec a Trois-Rivieres. Downloaded on January 08,2025 at 21:44:39 UTC from IEEE Xplore. Restrictions apply.

2.3 Conclusion

This chapter aims to investigate the impact of multi-stack FC system advantages on its performance and operating cost and compare it with a single-stack FC system in a FC-HEV using a developed EMS. The single-stack FC-HEV in this study consists of a 2000-W Horizon FC, while the multi-stack system uses four 500-W Horizon FCs. The operating cost includes hydrogen consumption and FC degradation costs. The main objective of this optimization problem is to select an optimal FC power signal, as the control variable, to minimize operating cost. To achieve this, a hierarchical EMS is proposed for the multi-stack FC system, and the results are compared with those from DP, a well-accepted benchmark. In the multi-stack FC system, a rule-based strategy is used in the first layer of the EMS to determine how many FCs should participate in the optimization problem of the second layer, where ECMS is responsible for power distribution. The results illustrate that the hydrogen consumption, degradation, and total operating cost of the multi-stack FC system are lower than those of the single-stack system. Therefore, in terms of operating cost, the multi-stack FC system is a suitable choice for a FC-HEV. Additionally, the results show that the multi-stack FC system operates in the safe zone (high-efficiency zone) for a greater portion of its total performance time compared to the single-stack FC system.

Chapter 3 - Designing an Advanced EMS for a Multi-Stack FC-HEV

3.1 Introduction

In Chapter 2, it is analytically demonstrated that the advantages of the multi-stack FC system lead to reduced operating cost and improved FC performance compared to the single-stack FC system. However, despite the notable advantages and potential of the multi-stack FC system on the hardware side, fully operationalizing these benefits requires an advanced EMS as the core of power control on the software side. On the other hand, the operating cost of a multi-stack FC system, consisting of hydrogen consumption and FC degradation, remains an open issue that requires further development. In addition, distributing optimal power between sub-stacks to reduce hydrogen consumption and increase FC longevity is a challenging task that requires a dependable EMS.

To develop the multi-stack FC system performance, many recent studies have focused on OB-EMS strategies. However, most of these OB-EMSs rely on a single time-point assumption, only considering the current time step to make control decisions, without accounting for future events or adjusting power distribution accordingly. In optimal control problems, it has been proven that anticipating future events leads to decisions that are closer to global optimization results. Therefore, employing a multiple time-point strategy with prediction can improve EMS outcomes, bringing them closer to global optimization approaches. For this purpose, this chapter is dedicated to designing a predictive health-conscious EMS (PHC-EMS) for a multi-stack FC-HEV to enhance the performance of the multi-stack system.

3.2 Paper 2: Predictive Health-Conscious Energy Management Strategy of a Hybrid Multi-Stack Fuel Cell Vehicle

Authors: Mohammadreza Moghadari, Mohsen Kandidayeni, Loïc Boulon, and Hicham Chaoui.

Journal: IEEE Transactions on Vehicular Technology.

Publication status: Published (11/12/2024).

3.2.1 Methodology

In this chapter, a PHC-EMS is developed to minimize the total operating cost of a multi-stack FC-HEV. The results of the proposed EMS are compared with those of DP, a well-known global optimization algorithm, and ECMS, a single time-point strategy. The proposed PHC-EMS consists of three main parts, as shown in Figure 3-1. The first part is a rule-based strategy in the upper layer, used to designate how many FCs should be activated to participate in the optimization process. The second part is an MPC, developed in the lower layer, responsible for distributing optimal power among the FCs and the battery. The third part is a driving cycle predictor, called SBLSTM, a novel approach for predicting vehicle velocity. The following sections provide detailed explanations of these three components.

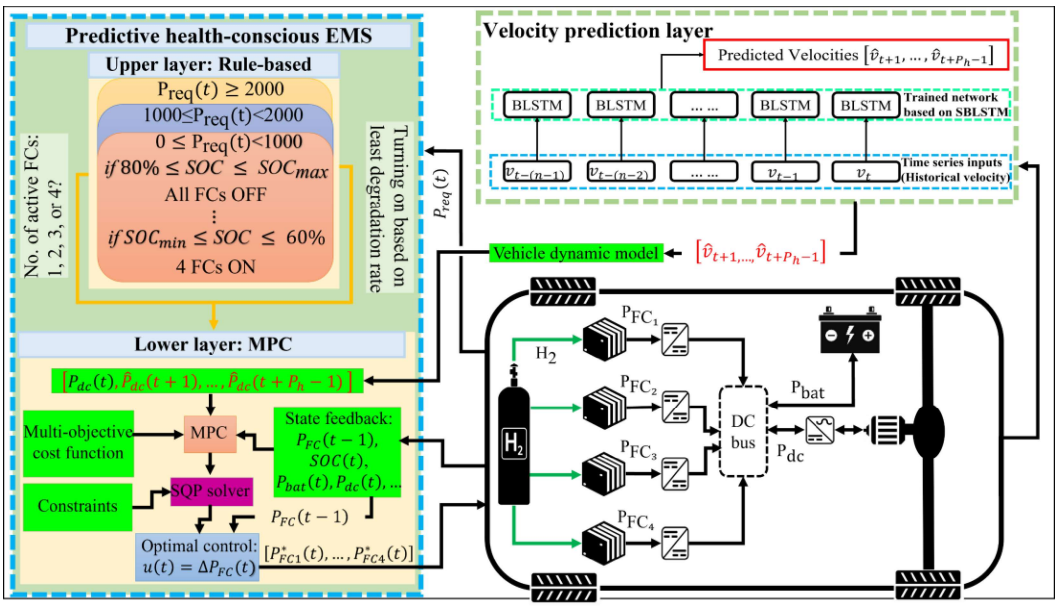

Figure 3-1- Schematic of PHC-EMS concept.

1) Upper Layer: Rule-Based Strategy

The performance differences among sub-stacks affect the operating cost of a multi-stack system in two key ways: 1) Reducing the rate of FC degradation and 2) Lowering hydrogen consumption. At each time step, the upper layer selects the minimum number of FCs needed based on their degradation rates. For example, if two FCs are required, it selects those with the lowest degradation. If FC1 and FC4 are less degraded than FC2 and FC3, FC1 and FC4 are used, while the others are turned off to prevent additional degradation. In other words, FCs with higher output power and lower voltage degradation are considered younger and are given the highest priority for participation in the lower layer. As a result, the upper layer aims to keep all sub-stacks at a similar degradation rate, which is crucial in a multi-stack FC system. This approach enhances system reliability and durability while also reducing operating cost. Another goal of the upper layer is to activate the minimum number of FCs to lower hydrogen consumption, which significantly impacts

operating cost. By determining when to activate or deactivate FCs, the upper layer aims to turn off unnecessary FCs and minimize hydrogen consumption.

2) Lower Layer: MPC

Following the notion of the receding horizon, MPC employs a nonlinear model of the process to forecast and optimize the system's future behavior [133]. The first elements of finite horizon optimal control sequences are calculated repeatedly along the closed-loop solution in MPC. When using MPC, the controller solves an optimal control problem at each sampling instant, producing an optimal sequence of future input values that guides the process toward the desired state. At the subsequent sampling time, only the first component of this optimal sequence is applied to the process [133]. The nonlinear problem is formulated as a state-space model in MPC. Typically, in such a problem, the SOC is a state variable, and FC power is the control variable. This study uses the increment of FC power as the control variable. The utilized multi-objective cost function in this study is based on operating cost ($). The total operating cost consists of hydrogen consumption (C_{H_2}), FC degradation ($C_{FC,deg}$), and battery degradation ($C_{bat,deg}$).

3) Velocity Predictor (SBLSTM)

This study aims to go beyond typical prediction methods by using a new approach to improve prediction accuracy. Accurate velocity prediction significantly impacts the performance of the PEMS and can make a substantial difference. To achieve this, this study uses SBLSTM networks to boost prediction accuracy and performance. Deep neural networks, such as the LSTM network, can process historical velocity data as motion information for better prediction. LSTM is a robust variant of the recurrent neural network (RNN) that solves the gradient vanishing problem [134]. However, relevant information

may be filtered out or not properly conveyed through the chain-like gated structure in a time series prediction process. Consequently, this study uses a bidirectional LSTM (BLSTM), which can handle both forward and backward dependencies, as part of the network structure. Deep BLSTM architectures consist of several stacked BLSTM hidden layers, where the output of one BLSTM hidden layer serves as the input for the next. As a result, this study applies the stacked layers technique, which enhances the power of neural networks.

3.2.2 Summary of the Results Analysis

To evaluate the effectiveness of PHC-EMS, the results are compared with DP as a benchmark and ECMS as a single time-point EMS. Two different driving cycles (INRETS and WVUINTER) are employed in this investigation to analyze the performance of the proposed EMS.

According to Table 3-1, for the INRETS driving cycle, DP spends less time in the high load zone ($0.8\,P_{max}$) than other strategies and consumes less hydrogen. PHC-EMS performs similarly to DP, consuming 4.363% more hydrogen than DP and 8.958% less hydrogen than ECMS. PHC-EMS spends less time in both the high and low load ($0.2\,P_{max}$) zones compared to ECMS, resulting in lower FC degradation costs.

Table 3-1- Analytical comparison between three strategies for INRETS driving cycle.

Strategy	H_2 Consumption (g)	High load (s)	Low load (s)
DP	16.640	1304	5356
PHC-EMS	17.449	1631	5618
ECMS	19.012	1683	5697

Figure 3-2 shows the total operating costs of DP, PHC-EMS, and ECMS for the INRETS driving cycle. The total operating costs of DP, PHC-EMS, and ECMS are 12.215, 12.688, and 13.342 cents, respectively. DP, as a benchmark for optimal control decision problems, achieves the best result. Hydrogen consumption is the most critical component of the operating cost in a multi-stack FC-HEV. The proposed strategy in this study achieves results close to DP in terms of hydrogen consumption while preventing a significant increase in FC and battery degradation. The total operating cost of PHC-EMS is 3.728% higher than DP and 5.154% lower than ECMS.

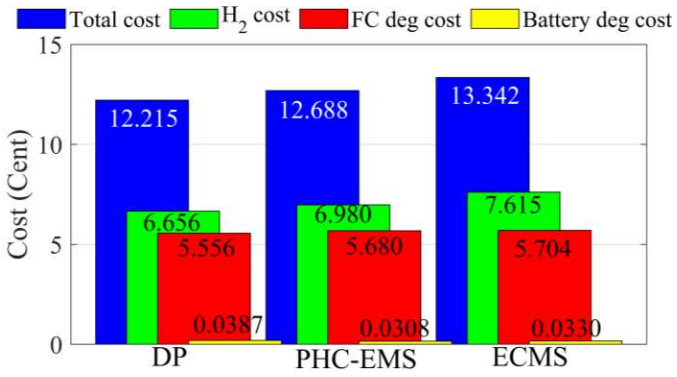

Figure 3-2- Total cost comparison between three different strategies for INRETS driving cycle.

Table 3-2 compares the effectiveness of the three strategies regarding hydrogen consumption and total working time in high and low load zones for the WVUINTER driving cycle. According to Table 3-2, DP has achieved the lowest cost, as expected. The results of PHC-EMS show that the FC system operates 17 s less in the high load zone and 22 s less in the low load zone compared to ECMS, which leads to lower degradation costs. The results demonstrate the potential of PHC-EMS to reduce hydrogen consumption. The proposed strategy consumes 2.553% more hydrogen than DP and 5.106% less than ECMS.

Table 3-2- Analytical comparison between three strategies for WVUINTER driving cycle.

Strategy	H_2 Consumption (g)	High load (s)	Low load (s)
DP	27.252	2508	2664
PHC-EMS	27.966	2839	2971
ECMS	29.394	2856	2993

Figure 3-3 indicates the total cost comparison among DP, PHC-EMS, and ECMS under the WVUINTER driving cycle. 16.244, 16.654, and 17.245 cents, respectively, are the total operational costs for DP, PHC-EMS, and ECMS. The total operating cost of PHC-ESM is 2.462% more than DP, and 3.550% less than ECMS.

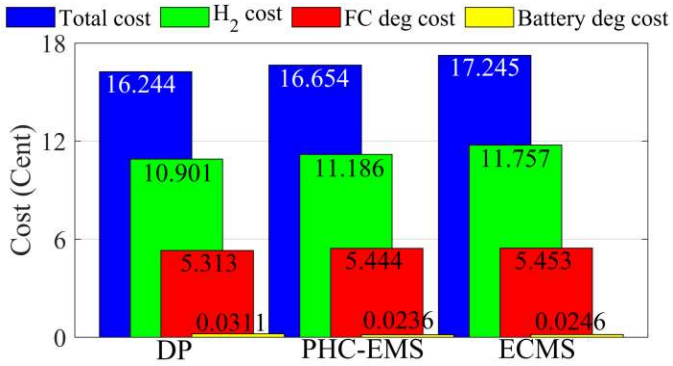

Figure 3-3- Total cost comparison between three different strategies for WVUINTER driving cycle.

Predictive Health-Conscious Energy Management Strategy of a Hybrid Multi-Stack Fuel Cell Vehicle

Mohammadreza Moghadari, Mohsen Kandidayeni, *Member, IEEE*, Loïc Boulon, *Senior Member, IEEE*, and Hicham Chaoui, *Senior Member, IEEE*

***Abstract*—The use of a multi-stack fuel cell (FC) hybrid electric vehicle (HEV) has recently attracted a lot of attention as a key to enhance system modularity, efficiency, and redundancy. An essential challenge here is the high operating cost of the FC-HEV, which includes the cost of hydrogen, FC degradation, and energy storage system (ESS). For this purpose, this study proposes a predictive health-conscious (PHC) energy management strategy (EMS) to reduce the total operating cost of a multi-stack FC-HEV. The proposed EMS is a multi-layer strategy. In the upper layer, a rule-based strategy is devised to determine how many FCs should be activated considering the degradation of FCs, requested power, and battery state of charge (SOC) to decrease the hydrogen consumption and prevent extreme FC degradation. The lower layer is a real-time optimization algorithm called model predictive control (MPC) that employs its predictive ability to share the optimal power between FCs and the battery. Unlike the other studies, a new velocity predictor, stacked bidirectional long short-term memory (SBLSTM) networks, is utilized in the lower layer to provide accurate future velocity prediction for the MPC. The performance of the proposed strategy is benchmarked with dynamic programming (DP) and equivalent consumption minimization strategy (ECMS) under two different driving cycles. The obtained results indicate that the proposed PHC-EMS achieves close results to DP (with maximum of 3.728% difference) while outperforming ECMS up to 5.154%.**

***Index Terms*—Fuel cell degradation, fuel cell hybrid electric vehicle, long short-term memory, modular fuel cell system, predictive energy management strategy.**

I. Introduction

FUEL cell (FC) hybrid electric vehicle (HEV) is one of the most potential candidates for the electrification of vehicles [1], [2]. Proton exchange membrane fuel cell (PEMFC) is an appealing choice for vehicular applications among the different types of FC because it has the right size and weight, works at a low temperature, has a high power density, and has a low risk of corrosion [3]. Pure FC power systems have a slow dynamic response, making it difficult to produce power peaks during start-up and acceleration. Furthermore, pure FC systems cannot recover the energy created during braking [4].

Therefore, a FC system is typically combined with an energy storage system (ESS) to provide power peaks and absorb regenerative energy while reducing hydrogen consumption and degradation [5]. Despite the noteworthy merits of FC, the commercialization of FC technology in the transportation sector is still constrained by technical and scientific obstacles, such as hydrogen storage infrastructure, high operating cost, FC confined lifetime, low durability, and low reliability [6]. Furthermore, in real-world applications such as vehicles, FC load profile includes start/stop cycling, low-power operation, high-power operation, and quick load shifting cycles. These sorts of power demands cause irreversible and permanent degradation, which can expedite the failure of the FC [7]. The US Department of Energy (DOE) has set a lifespan target of 150000 miles (8000 hours) in a passenger vehicle for PEMFCs [8]. Using several low-power FC stacks, known as a multi-stack FC system, instead of a single high-power FC stack can be considered a suitable solution to overcome some of the mentioned barriers like FC high operating cost, FC confined lifetime, low reliability, and low durability [9]. The multi-stack FC system potentially could have technical advantages such as higher efficiency, higher output power, and longer longevity over the single-stack FC [9], [10]. A major benefit of multi-stack FC systems is that they are more efficient than single-stack FC systems. Single-stack systems have only one peak efficiency point, while multi-stack systems have several high efficiency points, boosting the overall efficiency [9], [11]. One of the key features of the multi-stack system is its redundancy. This means that even if some sub-stacks fail and stop generating power, the entire system can still operate. The system isolates the malfunctioning sub-stacks, allowing the rest to continue functioning. When the faulty sub-stacks recover from malfunctions like flooding or drying out, they can rejoin the system and resume their operation [12]. In single-stack FC-HEVs, a FC stack failure greatly impacts performance. A multi-stack system's modular design allows faulty stacks to be replaced without disrupting the electrical connection, improving maintainability and performance [13], [14]. Moreover, multi-stack FC aids in the decrease of individual stack degradation and increases the overall stability of the system [15]. However, the mentioned potentials of the multi-stack FC systems depend on the adopted configuration and energy management strategy (EMS) [9], [16], [17]. The parallel configuration outperforms other types of multi-stack FC configurations in terms of space

Received 11 December 2023; revised 5 July 2024 and 10 September 2024; accepted 26 November 2024. Date of publication 11 December 2024; date of current version 18 April 2025. The review of this article was coordinated by Prof. Ching-Ming Lai. *(Corresponding author: Mohammadreza Moghadari.)*

Mohammadreza Moghadari, Mohsen Kandidayeni, and Loïc Boulon are with the Hydrogen Research Institute, Electrical and Computer Engineering Department, Université du Québec à Trois-Rivières, Trois-Rivières, QC G8Z 4M3, Canada (e-mail: mohammadreza.moghadari@uqtr.ca; loic.boulon@uqtr.ca; mohsen.kandi.dayeni@uqtr.ca).

Hicham Chaoui is with the Intelligent Robotic and Energy Systems (IRES) Research Group, Department of Electronics, Carleton University, Ottawa, ON K1S 5B6, Canada (e-mail: hicham.chaoui@carleton.ca).

Digital Object Identifier 10.1109/TVT.2024.3512204

0018-9545 © 2024 IEEE. All rights reserved, including rights for text and data mining, and training of artificial intelligence and similar technologies. Personal use is permitted, but republication/redistribution requires IEEE permission. See https://www.ieee.org/publications/rights/index.html for more information.

Authorized licensed use limited to: Universite du Quebec a Trois-Rivieres. Downloaded on April 21,2025 at 18:19:44 UTC from IEEE Xplore. Restrictions apply.

flexibility, performance, and efficiency [9], [11], [16]. The multi-stack FC system is a mandatory option for heavy-duty cycles, but due to the its notable benefits, it can be used for other applications, such as passenger vehicles.

A multi-stack FC-HEV consisting of several power sources with different characteristics needs a mature EMS to distribute the power, which has a crucial role in reducing fuel consumption and increasing system efficiency and FC lifespan [18]. EMSs are typically classified into two categories: rule-based and optimization-based [19]. The rule-based techniques are real-time and can be used quickly with specialized expertise and experience. However, predetermined rules cannot guarantee optimal performance [19], [20]. Optimization-based approaches are classified into global and local optimization. Dynamic programming (DP), which needs the whole driving cycle information in advance, is normally used as a global optimization and benchmark. Well-known local optimization strategies include approaches like model predictive control (MPC), equivalent consumption minimization strategy (ECMS) [19], [20].

Appropriate power distribution in multi-stack FC-HEV, considering the improvement of fuel consumption, system efficiency, and FC lifetime is a challenging task. For this purpose, in recent years, most of the papers have focused on optimization-based EMS in multi-stack FC-HEV to ameliorate the system performance.

For the multi-stack FC system, [21] suggests an optimal coordinating method. This method can produce the efficiency distribution function using a model of each stack's energy consumption. Experiments with 100-kW stacks confirm the method's efficacy. The study of [22] proposes a unique decentralized convex optimization framework based on the auxiliary problem notion to address a multi-objective power allocation strategy issue in a multi-stack FC. To prevent adverse loading circumstances that could degrade the sub-stacks, [23] proposes a predictive soft loading approach with an upgraded overall efficiency maximization strategy for dual-stack FC systems. The authors of [24] propose a power allocation strategy for the multi-stack FC to narrow the performance difference between the FCs and extend the system's lifetime. To increase fuel economy and the longevity of the FC stacks, the study in [25] suggests an EMS that considers system operating cost and service life. According to testing data, the suggested technique can increase system efficiency while lowering operating cost by 15.85% and 9.75%. In [26], an SQP-based ECMS is used for a hybrid vehicle with a FC, battery, and supercapacitor. This study demonstrates that the proposed strategy can save more fuel than a rule-based one.

However, most of the discussed optimization-based EMSs are based on a single time-point assumption that just considers the current time step to make the control decision. They do not have the prediction to consider future events and split the power accordingly. In optimal control problems, it has been proven that awareness of the future event leads to making an optimal decision near the global optimization results. Therefore, using a multiple time-point strategy that has the prediction can make the EMS result better and closer to the global optimization approaches. In this regard, MPC is a potential tool whose applicability in the domain of FC-HEVs has been well-proved. In [27], the authors propose a multi-objective predictive EMS based on MPC, velocity forecasting, and driving pattern recognition. The suggested EMS can maintain SOC around the reference, reduce fuel consumption by 6.67%, and avoid PEMFC degradation. The study in [28] presents a health-conscious EMS based on MPC for FC-HEVs. The results of simulation and real-time experiments demonstrated that the proposed strategy is a viable option for constructing cost-effective EMSs. The authors of [29] propose a cost-optimal, predictive EMS method for a FC-HEV. The effectiveness of this approach is assessed while taking into account different prediction horizon lengths and prediction uncertainty. In [30], MPC is used to implement the suggested strategy, which includes both hydrogen consumption and energy source degradation in the multi-objective cost function.

A vehicle velocity prediction-based MPC is proposed for a FC-HEV in [31]. Under the same objective function, the suggested method has a 3.74% lower overall operating cost than the normal MPC. In [32], a predictive control strategy based on a new velocity predictor is proposed for a plug-in FC vehicle. This method decreases hydrogen consumption by 4.99% compared to the ECMS, and by 17.07% versus the rule-based control strategy. In [33], a hierarchical MPC-based EMS for a FC hybrid construction vehicle is proposed. The simulations with cyclic loads indicate that the suggested prediction methodology is accurate.

Regarding MPC-based EMSs, some studies assume that the predicted vehicle velocity remains unchanged during the prediction horizon, always equal to the current velocity, or that the driving cycle is already known [28], [29], [34]. Even though these hypotheses make MPC viable for vehicle applications, it is too perfect for producing reliable predictions, which hinders MPC's effectiveness. Prediction of vehicle velocity, as the external disturbance has a key role in the optimal and accurate response of MPC. Vehicle velocity changes can affect the durability of power sources and fuel economy [35]. The outputs of MPC without including velocity prediction are far from optimality and accuracy, hence MPC needs to regulate its results depending on the vehicle's future velocity. Therefore, adopting a powerful velocity predictor that enables the system to accurately anticipate future velocities is crucial.

According to the literature review on predictive EMS, the prediction improves the optimal control results in terms of fuel consumption, FC and battery lifespan, and total operating cost. According to the literature review, most of the studies that use predictive EMS are connected to single-stack FC-HEVs, and applying predictive EMS in multi-stack FC-HEVs is really scarce. As a result, this paper proposes a predictive health-conscious EMS (PHC-EMS) for a multi-stack FC-HEV to improve the multi-stack system's performance in vehicular applications. This study's theoretical contributions have four main parts:

1) Utilizing a PHC-EMS: Unlike single time-point methods that focus solely on the current state of the system to optimize power distribution, this study adds a predictive aspect to the EMS for multi-stack FC-HEVs, bringing the results closer to those of global optimization methods. Additionally, the proposed EMS is health-conscious, as it optimizes power distribution by considering the state of

Authorized licensed use limited to: Universite du Quebec a Trois-Rivieres. Downloaded on April 21,2025 at 18:19:44 UTC from IEEE Xplore. Restrictions apply.

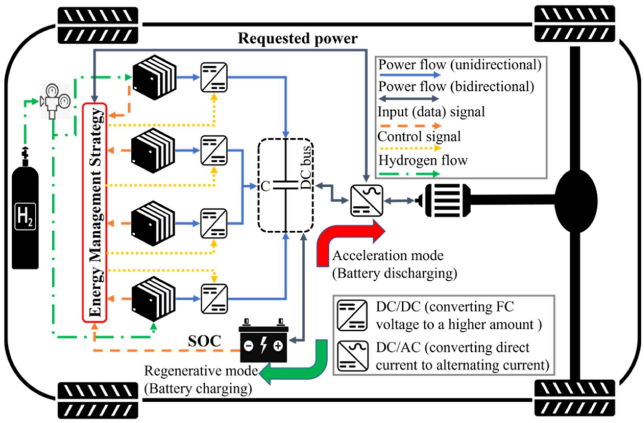

Fig. 1. The architecture of the multi-stack system's powertrain.

health (SOH) of the FCs and battery, thereby increasing the durability of the power sources.

2) Employing hierarchical EMS: The proposed EMS consists of two layers. The upper layer is a rule-based EMS that determines how many FCs should be activated in each time step. It sorts the FCs from most degraded to least degraded, giving priority to the FCs with the lowest degradation rates to participate in the lower layer. The goals of the upper layer are:

a) Preventing further degradation of the most degraded FCs and ensuring that all FCs have a close degradation rate.

b) Deactivating unnecessary FCs to reduce hydrogen consumption.

The lower layer is an MPC that, based on the active FCs selected by the upper layer, optimally distributes power between the FCs and the battery.

3) Novel velocity predictor: Unlike most studies that use conventional methods, this study aims to go beyond by employing a novel deep neural network approach to improve prediction accuracy. This study uses a stacked bidirectional long short-term memory (SBLSTM) network to forecast vehicle velocities. SBLSTM enhances the effectiveness of the MPC by providing reliable and precise velocity predictions.

4) Results comparison: This study aims to compare the results of PHC-EMS with DP as a benchmark and ECMS as a single time-point strategy. This comparison demonstrates the robustness of PHC-EMS in achieving optimal results, balancing computational burden, and ensuring feasibility in real-world applications.

The remainder of this project is organized as follows. Section II covers vehicle modeling. The EMS system is explained in Section III. The obtained results are discussed in Section IV, and the conclusion is provided in Section V.

II. Modeling

A. Multi-Stack FC-HEV Powertrain Configuration

The hybrid powertrain with a multi-stack FC design is investigated in this study. Fig. 1 shows the multi-stack powertrain, which includes a battery pack and four 500-W PEMFCs as its main power sources. A semi-active design is used in this configuration, with the battery pack connected to the bus directly and the FCs connected to it through unidirectional DC-DC converters [31]. According to Fig. 1, C is the DC bus capacitor. Without the capacitor, the motor's performance is affected by the switching of the rectifier's side switches. In other words, the DC bus capacitor functions as a filter [36]. It is important to mention that the 2 kW total power configuration of the FCs is specifically designed for a low velocity vehicle like Nemo [37]. In this study, the main power of FC-HEV is supplied by FCs. The battery's size is not large, and its primary role is to compensate for the FC's slow dynamic response and provide peak powers.

TABLE I
Technical Parameter of the Vehicle

Parameters	Value
Coefficient of rolling friction c_r	0.015
The total mass of the vehicle M	896 kg
Gravitational acceleration g	9.81 m/s^2
The slope of the road θ	0°
Air density ρ_{air}	1.2 kg/m^3
Aerodynamic drag coefficient c_d	0.42
The contact area of the vehicle's front surface A_{ad}	4 m^2
Top speed	40 km/h

The requested power (P_{req}) can be computed as follows based on a road vehicle longitudinal dynamics.

$$P_{req} = v \;\; F_{req} = (F_r + F_{ad} + F_a)\, v \tag{1}$$

$$\begin{cases} F_r = c_r\, M\, g\, \cos(\theta) \\ F_{ad} = \frac{1}{2}\, \rho_{air}\, c_d\, A_{ad}\, v^2 \\ F_a = M \frac{dv(t)}{dt} \end{cases} \tag{2}$$

where F_r represents the rolling friction of the tires, it is important to note that the driving environment is flat, and the road slope is 0°. F_{ad} is the force of aerodynamic resistance, F_a is the acceleration force, and v is the vehicle velocity. Table I illustrates the vehicle's technical parameters. The battery and the FC provide the requested power required for the driving cycle, and their combined power is delivered via the DC bus (P_{dc}) by (3).

$$\begin{aligned} P_{dc} &= P_{bat} + P_{FC}\, \eta_{DC-DC} \\ &= \begin{cases} \frac{P_{req}}{\eta_{drive}\, \eta_{em}\, \eta_{DC-AC}}, & P_{req} \geq 0 \\ P_{req}\, (\eta_{drive}\, \eta_{em}\, \eta_{DC-AC}), & P_{req} < 0 \end{cases} \end{aligned} \tag{3}$$

where η_{drive}, η_{em}, η_{DC-AC}, and η_{DC-DC} indicate, respectively, the efficiency of the driving line, the electric motor, the DC-AC inverter, and the DC-DC converter. It should be noted that P_{req} consists of driving and braking modes, and in this investigation, the focus is on the driving mode.

B. FC Model

In this paper, four Horizon 500-W FCs are employed to form a multi-stack power train architecture. The same FC technology discussed in this study has been utilized in other investigations as well [22], [38]. Since there is no accurate and complete model of the FC, and most FC models have inaccuracies that might diverge

Authorized licensed use limited to: Universite du Quebec a Trois-Rivieres. Downloaded on April 21,2025 at 18:19:44 UTC from IEEE Xplore. Restrictions apply.

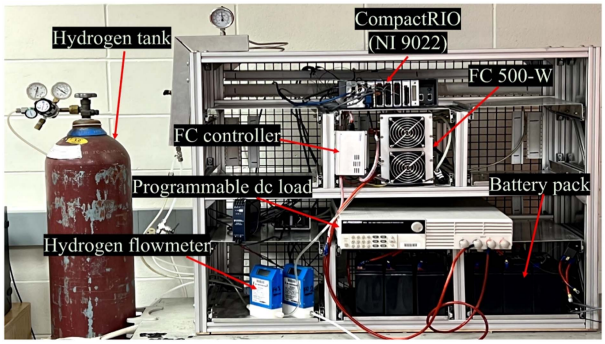

Fig. 2. The hydrogen research institute's PEMFC test bench at the university of quebec in trois-rivieres (UQTR).

TABLE II
FC SPECIFICATION

Horizon 500-W (PEM)	
Number of cells	24
Rated Power	500 W
Voltage range	12-23 V
Maximum current	40 A
H2 pressure	0.5 to 0.6 bar
Rated H2 flow	7 SLPM
Weight (with fan & casing)	2.52 kg (±50grams)

TABLE III
COEFFICIENT VALUES OF (4)–(5)

Coefficients	Values
b_1, b_2, b_3, b_4, b_5	1.353×10^{-5}, -0.001, 0.046, -0.663, 22.390
a_1, a_1, a_3	1.470×10^{-8}, 1.080×10^{-5}, 2.450×10^{-4}

from the true performance of the FC and impact the EMS results, this research utilizes experimental data of FC characteristics curves. The curves of Horizon 500-W have been obtained from a developed test bench presented in Fig. 2. The FC system's specifications are provided in Table II. The setup shown in Fig. 2 has been developed at the Hydrogen Research Institute of the University of Quebec in Trois-Rivières (UQTR). According to Fig. 2, a Horizon 500-W is linked to a National Instrument CompactRIO utilizing a PEMFC controller. Every 100 ms, data are sent via Ethernet from the CompactRIO to the PC, and the FC system voltage, current, and hydrogen consumption are recorded. An 8514 BK Precision DC Electronic Load is used to request load profiles from the PEMFC. As seen in (4)–(5), the fitted polarization and hydrogen consumption models are polynomial functions of current and FC power.

$$V\ (I) = b_1\ I^4 + b_2 I^3 + b_3 I^2 + b_4 I + b_5 \tag{4}$$

$$H_2\ (P_{FC}) = a_1\ P_{FC}^2 + a_2 P_{FC} + a_3 \tag{5}$$

Table III introduces the values of all the coefficients in (4)–(5). The experimental data of polarization, hydrogen consumption, and FC system efficiency for the Horizon 500-W PEMFC are shown in Fig. 3.

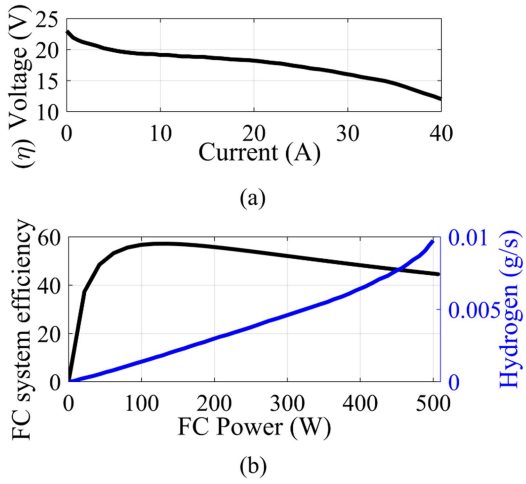

Fig. 3. The experimental data of the horizon 500-W characteristic curves: (a) Polarization; (b) hydrogen consumption and FC system efficiency.

TABLE IV
THE PEMFC DEGRADATION RATE (CELL LEVEL)

Operating state	Rate of degradation
Start-stop cycle ($\delta_{on/off}$)	13.79 $\frac{\mu V}{cycle}$ [40]
High load (δ_{high})	10.00 $\frac{\mu V}{h}$ [40]
Low load (δ_{low})	8.66 $\frac{\mu V}{h}$ [41]
Transition load (δ_{tran})	0.0441 $\frac{\mu V}{\Delta kW}$ [41]

C. FC Degradation Model

Degradation of the FC is a normal and unavoidable process that can result in a reduction in the voltage.

Since each PEMFC component degrades differently, it is hard to capture component-level degradation and its influence on other components. As a result, the stack level is usually considered for modeling FC degradation [39]. Four working conditions are normally recognized as the leading causes of degradation in a PEMFC. The start-stop operation, high load, low load, and transition load are these four operational circumstances [29], [30], [39]. The dominant and significant influence on voltage degradation is caused by the start-stop cycle. This cycle can significantly reduce FC voltage [29]. Regarding other degradation factors, high loading is defined as when $P_{FC} \geq 0.8 \times P_{FC,\max}$, and low loading is defined when $P_{FC} \leq 0.2 \times P_{FC,\max}$. $P_{FC,\max}$ in Horizon 500-W is 500 W. The total voltage degradation (μV) of a cell is given by (6):

$$\Delta\ V_{cell} = \delta_{on/off}\ \ N_{on/off} + \delta_{high}\ T_{high} + \delta_{low}\ T_{low} + \delta_{tran}\ N_{tran} \tag{6}$$

where $\delta_{on/off}$, δ_{high}, δ_{low}, and δ_{tran} are the voltage cell rate degradation for each start-stop cycle, high load, low load, and transition load, respectively. In Table IV, the degradation rates are indicated. $N_{on/off}$ represents the number of start-stop cycles, T_{high} and T_{low} represent the time in seconds that the FC operates at high and low load, respectively, and N_{tran} represents the amount of the load change ($|\Delta P_{FC}| = P_{FC}\ (t) -$

Authorized licensed use limited to: Universite du Quebec a Trois-Rivieres. Downloaded on April 21,2025 at 18:19:44 UTC from IEEE Xplore. Restrictions apply.

TABLE V
CHARACTERIZATION OF BATTERY

SAFT Rechargeable lithium-ion battery cell	
Capacity	6 Ah
Maximum current	C/1 A
Nominal voltage	3.9 V
Number of cells in series	20
Coulombic efficiency	0.99

$P_{FC}(t-1)$). In this study, the FC degradation should be converted to cost ($) format to be used in the multi-objective cost function. Therefore, the cost of FC degradation is described by $C_{FC,deg}$.

$$C_{FC,deg} = C_{on/off} + C_{high} + C_{low} + C_{tran} \tag{7}$$

$C_{on/off}$ is the start-stop cycle degradation cost, computed by (8):

$$C_{on/off} = \frac{\delta_{on/off}\, N_{on/off,t}}{V_{EOL}}\, \varphi_{FC}\, P_{FC,rated}\,(\$) \tag{8}$$

where V_{EOL} is the voltage drop at the end of life (EOL) of the PEMFC (6000 μV), corresponding to a 10% decline in the FC voltage. $P_{FC,rated}$ is the FC rated power (in kW) that is 0.5kW, and φ_{FC} is the unit of FC system price (93 $/kW) [42]. The degradation cost resulting from the high and low load is indicated in (9)–(10).

$$C_{high} = \frac{\delta_{high}\frac{T_{high}}{3600}}{V_{EOL}}\, \varphi_{FC}\, P_{FC,rated}\ (\$) \tag{9}$$

$$C_{low} = \frac{\delta_{low}\frac{T_{low}}{3600}}{V_{EOL}}\, \varphi_{FC}\, P_{FC,\,rated}\ (\$) \tag{10}$$

It should be mentioned that in this paper each time step lasts 1 s. Therefore, T_{high} and T_{low} will be 1 if the FC operates in high or low load, respectively, since the FC works for one second in these loads. The transition load cost shown in (11) is related to the last portion of the degradation cost.

$$C_{tran} = \frac{\delta_{tran}\ |P_{FC}(t) - P_{FC}(t-1)|\ \Delta t}{V_{EOL}\ N_{cell}} \times \varphi_{FC}\ P_{FC,rated}\ (\$) \tag{11}$$

where N_{cell} is the number of cells in a stack.

D. Battery Model

An internal resistance-based model is used in this work to simulate the battery [43]. The battery's characteristics are shown in Table V. Fig. 4 illustrates how internal resistance and open-circuit voltage relate to battery SOC. The National Renewable Energy Laboratory's experimental tests have been used to derive the battery data [44]. The battery current (I_{bat}), bus voltage (V_{bus}), and SOC are shown in (12)–(14) respectively.

$$I_{bat} = \frac{V_{oc} - \sqrt{V_{oc}^2(SOC) - 4\,R_{bat}(SOC)\ P_{bat}}}{2\,R_{bat}(SOC)} \tag{12}$$

$$V_{bus} = V_{oc}\ (SOC) - I_{bat}\,R_{bat} \tag{13}$$

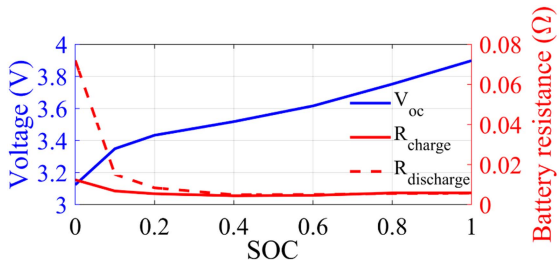

Fig. 4. The relationship between SOC and battery open-circuit voltage and resistance.

TABLE VI
PRE-EXPONENTIAL COEFFICIENT (B) AS A FUNCTION OF C-RATE

c-rate	c\2	2c	6c	10c
$B(c)$	31630	21681	12934	15512

$$SOC\ (t) = SOC\,(t_0) - \eta_{bat}\,\frac{\int_{t_0}^{t} I_{bat}\,dt}{Q_{bat}} \tag{14}$$

V_{oc} and R_{bat} are the battery's open-circuit voltage and internal resistance, respectively, and can be represented as a function of SOC. The battery's output power is denoted by P_{bat}, its nominal capacity is expressed by Q_{bat} (Ah), and its coulombic efficiency is indicated by η_{bat}.

E. Battery Degradation Model

Battery degradation is directly impacted by physical and electrical alterations and emerges as a reduction in battery capacity and an increase in internal resistance.

In this study, the capacity loss of the battery cell is simulated using a semi-empirical battery degradation model [45]. Considering the battery's initial capacity is 100%, the cell capacity loss can be calculated by (15) based on the Arrhenius equation.

$$\Delta\,Q_{cell} = B\,(c)\exp\left(\frac{-E_a\,(c)}{R_C T_C}\right) A(c)^z \tag{15}$$

where ΔQ_{cell} is the battery capacity loss in percentage (%), c is the c-rate, B is the pre-exponential factor dependent on the c-rate, which has various amounts for various c-rates according to Table VI. R_C and T_C are constant of the ideal gas (8.31 J/mol. K), and battery cell temperature (K), respectively. A is the battery discharge throughput (Ah) that is a function of c-rate, and z is the power-law coefficient that considers 0.55 [45]. The activation energy E_a (J/mol) as a function of c-rate can be calculated by (16) [45].

$$E_a\ (c) = 31700 - 370.3c \tag{16}$$

It should be mentioned that the authors of [45] use 1c (c = 1), which is equivalent to 2 A, by de-rating the nominal battery cell capacity from 2.3 Ah to 2 Ah to provide (16) and Table VI. In this study, c-rate changes with battery current, and interpolation is used to update the value of the $B(c)$ related to the c-rate. When a battery approaches its EOL in a vehicle application, it has lost 20% of its capacity. Therefore, based on EOL, the

Authorized licensed use limited to: Universite du Quebec a Trois-Rivieres. Downloaded on April 21,2025 at 18:19:44 UTC from IEEE Xplore. Restrictions apply.

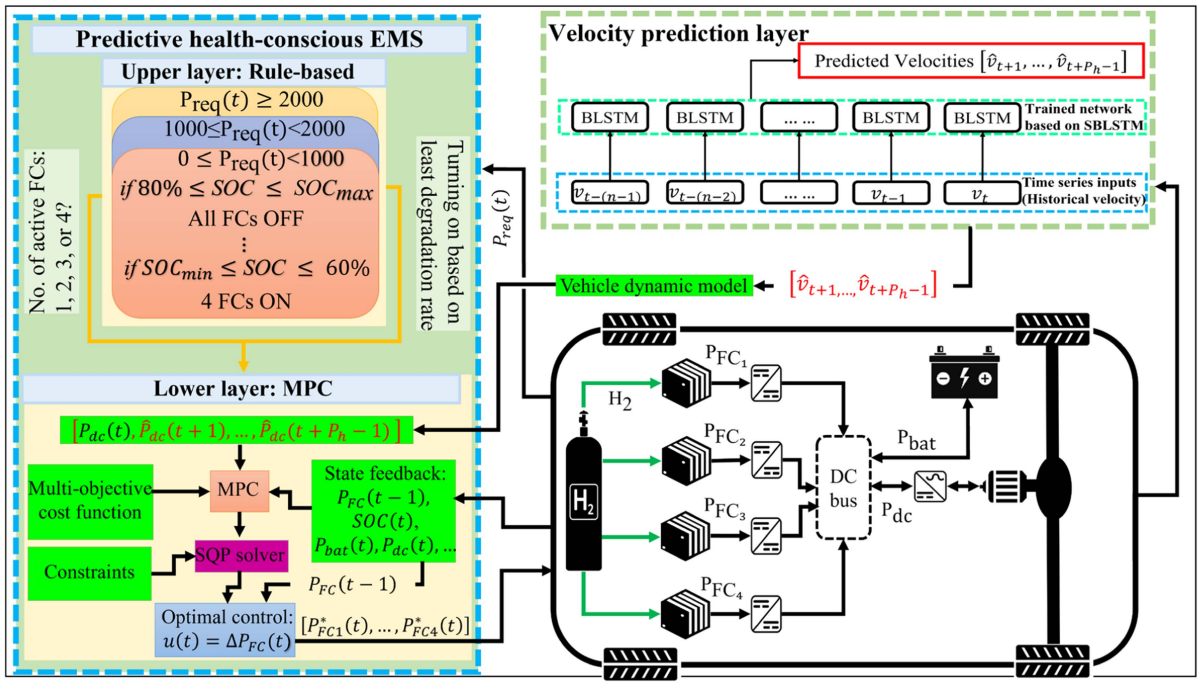

Fig. 5. The PHC- EMS basic idea.

relevant battery throughput (Ah) can be calculated by (17). The battery's total number of cycles until it reaches its EOL is shown in (18) [46].

$$A_{EOL}(c) = \left[\frac{20}{B(c)\exp\left(\frac{-E_a(c)}{R_C T_C}\right)}\right]^{1/z} \tag{17}$$

$$N_{EOL}(c) = \frac{A_{EOL}(c)}{Q_{cell}} \tag{18}$$

Therefore, the battery state of health (SOH) and rate of SOH alteration can be defined by (19) [46].

$$SOH(t) = 1 - \frac{\int_0^t |I_{batt,cell}(t)|\,dt}{2\,N_{EOL}(c)\;Q_{cell} * 3600}$$

$$\dot{SOH}(t) = -\frac{|I_{batt,cell}(t)|\,\Delta t}{2\,N_{EOL}(c)\;Q_{cell} * 3600} \tag{19}$$

where $I_{batt,cell}$ represents the current flowing through a single cell, the initial SOH is assumed to be 100%. (20) show the relationship between capacity reduction and battery internal resistance [47].

$$R_{inc}(t) = \frac{Q_{loss}(t) - 0.0073}{13.656} \tag{20}$$

where $Q_{loss}(t)$ is the amount of capacity reduction in each sampling time, and $R_{inc}(t)$ is the amount of increased battery internal resistance.

III. Energy Management Strategy

A PHC-EMS is developed in this investigation to reach the minimum total operating cost. The results of the proposed EMS are compared with the DP, a well-known global optimization algorithm, and ECMS.

A. PHC-EMS

The proposed PHC-EMS consists of three main parts, as shown in Fig. 5. The first part is a rule-based strategy called the upper layer that is used to designate how many FC should be turned on and take part in the optimization layer. The second part is an MPC, developed in the lower layer, employed to distribute optimal power among FCs and the battery. The third part is a driving cycle predictor called SBLSTM, a novel approach for predicting velocity. The following sections introduce these three parts in detail.

1) Upper Layer: Rule-Based Strategy: Operating all active FCs in the same manner throughout an entire driving cycle in a multi-stack system is unrealistic and can increase operating cost. In some circumstances, turning off some stacks during the driving cycle can reduce hydrogen consumption and enhance system reliability and durability. Therefore, a dependable and advanced EMS should be able to deactivate or reduce the output power of sub-stacks to prevent further degradation and decrease hydrogen consumption. The rules of this layer are shown in Table VII. The performance differences among sub-stacks affect the operating cost of a multi-stack system in two key ways: 1) Reducing the rate of FC degradation, and 2) Lowering hydrogen consumption.

At each time step, the upper layer selects the minimum number of FCs needed based on their degradation rates. For example, if two FCs are required, it chooses those with the lowest degradation. If FC1 and FC4 are less degraded than FC2 and FC3, FC1 and FC4 are used, while the others are turned off to prevent

Authorized licensed use limited to: Universite du Quebec a Trois-Rivieres. Downloaded on April 21,2025 at 18:19:44 UTC from IEEE Xplore. Restrictions apply.

TABLE VII
RULES OF UPPER LAYER STRATEGY

Conditions \ P_{req}	Range of requested power (kW)		
	$0 \le P_{req} < 1$	$1 \le P_{req} < 2$	$P_{req} > 2$
	Number of active FCs		
$80 \le SOC < SOC_{max}$	All OFF	2 FCs	3 FCs
$70 \le SOC < 80$	1 FC	3 FCs	4 FCs
$60 \le SOC < 70$	3 FCs	4 FCs	4 FCs
$SOC_{min} \le SOC < 60$	4 FCs	4 FCs	4 FCs

additional degradation. In other words, FCs with higher output power and lower voltage degradation are considered younger and are given the highest priority for participation in the lower layer. As a result, the upper layer aims to keep all sub-stacks at a similar degradation rate, which is crucial in a multi-stack FC system. This approach enhances system reliability and durability while also reducing operating cost. On the other hand, another goal of the upper layer is to activate the minimum number of FCs to lower hydrogen consumption, which significantly impacts operating cost. By determining when to activate or deactivate FCs, the upper layer aims to turn off unnecessary FCs and minimize hydrogen consumption. In addition, using a rule-based EMS enhances the system's capability for real-world applications because the upper layer minimizes the number of active FCs at each time step, reducing the size of the control parameter matrices and decreasing the computational burden.

2) Lower Layer: MPC: Following the notion of the receding horizon, MPC employs a nonlinear model of the process to forecast and optimize the system's future behavior [48]. The first elements of finite horizon optimal control sequences are calculated repeatedly along the closed loop solution in MPC. When using MPC, the controller solves an optimal control problem at each sampling instant, producing an optimal succession of future input values that guides the process toward the desired state. At the subsequent sampling time, only the first component of this optimal sequence is applied to the process [48]. The nonlinear problem is written as the state-space model in MPC. Typically, in such a problem the SOC is a state variable and FC power is the control variable. This study uses the increment of FC power as a control variable, and the state-space formulation is written as (21)–(22).

$$\Delta x\ (t+1) = A\Delta x\,(t) + B\Delta u\,(t) + E\Delta d\,(t) \tag{21}$$

$$\begin{cases} \Delta x\ (t) = \Delta SOC\ (t) = \frac{SOC(t)-SOC(t-1)}{\Delta t} \\ \Delta u\ (t) = \Delta P_{FC}\ (t) = \frac{P_{FC}(t)-P_{FC}(t-1)}{\Delta t} \\ \Delta d\ (t) = \Delta P_{dc}\ (t) = \frac{P_{dc}(t)-P_{dc}(t-1)}{\Delta t} \end{cases} \tag{22}$$

where $x(t)$ is the SOC, $u(t)$ is the FC power, and $d(t)$ is the requested power that is modeled as a disturbance in this formulation. A, B, *and* E are the matrix of coefficients. t shows the time step and Δt is the sampling time that considers 1s in this study. Prediction horizon (P_h), and control horizon (C_h) are two important parameters in MPC. P_h is often equal to or larger than C_h in a typical MPC. In this paper, P_h and C_h are equal and set to 10 s same as the predicted velocity horizon. The utilized multi-objective cost function is based on operating cost ($). The total operating cost consists of hydrogen consumption (C_{H_2}), FC degradation ($C_{FC,deg}$), and battery degradation ($C_{bat,deg}$). Among the sequence of FC optimal powers over the prediction horizon $[\Delta P^*_{FC}(t),\ \Delta P^*_{FC}(t+1), \ldots,\ \Delta P^*_{FC}(t+P_h-1)$, MPC selects the first element as the optimal result based on the receding horizon principle.

$$\min_{\Delta P_{FC}(t+k), k\in\{0,1,\ldots,P_h-1\}} J_t = C_{H_2,t} + C_{FC,deg,t} + C_{bat,deg,t} + k_{SOC,t}\ (\$) \tag{23}$$

$C_{H_2,t}$ is the total hydrogen consumption of four FCs over the t^{th} horizon.

$$C_{H2,t} = \alpha_{H_2}\ (C_{H2,FC1,t} + \ldots + C_{H2,FC4,t})\ (\$) \tag{24}$$

The hydrogen consumption of each FC is a polynomial function of FC power, as shown in (4). α_{H_2} is the cost of hydrogen per kilogram (4 $/kW). The cost of FC degradation ($C_{FC,deg,t}$) was explained with details in the FC degradation part. The cost of battery degradation ($C_{bat,deg,t}$) over the t^{th} horizon can be calculated as follows.

$$C_{bat,deg,t} = (SOH\,(t) - SOH\,(t+P_h)\ \varphi_{bat}\ P_{bat,rated}\ (\$) \tag{25}$$

where φ_{bat} is the unit of battery pack price (178.41 $/kWh), and $P_{bat,rated}$ is the battery pack total power which is 0.55 kWh. The last part of the multi-objective cost function is $k_{SOC,t}$ that is a penalty term to ensure the battery charge-sustaining approach.

$$k_{SOC,t} = w_{SOC} \sum_{k=0}^{P_h} (SOC\,(t+k) - SOC_{int})^2 \tag{26}$$

where w_{SOC} is a penalty gain that needs to be tuned. In the simulation, SOC for all EMSs must end at the same point for fair comparison. To achieve this, the penalty gain is tuned for each driving cycle, ensuring SOC returns to its initial level. Therefore, w_{SOC} is the only parameter needing adjustment ensuring unbiased EMS comparisons. The considered constraints on the FC operation are as follows.

$$\begin{cases} P_{FC,\min} \le P_{FC}\,(t+k) \le P_{FC,\max} \\ \Delta P_{FC,\min} \le P_{FC}\,(t+k) - P_{FC}\,(t+k-1) \le \Delta P_{FC,\max} \end{cases} \tag{27}$$

$P_{FC,\min}$ is zero, $P_{FC,\max}$ is 500 W, and $\Delta P_{FC,\min}$ and $\Delta P_{FC,\max}$ are -50 and 50 W/s respectively. Battery constraints consist of battery power, SOC, and SOH as follows.

$$\begin{cases} SOC\ (0) = 70\% \\ SOC_{\min} \le SOC\,(t+k) \le SOC_{\max} \\ SOH\,(0) = 100\% \\ SOH_{\min} \le SOH\,(t+k) \le SOH_{\max} \\ P_{bat,\min} \le P_{bat}\,(t+k) \le P_{bat,\max} \end{cases} \tag{28}$$

where $SOC_{\min}$ is 50%, $SOC_{\max}$ is 90%, $SOH_{\min}$ is 0%, and $SOH_{\max}$ is 100%. $P_{bat,\min}$ and $P_{bat,\max}$ are -1900 and

Authorized licensed use limited to: Universite du Quebec a Trois-Rivieres. Downloaded on April 21,2025 at 18:19:44 UTC from IEEE Xplore. Restrictions apply.

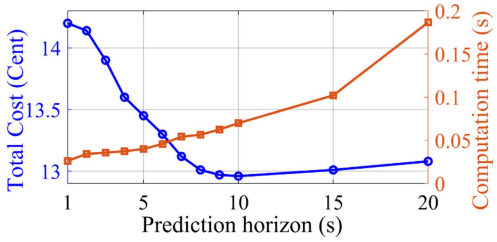

Fig. 6. Comparison of total cost and computation time per step as a function of P_h.

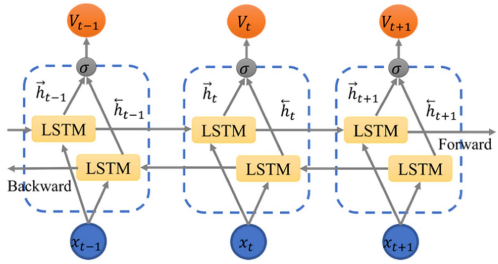

Fig. 7. The BLSTM unfolded structure in three successive steps.

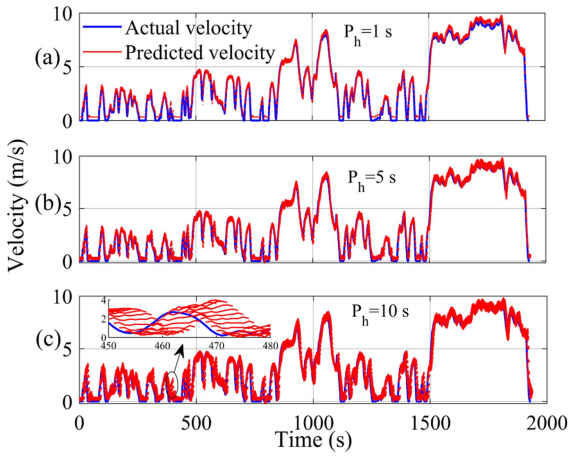

Fig. 8. SBLSTM performance in three different prediction horizons for INRETS driving cycle.

1900 W respectively. The sequential quadratic programming (SQP) algorithm is a common algorithm for solving a receding horizon optimization problem among the numerous optimization algorithms. The convergence and computational efficacy of the SQP are satisfactory to use in a real-time application like FC-HEVs [22], [29].

3) Impact of P_h on Total Cost and Computational Time: In the MPC approach choosing a suitable P_h is very important and affects the optimal results. By increasing P_h, the computation time increases, and total cost decreases. According to Fig. 6, $P_h = 10\ s$ has the minimum total cost and its computation time per step is appropriate for real-time problems. Fig. 6 indicates that when the P_h exceeds 10 s, the accuracy of MPC results declines. This decrease is a result of the diminishing quality and precision of predicted velocities beyond the 10 s. As a result, following MPC theory, augmenting the P_h results in improved and more precise outcomes. However, as depicted in Fig. 6, the decline in MPC result accuracy beyond the $P_h = 10\ s$ is associated with the reduction of accuracy in predicted velocities after 10 s.

4) Velocity Predictor (SBLSTM): This study aims to go beyond typical prediction methods by using a new approach to improve accuracy. Accurate velocity prediction significantly impacts the performance of the predictive EMS and can make a big difference. To achieve this, the authors use SBLSTM networks to boost prediction accuracy and performance. Deep neural networks, such as the LSTM network, can be used to process historical velocity series as motion information for better prediction. LSTM is a strong variant of the recurrent neural network (RNN) that has solved the gradient vanishing problem [49]. The information in the LSTM is normally transmitted positively from time step $t-1$ to time step t. As a result, the LSTM structure only uses forward dependencies. However, it is quite likely that relevant information is filtered out or not properly conveyed via the chain-like gated structure in a time series prediction process. Consequently, it could be beneficial to consider backward dependencies, which transfer information in the other direction. As a consequence, in this study, a bidirectional LSTM (BLSTM) with the capacity to handle both forward and backward dependencies is used as a component of the network structure. In Fig. 7, the structure of an unfolded BLSTM layer, which has a forward LSTM layer and a backward LSTM layer, is described.

The forward layer output sequence, $\vec{h}$, is computed iteratively using positive sequence inputs from time $t-n$ to time $t-1$, whereas the backward layer output sequence, $\overleftarrow{h}$, is created using inputs from time $t-1$ to $t-n$. The BLSTM layer produces an output vector, V_t, in which each element is computed by (29).

$$V_t = \sigma\left(\vec{h}, \overleftarrow{h}\right) \tag{29}$$

where σ is the activation function. The input data (x_t) is the historical velocity sequence, and the output data (V_t) is the predicted velocity sequence.

Deep BLSTM architectures are networks with several stacked BLSTM hidden layers, where the output of one BLSTM hidden layer is used as the input for the next BLSTM hidden layer. This study utilized 11 different driving cycles for training, which together form a combined driving cycle with a total duration of 11170 s. Fig. 8 shows the comparison between predicted and actual velocities of the INRETS driving cycle by the SBLSTM approach. This study uses the stacked layers technique, which can improve the power of neural networks. Root Mean Square Error (RMSE) and R-square are presented in Table VIII. According to the results, RMSE increases by increasing P_h.

TABLE VIII
PERFORMANCE COMPARISON OF THREE DIFFERENT VELOCITY PREDICTORS

P_h (second)	RMSE (m/s)			R-square		
	SBLSTM	BLSTM	LSTM	SBLSTM	BLSTM	LSTM
1 *s*	0.211	0.332	0.385	0.994	0.989	0.981
5 *s*	0.560	0.692	0.765	0.955	0.942	0.925
10 *s*	0.955	1.001	1.225	0.866	0.858	0.851

Authorized licensed use limited to: Universite du Quebec a Trois-Rivieres. Downloaded on April 21,2025 at 18:19:44 UTC from IEEE Xplore. Restrictions apply.

Table VIII illustrates that the SBLSTM has a solid capacity to predict the far future velocities with minimum RMSE compared to other methods. It is worth mentioning that the SBLSTM algorithm takes 15 s of previous velocities in each time step as historical data and predicts future velocities.

B. Dynamic Programming (DP)

As stated in the previous sections, DP is an appropriate baseline for validating the outcomes of new EMSs for FC-HEVs. DP, as a global optimization, is aware of the whole driving cycle in advance. In each step, DP by knowing what is happening in the future takes control actions. The MATLAB code described in [50] is used in this study to solve the energy management problem using the DP algorithm. According to (30), the state and control variables must be identified in the DP as the initial stage. This research considers SOC as the state variable (x_k), whereas FC power is regarded as the control signal (u_k).

$$\begin{cases} x_{k+1} = F\left(x_k, u_k\right) + x_k, \ k = 0, 1, \ldots, N-1 \\ x_k = SOC \\ u_k = P_{FC} \\ N = \frac{t_f}{t_s} + 1 \end{cases} \tag{30}$$

where t_f is the time at the end of the driving cycle, and t_s is the sampling time. The subsequent step is to discretize the continuous-time model into the discrete-time model, as shown in (31). The multi-objective cost function of DP is shown in (31). The constraints for the DP problem are the same as those established for MPC.

$$J_t = \min \sum_{t=0}^{N-1} C_{H_2}\left(t\right) + C_{FC,deg}\left(t\right) + C_{bat,deg}\left(t\right) \ (\$) \tag{31}$$

C. Equivalent Consumption Minimization Strategy (ECMS)

One of the real-time optimization-based EMSs is ECMS which tries to convert battery electrical energy to equivalent hydrogen consumption to reduce the overall hydrogen consumption of the FC system [26]. The ECMS Hamiltonian function is shown in (32).

$$C_{H_2}\left(t\right) = C_{H_2,FC}\ \left(t\right) + k\, C_{H_2,bat}\left(t\right) \tag{32}$$

$C_{H_2,FC}$ represents the hydrogen consumption of the FC, $C_{H_2,bat}$ is the equivalent hydrogen consumption of the battery. k is a penalty coefficient and its role in this strategy is to regulate the equivalent fuel consumption of the battery system to minimize the difference from the target SOC [10]. The battery equivalent hydrogen consumption is a function of the FC average hydrogen consumption, average power, the battery power, and the battery's efficiency during charging and discharging [51]. The coefficient k is calculated as shown in (33).

$$k = 1 - \frac{2\,\omega\ \left(SOC\left(t\right) - 0.5\left(SOC_{\max} + SOC_{\min}\right)\right)}{SOC_{\max} + SOC_{\min}} \tag{33}$$

ω is a balance coefficient that affects the rate of change in the SOC and should be set according to the driving cycle. ECMS is categorized as local optimization-based EMS, making instantaneous decisions based on the current state of the system without considering future events. In other words, ECMS employs the current vehicle velocity and takes the control action based on the instantaneous velocity. Regarding ECMS, in each time step, the next velocity ($\hat{v}(t+1)$) is predicted based on the historical velocity matrix then requested power is calculated and sent to the ECMS as an EMS unit. Therefore, the ECMS employs the predicted velocity for the next time step. To make a fair comparison between DP, PHC-EMS, and ECMS, the cost function of all three approaches should be the same. The multi-objective cost function of ECMS is the same as MPC and DP, which consists of hydrogen consumption, FC degradation, and battery degradation. The constraints for the ECMS are the same as those established for MPC and DP.

TABLE IX
METHODOLOGY COMPARISON

Features	DP	PHC-EMS	ECMS
Optimality	Global	Local	Local
Approach	Multiple time-point	Multiple time-point	Single time-point
Awareness of the future	Yes	Yes	No
Computational time per step (ms)	370	70	37
Total computational burden	709 s	135 s	71 s
Feasibility for real-world applications	No	Yes	Yes

D. Analyzing Complexity, Computational Time, and Feasibility in Real-World Application for Three Different EMSs

This section is dedicated to a comparison between different features of the DP, PHC-EMS, and ECMS. The results in Table IX are based on the INRETS driving cycle, which lasts 1925 s. According to the results, ECMS shows better real-time performance compared to PHC-EMS and DP. This is because ECMS focuses only on the present moment without considering future events. For PHC-EMS, the computational time per step is around 70 ms, which is higher than ECMS with 37 ms. This difference occurs because PHC-EMS utilizes a prediction horizon of 10 s, requiring the solution of larger matrices than ECMS. Although PHC-EMS has a slightly longer computational time per step, the results indicate that this leads to better operating cost and power distribution. This is reasonable as a bit more computational effort can yield better outcomes. DP has a computational time per step of approximately 370 ms, which is significantly longer than both ECMS and PHC-EMS. The reason for this is that DP needs to process the entire driving cycle beforehand, resulting in a longer time to generate optimal results. In terms of total computational time, ECMS takes 71 s, PHC-EMS takes 135 s, and DP takes 709 s. This shows that DP is not suitable for real-time applications like FC-HEV.

According to the results, PHC-EMS sacrifices a reasonable amount of time by adding complexity to the EMS to achieve better results and reduce the operating cost of multi-stack FC-HEVs. As shown in Table IX, the computational time of PHC-EMS is suitable for real-world applications, and the slight

Authorized licensed use limited to: Universite du Quebec a Trois-Rivieres. Downloaded on April 21,2025 at 18:19:44 UTC from IEEE Xplore. Restrictions apply.

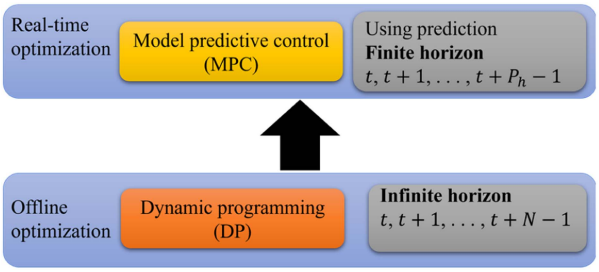

Fig. 9. MPC creation from DP concept.

increase in computational burden compared to ECMS does not compromise the applicability of PHC-EMS for real-world use. As a result, PHC-EMS has a viable capacity for use in real-time applications and experimental tests, thanks to its reasonable computational time. PHC-EMS could be a reasonable compromise between a single time-point strategy like ECMS and offline optimization like DP. PHC-EMS by using the prediction is a multiple time-point strategy that considers a finite prediction horizon and its results are near the global optimal. According to Fig. 9, PHC-EMS is a bridge between local and global optimization by using prediction and considering a finite prediction horizon. PHC-EMS tackles DP shortcomings such as offline applicability and high computational burden by considering a finite horizon and using receding horizon principle. As a result, there is a trade-off between computational time and optimal results. According to the results and Table IX, the multi-stack FC-HEV under PHC-EMS achieves lower operating cost by reasonably increasing computational time. This strategy uses prediction to improve results. Table IX shows that the computational time of PHC-EMS is within a reasonable and feasible range for real-world applications. Therefore, it is worth using PHC-EMS because it can achieve lower operating cost, which is crucial in a multi-stack configuration.

All simulations and methods in this paper were executed using MATLAB on a system equipped with an Intel Core i7-6500 CPU operating at 3.30 GHz (base frequency) and 2.50 GHz (max turbo frequency), with a clock speed of 2592 Mhz, featuring 2 cores and 4 logical processors.

IV. Result and Discussion

This section evaluates the effectiveness of the PHC-EMS and compares the results to DP as a benchmark and ECMS as a single time-point EMS. Two different driving cycles are employed in this investigation to analyze the performance of the proposed EMS. Fig. 10 presents the utilized driving cycles.

A. Results Analysis Under INRETS Driving Cycle

Fig. 11(b)–(e) demonstrates the FCs power distribution with three different strategies. Each strategy's primary goal is to decrease the overall operating cost, including hydrogen consumption, FC degradation, and battery degradation

From 0 to 870 s, the driving cycle is in low velocity mode. During this time, the FCs in the PHC-EMS work less and are off most of the time, and the battery has enough power to supply

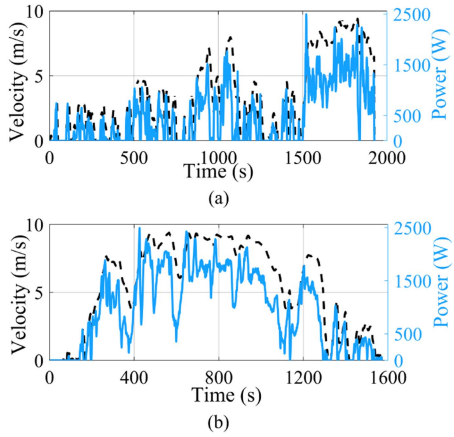

Fig. 10. Driving cycles: (a) INRETS; (b) WVUINTER.

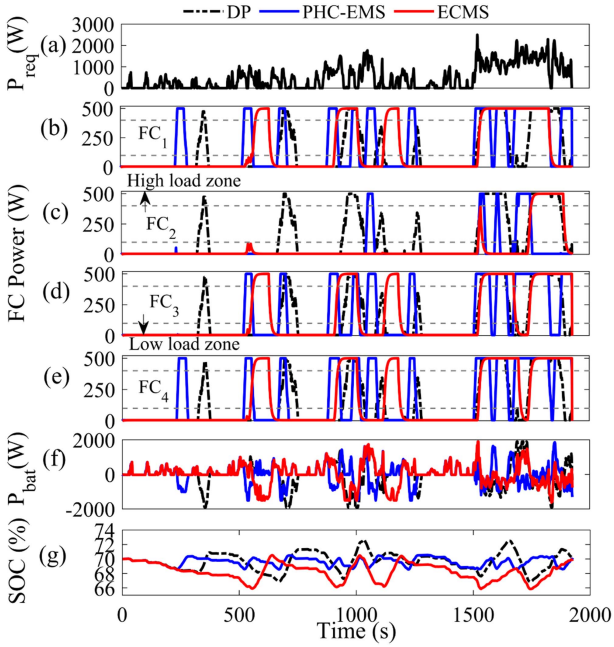

Fig. 11. Results comparison between three different strategies for the INRETS driving cycle: (a) Requested power; (b) FC_1 power; (c) FC_2 power; (d) FC_3 power; (e) FC_4 power; (f) battery power; (g) SOC.

the requested power. According to Fig. 11(b)–(e), FC1 and FC4 work more than FC3 and FC2, due to the rotation rule of the upper layer, which indicates that FC1 and FC4 are less degraded and younger than FC2 and FC3 and have the highest priority to share power. In other words, the proposed PHC-EMS states that two FCs are often sufficient to deliver the requested power in the low velocity zone, and the remaining FCs work less. Indeed, the role of the upper layer in FC power distribution is to utilize the minimum number of active FCs to reduce both FC degradation rate and hydrogen consumption. At each time step, the criteria for choosing the active FCs are those with the lowest degradation. This approach enables the system to deactivate the most degraded FCs, preventing further degradation and ensuring that all FCs have similar degradation rate, which is an important factor in multi-stack FC-HEVs. On the other hand,

Authorized licensed use limited to: Universite du Quebec a Trois-Rivieres. Downloaded on April 21,2025 at 18:19:44 UTC from IEEE Xplore. Restrictions apply.

TABLE X
ANALYTIC COMPARISON BETWEEN THREE STRATEGIES FOR INRETS DRIVING CYCLE

Strategy	H_2 Consumption (g)	High load (s)	Low load (s)
DP	16.640	1304	5356
PHC-EMS	17.449	1631	5618
ECMS	19.012	1683	5697

the upper layer attempts to use the minimum number of FCs at each time step to reduce hydrogen consumption by deactivating unnecessary sub-stacks.

From Fig. 11(b)–(e), the proposed PHC-EMS activates two FCs (FC1 and FC4) at around 250 s, followed by DP, which utilizes all the FCs at approximately 350 s. However, ECMS does not activate any FCs during the first 500 s when the requested power is low. From 871 to 1270 s the driving cycle is in the medium velocity mode and for meeting the requested power and sustaining SOC more FCs should share the power. In the medium velocity sector, FC1, FC3, and FC4 are less degraded and known as the younger FCs in the PHC-EMS and they work more than FC2. From 1271 to 1500, the driving cycle is again in the low velocity zone and all FCs are off because the battery supplies the requested power. The velocity is high from 1501 s to the end of the driving cycle, and all FCs should operate at high power to fulfill the requested power and SOC. Because DP is aware of the whole driving cycle it prefers to turn off all FCs or reduces their output power uniformly instead of activating some of the FCs. In fact, DP by choosing the best trajectory of the battery SOC employs the battery power efficiently to reduce the FCs output power and degradation. That is why the FCs in the DP spend less time in high and low load zones. The comparison of the power signals during this time span shows that ECMS operates the FCs in their high power zones more frequently than the other strategies to sustain SOC, as it activates the FCs later than the others at the start of the driving cycle. Table X shows the analytic results of DP, PHC-EMS, and ECMS from Fig. 11(b)–(e) that compare hydrogen consumption and total time working in high and low power zones. The total time of high and low power zones is the sum of four FCs. It is noteworthy that each FC has one start-stop cycle during the driving cycle.

According to Table X, DP spends less time in high load zone than other strategies and consumes less hydrogen. PHC-EMS shows close performance to DP by consuming 4.363% more hydrogen than DP and 8.958% less hydrogen than ECMS. PHC-EMS spends less time in high and low load zones than ECMS, leading to less FC degradation cost.

Fig. 11(f) and (g) illustrates the battery power and SOC trajectory obtained from the three different strategies. According to Fig. 11(g), due to awareness of the whole driving cycle, DP tries to use the higher domain of SOC to reduce FC degradation and hydrogen consumption. SOC trajectory reveals PHC-EMS prediction capacity. According to Fig. 11(g), since ECMS tries to reduce hydrogen consumption as a prominent part of the total operating cost, the battery SOC decreases until 550 s. However, since it is not a predictive approach, it just focuses on the current step time. This intrinsic characteristic can increase hydrogen consumption and FC degradation in some working

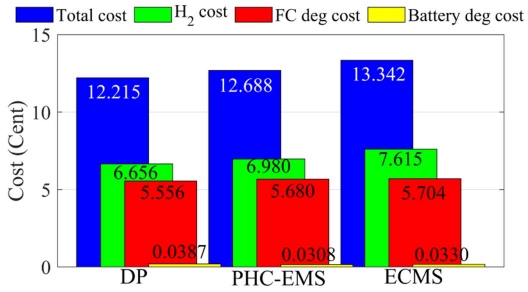

Fig. 12. Total cost comparison between three different strategies for INRETS driving cycle.

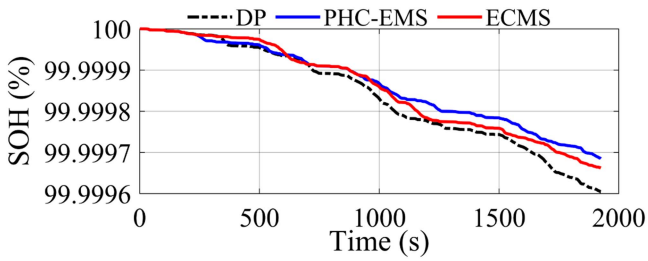

Fig. 13. Battery SOH trajectory analysis among three different strategies for INRETS driving cycle.

points because FCs need to operate more to sustain SOC and supply the requested power. On the other hand, due to the predictive feature of PHC-EMS, it decreases battery SOC up to 250 s and then recharges the battery.

This difference in SOC trajectory shows that PHC-EMS can perform better than a single time-point strategy like ECMS by considering future events. According to Fig. 11(g), DP utilizes the SOC in a wider range to reduce the total operating cost because the cost of the battery degradation is less than others and it is better to sacrifice the battery degradation in favor of the total cost reduction.

Fig. 12 shows the total operating cost of DP, PHC-EMS, and ECMS. The total operating cost of DP, PHC-EMS, and ECMS are 12.215, 12.688, and 13.342 cents, respectively. DP as a benchmark for optimal control decision problems has the best result. Hydrogen consumption is the most critical part of the operating cost in the multi-stack FC-HEV. The proposed strategy in this paper can lead to close results to DP in terms of hydrogen consumption while preventing an extreme increase in the degradation of FC and battery. The total operating cost of PHC-EMS is 3.728% more than DP, and 5.154% less than ECMS.

Fig. 13 shows the battery SOH trajectory across different strategies. According to Figs. 11(g) and 13, DP utilizes a broader SOC range to reduce operating cost. However, this usage pattern decreases the battery SOH. In fact, due to the lower weight of battery degradation cost compared to hydrogen cost and FC degradation cost, as shown in Fig. 12, DP prefers to sacrifice battery health in favor of reducing total operating cost. PHC-EMS uses a tighter SOC range, resulting in less battery SOH degradation compared to DP and ECMS. According to Fig. 13,

Authorized licensed use limited to: Universite du Quebec a Trois-Rivieres. Downloaded on April 21,2025 at 18:19:44 UTC from IEEE Xplore. Restrictions apply.

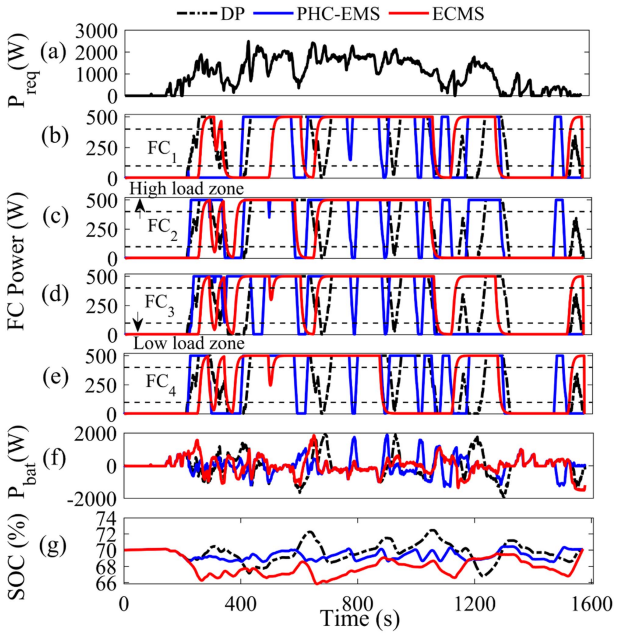

Fig. 14. Results comparison between three different strategies for the WVUINTER driving cycle: (a) Requested power; (b) FC_1 power; (c) FC_2 power; (d) FC_3 power; (e) FC_4 power; (f) battery power; (g) SOC.

TABLE XI
ANALYTIC COMPARISON BETWEEN THREE STRATEGIES FOR WVUINTER DRIVING CYCLE

Strategy	H_2 Consumption (g)	High load (s)	Low load (s)
DP	27.252	2508	2664
PHC-EMS	27.966	2839	2971
ECMS	29.394	2856	2993

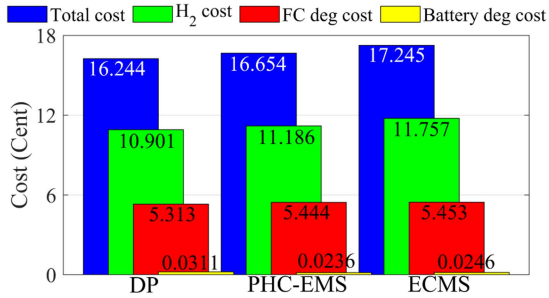

Fig. 15. Total cost comparison between three different strategies for WVUINTER driving cycle.

while the difference in SOH may appear minimal due to the length of the driving cycle in this study, its practical significance is crucial for the long-term operation of the system, as it impacts the battery degradation rate, multi-stack FC-HEV operating cost, and overall system reliability. For this purpose, the goal of designing the PHC-EMS is to account for the health state of the multi-stack FC-HEV components while managing optimal power distribution.

This approach aims to maintain the power sources in good condition, making the multi-stack FC-HEV more cost-effective and reliable.

B. Results Analysis Under WVUINTER Driving Cycle

WVUINTER is a high velocity driving cycle and can be a good choice to assess the performance of the proposed strategy in this work. Fig. 14(b)–(e) shows the power distribution for each FC under three different strategies. According to Fig. 14(b)–(e), from 0 to 400 s, the driving cycle is in the medium velocity mode, and the PHC-EMS decides to employ 3 FCs during this period. From 0 to 250 s, all FCs are off and the battery is enough to supply the requested power. From 251 to 400 s, the PHC-EMS designates that FC2 and FC3 should operate more than FC4 because they are less degraded than FC1 and FC4. In this period, the ECMS turns on all FCs to meet the requested power and battery SOC. From 401 to 1200 s, almost all FCs work in high power most of the time because the driving cycle is in high velocity mode. Fig. 14(b)–(e) illustrates that in high velocity mode, FCs in the ECMS work more time in high power than those in the PHC-EMS. From 1201 s to the end of the driving cycle, the FCs are off most of the time because the driving cycle is in low velocity mode. In this period, FCs in the ECMS work harder compared with FCs in the PHC-EMS. DP with knowledge of the whole driving cycle prefers to employ the FCs equally during the entire driving cycle. Since this driving cycle represents a high velocity driving condition, each FC should perform in the high load zone for more time to supply the requested power and sustain the battery SOC. Therefore, an effective strategy should be able to reduce the FC operation time in the high load zone in this condition to diminish the degradation and hydrogen consumption. This is due to the fact that the operation in the high load zone causes the highest degradation rate after the start-stop cycle.

Table XI compares the effectiveness of the three strategies regarding hydrogen consumption and total working time in high and low load zones. According to Fig. 14(b)–(e) and Table XI, DP has achieved the lowest cost as expected. The results of PHC-EMS show that the FC system works 17s and 22s less than ECMS in the high and low load zones throughout the driving cycle and consumes less hydrogen. The results show the potential of the PHC-EMS to reduce the total operating cost. The proposed strategy consumes 2.553% of hydrogen more than DP and 5.106% less than ECMS.

Fig. 15 indicates the total cost comparison among DP, PHC-EMS, and ECMS under the WVUINTER driving cycle. 16.244, 16.654, and 17.245 cents, respectively, are the total operating costs for DP, PHC-EMS, and ECMS.

The battery SOH trajectory for the three different strategies is shown in Fig. 16. According to Figs. 14(g) and 16, DP utilizes a wider SOC range, resulting in greater battery SOH degradation compared to PHC-EMS and ECMS. This occurs because, according to Fig. 15, the cost of battery degradation is significantly lower than the costs associated with hydrogen consumption and FC degradation, prompting DP to sacrifice the cheaper component to minimize total operating cost. In contrast, PHC-EMS uses a narrower SOC range and maintains the best SOH among all the strategies. The results indicate that PHC-EMS can achieve closer outcomes to DP, and this performance originates from the predictive and heal-conscious ability

Authorized licensed use limited to: Universite du Quebec a Trois-Rivieres. Downloaded on April 21,2025 at 18:19:44 UTC from IEEE Xplore. Restrictions apply.

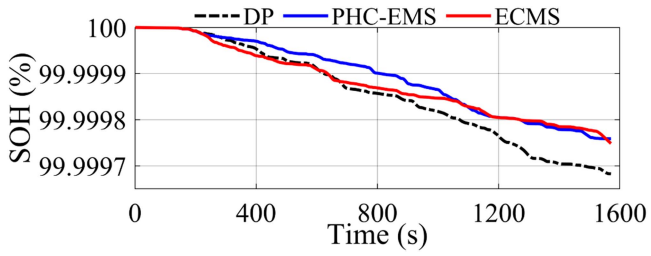

Fig. 16. Battery SOH trajectory analysis among three different strategies for WVUINTER driving cycle.

of the proposed strategy. The total operating cost of PHC-EMS is 2.462% more than DP, and 3.550% less than ECMS.

In summary, while DP remains the benchmark for optimal solutions, its computational burden limits its practical use in real-time applications. PHC-EMS, on the other hand, offers a practical alternative, providing nearly optimal results with reasonable computational burden, making it an excellent choice for real-world FC-HEV applications. The slight increase in operating cost is a sensible trade-off for the significant gains in computational efficiency and real-time applicability.

C. The Effectiveness of the PHC-EMS and Velocity Predictor

This section aims to analyze the effectiveness of the upper layer and SBLSTM, as well as their impact on the results of the PHC-EMS.

1) Effectiveness of the PHC-EMS: To demonstrate the effectiveness of the proposed EMS, the results of the PHC-EMS are compared with the conventional MPC under the INRETS driving cycle. The objective function of both the PHC-EMS and the conventional MPC is the same. However, in the conventional MPC, the upper layer is removed, and only the conventional MPC is responsible for distributing power among the FCs and the battery. In other words, this part aims to highlight the role and importance of the two-layer EMS for a multi-stack FC-HEV. In the upper layer, the main purpose of activating the minimum number of FCs is to reduce hydrogen consumption, which has the greatest impact on operating cost. In fact, by deciding when to activate or deactivate the FCs, the upper layer aims to reduce unnecessary fuel consumption that can occur in conventional MPC, where all FCs operate in a similar manner. The results in Fig. 17 show that FCs under the PHC-EMS operate for 5618 s in the low load zone, whereas FCs under conventional MPC operate for only 4300 s in this zone. The 1318 s difference demonstrates that the upper layer in the PHC-EMS effectively reduces the number of active FCs in unnecessary situations to lower hydrogen consumption, which explains why the FCs under PHC-EMS spend more time in the low load zone. The results in Fig. 17 also show that FCs under PHC-EMS operate for 1631 s in high load zones, whereas FCs under conventional MPC operate for 1804 s. Operating in the high load zone for a longer time is another reason for the higher hydrogen consumption in conventional MPC, further demonstrating the effectiveness of the upper layer in PHC-EMS.

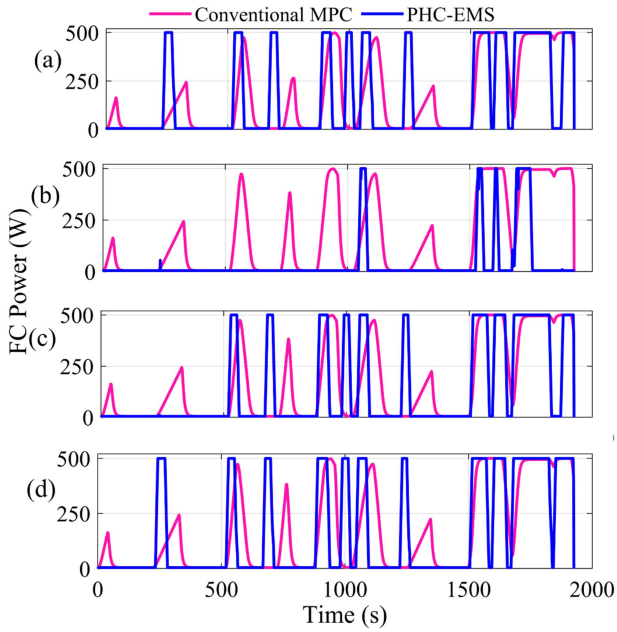

Fig. 17. FCs power distribution under the conventional MPC and PHC-EMS for INRETS driving cycle: (a) FC_1 power; (b) FC_2 power; (c) FC_3 power; (d) FC_4 power.

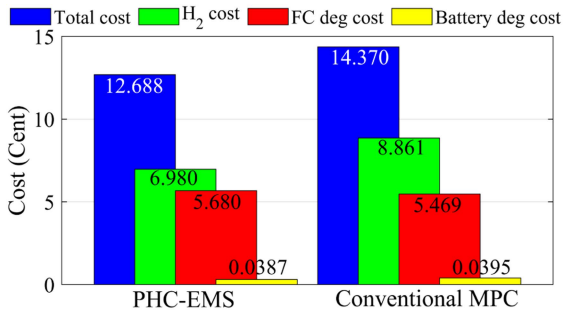

Fig. 18. Total cost comparison between conventional MPC and PHC-EMS for INRETS driving cycle.

According to Fig. 18, the total cost of the PHC-EMS is 11.7% less than that of the conventional MPC. While the degradation cost under conventional MPC is slightly less than that under PHC-EMS, hydrogen consumption plays a key role, and it is lower in PHC-EMS compared to conventional MPC. The results of the PHC-EMS demonstrate that incorporating a suitable and reasonable rule-based layer can lead to improved performance.

2) Effectiveness of the SBLSTM: The quality of the predicted velocities in the MPC is undeniable and can significantly affect the effectiveness of the MPC. The prediction of vehicle velocity plays a crucial role in ensuring the optimal and accurate response of MPC.

Variations in vehicle velocity can influence the durability of power sources and affect fuel economy [35]. The outputs of standard MPC, without velocity prediction, are usually not optimal or accurate. Therefore, MPC needs to adjust its results based on predicted future vehicle velocity. As a result, in real-world applications, knowing the entire driving cycle in advance is impossible. Therefore, a velocity predictor is needed

Authorized licensed use limited to: Universite du Quebec a Trois-Rivieres. Downloaded on April 21,2025 at 18:19:44 UTC from IEEE Xplore. Restrictions apply.

TABLE XII
TOTAL COST COMPARISON BETWEEN THREE VELOCITY PREDICTORS FOR INRETS DRIVING CYCLE

Velocity predictor	SBLSTM	BLSTM	LSTM
Total cost (Cent)	12.688	13.169	13.350

to anticipate future velocities as disturbances for the MPC. For this purpose, this study utilizes a novel velocity predictor called SBLSTM. To demonstrate the effectiveness of the proposed predictor, the results of the SBLSTM are compared with BLSTM and LSTM. According to Table VIII and Fig. 8, the SBLSTM predicts future velocities with higher accuracy than BLSTM and LSTM. The total operating cost of the multi-stack FC-HEV under the PHC-EMS is evaluated using three different velocity predictors for the INRETS driving cycle. According to Table XII, due to the high prediction accuracy of the SBLSTM, the total operating cost with the SBLSTM predictor is 3.653% less than with the BLSTM predictor and 4.959% less than with the LSTM predictor.

V. CONCLUSION

This paper aims to reduce the total operating cost of the multi-stack FC-HEV alongside relieving the degradation of FCs and battery. In this regard, a PHC-EMS is put forward to decrease the total operating cost. The proposed strategy is a multi-layer one that consists of rule-based and optimization strategies. In the upper layer, a rule-based strategy is contrived to designate the number of active FCs in each time step according to the degradation of FCs, requested power, and SOC. This layer is designed to hinder more degradation of each FC and help with less hydrogen consumption. In the lower layer, MPC, as a predictive real-time optimization algorithm, is employed to take the optimal control decision between FCs and the battery. This paper uses a novel deep neural network approach called SBLSTM. The prediction results of the proposed predictor show high accuracy. Two different driving cycles are used to assess the performance of the PHC-EMS. The results are compared with DP and ECMS to indicate the proposed strategy's effectiveness. The results of the INRETS driving cycle show that the total operating cost of PHC-EMS is 3.728% more than DP and 5.154% less than ECMS. In the WVUINTER driving cycle, the results illustrate that the total operating cost of PHC-EMS is 2.462% more than DP and 3.550% less than ECMS. Consequently, the proposed strategy can be a convincing choice to be used in real-time for the energy management of a multi-stack FC-HEV.

A. Future Work

1) In future, the first layer can be replaced with an optimization method to study its influence over the optimality of the performance. On the other hand, the prediction can be added to the proposed EMS to determine the number of active FC in each time step based on the future requested power.
2) This study evaluates the proposed EMS in two phases. The first phase involves comparing it with the ECMS and using DP as a benchmark to demonstrate its effectiveness. The second phase focuses on implementing the proposed EMS in a hardware-in-the-loop (HIL) setup, planned for future use, to enhance the evaluation and validation of the EMS results, ensuring its real-world applicability and performance.

REFERENCES

[1] Z. P. Cano et al., "Batteries and fuel cells for emerging electric vehicle markets," *Nat. Energy*, vol. 3, no. 4, pp. 279–289, 2018, doi: 10.1038/s41560-018-0108-1.
[2] A. Makhsoos, M. Kandidayeni, B. G. Pollet, and L. Boulon, "A perspective on increasing the efficiency of proton exchange membrane water electrolyzers– A review," *Int. J. Hydrogen Energy*, vol. 8, pp. 5341–15370, 2023, doi: 10.1016/j.ijhydene.2023.01.048.
[3] B. Tanç, H. T. Arat, E. Baltacıoğlu, and K. Aydın, "Overview of the next quarter century vision of hydrogen fuel cell electric vehicles," *Int. J. Hydrogen Energy*, vol. 44, no. 20, pp. 10120–10128, 2019, doi: 10.1016/j.ijhydene.2018.10.112.
[4] H. S. Das, C. W. Tan, and A. H. M. M. Yatim, "Fuel cell hybrid electric vehicles: A review on power conditioning units and topologies," *Renewable Sustain. Energy Rev.*, vol. 76, no. 3, pp. 268–291, 2017, doi: 10.1016/j.rser.2017.03.056.
[5] H. Bakhshi Yamchi, H. Shahsavari, N. Taghizadegan Kalantari, A. Safari, and M. Farrokhifar, "A cost-efficient application of different battery energy storage technologies in microgrids considering load uncertainty," *J. Energy Storage*, vol. 22, no. 10, pp. 17–26, 2019, doi: 10.1016/j.est.2019.01.023.
[6] E. Ogungbemi, T. Wilberforce, O. Ijaodola, J. Thompson, and A. G. Olabi, "Selection of proton exchange membrane fuel cell for transportation," *Int. J. Hydrogen Energy*, vol. 46, no. 40, pp. 30625–30640, 2020, doi: 10.1016/j.ijhydene.2020.06.147.
[7] A. Jacome, D. Hissel, V. Heiries, M. Gerard, and S. Rosini, "Prognostic methods for proton exchange membrane fuel cell under automotive load cycling: A review," *IET Elect. Syst. Transp.*, vol. 10, no. 4, pp. 369–375, 2020, doi: 10.1049/iet-est.2020.0045.
[8] D. Energy, "2019 annual progress report: DOE hydrogen and fuel cells program," *DOE Hydrogen Fuel Cells Prog.*, vol. 9, no. 4, 2020, Art. no. 993.
[9] N. Marx, L. Boulon, F. Gustin, D. Hissel, and K. Agbossou, "A review of multi-stack and modular fuel cell systems: Interests, application areas and on-going research activities," *Int. J. Hydrogen Energy*, vol. 39, no. 23, pp. 12101–12111, 2014, doi: 10.1016/j.ijhydene.2014.05.187.
[10] T. Wang, Q. Li, L. Yin, W. Chen, E. Breaz, and F. Gao, "Hierarchical power allocation method based on online extremum seeking algorithm for dual-PEMFC/battery hybrid locomotive," *IEEE Trans. Veh. Technol.*, vol. 70, no. 6, pp. 5679–5692, Jun. 2021, doi: 10.1109/TVT.2021.3078752.
[11] H. Wang, A. Gaillard, Z. Li, R. Roche, and D. Hissel, "Multiple-fuel cell module architecture investigation: A key to high efficiency in heavy-duty electric transportation," *IEEE Veh. Technol. Mag.*, vol. 17, no. 3, pp. 94–103, Sep. 2022, doi: 10.1109/MVT.2022.3179801.
[12] S. Zhou, G. Zhang, L. Fan, J. Gao, and F. Pei, "Scenario-oriented stacks allocation optimization for multi-stack fuel cell systems," *Appl. Energy*, vol. 308, no. 4, 2022, Art. no. 118328, doi: 10.1016/j.apenergy.2021.118328.
[13] Y. Yan, Q. Li, W. Chen, W. Huang, and J. Liu, "Hierarchical management control based on equivalent fitting circle and equivalent energy consumption method for multiple fuel cells hybrid power system," *IEEE Trans. Ind. Electron.*, vol. 67, no. 4, pp. 2786–2797, Apr. 2020, doi: 10.1109/TIE.2019.2908615.
[14] J. Zhou, J. Liu, Y. Xue, and Y. Liao, "Total travel costs minimization strategy of a dual-stack fuel cell logistics truck enhanced with artificial potential field and deep reinforcement learning," *Energy*, vol. 239, 2022, Art. no. 121866, doi: 10.1016/j.energy.2021.121866.
[15] X. Li, Z. Shang, F. Peng, L. Li, Y. Zhao, and Z. Liu, "Increment-oriented online power distribution strategy for multi-stack proton exchange membrane fuel cell systems aimed at collaborative performance enhancement," *J. Power Sources*, vol. 512, no. 5, 2021, Art. no. 230512, doi: 10.1016/j.jpowsour.2021.230512.
[16] S. Zhou et al., "A review on proton exchange membrane multi-stack fuel cell systems: Architecture, performance, and power management," *Appl. Energy*, vol. 310, no. 1, 2022, Art. no. 118555, doi: 10.1016/j.apenergy.2022.118555.

Authorized licensed use limited to: Universite du Quebec a Trois-Rivieres. Downloaded on April 21,2025 at 18:19:44 UTC from IEEE Xplore. Restrictions apply.

[17] M. Moghadari, M. Kandidayeni, L. Boulon, and H. Chaoui, "Operating cost comparison of a single-stack and a multi-stack hybrid fuel cell vehicle through an online hierarchical strategy," *IEEE Trans. Veh. Technol.*, vol. 72, no. 1, pp. 267–279, Jan. 2023, doi: 10.1109/TVT.2022.3205879.

[18] S. Zendegan, A. Ferrara, S. Jakubek, and C. Hametner, "Predictive battery state of charge reference generation using basic route information for optimal energy management of heavy-duty fuel cell vehicles," *IEEE Trans. Veh. Technol.*, vol. 70, no. 12, pp. 12517–12528, Dec. 2021, doi: 10.1109/TVT.2021.3121129.

[19] Y. Huang et al., "A review of power management strategies and component sizing methods for hybrid vehicles," *Renewable Sustain. Energy Rev.*, vol. 96, no. 4, pp. 132–144, 2018, doi: 10.1016/j.rser.2018.07.020.

[20] T. Teng, X. Zhang, H. Dong, and Q. Xue, "A comprehensive review of energy management optimization strategies for fuel cell passenger vehicle," *Int. J. Hydrogen Energy*, vol. 45, no. 39, pp. 20293–20303, 2020, doi: 10.1016/j.ijhydene.2019.12.202.

[21] Y. Yan, Q. Li, W. Chen, W. Huang, J. Liu, and J. Liu, "Online control and power coordination method for multistack fuel cells system based on optimal power allocation," *IEEE Trans. Ind. Electron.*, vol. 68, no. 9, pp. 8158–8168, Sep. 2021, doi: 10.1109/TIE.2020.3016240.

[22] A. Khalatbarisoltani, M. Kandidayeni, L. Boulon, and X. Hu, "Power allocation strategy based on decentralized convex optimization in modular fuel cell systems for vehicular applications," *IEEE Trans. Veh. Technol.*, vol. 9545, no. 12, pp. 14563–14574, Dec. 2020, doi: 10.1109/tvt.2020.3028089.

[23] C. Zhang, T. Zeng, Q. Wu, C. Deng, S. H. Chan, and Z. Liu, "Improved efficiency maximization strategy for vehicular dual-stack fuel cell system considering load state of sub-stacks through predictive soft-loading," *Renewable Energy*, vol. 179, pp. 929–944, 2021, doi: 10.1016/j.renene.2021.07.090.

[24] T. Wang, Q. Li, X. Wang, W. Chen, E. Breaz, and F. Gao, "A power allocation method for multistack PEMFC system considering fuel cell performance consistency," *IEEE Trans. Ind. Appl.*, vol. 56, no. 5, pp. 5340–5351, Sep./Oct. 2020, doi: 10.1109/TIA.2020.3001254.

[25] Q. Li et al., "An energy management strategy considering the economy and lifetime of multi-stack fuel cell hybrid system," *IEEE Trans. Transp. Electrific.*, vol. 9, no. 2, pp. 3498–3507, Jun. 2022, doi: 10.1109/TTE.2022.3218505.

[26] H. Li, A. Ravey, A. N'Diaye, and A. Djerdir, "A novel equivalent consumption minimization strategy for hybrid electric vehicle powered by fuel cell, battery and supercapacitor," *J. Power Sources*, vol. 395, no. 2, pp. 262–270, 2018, doi: 10.1016/j.jpowsour.2018.05.078.

[27] Y. Ma, C. Li, and S. Wang, "Multi-objective energy management strategy for fuel cell hybrid electric vehicle based on stochastic model predictive control," *ISA Trans.*, vol. 131, no. 1, pp. 178–196, 2022, doi: 10.1016/j.isatra.2022.04.045.

[28] M. Sellali et al., "Multi-objective optimization-based health-conscious predictive energy management strategy for fuel cell hybrid electric vehicles," *Energies*, vol. 15, no. 4, 2022, Art. no. 1318, doi: 10.3390/en15041318.

[29] X. Hu, C. Zou, X. Tang, T. Liu, and L. Hu, "Cost-optimal energy management of hybrid electric vehicles using fuel cell/battery health-aware predictive control," *IEEE Trans. Power Electron.*, vol. 35, no. 1, pp. 382–392, Jan. 2020, doi: 10.1109/TPEL.2019.2915675.

[30] Y. Zhou, A. Ravey, and M.-C. C. Péra, "Real-time cost-minimization power-allocating strategy via model predictive control for fuel cell hybrid electric vehicles," *Energy Convers. Manag.*, vol. 229, no. 9, 2021, Art. no. 113721, doi: 10.1016/j.enconman.2020.113721.

[31] S. Quan, Y.-X. X. Wang, X. Xiao, H. He, and F. Sun, "Real-time energy management for fuel cell electric vehicle using speed prediction-based model predictive control considering performance degradation," *Appl. Energy*, vol. 304, no. 8, 2021, Art. no. 117845, doi: 10.1016/j.apenergy.2021.117845.

[32] X. Lin, Z. Wang, and J. Wu, "Energy management strategy based on velocity prediction using back propagation neural network for a plug-in fuel cell electric vehicle," *Int. J. Energy Res.*, vol. 45, no. 2, pp. 2629–2643, 2021, doi: 10.1002/er.5956.

[33] T. Li, H. Liu, H. Wang, and Y. Yao, "Hierarchical predictive control-based economic energy management for fuel cell hybrid construction vehicles," *Energy*, vol. 198, 2020, Art. no. 117327, doi: 10.1016/j.energy.2020.117327.

[34] D. F. Pereira, F. d. C. Lopes, and E. H. Watanabe, "Nonlinear model predictive control for the energy management of fuel cell hybrid electric vehicles in real time," *IEEE Trans. Ind. Electron.*, vol. 68, no. 4, pp. 3213–3223, Apr. 2021, doi: 10.1109/TIE.2020.2979528.

[35] Y. Zhou, A. Ravey, and M. C. Péra, "A survey on driving prediction techniques for predictive energy management of plug-in hybrid electric vehicles," *J. Power Sources*, vol. 412, no. 9, pp. 480–495, 2019, doi: 10.1016/j.jpowsour.2018.11.085.

[36] M. H. Rashid, *Electronics Handbook*. Boca Raton, FL, USA: CRC, 2011.

[37] F. Martel, S. Kelouwani, Y. Dubé, and K. Agbossou, "Optimal economy-based battery degradation management dynamics for fuel-cell plug-in hybrid electric vehicles," *J. Power Sources*, vol. 274, pp. 367–381, 2015, doi: 10.1016/j.jpowsour.2014.10.011.

[38] A. M. I. Fernandez, M. Kandidayeni, L. Boulon, and H. Chaoui, "An adaptive state machine based energy management strategy for a multi-stack fuel cell hybrid electric vehicle," *IEEE Trans. Veh. Technol.*, vol. 69, no. 1, pp. 220–234, Jan. 2020, doi: 10.1109/TVT.2019.2950558.

[39] M. Yue, S. Jemei, R. Gouriveau, and N. Zerhouni, "Review on health-conscious energy management strategies for fuel cell hybrid electric vehicles: Degradation models and strategies," *Int. J. Hydrogen Energy*, vol. 44, no. 13, pp. 6844–6861, 2019, doi: 10.1016/j.ijhydene.2019.01.190.

[40] T. Fletcher, R. Thring, and M. Watkinson, "An energy management strategy to concurrently optimise fuel consumption & PEM fuel cell lifetime in a hybrid vehicle," *Int. J. Hydrogen Energy*, vol. 41, no. 46, pp. 21503–21515, 2016, doi: 10.1016/j.ijhydene.2016.08.157.

[41] H. Chen, P. Pei, and M. Song, "Lifetime prediction and the economic lifetime of proton exchange membrane fuel cells," *Appl. Energy*, vol. 142, pp. 154–163, 2015, doi: 10.1016/j.apenergy.2014.12.062.

[42] J. Marcinkoski et al., "DOE hydrogen and fuel cells program record," *DOE Hydrogen Fuel Cells Program. Rec.*, vol. 15015, pp. 1–9, 2015. [Online]. Available: https://www.hydrogen.energy.gov/pdfs/15015_fuel_cell_system_cost_2015.pdf

[43] M. Kandidayeni, A. Macias, L. Boulon, and S. Kelouwani, "Investigating the impact of ageing and thermal management of a fuel cell system on energy management strategies," *Appl. Energy*, vol. 274, no. 6, 2020, Art. no. 115293, doi: 10.1016/j.apenergy.2020.115293.

[44] V. H. Johnson, "Battery performance models in ADVISOR," *J. Power Sources*, vol. 110, no. 2, pp. 321–329, 2002, doi: 10.1016/S0378-7753(02)00194-5.

[45] J. Wang et al., "Cycle-life model for graphite-LiFePO4 cells," *J. Power Sources*, vol. 196, no. 8, pp. 3942–3948, 2011, doi: 10.1016/j.jpowsour.2010.11.134.

[46] S. Ebbesen, P. Elbert, and L. Guzzella, "Battery state-of-health perceptive energy management for hybrid electric vehicles," *IEEE Trans. Veh. Technol.*, vol. 61, no. 7, pp. 2893–2900, Sep. 2012, doi: 10.1109/TVT.2012.2203836.

[47] L. Chen, Z. Lü, W. Lin, J. Li, and H. Pan, "A new state-of-health estimation method for lithium-ion batteries through the intrinsic relationship between ohmic internal resistance and capacity," *J. Int. Meas. Confederation*, vol. 116, no. 11, pp. 586–595, 2018, doi: 10.1016/j.measurement.2017.11.016.

[48] L. Grüne and J. Pannek, "Nonlinear model predictive control," in *Nonlinear Model Predictive Control: Theory and Algorithms*. Cham, Switzerland: Springer, 2017, pp. 45–69.

[49] Z. Zhao, W. Chen, X. Wu, P. C. Y. Chen, and J. Liu, "LSTM network: A deep learning approach for Short-term traffic forecast," *IET Intell. Transp. Syst.*, vol. 11, no. 2, pp. 68–75, 2017, doi: 10.1049/iet-its.2016.0208.

[50] W. Zhou, L. Yang, Y. Cai, and T. Ying, "Dynamic programming for new energy vehicles based on their work modes Part II: Fuel cell electric vehicles," *J. Power Sources*, vol. 407, no. 10, pp. 92–104, 2018, doi: 10.1016/j.jpowsour.2018.10.048.

[51] L. Xu, J. Li, J. Hua, X. Li, and M. Ouyang, "Optimal vehicle control strategy of a fuel cell/battery hybrid city bus," *Int. J. Hydrogen Energy*, vol. 34, no. 17, pp. 7323–7333, 2009, doi: 10.1016/j.ijhydene.2009.06.021.

Mohammadreza Moghadari received the B.S. degree in mechanical engineering from Islamic Azad University, Tehran, Iran, in 2015, and the M.S. degree (Hons.) in automotive engineering from the Iran University of Science and Technology, Tehran, in 2018. His research focuses on proton exchange membrane fuel cell (PEMFC) technology. He began his Ph.D. studies in 2020 with the Hydrogen Research Institute, Université du Québec à Trois-Rivières, Trois-Rivières, QC, Canada. Since 2016, he has authored or coauthored numerous articles in leading SCI journals and has actively served as a reviewer for several academic journals. His research interests include PEMFC systems, energy management strategies, optimization-based control, and fault-tolerant strategies for hybrid vehicles.

Authorized licensed use limited to: Universite du Quebec a Trois-Rivieres. Downloaded on April 21,2025 at 18:19:44 UTC from IEEE Xplore. Restrictions apply.

Mohsen Kandidayeni (Member, IEEE) was born in Tehran, Iran, in 1989. His academic journey has followed diverse paths. He received the B.S. degree in mechanical engineering in 2011, the M.S. degree (Hons.) in mechatronics from Arak University, Iran, in 2014, and the Ph.D. degree (Hons.) in electrical engineering from the University of Quebec, Trois-Rivières(UQTR), QC, Canada, in 2020. From 2020 to 2024, he held various academic roles, including Postdoctoral Fellow with the Electric Transport, Energy Storage, and Conversion Lab (eTESC) with Université de Sherbrooke, Research Associate with the Hydrogen Research Institute (HRI) of UQTR, and Technical Project Manager with HRI. He is currently an Assistant Professor with the Department of Electrical and Computer Engineering, UQTR. He has actively contributed to research by authoring, co-authoring, and reviewing numerous scholarly articles. His academic output includes more than 75 journal and conference publications. His research interests include energy-related topics such as hybrid electric vehicles, fuel cell systems, energy management, multiphysics systems, modeling, and control. He was the recipient of several prestigious awards and honors throughout his academic career, including the Doctoral and Postdoctoral Scholarship from the Fonds de recherche du Québec – Nature et technologies (FRQNT), the Best PhD Thesis Award, and the Third Prize in the Energy Research Challenge from the Quebec Ministry of Energy and Natural Resources.

Loïc Boulon (Senior Member, IEEE) received the master's degree in electrical and automatic control engineering from the University of Lille, Lille, France, in 2006, and the Ph.D. degree in electrical engineering from the University of Franche-Comté, Besançon, France. Since 2010, he has been a Professor with Université du Québec (UQTR), Trois-Rivières, QC, Canada, attaining the rank of Full Professor in 2016, and the Deputy Director of the Hydrogen Research Institute since 2019. His research interests include modeling, control, and energy management of multiphysics systems, with interests spanning hybrid electric vehicles, energy and power sources, such as fuel cells, batteries, and ultracapacitors. He has authored more than 140 peer-reviewed papers in international journals and conferences and has delivered over 40 invited talks worldwide. In 2022, he was recognized as one of the top 10 most prolific authors globally in "Proton Exchange Membrane Fuel Cell (PEMFC)" research and ranked in the top 20 for "Plug-in Hybrid Vehicles," as identified by Elsevier SciVal. In 2015, he was the General Chair of the IEEE Vehicular Power and Propulsion Conference in Montréal, Canada. He is VP-Motor Vehicles Vehicles for the IEEE Vehicular Technology Society. He founded the "International Summer School on Energetic Efficiency of Connected Vehicles" and the "IEEE VTS Motor Vehicle Challenge." He holds the prestigious Canada Research Chair in Energy Sources for Vehicles of the Future and is the Director of the Réseau Québécois sur l'Énergie Intelligente.

Hicham Chaoui (Senior Member, IEEE) received the Ph.D. degree in electrical engineering (with honors) from the University of Quebec, Trois-Rivières, QC, Canada, in 2011. His career has spanned both academia and industry in the field of control and energy systems. From 2007 to 2014, he held various engineering and management positions in the Canadian industry. He is currently a Faculty Member with Carleton University, Ottawa, ON, Canada. His scholarly work has resulted in over 200 journal and conference publications. He is a registered Professional Engineer in the province of Ontario. He is also an Associate Editor for IEEE TRANSACTIONS ON POWER ELECTRONICS, IEEE TRANSACTIONS ON VEHICULAR TECHNOLOGY, and several other journals. He was the recipient of the Best Thesis Award and the Governor General of Canada Gold Medal Award. He is also a recipient of the FED Research Excellence Award, the Early Researcher Award from the Government of Ontario, and the Top Editor Recognition from both the IEEE Vehicular Technology Society and the IEEE Power Electronics Society.

Authorized licensed use limited to: Universite du Quebec a Trois-Rivieres. Downloaded on April 21,2025 at 18:19:44 UTC from IEEE Xplore. Restrictions apply.

3.3 Conclusion

Alongside the operating cost of the multi-stack FC system, which is one of the main challenges, allocating suitable power between sub-stacks to reduce hydrogen consumption and increase the lifespan of sub-stacks is a challenging task that requires further development in EMS. In this regard, designing an advanced EMS can address the mentioned challenges to a great extent.

For this purpose, this chapter aims to design a PHC-EMS to distribute optimal power between sub-stacks and the battery, reducing operating cost and increasing the longevity of power sources. The proposed EMS is a multi-layer one that consists of rule-based and optimization strategies. In the upper layer, a rule-based strategy is developed to determine the number of active FCs at each time step based on FC degradation, requested power, and SOC. This layer aims to minimize FC degradation and reduce hydrogen consumption. In the lower layer, MPC, as a predictive real-time optimization algorithm, is employed to take the optimal control decision between FCs and the battery. This paper uses a novel deep neural network approach called SBLSTM. The results of the proposed predictor show high accuracy. Two different driving cycles are used to assess the performance of the PHC-EMS. The results are compared with DP and ECMS to indicate the proposed strategy's effectiveness. The results of the INRETS driving cycle show that the total operating cost of PHC-EMS is 3.728% more than DP and 5.154% less than ECMS. In the WVUINTER driving cycle, the results illustrate that the total operating cost of PHC-EMS is 2.462% more than DP and 3.550% less than ECMS. Consequently, the proposed strategy can be a convincing choice to be used in real-time for the energy management of a multi-stack FC-HEV.

Chapter 4 - Integration of Water Management into the EMS Through an Adaptive Purge Strategy

4.1 Introduction

Voltage, as the output of the FC, is one of the most critical operating parameters and has a significant impact on PEMFC performance. Additionally, voltage serves as an indicator of FC health, where any voltage drop signals a malfunction or fault in the operation of the FC. As a result, the performance of the FC is sensitive and depends on FC voltage. In this regard, maintaining FC voltage stability to mitigate voltage drops and fluctuations is crucial to ensure the FC meets the requested power. Moreover, stable voltage enables the proper and more efficient operation of power electronics and simplifies the control of FC output power. However, due to the various dynamic conditions in real-world applications, FC voltage is prone to drops and instability. One of the main contributors to voltage drops and instability is water management faults, which have a direct impact on FC voltage performance. Water management faults, particularly flooding, can reduce the PEMFC system's output voltage and power in the short term. If not addressed promptly, they can result in long-term issues such as corrosion of the catalyst's carbon substrate and membrane degradation, ultimately leading to PEMFC failure. One of the feasible and economical solutions to improve water management in PEMFCs is the use of a purge valve. Using the purge valve is an effective method because it can promptly remove accumulated water on the anode side and help the PEMFC quickly recover to a normal and healthy condition. However, determining an appropriate purge strategy is crucial for water management. As unstable voltage is a consequence of water management faults,

maintaining voltage stability through an appropriate purge strategy ensures effective water management in the PEMFC. Despite the effectiveness of the purge method in PEMFCs, an important issue with this system is the wasted hydrogen during the purge. When the purge valve opens, it creates a pressure difference that drives hydrogen flow, removing water from the anode while also discharging hydrogen. Since hydrogen is an expensive fuel and a crucial component of PEMFCs, considering wasted hydrogen when designing a suitable purge strategy is essential, especially in real-time applications like vehicular systems, as it significantly impacts system efficiency and FC operating cost. As a result, an efficient purge strategy should reduce water management faults to achieve voltage stability while also minimizing wasted hydrogen during the purge to enhance PEMFC efficiency and lower operating cost.

Despite the critical role of current in PEMFC performance, a review of the literature reveals that current variations have largely been overlooked when designing purge strategies. To address this gap, the primary aim of this paper is to design an adaptive efficient purge strategy through experimental analysis. This strategy is intended to reduce water management faults, enhance voltage stability, and minimize hydrogen consumption. The proposed purge strategy is adjustable to accommodate different current levels.

The literature review illustrates that, despite the critical importance of water management for FC voltage in real-world applications, the integration of water management into an EMS has not been addressed. In this context, the second aim of this paper is to distribute optimal power between the FCs and the battery while considering the effect of water management on voltage stability through an adaptive efficient purge strategy.

4.2 Paper 3: Integration of Water Management into the Energy Management Strategy for a Fuel Cell Vehicle

Authors: Mohammadreza Moghadari, Mohsen Kandidayeni, Ashkan Makhsoos, Loïc Boulon, and Hicham Chaoui.

Journal: IEEE Transactions on Industrial Electronics.

Publication status: Under Review (with comments received).

4.2.1 Methodology

4.2.1.1 Design of a Purge Strategy Through Experimental Analysis

A. Experimental Setup

This study utilizes the H-500 DEA-PEMFC at the Hydrogen Research Institute, Université du Québec à Trois-Rivières (UQTR). The air-cooled open-cathode DEA-PEMFC, manufactured by Horizon Fuel Cell Technologies, consists of 24 single cells with platinum electrocatalysts on both sides. In air-cooled FCs, air functions as both an oxidizer and a coolant, with airflow adjustable via an axial fan [110]. The experimental setup connects the PEMFC to a National Instruments CompactRIO through PEMFC controller, which manages tasks such as regulating stack temperature through fan control, hydrogen valve operation, and purge interval and duration. The hydrogen supply system includes a tank, pressure regulator, supply valve, purge valve, and flowmeter, with pressure maintained between 0.45 and 0.55 bar. Dry hydrogen (99.999% purity) flows at rates of 0–6.5 L/min, depending on stack power requirements.

The proposed study aims to analyze various combinations of purge intervals and durations to evaluate voltage stability as a consequence of water management across different currents, ranging from 1 A to 42 A. Table 4-1 illustrates the experimental plan, where 8 purge durations are analyzed for each purge interval. In each test, the H-500 DEA-PEMFC runs for 10 minutes to reach a steady state. The data from the last 100 s is collected for analysis. After each test, the PEMFC is turned off for 30 minutes before the next test begins.

Table 4-1- Experimental plan.

Purge combinations		Current levels
Purge interval (s)	Purge duration (ms)	1 A, 2 A, 3A, …, 41 A, 42 A
8, 10, 12, 14, 16, 18, 20	100,200,300,400,500,6007001000	

B. Voltage Behavior Analysis

As any malfunction in water management directly impacts voltage stability, this study analyzes voltage behavior to evaluate water management under different purge strategies. For this purpose, the voltage behavior is analyzed for four different currents (10 A, 20 A, 30 A, and 42 A), representing low, medium, and high current operation levels. In the voltage behavior analysis, 100 mV is selected as the threshold for unstable voltage, as exceeding this value can lead to water management faults.

1) Voltage Analysis of the Manufacturer's Suggested Non-Adaptive Purge Strategy

The first step evaluates the purge period recommended by the H-500 manufacturer: a 10 s interval and 100 ms duration. Figure 4-1(a)-(d) shows voltage behavior, and Figure 4-1(e) displays purge valve status. At 10 A and 20 A, average voltage drops during the purge interval are 25 mV and 21.11 mV, respectively, below the 100 mV threshold, indicating safe

operation without water management faults. However, at 30 A and 42 A, voltage drops are 250 mV and 553 mV, exceeding the threshold. Figure 4-1(c)-(d) demonstrate that a 100 ms purge duration fails to remove excess water, leading to flooding and voltage drops after the purge. The 10 s purge interval and 100 ms purge duration recommended by the manufacturer are unsuitable for high currents and result in reduced PEMFC performance. The results highlight the importance of an appropriate purge strategy to improve water management and maintain voltage stability, especially at high currents, which is critical for FC performance.

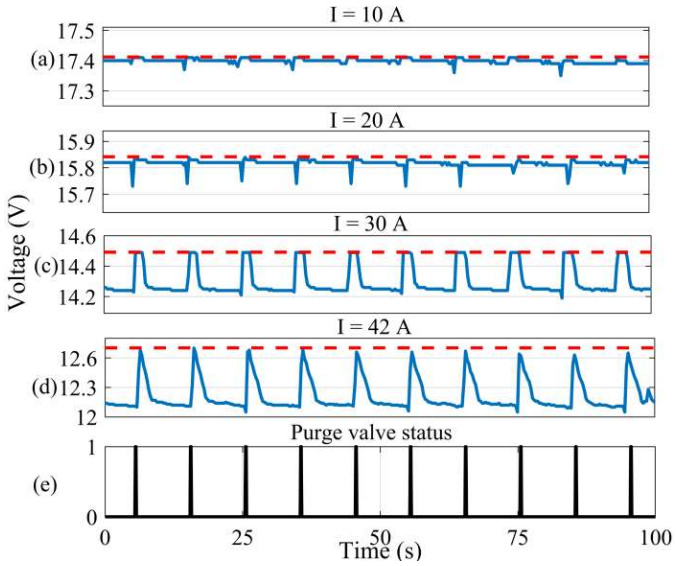

Figure 4-1- Voltage behavior for a 10 s purge interval and 100 ms purge duration at different currents: a) 10 A; b) 20 A; c) 30 A; d) 42 A; e) Purge valve status.

2) The Impact of Purge Interval and Duration on Voltage Stability

This section analyzes the impact of purge interval and duration on water management and voltage behavior. Purge intervals of 8 s, 14 s, and 20 s are selected as samples to demonstrate PEMFC voltage behavior under different combinations of purge intervals and durations. Figure 4-2(a)-(d) shows voltage behavior for an 8 s purge interval and a 100 ms

purge duration. Table 4-2 provides average voltage drops during the purge interval. For 10 A and 20 A currents, this duration is suitable, as the average voltage drop remains below 100 mV, indicating balanced water management. However, for higher currents like 30 A and 42 A, it fails to evacuate excess water efficiently, leading to flooding. Figure 4-2(f)-(i) illustrate voltage behavior for the 8 s purge interval and a 200 ms purge duration. As shown in Table 4-2, this duration is suitable for all currents, maintaining average voltage drops below 100 mV.

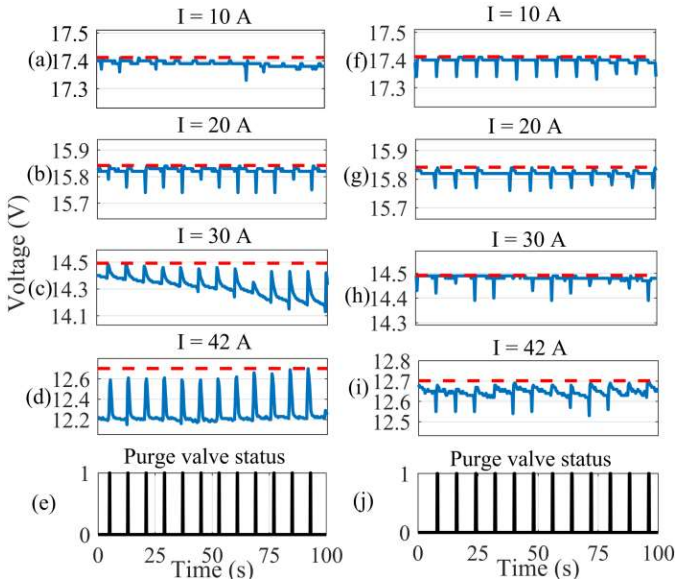

Figure 4-2- Voltage behavior for a purge interval of 8 s and a 100 ms duration: (a)-(e), and for a purge interval of 8 s with a 200 ms duration: (f)-(j).

Table 4-2- Average voltage drops for a purge interval of 8 s with different purge durations.

Purge interval (s) - Purge duration (ms)					
8 - 100	Current (A)	10	20	30	42
	Voltage drop (mV)	15	19.10	162.5	420
8 - 200	Voltage drop (mV)	13.33	17	15.83	51.82

Figure 4-3(a)-(d) illustrates PEMFC voltage behavior for a 14 s purge interval and a 100 ms purge duration. Table 4-3 shows the average voltage drops for 14 s purge interval under different purge durations. For 30 A and 42 A currents, a 100 ms duration is insufficient, with voltage drops exceeding 100 mV, failing to recover PEMFC performance. Figure 4-3(f)-(i) shows voltage behavior for the same interval with a 200 ms purge duration. Table 4-3 indicates that this duration is still insufficient for 42 A, failing to ensure voltage stability.

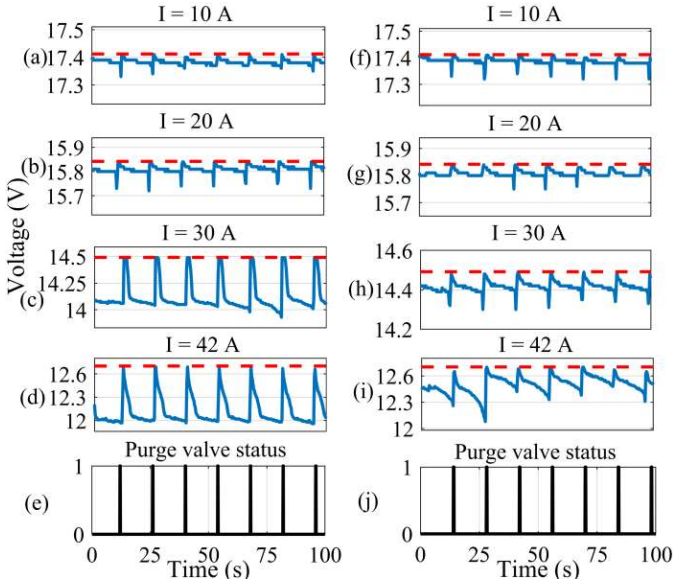

Figure 4-3- Voltage behavior for a purge interval of 14 s and a 100 ms duration: (a)-(e), and for a purge interval of 14 s with a 200 ms duration: (f)-(j).

Table 4-3- Average voltage drops for a purge interval of 14 s with different purge durations.

Purge interval (s) - Purge duration (ms)					
14 - 100	Current (A)	10	20	30	42
	Voltage drop (mV)	28.33	38.33	463.67	698.19
14 - 200	Voltage drop (mV)	23.33	36.67	83.33	220
14 - 300	Voltage drop (mV)	18.25	30	73.26	136.67
14 - 400	Voltage drop (mV)	13	27.55	66.67	93.13

For a 14 s interval and a 300 ms purge duration, Table 4-3 reveals it is insufficient at 42 A, with voltage drops exceeding 100 mV. According to Table 4-3, for a 14 s purge interval, a purge duration of 400 ms is suitable for efficient water management, as the voltage drops for all currents remain below 100 mV.

In this study, the maximum purge interval is 20 s. Table 4-4 shows that shorter purge durations, such as 100 ms and 200 ms, are unsuitable, as they lead to flooding and unstable voltage, especially at higher currents. Similarly, 300 ms and 400 ms durations are insufficient, with average voltage drops exceeding 100 mV at 30 A and 42 A. A 500 ms purge duration is suitable for 10 A, 20 A, and 30 A, but at 42 A, the voltage drop exceeds 100 mV, indicating a water management fault. To maintain voltage stability across all current levels, the purge duration must be increased. Figure 4-4 and Table 4-4 demonstrate that a 600 ms purge duration is suitable for a 20 s interval, as the voltage drop for all currents remains below 100 mV, ensuring stable PEMFC performance.

Table 4-4- Average voltage drops for a purge interval of 20 s with different purge durations.

Purge interval (s) - Purge duration (ms)					
20 - 100	Current (A)	10	20	30	42
	Voltage drop (mV)	65	132.50	732.50	917.50
20 - 200	Voltage drop (mV)	45	80	475	525.67
20 - 300	Voltage drop (mV)	35.33	73.33	235	242.50
20 - 400	Voltage drop (mV)	25.33	50	102.50	195.33
20 - 500	Voltage drop (mV)	23.57	35	82	113.76
20 - 600	Voltage drop (mV)	20	27.50	75	72.50

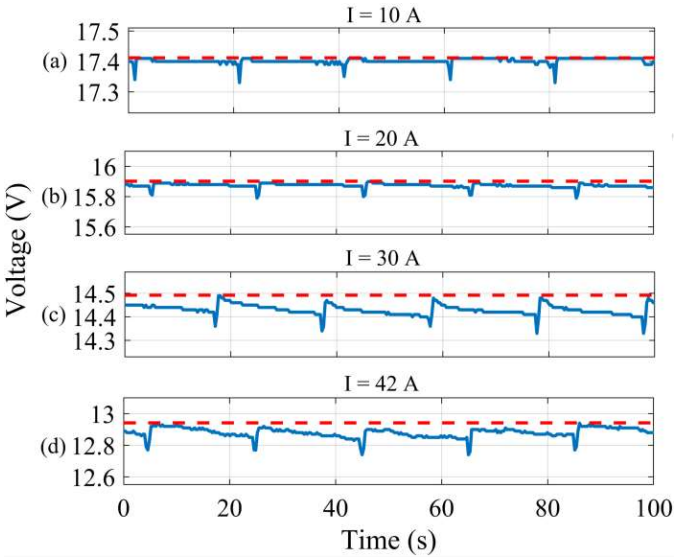

Figure 4-4- Voltage behavior for a 20 s purge interval and 600 ms purge duration at different currents: a) 10 A; b) 20 A; c) 30 A; d) 42 A; e) Purge valve status.

Table 4-5 shows the appropriate purge durations for all purge intervals used in this study, which reduce the risk of water management faults and maintain voltage stability across all current levels. Based on the analysis of purge intervals and durations, for a constant purge interval, increasing the purge duration mitigates water management faults and stabilizes voltage. Conversely, for a constant purge duration, increasing the purge interval leads to increased water management faults and unstable voltage. According to Table 4-5, for the 10 s purge interval suggested by the manufacturer, a purge duration of 300 ms is suitable for all current levels. The experimental results indicate that the voltages in low and medium current zones are not highly sensitive to variations in purge interval and duration. However, the voltage in high current zones is more sensitive to the purge strategy, as the PEMFC is more susceptible to flooding in this region.

Table 4-5- Appropriate purge duration for each purge interval.

Purge interval (s)	Appropriate purge duration (ms)
8	200
10	300
12	300
14	400
16	500
18	500
20	600

C. Impact of the Purge Strategy on Hydrogen Consumption

To assess the purge strategy's impact on hydrogen consumption in the H-500 DEA-PEMFC, Figure 4-5 presents results under a fixed 8 s purge interval with varying durations (200–1000 ms). The aim is to quantify hydrogen wasted during purging. Voltage remains stable across all strategies. Experimental data show a sharp hydrogen flow spike each time the purge valve opens, indicating wasted hydrogen. Total hydrogen consumption combines this waste with the hydrogen used for power generation, averaged over the test duration. The "Baseline" in Figure 4-5 represents only the electrochemically consumed hydrogen. As purge duration increases, more hydrogen is wasted, reducing system efficiency. Thus, minimizing purge waste is crucial for improving overall PEMFC efficiency, even with stable voltage.

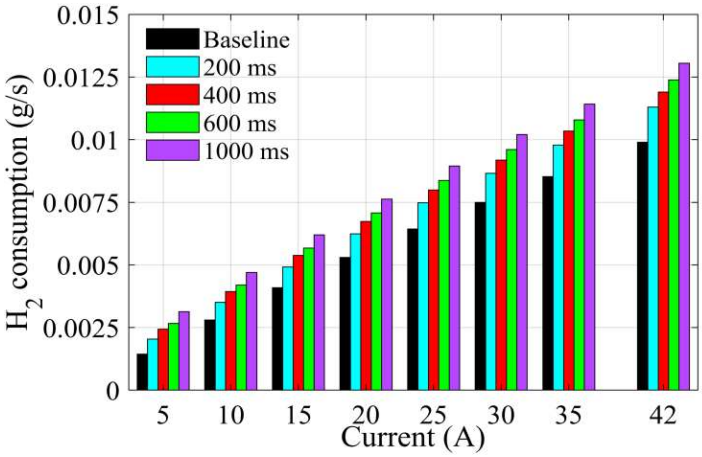

Figure 4-5- Hydrogen consumption based on: (a) Power; (b) Current.

Figure 4-6 shows the amount of wasted hydrogen during different purge durations when the purge valve is open. According to Figure 4-6, as the current level increases, the amount of wasted hydrogen decreases for a constant purge duration. The reason is that increasing the FC current, while keeping the hydrogen inlet pressure constant, causes more hydrogen to be consumed at the anode. This lowers the hydrogen partial pressure, reducing the pressure difference between the inside and outside of the anode. On the other hand, at high current levels, water accumulation can block the porous media and reactant areas, reducing hydrogen availability and lowering hydrogen partial pressure [135].

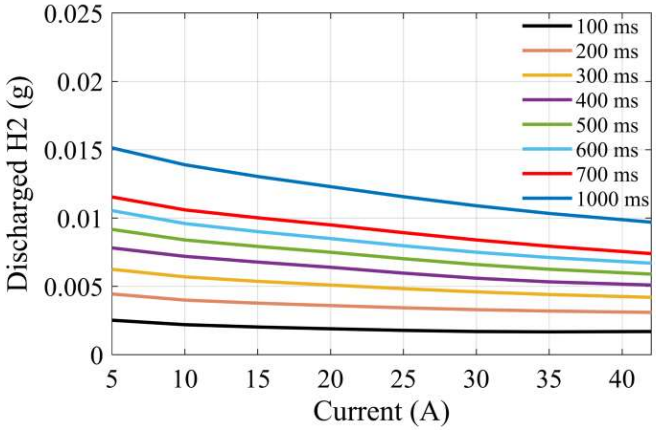

Figure 4-6- The amount of hydrogen discharged for different purge durations.

D. Designing an Adaptive Efficient Purge Strategy

PEMFC performance is sensitive to current variations, and static purge strategies can lead to poor water management, reduced voltage stability, higher hydrogen consumption, and lower efficiency. This section focuses on designing an adaptive efficient purge strategy suitable for varying current levels. An adaptive efficient purge strategy consists of two steps. 1) The first step involves analyzing different combinations of purge intervals and durations for each current level to determine how many combinations result in effective water management, defined as a voltage drop below 100 mV. 2) The second step is to examine hydrogen consumption. From the purge combinations that keep the voltage stable, the one with the lowest hydrogen consumption is selected.

Figure 4-7 illustrates the process of selecting an adaptive efficient purge strategy based on different current levels. The red stems represent combinations of purge intervals and durations that cause water management faults, with the voltage drop exceeding the 100 mV threshold. The blue stems indicate combinations that result in effective water management, with the voltage drop remaining below 100 mV. Among the combinations with voltage drops under 100 mV, the one with the lowest hydrogen consumption is chosen as the efficient purge strategy, marked by the green stem. As shown in Figure 4-7, low current levels, such as 10 A, are not sensitive to water management, as the voltage drop for all combinations remains below 100 mV.

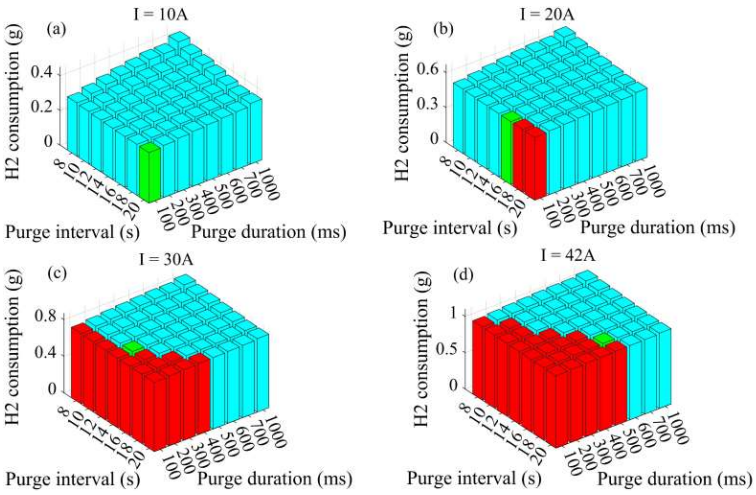

Figure 4-7- Adaptive efficient purge strategy selection for different current levels: (a) 10 A; (b) 20 A; (c) 30 A; (d) 42 A.

Figure 4-8 compares the adaptive efficient purge strategy proposed in this study with the manufacturer's recommended strategy for different current levels of the H-500 DEA-PEMFC. The manufacturer's suggested strategy uses a constant 10.1 s purge period, consisting of a 10 s purge interval and a 100 ms purge duration, applied uniformly for all current levels, as shown in Figure 4-8(a)-(b). According to Figure 4-8(c), the manufacturer’s purge strategy works effectively up to 24 A. However, it fails to mitigate water management faults and maintain voltage stability at higher currents, where voltage drops exceed 100 mV. As shown in Figure 4-8(c), the voltage drop in the adaptive efficient purge strategy remains below 100 mV at all current levels, demonstrating the effectiveness of the proposed strategy in water management. As illustrated in Figure 4-8(a)-(b), for low currents, the proposed strategy selects the longest purge interval and the shortest purge duration to minimize hydrogen consumption and enhance energy efficiency.

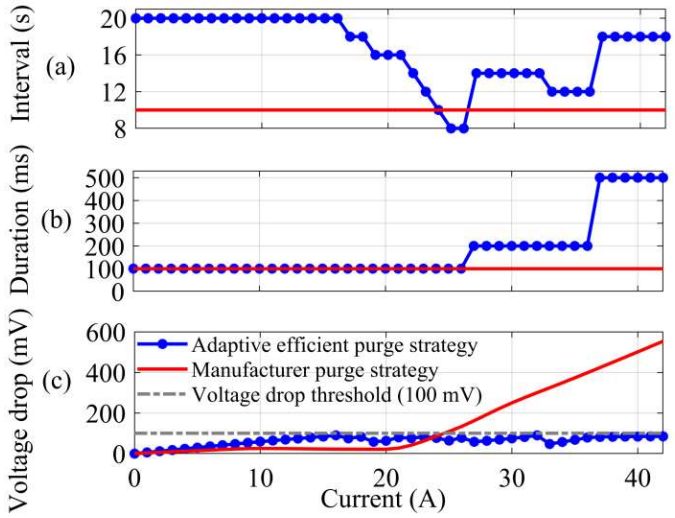

Figure 4-8- Purge strategies comparison: a) Purge interval; b) Purge duration; c) Voltage drop.

4.2.1.2 Integrating Water Management into the Energy Management Strategy

A. Hardware-in-the-Loop Setup

To evaluate the effectiveness of the proposed purge strategy for water management in real-time applications, this study integrates water management into the EMS through a HIL platform for a multi-stack hybrid powertrain case study designed for a low-speed vehicle called Nemo [136]. The powertrain includes four H-500 DEA-PEMFCs, a three-phase induction motor, and a battery pack. In this powertrain configuration, the battery pack connects directly to the bus, while the FCs are connected through unidirectional DC-DC converters. The proposed strategy consists of an EMS level and a purge strategy level. The EMS level determines the optimal power distribution between the sub-stacks and the battery. The proposed purge strategy receives the DEA-PEMFC reference current from the EMS level, determines the efficient purge strategy to mitigate water management faults based on it, and sends the control signal to the DEA-PEMFC controller. The HIL platform is shown in Figure 4-9. According to Figure 4-9, two H-500 DEA-PEMFCs in this platform

are employed as real components, while the other two PEMFCs are virtual and used as emulators. It should be mentioned that the other components of this platform are represented by mathematical models. The PEMFCs are connected to a National Instruments CompactRIO (NIcRIO-9022) through their controller. The CompactRIO connects to the PC running LabVIEW software using an Ethernet connection. Data is transferred between the CompactRIO and the PC every 100 ms. At each sampling time, experimental data such as FC voltage, current, and hydrogen flow rate are recorded and collected. Two 8514 BK Precision DC Electronic Loads are used to request load profiles imposed by the DC-DC converter on the PEMFC stacks.

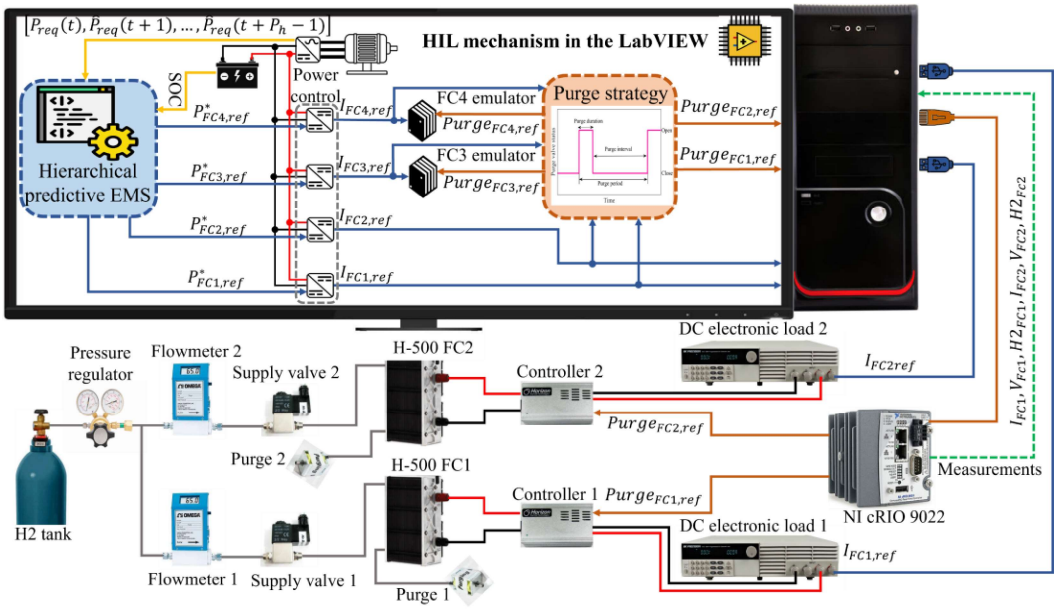

Figure 4-9- HIL mechanism integrated water management in the EMS.

B. Energy Management Strategy

In this study, a HPEMS is used to distribute optimal power. The first layer is a rule-based strategy that decides how many FCs should be activated and participate in the second

layer. The second layer is a MPC that, based on the information from the first layer and system constraints, determines optimal power between the FCs and the battery.

4.2.2 Summary of the Results Analysis

This section aims to evaluate the performance of the integrated water management into the EMS (IWM-EMS) using the proposed purge strategy. This study proposes an adaptive IWM-EMS (AIWM-EMS), where an adaptive efficient purge strategy is integrated into the EMS. The performance of the AIWM-EMS is compared with that of the non-adaptive IWM-EMS (NAIWM-EMS), which incorporates the manufacturer's non-adaptive purge strategy into the EMS. The performance and effectiveness of the two WM-EMSs are compared under the WLTC-class3 driving cycle.

Figure 4-10(a)-(d) shows FC power distribution, and Figure 4-10(e) presents battery SOC for IWM-EMSs under the WLTC-class3 driving cycle. The AIWM-EMS uses an adaptive purge strategy based on reference current to mitigate water management faults, maintain voltage stability, and minimize hydrogen consumption. In contrast, the NAIWM-EMS applies a constant purge strategy for all current levels. In the HIL structure, a PID controller regulates FC current to track the reference power accurately. FC1 and FC2 are real PEMFCs, with experimental data (current, voltage, and hydrogen consumption) collected via CompactRIO, while FC3 and FC4 are emulators. According to Figure 4-10(a)-(d), in high-power zones, such as from 1113 s to 1372 s and 1546 s to 1770 s, the FCs must operate at high currents to meet the requested power. FCs operating under the AIWM-EMS can supply the requested power because water management faults are effectively reduced, and the voltage drop for all currents is kept below the 100 mV threshold, as shown in Figure 4-8. To meet the requested power, FCs under the NAIWM-EMS must operate at

higher currents than those under the AIWM-EMS to compensate for the higher voltage drop. FCs under the NAIWM-EMS operate at lower power at the maximum FC current. With the maximum current set to 42 A, the FCs under NAIWM-EMS cannot exceed this current to compensate for the voltage drop and must operate at reduced power. Operating at reduced power causes FCs in the NAIWM-EMS to work longer in the high-power zone compared to those in the AIWM-EMS to meet the requested power and maintain battery SOC, resulting in a different SOC trajectory, as shown in Figure 4-10(e).

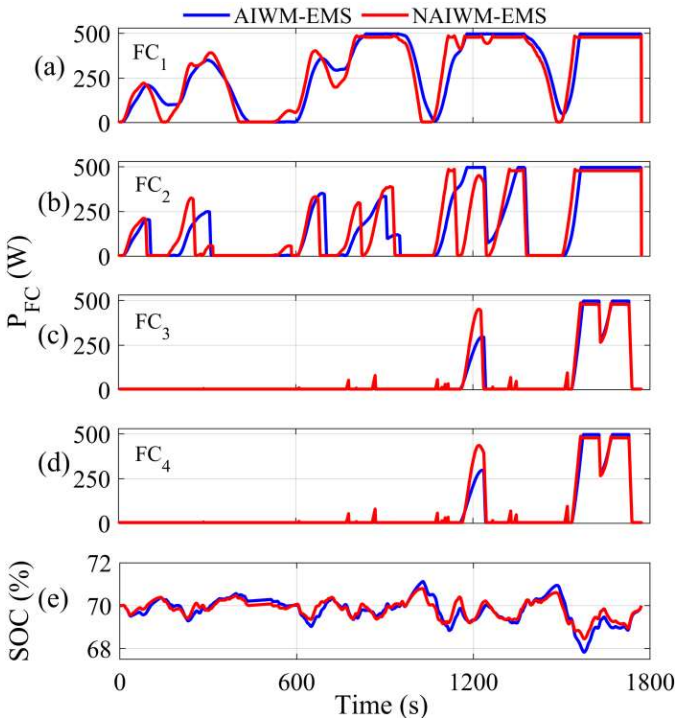

Figure 4-10- AIWM-EMS and NAIWM-EMS performance under the WLTC-class3 driving cycle: a) FC_1 power; b) FC_2 power; c) FC_3 power; d) FC_4 power; e) Battery SOC.

Figure 4-11 illustrates the voltage drop caused by water management faults in the PEMFCs during the driving cycle. The voltage drop of the FCs under the AIWM-EMS remains below 100 mV throughout the driving cycle, indicating that this approach effectively mitigates water management faults. However, the voltage drop of the FCs under

the NAIWM-EMS exceeds 100 mV, particularly in high-power zones, indicating water flooding faults due to the use of a non-adaptive purge strategy.

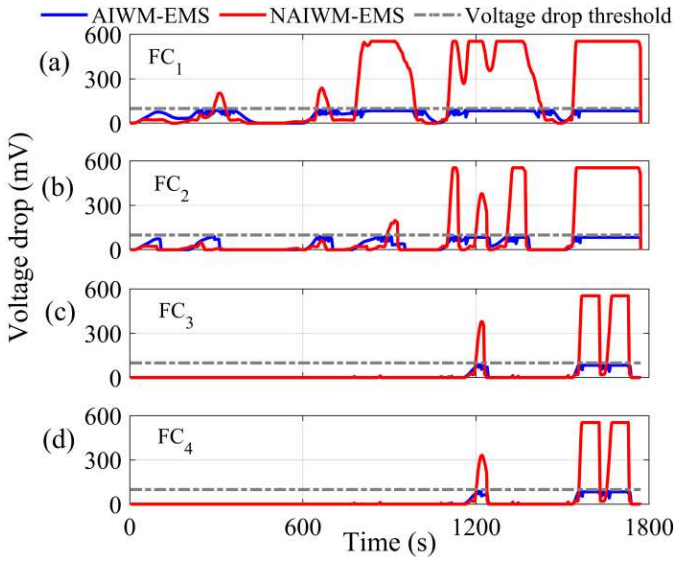

Figure 4-11- Voltage drop comparison between AIWM-EMS and NAIWM-EMS: a) FC_1; b) FC_2; c) FC_3; d) FC_4.

Figure 4-12 shows a comparison of the total wasted hydrogen when the purge valve is open. The total wasted hydrogen in the AIWM-EMS is 1.128 g, while it is 1.533 g in the NAIWM-EMS. According to Figure 4-12, the total wasted hydrogen in the AIWM-EMS is 26.42% less than in the NAIWM-EMS. The results of Figure 4-11 and Figure 4-12 demonstrate the effectiveness of the AIWM-EMS in mitigating water management faults, maintaining FC voltage stability and minimizing hydrogen consumption across different current levels.

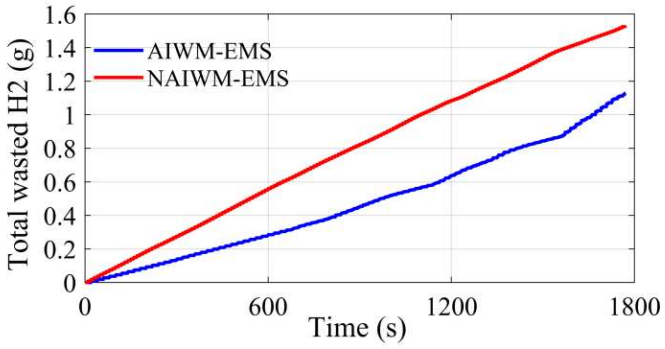

Figure 4-12- Total wasted hydrogen during the purge strategies.

Figure 4-13 compares the total operating cost of the FC-HEV under the AIWM-EMS and NAIWM-EMS. According to Figure 4-13, the cost of hydrogen consumption in the AIWM-EMS is 4.09% lower than in the NAIWM-EMS. The results also show that the cost of FC degradation in the AIWM-EMS is 8.12% less than in the NAIWM-EMS. Under the NAIWM-EMS, the FCs operate at reduced power at maximum current, leading to longer operation at high power to meet the requested power and maintain battery SOC, which increases FC degradation. The cost of battery degradation in the AIWM-EMS is slightly higher than in the NAIWM-EMS because the AIWM-EMS utilizes a wider range of battery SOC. Finally, the results show that the total operating cost in the AIWM-EMS is 5.21% lower than in the NAIWM-EMS.

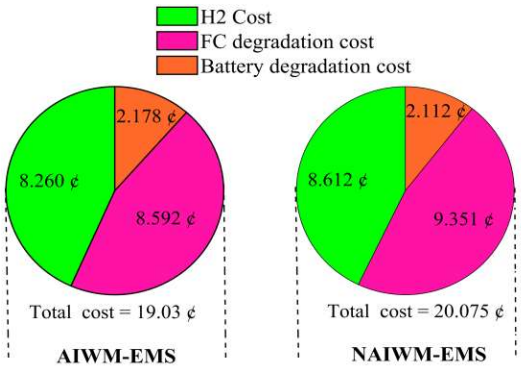

Figure 4-13- FC-HEV operating cost comparison.

Figure 4-14 shows the efficiency distribution of all FCs in the FC-HEV under the AIWM-EMS and NAIWM-EMS. The results show that the FCs operates 78.36% of the driving cycle time in an efficiency zone of 45% or higher, while in the NAIWM-EMS, the FCs operate 62% of the driving cycle time in this zone.

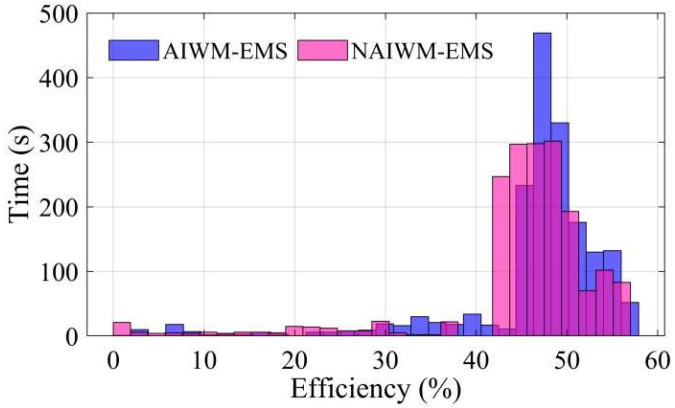

Figure 4-14- FC system efficiency distribution comparison.

Integration of Water Management into the Energy Management Strategy for a Fuel Cell Vehicle

Mohammadreza Moghadari, *Student Member, IEEE*, Mohsen Kandidayeni, *Member, IEEE*, Ashkan Makhsoos, *Student Member, IEEE,* Loïc Boulon, *Senior Member, IEEE*, and Hicham Chaoui, *Senior Member, IEEE*

***Abstract*— Unlike other studies that focus solely on determining the optimal power distribution for a fuel cell hybrid electric vehicle (FC-HEV), this paper aims to integrate water management into the energy management strategy (EMS) by designing an adaptive efficient purge strategy. This study investigates the impact of integrated water management into the EMS (IWM-EMS) on the performance and operating cost of FC-HEV. The IWM-EMS consists of two levels: the first level is the EMS, which determines the optimal power, and the second level is the proposed purge strategy. The proposed IWM-EMS in this study is the adaptive IWM-EMS (AIWM-EMS), which utilizes an adaptive efficient purge strategy that can adjust based on the FC reference current. Another IWM-EMS is the non-adaptive IWM-EMS (NAIWM-EMS), which utilizes a constant purge strategy suggested by the FC manufacturer for all current levels. The results show that the FC-HEV under the AIWM-EMS consumes 4.09% less hydrogen than the NAIWM-EMS and reduces total operating cost by up to 5.21%. In addition, 78.36% of the FCs' operating time is spent in the high-efficiency zone.**

***Index Terms*— Energy management strategy, proton exchange membrane fuel cell, purge strategy, voltage stability, water management.**

I. Introduction

A. Literature Review

ALIGNED with green transportation policies, fuel cell hybrid electric vehicles (FC-HEVs) have gained significant attention in the field of vehicle electrification, with widespread development in many countries around the world [1]. Proton exchange membrane fuel cells (PEMFCs) are employed as the primary power source in FC-HEVs due to their distinct characteristics, including high efficiency, low operating temperatures, rapid start-up times, and nearly zero emissions [2]. However, due to the slow dynamic response of the FC, a secondary power source, such as a battery or supercapacitor (SC), is utilized in FC-HEVs [3]. In FC-HEVs, due to the existence of multiple power sources with distinct characteristics, an energy management strategy (EMS) is needed to effectively manage power distribution [4], [5]. According to the literature, EMSs typically fall into three main categories: rule-based (RB), optimization-based (OB), and learning-based (LB) [6]. In the literature, various EMSs and their combinations are explored. The study in [7] proposes a frequency-decoupling EMS using fuzzy control for a FC-HEV. The proposed strategy enhances power performance, reduces FC degradation, and improves fuel economy by 7.94%. In [8], the authors propose an adaptive state machine as a RB-EMS for a multi-stack FC-HEV. The proposed EMS improves fuel efficiency and reduces FC degradation. In [9], a nonlinear model predictive control (NMPC)-based EMS is proposed for FC-HEVs. The results show that the proposed EMS enhances fuel efficiency, minimizes hydrogen consumption, and reduces FC degradation. The study in [10] proposes an online efficiency-optimized EMS for a FC-HEV. The results show an efficiency increase to 53% and a reduction in computational burdens. In [11], a hierarchical EMS for a FC-HEV using deep reinforcement learning (DRL) is developed. The proposed EMS improves FC lifespan and enhances fuel economy by 16.8%. The paper in [12] presents a three-level EMS for FC-HEV, utilizing a dual-reward Q-learning algorithm. This strategy improves energy efficiency by 8% and reduces FC degradation.

B. Impact of Water Management on Voltage Stability

In real-time applications like vehicles, the performance, durability, and reliability of PEMFC systems are challenging and largely depend on effective water management [13]. PEMFC performance highly depends on the membrane's hydration level, and an imbalance in hydration can reduce proton conductivity and lower overall performance. Water transport in a PEMFC involves three main processes that influence membrane’s water balance and overall performance. The first is water generation on the cathode side during the oxygen reduction reaction, which increases with current. The second process is back diffusion, where water moves from the cathode to the anode due to concentration differences. The third is electro-osmotic drag, which pulls water molecules, along with protons through the membrane toward the cathode [14], [15]. Water flooding and membrane drying out are two common faults in PEMFC associated with water management malfunctions [16]. An increase in the membrane's hydration level can lead to flooding, which restricts the access of reactant gases and reduces PEMFC performance. Back diffusion is a key contributor to this issue. On the other hand, a decrease in membrane hydration causes drying out, leading to higher membrane resistance and reduced proton conductivity. Electro-osmotic drag is a primary factor contributing to drying out [16], [17]. Flooding and drying out can reduce the PEMFC output voltage and power in the short term. If not resolved promptly, they can result in long-term effects, eventually leading to PEMFC failure [17].

One of the feasible and economical solutions to improve water management in PEMFCs is the use of a purge valve. This approach is particularly common in dead-end anode (DEA) PEMFCs [13]. Using the purge valve is an effective method for promptly removing accumulated water and helping the PEMFC quickly return to a normal and healthy condition. Determining an appropriate purge strategy is crucial for effective water management. Some studies focus on analyzing the impact of different purge strategies on the water content inside the PEMFC [18]–[21]. However, this approach relies on a precise model to estimate the water content, which is challenging due to the complexity and multi-physics nature of PEMFCs. Consequently, it may not effectively enhance water

management. One important aspect of designing a suitable purge strategy is its effectiveness in real-time applications. Using a precise water content model requires a three-dimensional approach, which is complex and increases the computational burden. This can compromise the real-time applicability of purge strategy design. Moreover, an accurate dynamic model of water content depends on several parameters, which remains a limitation in current studies.

Voltage, as the output of a FC system, is a vital parameter with a significant impact on FC performance. It acts as an indicator, where any drop signals a malfunction in the FC. On the other hand, in real-world applications such as FC-HEVs, quickly detecting water management faults and taking appropriate action to resolve them and restore PEMFC performance is highly important. PEMFC voltage is a dependable indicator of performance and can be measured easily without the need for complex sensors. Therefore, to avoid the complexity and inaccuracies of water content models, voltage monitoring (VM) is a reliable and widely used method for improving water management and detecting PEMFC malfunctions in real-world applications [16]. As unstable voltage is a consequence of water management faults, maintaining voltage stability through an appropriate purge strategy ensures effective water management in the PEMFC. In this regard, many studies on purge strategies focus on voltage stability as the output of the PEMFC system to improve water management. These types of studies focus on designing suitable purge strategies to achieve effective water management by analyzing voltage stability [22]–[24]. In these studies, voltage is considered stable if the drop during the purge interval is less than 100 mV [22], [23], [25]. Fig. 1 shows the effect of the purge strategy on water management and voltage stability at 42 A in an H-500 DEA-PEMFC with a 20 s purge interval. The dashed red line represents the desired voltage, while the blue line displays experimental data. At 42 A, a 100 ms purge duration fails to remove accumulated water, resulting in flooding and a 917.5 mV voltage drop, which exceeds the stability limit. A 600 ms duration guarantees proper water management and reduces the voltage drop to 72.5 mV.

Despite the effectiveness of the purge method in PEMFCs, an important issue with this system is the wasted hydrogen during the purge. Since hydrogen is an expensive fuel, considering wasted hydrogen when designing a suitable purge strategy is essential, as it significantly impacts system efficiency and PEMFC operating cost [13], [26]. However, there are few studies focused on designing an efficient purge strategy that maintains voltage stability while minimizing hydrogen consumption [27]–[29].

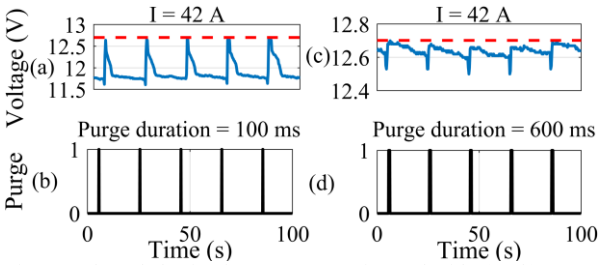

Fig. 1. Voltage behavior for a 20 s purge interval with: (a)-(b) a 100 ms purge duration; and (c)-(d) a 600 ms purge duration.

C. Contributions

PEMFC operating current plays a key role in water management. An increase in PEMFC current intensifies water flooding [30]. Although in some commercial PEMFC systems purge parameters are tuned with current levels, the literature review illustrates that academic and laboratory-scaled studies on purge strategies in PEMFCs focus only on designing a constant, non-adaptive purge strategy for all current levels. Due to current changes in real-world applications and the sensitivity of PEMFC performance to the output current, designing an adaptive purge strategy that can adjust to different current levels can reduce the risk of water management faults and improve PEMFC voltage stability. However, despite the critical role of current in PEMFC performance and voltage behavior, considering current variations when designing a purge strategy is rarely addressed. As a result, since in real-world applications PEMFC operating conditions are always dynamically changing, the first contribution of this study is to design a purge strategy that can adapt to various dynamic conditions. In this regard, an adaptive efficient purge strategy is proposed, which adjusts based on the PEMFC operating current.

In vehicular applications, water management faults are the most common issues and cause unstable or decreased voltage. In real-world applications like FC-HEVs, voltage stability is crucial to ensure the requested power is supplied. As a result, considering water management and its effect on voltage stability is crucial in real-world applications. Despite its critical importance in real-world applications, the integration of water management into an EMS has not been addressed. In this regard, the second contribution of this paper is the design of an integrated water management into the EMS (IWM-EMS) utilizing an adaptive efficient purge strategy. The proposed purge strategy is implemented in a hardware-in-the-loop (HIL) setup to evaluate its effectiveness.

II. Design of a Purge Strategy Through Experimental Analysis

A. Experimental Setup

This study utilizes an air-cooled open-cathode DEA-PEMFC manufactured by Horizon Fuel Cell Technologies for experiments at the Hydrogen Research Institute's test center, located at the Université du Québec à Trois-Rivières (UQTR) [31]. Table I shows the technical characteristics of the H-500 DEA-PEMFC. To develop a suitable purge strategy that avoids water management faults and ensures stable PEMFC voltage, this study conducts extensive tests using seven purge intervals (8–20 s) and eight purge durations (100–1000 ms) across current levels ranging from 1 to 42 A. Table II illustrates the proposed experimental plan. The 8 s interval is used to assess water management and voltage behavior below the 10 s purge interval recommended by manufacturers, while the 20 s interval is used to examine the effects of a longer purge interval. Purge durations are selected based on the chosen purge interval range.

TABLE I
Technical Characteristics of the H-500 DEA-PEMFC

Number of cells	24
Rated Power	500W
Voltage range	12-23 V
Maximum current	42 A
Operating temperature	0 - 65 °C
Cooling system	Cooling fan (ambient air)

TABLE II
EXPERIMENTAL PLAN

Purge combinations		Current levels
Purge interval (s)	Purge duration (ms)	1 A, 2 A, 3A, …, 41 A, 42 A
8, 10, 12, 14, 16, 18, 20	100,200, 300, 400, 500, 600 700 1000	

While most studies and PEMFC data sheets recommend a minimum duration above 100 ms, this study uses 100 ms to investigate its effect on water management and voltage stability. The 1000 ms duration is defined as the upper limit, considered a safe and conservative choice. Experimental results confirm that combining this maximum duration with various intervals ensures effective water removal and maintains voltage stability.

In each test, the H-500 DEA-PEMFC runs for 10 minutes to reach a steady state. The data from the last 100 s is collected for analysis. In the developed PEMFC test center, the ambient temperature and humidity are 21 °C and 46%, respectively, and a control system maintains these environmental conditions during the experiments to improve the quality of the experimental results. It should be noted that the PEMFC fan duty cycle is 80% to ensure the stack temperature stays within a safe range during the purge strategy tests.

B. Voltage Behavior Analysis

In this section, the voltage behavior is analyzed for four different currents (10 A, 20 A, 30 A, and 42 A), representing low, medium, and high current levels. In the voltage behavior analysis, 100 mV is selected as the threshold for unstable voltage, as exceeding this value can lead to water management faults.

1) Voltage Analysis of the Manufacturer's Suggested Non-Adaptive Purge Strategy: The purge strategy suggested by the H-500 manufacturer consists of a purge interval of 10 s and a duration of 100 ms. Fig. 2(a)-(d) shows the voltage behavior, and Fig. 2(e) displays the status of the purge valve. As shown in Fig. 2(a)-(b), the average voltage drops during the purge intervals are 25 mV at 10 A and 21.11 mV at 20 A, indicating that the PEMFC is operating safely without water management faults. According to Fig. 2(c)-(d), the average voltage drops are 250 mV for 30 A and 553 mV for 42 A, exceeding the 100 mV threshold. Fig. 2(c)-(d) demonstrates that the 10 s purge interval and 100 ms purge duration recommended by the manufacturer are unsuitable for high currents and result in flooding and voltage drop. strategy to improve water management and maintain voltage stability, especially at high currents.

2) The Impact of Purge Interval and Duration on Voltage Stability: This section focuses on analyzing how changes in the purge interval and duration impact water management and voltage behavior. For this analysis, purge intervals of 8 s, 14 s, and 20 s are selected as samples to demonstrate PEMFC voltage behavior. Fig. 3(a)-(d) illustrates voltage behavior with a purge interval of 8 s and a 100 ms purge duration. The results highlight the importance of an appropriate purge. The average PEMFC voltage drops during the purge interval are provided in Table III. According to Fig. 3(a)-(b) and Table III, for an 8 s purge interval, the 100 ms purge duration is suitable for 10 A and 20 A, as the average voltage drop remains below 100 mV. However, it is not suitable for high currents like 30 A and 42 A. According to Fig. 3(f)-(i) and Table III, for the 8 s purge interval the 200 ms purge duration is suitable since the average voltage drop for all currents remains below 100 mV.

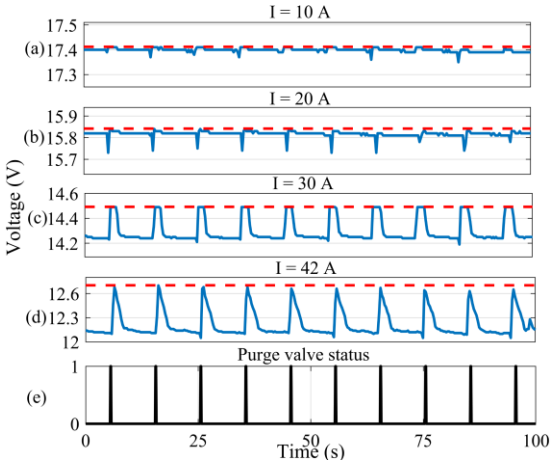

Fig. 2. Voltage behavior for a 10 s purge interval and 100 ms purge duration at different currents: a) 10 A; b) 20 A; c) 30 A; d) 42 A; e) Purge valve status.

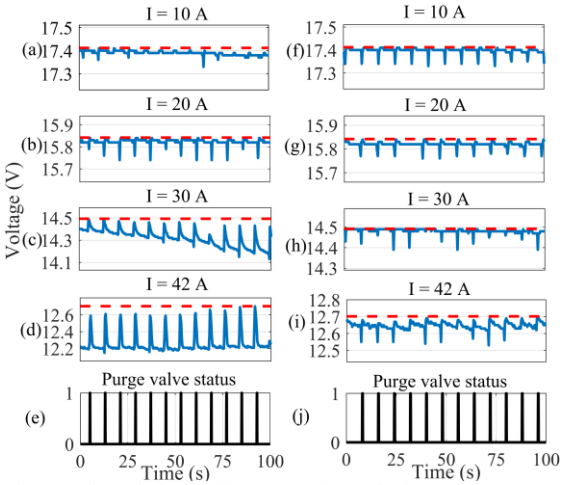

Fig. 3. Voltage behavior for a purge interval of 8 s and a 100 ms duration: (a)-(e), and for a purge interval of 8 s with a 200 ms duration: (f)-(j).

TABLE III
AVERAGE VOLTAGE DROPS FOR A PURGE INTERVAL OF 8 S WITH DIFFERENT PURGE DURATIONS.

Purge interval (s) - Purge duration (ms)					
8 - 100	Current (A)	10	20	30	42
	Voltage drop (mV)	15	19.10	162.5	420
8 - 200	Voltage drop (mV)	13.33	17	15.83	51.82

Fig. 4(a)-(d) shows the PEMFC voltage behavior with a purge interval of 14 s and a purge duration of 100 ms. According to Fig. 4(a)-(d) and Table IV, a 100 ms purge duration for current levels of 30 A and 42 A is insufficient to recover PEMFC performance. Fig. 4(f)-(i) indicates the voltage behavior with the 14 s purge interval and the 200 ms purge duration. The results of Fig. 4(f)-(i) and Table IV show that the 200 ms purge duration is not sufficient for a current of 42 A to remove the excess water and stabilize the voltage. According to Table IV, for a 14 s purge interval, a purge duration of 400 ms is suitable for an effective water management.

In this study, the maximum purge interval is 20 s. By analyzing different purge durations, Table V indicates that a

purge duration of 600 ms is suitable for a 20 s purge interval, as the voltage drop for all currents remains below 100 mV.

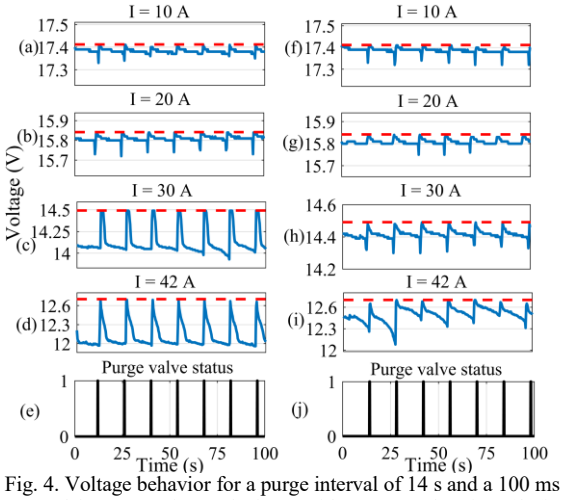

Fig. 4. Voltage behavior for a purge interval of 14 s and a 100 ms duration: (a)-(e), and for a purge interval of 14 s with a 200 ms duration: (f)-(j).

TABLE IV
AVERAGE VOLTAGE DROPS FOR A PURGE INTERVAL OF 14 S WITH DIFFERENT PURGE DURATIONS

Purge interval (s) - Purge duration (ms)					
14 - 100	Current (A)	10	20	30	42
	Voltage drop (mV)	28.33	38.33	463.67	698.19
14 - 200	Voltage drop (mV)	23.33	36.67	83.33	220
14 - 300	Voltage drop (mV)	18.25	30	73.26	136.67
14 - 400	Voltage drop (mV)	13	27.55	66.67	93.13

TABLE V
AVERAGE VOLTAGE DROPS FOR A PURGE INTERVAL OF 20 S WITH DIFFERENT PURGE DURATIONS

Purge interval (s) - Purge duration (ms)					
20 - 100	Current (A)	10	20	30	42
	Voltage drop (mV)	65	132.50	732.50	917.50
20 - 200	Voltage drop (mV)	45	80	475	525.67
20 - 300	Voltage drop (mV)	35.33	73.33	235	242.50
20 - 400	Voltage drop (mV)	25.33	50	102.50	195.33
20 - 500	Voltage drop (mV)	23.57	35	82	113.76
20 - 600	Voltage drop (mV)	20	27.50	75	72.50

Table VI shows the appropriate purge durations for all purge intervals used in this study. Based on the analysis of experimental results, for a constant purge interval, increasing the purge duration mitigates water management faults. Conversely, for a constant purge duration, increasing the purge interval leads to increased water management faults and unstable voltage.

C. Impact of the Purge Strategy on Hydrogen Consumption

To understand the effect of purge strategy on hydrogen consumption for the H-500 DEA-PEMFC, Fig. 5 shows the hydrogen consumption at various purge durations. For this purpose, the PEMFC is tested under a constant purge interval of 8 s as an example, combined with different purge durations (200 ms, 400 ms, 600 ms, and 1000 ms). The main goal of the proposed test is to analyze the impact of wasted hydrogen during purge process on the total hydrogen consumption. It should be noted that during the experiments, the PEMFC voltage remains stable under different purge strategies.

TABLE VI
APPROPRIATE PURGE DURATION FOR EACH PURGE INTERVAL

Purge interval (s)	Appropriate purge duration (ms)
8	200
10	300
12	300
14	400
16	500
18	500
20	600

The duration of each purge strategy test is 100 s, and hydrogen consumption data from the hydrogen flowmeter are recorded during the tests. According to the experimental data, when the purge valve opens, the hydrogen flow shows a peak in the recorded data. This peak represents the wasted hydrogen during the purge process. The total hydrogen consumption is the sum of the hydrogen flow at each current level and the wasted hydrogen during the purge process over the test period. This total is then divided by the test duration to express the result in grams per second. The black stem labeled "Baseline" represents only the hydrogen directly consumed electrochemically by the PEMFC stack to produce power at a given current, without considering the wasted hydrogen used during the purge process. According to Fig. 5, as the purge duration increases, the valve remains open longer, leading to more wasted hydrogen. For a given power with stable voltage, an increase in wasted hydrogen leads to higher total hydrogen consumption and a reduction in PEMFC system efficiency. Therefore, in addition to maintaining voltage stability, selecting a suitable and efficient purge strategy to minimize wasted hydrogen has a significant impact on overall PEMFC system efficiency. As a result, Fig. 5 illustrates that the wasted hydrogen during the purge process should not be neglected, as it significantly contributes to total hydrogen consumption and impacts the system efficiency of the PEMFC.

D. Designing an Efficient Purge Strategy

To efficiently select a suitable purge strategy, two criteria should be considered. The first is voltage stability, and the second is hydrogen consumption. Hydrogen consumption significantly affects energy efficiency and is a major contributor to the PEMFC operating cost. Therefore, an efficient purge strategy involves balancing the trade-off between maintaining voltage stability and minimizing hydrogen consumption. To illustrate this trade-off, this study analyzes the total energy loss (TEL).

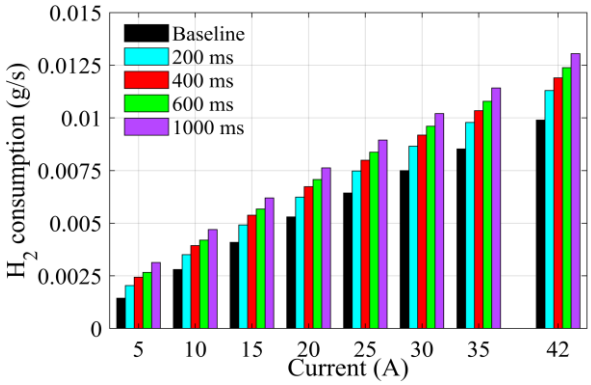

Fig. 5. Impact of wasted hydrogen during the purge process on total hydrogen consumption.

According to (1), the TEL comprises the electrical energy loss (EEL) resulting from the voltage drop and the hydrogen energy loss (HEL) due to the discharged hydrogen.

$$TEL\ (J) = EEL\ + HEL \tag{1}$$

The EEL is calculated as:

$$EEL\ (J) = N \times \int_0^{Purge\ period} (V_{desired} - V(t))\ I\ dt \tag{2}$$

where N is the number of purge periods within 100 s test, I represents the PEMFC current, $V_{desired}$ is the PEMFC nominal voltage for a given current, and $V(t)$ is the experimental PEMFC voltage. The HEL can be calculated using (3).

$$HEL\ (J) = N \times discharged\ H_2\ \times LHV \tag{3}$$

In (3), $discharged\ H_2$ represents the amount of wasted hydrogen in grams, and LHV stands for the lower heating value of hydrogen. To better understand the amount of energy loss, this study presents energy loss as a percentage of the total produced energy (TPE). The TPE is defined as:

$$TPE\ (J) = \left(N \times \int_0^{Purge\ period} (V(t))I\ dt\right) + TEL \tag{4}$$

Therefore, the ratio of energy loss to TPE is defined as:

$$\begin{aligned} TEL_r\ (\%) &= TEL/TPE \\ EEL_r\ (\%) &= EEL/TPE \\ HEL_r\ (\%) &= HEL/TPE \end{aligned} \tag{5}$$

Fig. 6 shows the ratio of energy loss to TPE as a percentage. Fig. 6 represents the average value for all currents to provide a clear perspective on energy loss. The results from Fig. 6(a) show that longer purge intervals reduce the frequency of purging, which results in lower hydrogen consumption and reduced HEL. However, longer intervals can increase the risk of water management faults and result in voltage drops and an increase in EEL. The results illustrate that up to a 12 s purge interval, the TEL decreases because hydrogen consumption is reduced as the purge interval increases, and the voltage drop is not severe. However, after the 12 s purge interval, although hydrogen consumption continues to decrease, the voltage drop caused by the longer purge interval becomes the dominant factor, leading to an increase in TEL. According to Fig. 6(b), across different purge durations, an increase in purge duration leads to a longer opening time of the purge valve, which results in increased HEL and reduces the risk of water management faults, leading to lower EEL. The results show that up to 500 ms, hydrogen consumption does not have a predominant effect, and the decrease in EEL and the reduced risk of water management faults cause a reduction in TEL. However, after 500 ms, the increase in hydrogen consumption becomes the predominant factor, leading to an increase in TEL. The results indicate that a long purge interval and short purge duration reduce HEL but increase EEL. On the other hand, a short purge interval and long purge duration reduce EEL but increase HEL.

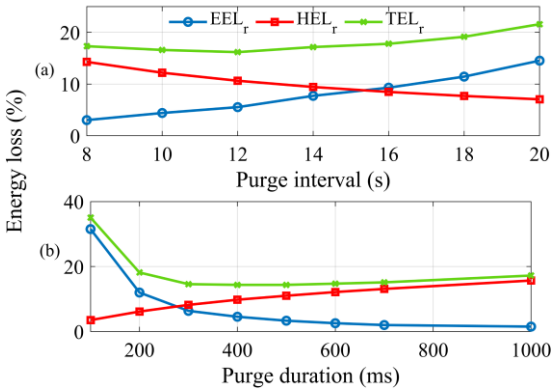

Fig. 6. Ratio of energy loss to TPE based on: (a) Purge interval; (b) Purge duration.

In summary, Fig. 6 illustrates that, in addition to EEL, which is related to voltage stability, HEL, which is related to hydrogen consumption, is equally important. As a result, selecting an efficient purge strategy to reduce TEL involves a trade-off between balancing hydrogen consumption (HEL) and voltage drop (EEL).

1) Adaptive Efficient Purge Strategy Framework: This section aims to design an adaptive efficient purge strategy that adjusts to different current levels. An adaptive efficient purge strategy consists of two steps. In the first step, all combinations of different purge intervals and durations, forming 56 various purge strategies, are analyzed for each current level from 1 A to 42 A. Among these, the combinations with a voltage drop of less than 100 mV are selected. The next step is to examine hydrogen consumption. Among the combinations that maintain voltage stability, the one with the lowest wasted hydrogen is selected as the efficient purge strategy. This procedure is repeated whenever the PEMFC operating current changes.

Fig. 7 illustrates the process of selecting an adaptive efficient purge strategy based on different current levels. It should be noted that the results shown in Fig. 7 are based on data extracted from the extensive experiments described in Section II. According to Fig. 7 the red stems represent combinations where the voltage drop exceeds 100 mV threshold which leads to water management faults. The blue stems represent combinations where the voltage drop stays below 100 mV which prevents water management faults.

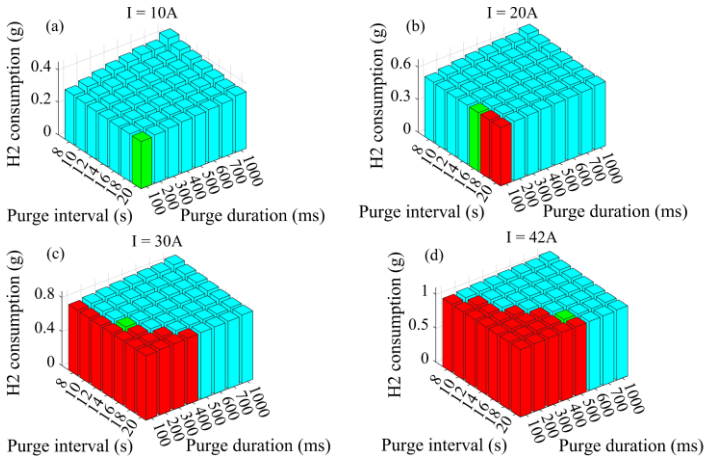

Fig. 7. Adaptive efficient purge strategy selection for different current levels: (a) 10 A; (b) 20 A; (c) 30 A; (d) 42 A.

Among the blue stems, which represent combinations with voltage drops under 100 mV, the one with the lowest wasted hydrogen is chosen as the efficient purge strategy and is marked by the green stem. As a result, the priority of the proposed purge strategy is to maintain voltage stability. The strategy initially selects purge combinations that ensure stable voltage. Then, among these combinations, the one with the minimum wasted hydrogen and lower hydrogen consumption is chosen as the efficient purge strategy. This procedure illustrates that the proposed purge strategy does not compromise voltage stability in order to reduce hydrogen consumption.

To illustrate the effectiveness of the proposed purge strategy, Fig. 8 compares the experimental results of the proposed purge strategy with the non-adaptive purge strategy recommended by the manufacturer. According to Fig. 8(a)-(b), the manufacturer's suggested strategy uses a constant purge period for all current levels. According to Fig. 8(c), the manufacturer's purge strategy works effectively up to 24 A. However, it fails to mitigate water management faults and maintain voltage stability at higher currents. As shown in Fig. 8(c), the proposed purge strategy keeps the voltage drop below 100 mV across different current levels due to its adaptive feature, demonstrating its effectiveness in improving water management.

III. Integrated Water Management into the Energy Management Strategy

A. Hardware-in-the-Loop Setup

To evaluate the effectiveness of the proposed purge strategy for water management in real-time application, this study aims to design an IWM-EMS through a HIL platform for a multi-stack hybrid powertrain case study used for a low-speed vehicle called Nemo [32]. The powertrain includes four H-500 DEA-PEMFCs, a three-phase induction motor, and a battery pack. The FCs serve as the main power source, while the battery pack is small, and its main role is to assist the FCs in supplying power peaks. In this powertrain configuration, the battery pack connects directly to the bus, while the FCs are connected through unidirectional DC-DC converters. The proposed IWM-EMS consists of an EMS level and a purge strategy level.

The proposed IWM-EMS is programmed in MATLAB and embedded into the LabVIEW environment. The time step of the proposed IWM-EMS is one second.

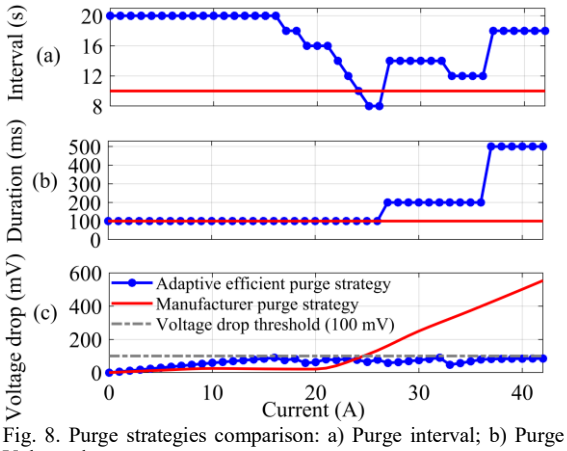

Fig. 8. Purge strategies comparison: a) Purge interval; b) Purge duration; c) Voltage drop.

In each time step, the IWM-EMS determines the optimal power of each sub-stack through the EMS level and the efficient purge strategy based on the reference current through the purge strategy level. After receiving the reference current and determining the efficient purge interval and duration, the control signal for the purge valve is sent to the PEMFC controller through the LabVIEW interface block.

The HIL platform is shown in Fig. 9. According to Fig. 9, two H-500 DEA-PEMFCs in this platform are employed as real components, while the other two PEMFCs are virtual and used as emulators. It should be mentioned that the other components of this platform are represented by mathematical models. The PEMFCs are connected to a National Instruments CompactRIO (NIcRIO-9022) through their controller. The CompactRIO connects to the PC running LabVIEW software using an Ethernet connection. Data is transferred between the CompactRIO and the PC every 100 ms. It should be mentioned that the time scale of flooding and drying out dynamics ranges from a few seconds to several minutes [33]. Therefore, the order of magnitude of the sampling rate (100 ms) is much faster than the characteristic time of flooding and drying out dynamics. In this regard, 100 ms is considered a conservative sampling rate to ensure a fast response to voltage changes caused by water management faults. At each sampling time, experimental data such as PEMFC voltage, current, and hydrogen flow rate are recorded and collected. Two 8514 BK Precision DC electronic loads are used to impose load profiles on the PEMFC stacks.

The model of the two PEMFC emulators is based on the Amphlett model, which is a semi-empirical model supported by a mechanistic background and has been widely used in many studies due to its strong capacity to model PEMFC output voltage [34]. The nominal output voltage of the PEMFC is calculated using (6).

$$V_{nominal} = N_{cell}(E_{Nernst} + V_{act} + V_{ohm} + V_{con}) \tag{6}$$

where N_{cell} is the number of cells, E_{Nernst} (V) is reversible potential, V_{act} (V), V_{ohm} (V), and V_{con} (V) are the activation loss, ohmic loss, and concentration loss, respectively. E_{Nernst} is calculated using (7):

$$E_{Nernst} = 1.299 - 0.85 \times 10^{-3}(T_{st} - 298.15) + 4.3085 \times 10^{-5}[0.5ln(P_{O2} + ln(P_{H2})]\, T_{st} \tag{7}$$

where T_{st} is the stack temperature (K), P_{O2} and P_{H2} are the oxygen and hydrogen partial pressures (N/m²). The formulation of V_{act} is shown in (8).

$$V_{act} = -[\xi_1 + \xi_2 T_{st} + \xi_3 T_{st} ln(CO_2) + \xi_4 T_{st} ln(i_{FC})] \tag{8}$$

where ξ_n (n = 1...4) are semi-empirical parameters, CO_2 is the oxygen concentration (mol/cm³), and i_{FC} is the PEMFC current (A). V_{ohm} and V_{con} can be calculated by:

$$V_{ohmic} = -i_{FC} R_{int} = -i_{FC}(\zeta_1 + \zeta_2 T_{st} + \zeta_3 i_{FC}) \tag{9}$$

$$V_{con} = B \times ln(1 - \frac{J}{J_{max}}) \tag{10}$$

where R_{int} (Ω) is the PEMFC equivalent internal resistance, ζ_n (n = 1...3) and B are semi-empirical coefficients, J is the actual current density (A/cm²), and J_{max} is the maximum current density (A/cm²).

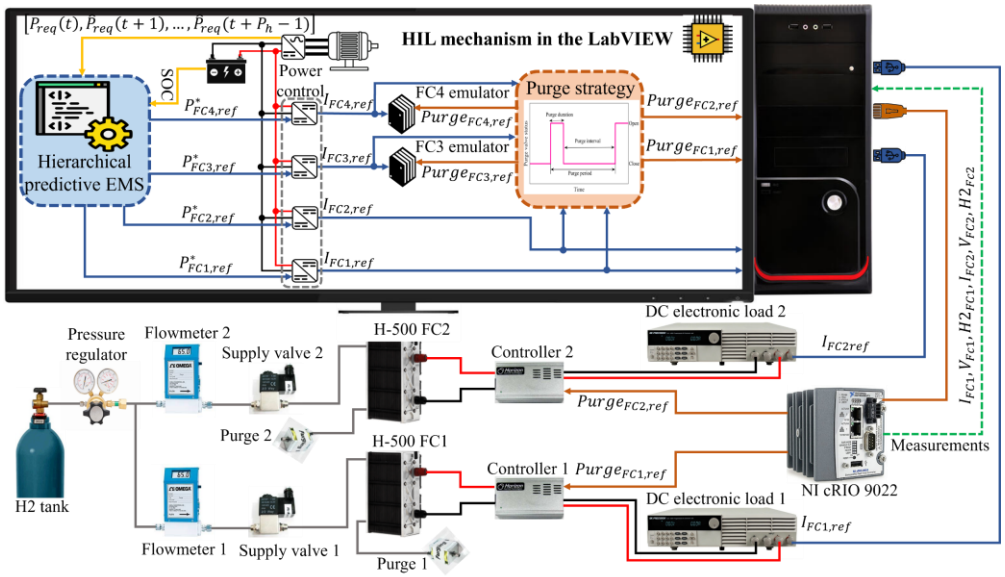

Fig. 9. HIL mechanism of the IWM-EMS.

Based on the data extracted from the extensive experiments, the voltage drop corresponding to different purge strategies for each current level is calculated and collected in a lookup table. In this regard, the PEMFC output voltage at each time step is calculated using (11).

$$V_{FC} = V_{nominal} - V_{drop} \tag{11}$$

where V_{drop} is the PEMFC voltage drop during the purge interval. The voltage drop is subtracted from the PEMFC output voltage model to make the model more realistic.

In the HIL setup, a PI controller is designed in the power control box to regulate the PEMFC current and ensure accurate tracking of the reference power. In this setup, when V_{FC} decreases due to a voltage drop, the PI controller increases the PEMFC operating current to reach the reference power.

B. Energy Management Strategy Level

In this study, a hierarchical predictive EMS (HPEMS) is used to distribute optimal power. The first layer is a rule-based strategy that decides how many FCs should be activated and participate in the second layer. The second layer is a model predictive control (MPC) that, based on the information from the first layer and system constraints, determines optimal power between the FCs and the battery.

Upper Layer

The upper layer is a rule-based EMS that uses a rotary state machine approach to determine how many sub-stacks should participate in the lower layer. This decision is made based on the requested power, battery SOC, and sub-stack degradation rates. In other words, at each time step, sub-stacks with lower degradation rates are given higher priority to participate in the lower layer of the EMS. For example, if two sub-stacks are sufficient to meet the requested power, the upper layer selects the two sub-stacks with the lowest degradation. As a result, the upper layer of the EMS serves two main purposes. First, it aims to balance degradation across all sub-stacks and prevent further degradation. Second, it helps reduce hydrogen consumption by determining when to activate or deactivate sub-stacks, keeping unnecessary FCs turned off when not required.

Lower Layer

The lower layer of the EMS employs MPC, a predictive optimization-based strategy. Based on the future vehicle velocities within a prediction horizon of 10 s and utilizing information from the upper layer regarding the number of active sub-stacks, the MPC minimizes a cost function to determine the optimal power distribution between the sub-stacks and the battery. In other words, at each time step, the lower layer determines the optimal power for each sub-stack, and the reference current corresponding to the optimal power is sent to the purge strategy level. The nonlinear problem is formulated as a state-space model in MPC. Usually, in this type of problem, the SOC is a state variable, and FC power is the control variable. In this study, the increment of FC power is used as the control variable, with the state-space formulation given by (12).

$$\Delta x(t+1) = A\Delta x(t) + B\Delta u(t) + D\Delta d(t) \tag{12}$$

where $x(t)$ represents the SOC, $u(t)$ is the FC power, and $d(t)$ is the requested power, modeled as a disturbance in this formulation. A, B, and D are matrices of coefficients and t indicates the time step. In this study the sampling time is set to 1 s. It should be noted that in this paper, prediction horizon (P_h) is set to 10 s. The MPC requires the vehicle's future velocities within the prediction horizon to determine the optimal power sequence. For this purpose, this study assumes that the entire driving cycle is already known, and at each time step, using the next 10 s of velocity data, the MPC determines the optimal power sequence. As shown in (13), the multi-objective cost function in this study is based on the total operating cost, which includes hydrogen consumption, FC degradation, and battery degradation.

$$\min_{\Delta P_{FC}(t+k),k\in\{0,1,\dots,P_h-1\}} J_t = C_{H_2,t} + C_{FC,deg,t} + C_{bat,deg,t} + k_{SOC,t} \ (\$) \quad (13)$$

where $C_{H_2,t}$ is the hydrogen consumption cost, $C_{FC,deg,t}$ is the FC degradation cost. and $C_{bat,deg,t}$ is the battery degradation cost. The final term in the multi-objective cost function, $k_{SOC,t}$, is a penalty term designed to enforce the battery charge-sustaining strategy and keep the SOC close to its initial value. In this study, the units for hydrogen price, FC system price, and battery pack price are 4 $/kg, 93 $/kW, and 178.41 $/kWh, respectively [35], [36]. FC operation constraints are shown in (14).

$$\begin{cases} P_{FC,min} \le P_{FC}(t+k) \le P_{FC,max} \\ \Delta P_{FC,min} \le P_{FC}(t+k) - P_{FC}(t+k-1) \le \Delta P_{FC,max} \end{cases} \quad (14)$$

$P_{FC,min}$ is set to zero, $P_{FC,max}$ is 500 W, and $\Delta P_{FC,min}$ and $\Delta P_{FC,max}$ are -50 W/s and 50 W/s, respectively. Battery constraints include battery power, SOC, and SOH, as shown in (15).

$$\begin{cases} SOC(0) = 70\% \\ SOC_{min} \le SOC(t+k) \le SOC_{max} \\ SOH(0) = 100\% \\ SOH_{min} \le SOH(t+k) \le SOH_{max} \\ P_{bat,min} \le P_{bat}(t+k) \le P_{bat,max} \end{cases} \quad (15)$$

where SOC_{min} is 50%, SOC_{max} is 90%, SOH_{min} is 0%, and SOH_{max} is 100%. The battery power limits, $P_{bat,min}$ and $P_{bat,max}$, are set to -1900 W and 1900 W, respectively. This study utilizes sequential quadratic programming (SQP) to solve the receding horizon optimization problem, which is a common algorithm for such applications. The convergence and computational efficiency of SQP are satisfactory for use in real-time applications [36], [37].

C. Purge Strategy Level

The second level of the proposed AIWM-EMS is the purge strategy section. This level uses an adaptive efficient purge strategy mechanism. The proposed purge strategy is based on a lookup table extracted from extensive experiments. At each time step, the purge strategy block receives the current reference from the EMS, determines the efficient purge strategy that maintains stable voltage and minimizes wasted hydrogen, and then sends the control signal to the purge valve through the PEMFC controller. It should be noted that, at each time step, the purge strategy level receives four different current values corresponding to the four sub-stacks. Based on the reference current of each sub-stack, it determines the efficient purge interval and duration.

IV. Result and Discussion

This section aims to evaluate the IWM-EMS performance. This study proposes an adaptive IWM-EMS (AIWM-EMS), where an adaptive efficient purge strategy is integrated into the EMS. The performance of the AIWM-EMS is compared with that of the non-adaptive IWM-EMS (NAIWM-EMS), which incorporates the manufacturer's non-adaptive purge strategy into the EMS. The performance and effectiveness of the two IWM-EMSs are compared under the WLTC-class3 driving cycle. Fig. 10 shows the driving cycle, with the right vertical axis representing the requested power and the left vertical axis representing the velocity.

Fig. 11(a)-(d) show the FC power distribution, and Fig. 11(e) presents the battery SOC. FC1 and FC2 are real PEMFCs in the HIL, with experimental data such as current, voltage, and hydrogen consumption collected via CompactRIO, while FC3 and FC4 are emulators. According to Fig. 11(a)-(d), in high-power zones, such as from 1113 s to 1372 s and 1546 s to 1770 s, the FCs must operate at high currents to meet the requested power. FCs operating under the AIWM-EMS can supply the requested power because water management faults are effectively mitigated and the FCs voltage remains stable. To meet the requested power, FCs under the NAIWM-EMS must operate at higher currents than those under the AIWM-EMS to compensate for the higher voltage drop. FCs under the NAIWM-EMS operate at lower power at the maximum FC current. With the maximum current set to 42 A, the FCs under NAIWM-EMS cannot exceed this current to compensate for the voltage drop and must operate at reduced power. Operating at reduced power causes FCs in the NAIWM-EMS to work longer in the high-power zone compared to those in the AIWM-EMS to meet the requested power and maintain battery SOC, resulting in a different SOC trajectory, as shown in Fig. 11(e).

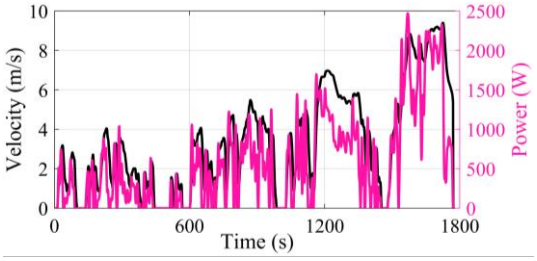

Fig. 10. WLTC-class3 driving cycle.

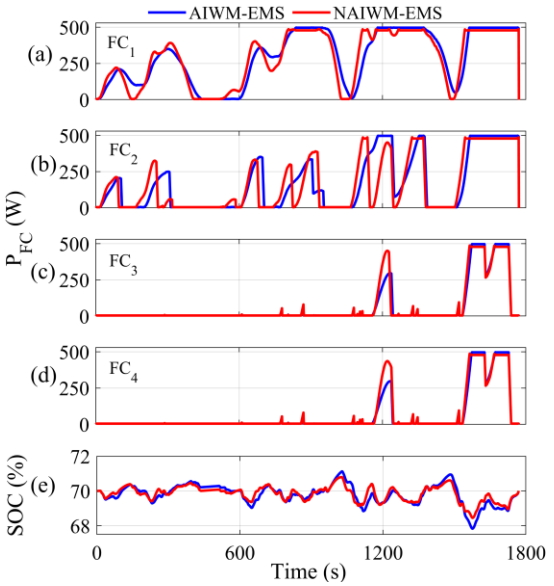

Fig. 11. AIWM-EMS and NAIWM-EMS performance under the WLTC-class3 driving cycle: a) FC_1 power; b) FC_2 power; c) FC_3 power; d) FC_4 power; e) Battery SOC.

Fig. 12 illustrates the voltage drop caused by water management faults in the PEMFCs during the driving cycle. The ultimate goal of a suitable purge strategy is to improve water management, reduce voltage drops, and enhance PEMFC voltage stability. The results of the HIL show that the AIWM-EMS consistently maintains voltage stability throughout the driving cycle, keeping voltage drops below 100 mV. This demonstrates the effectiveness of the proposed strategy in mitigating water management faults. These results highlight the robustness and quick response time of the adaptive strategy under real driving conditions. However, the voltage drop of the FCs under the NAIWM-EMS exceeds 100 mV, particularly in high-power zones, indicating water flooding faults due to the use of a non-adaptive purge strategy.

Fig. 13 shows a comparison of the total wasted hydrogen when the purge valve is open. During the driving cycle, opening the PEMFC purge valve causes a peak in the hydrogen flow data, which indicates the amount of wasted hydrogen during the purge process. Over the entire driving cycle, all hydrogen flow peaks are extracted and calculated as the total wasted hydrogen under two different purge strategies. The total wasted hydrogen in the AIWM-EMS is 1.128 g, while it is 1.533 g in the NAIWM-EMS. According to Fig. 13, the total wasted hydrogen in the AIWM-EMS is 26.42% less than in the NAIWM-EMS.

Fig. 14 compares the total operating cost of the FC-HEV under the AIWM-EMS and NAIWM-EMS. According to Fig. 14, the cost of hydrogen consumption in the AIWM-EMS is 4.09% lower than in the NAIWM-EMS.

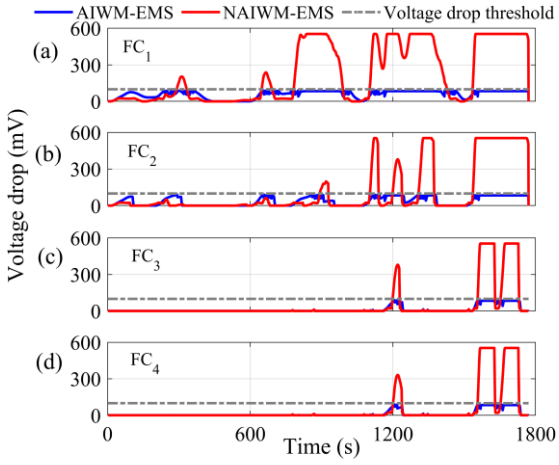

Fig. 12. Voltage drop comparison between AIWM-EMS and NAIWM-EMS: a) FC_1; b) FC_2; c) FC_3; d) FC_4.

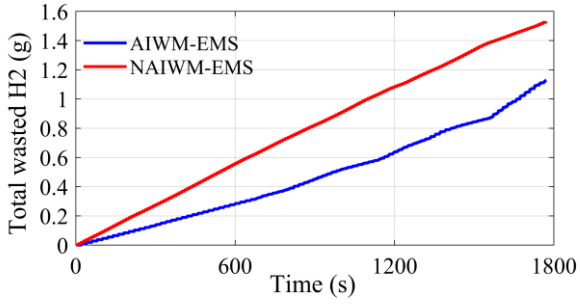

Fig. 13. Total wasted hydrogen during the purge strategies.

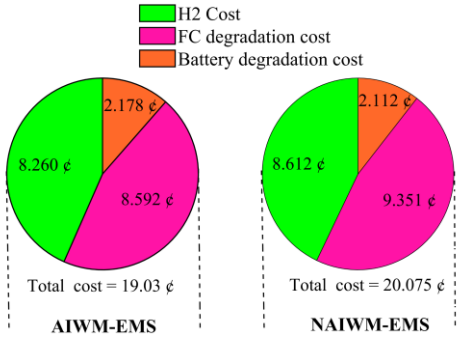

Fig. 14. FC-HEV operating cost comparison.

The results also show that the cost of FC degradation in the AIWM-EMS is 8.12% less than in the NAIWM-EMS. Under the NAIWM-EMS, the FCs operate at reduced power at maximum current, leading to longer operation at high power to meet the requested power and maintain battery SOC, which increases FC degradation. The results indicate that the total time spent in high power for all FCs in the AIWM-EMS is 1189 s, while in the NAIWM-EMS, the FCs spend 1263 s in the high-power zone. The cost of battery degradation in the AIWM-EMS is slightly higher than in the NAIWM-EMS because the AIWM-EMS utilizes a wider range of battery SOC. The results show that the total operating cost in the AIWM-EMS is 5.21% lower than in the NAIWM-EMS. As a result, according to the HIL results, the proposed strategy, due to its adaptability, can dynamically adjust to changes in the requested power. Compared to the constant and non-adaptive strategy, the ability of the proposed strategy to adapt to various dynamic conditions leads to improved voltage stability, lower hydrogen consumption, reduced FC degradation, and ultimately a lower operating cost. On the other hand, reducing the total operating cost of the FC has a direct impact on maintenance cost. Increased voltage stability and reduced FC degradation lead to a longer FC lifespan, which delays maintenance, reduces its frequency, and ultimately lowers maintenance cost.

Fig. 15 shows the system efficiency distribution of all sub-satcks in the FC-HEV. According to (16), the FC system efficiency is calculated as follows:

$$\eta_{FC\ system} = \frac{P_{FC,total}}{\dot{m}_{H_2,total}\, LHV_{H_2}} \tag{16}$$

where $P_{FC,total}$ is the total power output of the four sub-stacks, $\dot{m}_{H_2,total}$ is the total hydrogen consumption by the four sub-stacks, and LHV_{H_2} is the lower heating value of hydrogen, which is 120 MJ/kg.

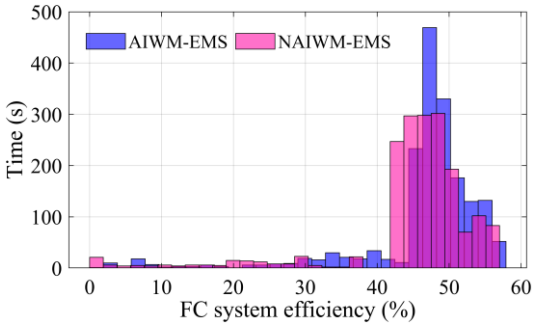

Fig. 15. FC system efficiency distribution comparison.

At each time step of the driving cycle, the FC system efficiency is calculated and recorded. To evaluate the impact of the AIWM-EMS on multi-stack FC performance, this study analyzes the multi-stack FC system efficiency over the entire driving cycle tested in the HIL. In this regard, according to the experimental results, the maximum system efficiency of the tested PEMFC is 46.5%, and the high-efficiency zone is defined as the region where the PEMFC system efficiency is equal to or greater than 45%. The high-efficiency zone is the area where the PEMFC achieves high performance and lower hydrogen consumption per unit of power output. In the AIWM-EMS, the FCs operate in a safe condition without water management faults, resulting in voltage drops below 100 mV. This prevents the FCs from operating at higher currents and increasing hydrogen consumption, thereby achieving higher efficiency, as shown in Fig. 15. Additionally, in the AIWM-EMS, the efficient purge strategy minimizes wasted hydrogen. Consequently, the FCs operates with higher efficiency compared to the NAIWM-EMS. However, it should be mentioned that increasing efficiency and reducing hydrogen consumption do not mean that the proposed strategy compromises voltage stability. The strategy first ensures voltage stability, and among the suitable purge strategies that maintain voltage stability, it selects the efficient one with minimum wasted hydrogen.

The results show that the FCs operate 78.36% of the driving cycle time in a high-efficiency zone, while in the NAIWM-EMS, the FCs operate 62% of the driving cycle time in the high-efficiency zone.

V. Conclusion

This study aims to integrate the impact of water management into the EMS for a FC-HEV. For this purpose, an IWM-EMS is designed with two levels. The first level is the HPEMS and the second level is the purge strategy. This paper proposes an AIWM-EMS in which an adaptive efficient purge strategy is embedded. The AIWM-EMS adapts to various dynamic conditions by adjusting the purge strategy based on the PEMFC operating current levels. On the other hand, the AIWM-EMS selects the efficient purge strategy to mitigate water management faults, enhance voltage stability, and minimize hydrogen consumption. The results of the AIWM-EMS are compared with the NAIWM-EMS, which includes a non-adaptive purge strategy recommended by the FC manufacturer. The results demonstrate the effectiveness of the AIWM-EMS in reducing water management faults, maintaining voltage stability across all current levels, and minimizing hydrogen consumption. The costs of hydrogen consumption and FC degradation in the FC-HEV under the AIWM-EMS are 4.09% and 8.12% lower, respectively, than in the NAIWM-EMS, and the total operating cost in the AIWM-EMS is reduced by 5.21% compared to the NAIWM-EMS. The results also show that the FCs under the AIWM-EMS works 78.36% of the operating time in the high-efficiency zone, compared to 62% under the NAIWM-EMS.

Future Work

1- To develop the proposed purge strategy and increase its effectiveness, a feasible option for future work is to expand the experiments and evaluate the strategy by considering changes in environmental conditions such as temperature and humidity.

2- Integrating an FC maintenance cost model into the total operating cost in future work will help account for all real-world FC expenses and enhance the practicality of the proposed purge strategy in real-world applications.

3- This study aimed to illustrate the importance of water management in PEMFC performance and operating cost. Thermal management and operating temperature can significantly affect water management and overall PEMFC performance. Therefore, in future work, the authors plan to enhance the performance and applicability of the proposed purge strategy by incorporating the effects of different cooling systems and thermal management into the water management approach.

References

[1] M. S. Munsi and R. P. Joshi, “Comprehensive Analysis of Fuel Cell Electric Vehicles: Challenges, Powertrain Configurations, and Energy Management Systems,” *IEEE Access*, vol. 12, no. September, pp. 145459–145482, 2024, doi: 10.1109/ACCESS.2024.3472704.

[2] X. Hu, J. Han, X. Tang, and X. Lin, “Powertrain Design and Control in Electrified Vehicles: A Critical Review,” *IEEE Trans. Transp. Electrif.*, vol. 7, no. 3, pp. 1990–2009, 2021, doi: 10.1109/TTE.2021.3056432.

[3] A. Prasanthi, H. Shareef, R. Errouissi, G. V. Murugesu, and M. Asna, “Optimal Sizing and Dynamic Energy Source Characteristics of Hybrid Electric Vehicles: A Comprehensive Review and Future Directions,” *IEEE Access*, vol. 12, no. March, pp. 44695–44729, 2024, doi: 10.1109/ACCESS.2024.3380464.

[4] A. Khalatbarisoltani, H. Zhou, X. Tang, M. Kandidayeni, L. Boulon, and X. Hu, “Energy Management Strategies for Fuel Cell Vehicles: A Comprehensive Review of the Latest Progress in Modeling, Strategies, and Future Prospects,” *IEEE Trans. Intell. Transp. Syst.*, vol. 25, no. 1, pp. 14–32, 2024, doi: 10.1109/TITS.2023.3309052.

[5] A. Moslehi, M. Kandidayeni, M. Hébert, and S. Kelouwani, “Investigating the impact of a fuel cell system air supply control on the performance of an energy management strategy,” *Energy Convers. Manag.*, vol. 325, p. 119374, 2025, doi: https://doi.org/10.1016/j.enconman.2024.119374.

[6] M. S. Munsi and H. Chaoui, “Energy Management Systems for Electric Vehicles: A Comprehensive Review of Technologies and Trends,” *IEEE Access*, vol. 12, no. December 2023, pp. 60385–60403, 2024, doi: 10.1109/ACCESS.2024.3371483.

[7] F. Tao, L. Zhu, Z. Fu, P. Si, and L. Sun, “Frequency decoupling-based energy management strategy for fuel cell/ battery/ultracapacitor hybrid vehicle using fuzzy control method,” *IEEE Access*, vol. 8, pp. 166491–166502, 2020, doi: 10.1109/ACCESS.2020.3023470.

[8] A. M. I. Fernandez *et al.*, “An Adaptive State Machine Based Energy Management Strategy for a Multi-Stack Fuel Cell Hybrid Electric Vehicle,” *IEEE Trans. Veh. Technol.*, vol. 69, no. 1, pp. 220–234, 2020, doi: 10.1109/TVT.2019.2950558.

[9] D. F. Pereira, F. D. C. D. C. Lopes, and E. H. Watanabe, “Nonlinear Model Predictive Control for the Energy Management of Fuel Cell Hybrid Electric Vehicles in Real Time,” *IEEE Trans. Ind. Electron.*, vol. 68, no. 4, pp. 3213–3223, 2021, doi: 10.1109/TIE.2020.2979528.

[10] Y. Zhang, R. Ma, D. Zhao, Y. Huangfu, and W. Liu, “An Online Efficiency Optimized Energy Management Strategy for Fuel Cell Hybrid Electric Vehicles,” *IEEE Trans. Transp. Electrif.*, vol. 9, no. 2, pp. 3203–3217, 2023, doi: 10.1109/TTE.2022.3214683.

[11] Z. Fu, H. Wang, F. Tao, B. Ji, Y. Dong, and S. Song, “Energy Management Strategy for Fuel Cell/Battery/Ultracapacitor Hybrid Electric Vehicles Using Deep Reinforcement Learning With Action Trimming,” *IEEE Trans. Veh. Technol.*, vol. 71, no. 7, pp. 7171–7185, 2022, doi: 10.1109/TVT.2022.3168870.

[12] Y. Zhang, R. Ma, D. Zhao, Y. Huangfu, and W. Liu, “A Novel Energy Management Strategy Based on Dual Reward Function Q-Learning for Fuel Cell Hybrid Electric Vehicle,” *IEEE Trans. Ind. Electron.*, vol. 69, no. 2, pp. 1537–1547, 2022, doi: 10.1109/TIE.2021.3062273.

[13] R. Ma, H. Dang, R. Xie, L. Xu, and D. Zhao, “Online Fault Diagnosis for Open-Cathode PEMFC Systems Based on Output Voltage Measurements and Data-Driven Method,” *IEEE Trans. Transp.*

Electrif., vol. 8, no. 2, pp. 2050–2061, 2022, doi: 10.1109/TTE.2021.3114194.
[14] G. Dotelli, R. Ferrero, P. G. Stampino, S. Latorrata, and S. Toscani, "PEM Fuel Cell Drying and Flooding Diagnosis With Signals Injected by a Power Converter," *IEEE Trans. Instrum. Meas.*, vol. 64, no. 8, pp. 2064–2071, 2015, doi: 10.1109/TIM.2015.2406051.
[15] S. G. Kandlikar, M. L. Garofalo, and Z. Lu, "Water management in a PEMFC: Water transport mechanism and material degradation in gas diffusion layers," *Fuel Cells*, vol. 11, no. 6, pp. 814–823, 2011, doi: 10.1002/fuce.201000172.
[16] J. Liu, Q. Li, H. Yang, Y. Han, S. Jiang, and W. Chen, "Sequence Fault Diagnosis for PEMFC Water Management Subsystem Using Deep Learning with t-SNE," *IEEE Access*, vol. 7, pp. 92009–92019, 2019, doi: 10.1109/ACCESS.2019.2927092.
[17] A. Alyakhni, L. Boulon, J. M. Vinassa, and O. Briat, "A Comprehensive Review on Energy Management Strategies for Electric Vehicles Considering Degradation Using Aging Models," *IEEE Access*, vol. 9, pp. 143922–143940, 2021, doi: 10.1109/ACCESS.2021.3120563.
[18] Z. Zhang *et al.*, "Research on shutdown purge characteristics of proton exchange membrane fuel cells: Purge parameters conspicuity and residual water," *Appl. Therm. Eng.*, vol. 249, no. May, p. 123437, 2024, doi: 10.1016/j.applthermaleng.2024.123437.
[19] G. Yang, K. Meng, Q. Deng, W. Chen, and B. Chen, "Numerical investigation and experimental verification of liquid water dynamic transfer characteristics in the flow field of PEMFC with dead-ended anode during gas purging," *Chem. Eng. J.*, vol. 491, no. December 2023, p. 152082, 2024, doi: 10.1016/j.cej.2024.152082.
[20] L. shi, P. Liu, M. Zheng, and S. Xu, "Numerical study on the mechanism of water and gas phase transition and water redistribution after purging based on two-dimensional multi-phase model," *Energy Convers. Manag.*, vol. 278, no. January, p. 116725, 2023, doi: 10.1016/j.enconman.2023.116725.
[21] T. Donateo, "Simulation Approaches and Validation Issues for Open-Cathode Fuel Cell Systems in Manned and Unmanned Aerial Vehicles," *Energies*, vol. 17, no. 4, 2024, doi: 10.3390/en17040900.
[22] T. Niu *et al.*, "Purge strategy analysis of proton exchange membrane fuel cells based on experiments and comprehensive evaluation method," *Fuel*, vol. 363, no. November 2023, p. 130970, 2024, doi: 10.1016/j.fuel.2024.130970.
[23] S. Liu *et al.*, "Study on the effect of purging time on the performance of PEMFC with dead-ended anode under gravity," *Renew. Energy*, vol. 200, no. October, pp. 1141–1151, 2022, doi: 10.1016/j.renene.2022.10.065.
[24] J. Shen, Z. Tu, and S. H. Chan, "Effect of gas purging on the performance of a proton exchange membrane fuel cell with dead-ended anode and cathode," *Int. J. Energy Res.*, vol. 45, no. 10, pp. 14813–14823, 2021, doi: 10.1002/er.6757.
[25] J. Yao *et al.*, "High-stability dead-end anode proton exchange membrane fuel cells by purge optimization," *J. Power Sources*, vol. 595, no. December 2023, 2024, doi: 10.1016/j.jpowsour.2024.234062.
[26] J. C. Kurnia, A. P. Sasmito, and T. Shamim, "Advances in proton exchange membrane fuel cell with dead-end anode operation: A review," *Appl. Energy*, vol. 252, no. November 2018, p. 113416, 2019, doi: 10.1016/j.apenergy.2019.113416.
[27] Q. Jian, L. Luo, B. Huang, J. Zhao, S. Cao, and Z. Huang, "Experimental study on the purge process of a proton exchange membrane fuel cell stack with a dead-end anode," *Appl. Therm. Eng.*, vol. 142, no. March, pp. 203–214, 2018, doi: 10.1016/j.applthermaleng.2018.07.001.
[28] Y. F. Lin and Y. S. Chen, "Experimental study on the optimal purge duration of a proton exchange membrane fuel cell with a dead-ended anode," *J. Power Sources*, vol. 340, pp. 176–182, 2017, doi: 10.1016/j.jpowsour.2016.11.039.
[29] I. Dashti, S. Asghari, M. Goudarzi, Q. Meyer, A. Mehrabani-Zeinabad, and D. J. L. Brett, "Optimization of the performance, operation conditions and purge rate for a dead-ended anode proton exchange membrane fuel cell using an analytical model," *Energy*, vol. 179, pp. 173–185, 2019, doi: 10.1016/j.energy.2019.04.118.
[30] J. Hong, J. Yang, Z. Weng, F. Ma, F. Liang, and C. Zhang, "Review on proton exchange membrane fuel cells: Safety analysis and fault diagnosis," *J. Power Sources*, vol. 617, no. June, p. 235118, 2024, doi: 10.1016/j.jpowsour.2024.235118.
[31] M. Kandidayeni *et al.*, "Efficiency Upgrade of Hybrid Fuel Cell Vehicles' Energy Management Strategies by Online Systemic Management of Fuel Cell," *IEEE Trans. Ind. Electron.*, vol. 0046, no. 6, pp. 1–1, 2021, doi: 10.1109/tie.2020.2992950.
[32] M. Kandidayeni *et al.*, "An Online Energy Management Strategy for a Fuel Cell/Battery Vehicle Considering the Driving Pattern and Performance Drift Impacts," *IEEE Trans. Veh. Technol.*, vol. 68, no. 12, pp. 11427–11438, 2019, doi: 10.1109/TVT.2019.2936713.
[33] E. Dijoux, N. Y. Steiner, M. Benne, M. C. Péra, and B. G. Pérez, "A review of fault tolerant control strategies applied to proton exchange membrane fuel cell systems," *J. Power Sources*, vol. 359, pp. 119–133, 2017, doi: 10.1016/j.jpowsour.2017.05.058.
[34] R. F. Mann, J. C. Amphlett, M. A. I. Hooper, H. M. Jensen, B. A. Peppley, and P. R. Roberge, "Development and application of a generalized steady-state electrochemical model for a PEM fuel cell," *J. Power Sources*, vol. 86, no. 1, pp. 173–180, 2000, doi: 10.1016/S0378-7753(99)00484-X.
[35] M. Moghadari, M. Kandidayeni, L. Boulon, and H. Chaoui, "Predictive Health-Conscious Energy Management Strategy of a Hybrid Multi-Stack Fuel Cell Vehicle," *IEEE Trans. Veh. Technol.*, vol. PP, pp. 1–16, 2024, doi: 10.1109/TVT.2024.3512204.
[36] X. Hu, C. Zou, X. Tang, T. Liu, and L. Hu, "Cost-optimal energy management of hybrid electric vehicles using fuel cell/battery health-aware predictive control," *IEEE Trans. Power Electron.*, vol. 35, no. 1, pp. 382–392, 2020, doi: 10.1109/TPEL.2019.2915675.
[37] A. Khalatbarisoltani, M. Kandidayeni, L. Boulon, and X. Hu, "Power Allocation Strategy based on Decentralized Convex Optimization in Modular Fuel Cell Systems for Vehicular Applications," *IEEE Trans. Veh. Technol.*, vol. 9545, no. c, pp. 14563–14574, 2020, doi: 10.1109/tvt.2020.3028089.

Mohammadreza Moghadari was born in Babol, Iran, in 1992. He received his B.S. in Mechanical Engineering from Islamic Azad University, Tehran, in 2015, and his M.S. (Hons.) in Automotive Engineering from Iran University of Science and Technology in 2018. He began his Ph.D. in 2020 at the Hydrogen Research Institute, Université du Québec à Trois-Rivières (UQTR), Canada. Since 2016, he has published numerous articles in leading SCI journals and served as a reviewer for academic journals. His research focuses on PEMFC systems management, energy management strategies, optimization-based control, and fault-tolerant strategies for hybrid vehicles.

Mohsen Kandidayeni (Member, IEEE) was born in Tehran, Iran, in 1989. He received his B.S. in mechanical engineering in 2011, an M.S. (Hons.) in mechatronics from Arak University, Iran, in 2014, and a Ph.D. (Hons.) in electrical engineering from the University of Quebec at Trois-Rivières (UQTR), Canada, in 2020. From 2020 to 2024, he served as a Postdoctoral Fellow at eTESC, Research Associate and Technical Project Manager at HRI, and is now an Assistant Professor at UQTR. He has authored over 75 journal and conference publications and actively reviews scholarly articles. His research interests include hybrid electric vehicles, fuel cell systems, energy management, multiphysics systems, modeling, and control. Recognized with awards like the FRQNT Doctoral and Postdoctoral Scholarship, Best PhD Thesis Award, and Third Prize in the Energy Research Challenge, he has made significant contributions to energy-related research.

Ashkan Makhsoos was born in Arak, Iran, in 1991. He holds an M.Sc. in Mechanical Engineering of Biosystems (Renewable Energies) from the University of Tehran (2017) and a B.Sc. from the University of Arak (2014), focusing on renewable energies and biofuels. He is a Ph.D. candidate in Electrical Engineering at the University of Quebec at Trois-Rivières, specializing in energy management of multi-stack Proton Exchange Membrane Water Electrolyzers (PEMWE) for hydrogen production from renewable energies. A member of the Institute for Hydrogen

Research (IHR), he contributes to green hydrogen projects and reviews for prestigious journals. His research interests include energy management, electrochemical modeling, and renewable energy systems.

Loïc Boulon (Senior Member, IEEE) received his Master's degree in Electrical and Automatic Control Engineering from the University of Lille, France, in 2006, and a Ph.D. in Electrical Engineering from the University of Franche-Comté, France. He has been a professor at Université du Québec à Trois-Rivières (UQTR) since 2010, becoming a Full Professor in 2016 and Deputy Director of the Hydrogen Research Institute in 2019. His research focuses on modeling, control, and energy management of multiphysics systems, including hybrid electric vehicles and energy sources like fuel cells, batteries, and ultracapacitors. Dr. Boulon has authored over 140 peer-reviewed publications and delivered more than 40 invited talks globally. In 2022, he was recognized among the top researchers in "Proton Exchange Membrane Fuel Cell (PEMFC)" and "Plug-in Hybrid Vehicles" by Elsevier SciVal. He is VP-Motor Vehicles for the IEEE Vehicular Technology Society, holds the Canada Research Chair in Energy Sources for Future Vehicles, and directs the Réseau Québécois sur l'Énergie Intelligente.

Hicham Chaoui (Senior Member, IEEE) received his Ph.D. in Electrical Engineering (with honors) from the University of Quebec, Trois-Rivières, Canada, in 2011. His career spans academia and industry, specializing in control and energy systems. From 2007 to 2014, he held engineering and management roles in the Canadian industry. Currently, he is a Faculty Member at Carleton University, Ottawa, Canada. Dr. Chaoui has authored over 200 journal and conference publications and is a registered Professional Engineer in Ontario. He serves as an Associate Editor for IEEE Transactions on Power Electronics, IEEE Transactions on Vehicular Technology, and other journals. His accolades include the Best Thesis Award, Governor General of Canada Gold Medal, FED Research Excellence Award, Early Researcher Award from the Government of Ontario, and Top Editor Recognition from IEEE Vehicular Technology Society and IEEE Power Electronics Society.

4.3 Conclusion

This chapter aims to integrate water management into the EMS using the proposed purge strategy in a multi-stack FC-HEV. In other words, the purpose of this chapter is to enhance the performance of FCs in the multi-stack system by addressing water management and its effect on FC voltage stability. In this regard, an IWM-EMS is designed with two levels. The first level is the HPEMS, which determines the optimal power distribution between the FCs and the battery. The second level is the purge strategy, which sets the purge timing based on the current received from the EMS. This paper proposes an AIWM-EMS in which an efficient purge strategy is embedded. Based on the reference current received from the first level, the efficient purge strategy evaluates different combinations of purge intervals and durations, selecting the one that mitigates water management faults to maintain voltage stability and minimize hydrogen consumption. The results of the AIWM-EMS are compared with the NAIWM-EMS, which includes a non-adaptive purge strategy recommended by the FC manufacturer and remains constant for all current levels. The results demonstrate the effectiveness of the AIWM-EMS in reducing water management faults, maintaining voltage stability across all current levels, and minimizing hydrogen consumption. The costs of hydrogen consumption and FC degradation in the FC-HEV under the AIWM-EMS are 4.09% and 8.12% lower, respectively, than in the NAIWM-EMS, and the total operating cost in the AIWM-EMS is reduced by 5.21% compared to the NAIWM-EMS. The results also show that the FCs under the AIWM-EMS works 78.36% of the operating time in the high-efficiency zone, compared to 62% under the NAIWM-EMS.

Chapter 5 - Conclusion

To reduce fossil fuel usage and align with policies promoting clean energy and green vehicles, FC-HEVs have gained significant attention in the automotive market due to their high efficiency, long driving range, and near-zero emissions. However, FC-HEVs face several challenges, such as high operating cost due to fuel consumption and FC degradation, limited FC lifespan, low reliability, and low durability, which hinder their mass production and commercialization. A promising and feasible solution to overcome these challenges is utilizing a multi-stack FC system, which provides significant advantages such as higher efficiency, the ability to operate in degraded mode, and improved reliability and durability. The multi-stack FC system, with several sub-stacks, requires an EMS as a software component to distribute power among the FCs and fully operationalize the potential and advantages of the multi-stack system. On the other hand, the operating cost of multi-stack FC systems is an open issue and requires an advanced EMS to optimally distribute power among sub-stacks, reducing fuel consumption and extending FC lifespan. As a result, the overall goal of this dissertation is to improve the performance of the multi-stack FC system in vehicular applications to reduce operating cost, increase FC durability and reliability, and enhance multi-stack FC system efficiency. In the first phase, this dissertation aims to investigate the impact of the advantages of a multi-stack FC system on the operating cost of a FC-HEV through an EMS. In the second phase, the purpose is to design and develop an advanced EMS to enhance the performance of a multi-stack FC-HEV and reduce operating cost. The proposed EMS uses a finite prediction horizon, enabling real-time application without prior knowledge of the full driving cycle. This

predictive approach outperforms single time-point strategies and achieves results near those of global optimization. Although the role of the EMS is to distribute optimal power among power sources, even an advanced EMS cannot guarantee that the FCs will operate properly and supply the requested power. FC voltage, as the output and a health indicator of the FC, is one of the most critical operating parameters, directly impacting FC performance. Stable voltage is essential for enhancing FC performance. Unstable voltage can result in reduced PEMFC output power and an inability to meet the requested power. In real-world applications, one of the key factors affecting voltage is water management. Water management faults cause voltage drops, reduce voltage stability, and negatively impact FC performance. Therefore, the third phase aims to improve the performance of the multi-stack FC system by integrating water management into the EMS.

To achieve the goals of this thesis, three main stages are conducted, which are explained in Chapter 2, Chapter 3, Chapter 4.

Despite the emphasis on the important and practical properties of multi-stack FC systems in most studies, the impact of their advantages and potential on the performance and operating cost of FC-HEVs has not been thoroughly investigated. For this purpose, this chapter compares the operating cost, FC efficiency, and FC durability of a multi-stack FC system consisting of four 500-W PEMFCs with a single-stack 2000-W PEMFC in a FC-HEV. The operating cost includes hydrogen consumption and FC degradation costs. This chapter introduces a hierarchical EMS for the multi-stack FC system, and the results are compared with those from DP, a well-accepted benchmark in this field. In the multi-stack FC system, a RB strategy is used in the first layer of the EMS to determine the number of FCs that should participate in the optimization problem of the second layer, where ECMS is

responsible for power distribution. The results show that the hydrogen consumption, degradation, and total operating cost of the multi-stack FC system are lower than those of the single-stack FC system. Therefore, according to the analytical comparison, the advantages of the multi-stack FC system can reduce the operating cost, making the multi-stack FC system a suitable choice for a FC-HEV.

After demonstrating that the multi-stack FC system is a feasible and reliable option for vehicular applications than the single-stack system, Chapter 3 focuses on designing an advanced EMS for a multi-stack FC-HEV to enhance its performance. The literature review shows that the prediction aspect has been overlooked by researchers during the development of EMSs for multi-stack FC-HEVs. As a result, Chapter 3 proposes a PHC-EMS for a multi-stack FC-HEV to improve the performance of the multi-stack FC system in vehicular applications. This chapter utilizes HPEMS to reduce fuel consumption, minimize degradation of power sources, and extend the lifespan of sub-stacks in a multi-stack FC system. In the upper layer, a RB strategy is devised to determine the number of active FCs at each time step based on FC degradation, requested power, and SOC. This layer is designed to minimize FC degradation and reduce hydrogen consumption. In the lower layer, MPC, a predictive and real-time optimization algorithm, is employed to make optimal control decisions between the FCs and the battery. A speed predictor is needed to forecast future vehicle velocities, for which this work utilizes a novel deep neural network approach called SBLSTM. The prediction results show high accuracy. Two different driving cycles are used to assess the PHC-EMS performance, with comparisons to DP and ECMS to demonstrate its effectiveness. In the INRETS driving cycle, the total operating cost of PHC-EMS is 3.728% higher than DP and 5.154% lower than ECMS. In the

WVUINTER driving cycle, the total operating cost of PHC-EMS is 2.4162% higher than DP and 3.550% lower than ECMS. Consequently, the proposed strategy is a convincing choice for real-time energy management of a multi-stack FC-HEV.

The role of an EMS is to distribute optimal power between the FCs and the battery to achieve objectives such as reducing operating cost. However, to supply the reference power sent from the EMS, the PEMFCs must operate properly and be in a safe and healthy condition. In this regard, changes in FC operating parameters have a significant and undeniable effect on performance of the FC. One of these operating parameters is voltage, which is important because it directly impacts the FC output power, hydrogen consumption, and efficiency. On the other hand, FC voltage acts as a health and performance indicator for the FC, where any changes or drops indicate potential malfunctions in the PEMFC. Therefore, voltage stability plays a crucial role in the proper performance of a PEMFC and should be supervised and controlled. PEMFC voltage performance relies heavily on its water content, and water management is one of the most critical factors directly affecting PEMFC voltage. Therefore, water management faults, such as flooding, can lead to voltage drops and reduced PEMFC performance. One of the feasible and economical solutions to improve water management in PEMFCs is the use of a purge valve. For this purpose, Chapter 4 aims to enhance the performance of the multi-stack FC system without redesigning the EMS by utilizing the IWM-EMS. The output current is a crucial factor influencing water management. As the current in a PEMFC increases, water flooding becomes more severe, leading to performance degradation and voltage instability. Consequently, the operating current significantly impacts water management in a PEMFC. For this purpose, this chapter aims to develop effective water

management by designing an adaptive purge strategy that can adjust to different current levels. Furthermore, the proposed purge strategy aims to minimize wasted hydrogen during the purging process to enhance FC efficiency and reduce hydrogen consumption. Therefore, this chapter proposes a water management, where an adaptive efficient purge strategy is integrated into the EMS (AIWM-EMS). The proposed AIWM-EMS in Chapter 4 consists of two levels. The first level is the HPEMS, designed in Chapter 3, which determines the optimal power for each sub-stack and sends the reference current to them. The second level is the water management, which receives the reference current from the EMS and selects the efficient purge strategy based on the reference current to maintain voltage stability. The proposed AIWM-EMS is implemented in the HIL to evaluate its effectiveness, with the results compared to those of a non-adaptive water management strategy, where the manufacturer's non-adaptive purge strategy is integrated into the EMS (NAIWM-EMS). The results indicate that hydrogen consumption and FC degradation costs in the multi-stack FC-HEV under the proposed AIWM-EMS are 4.09% and 8.12% lower, respectively, compared to the NAIWM-EMS, leading to a total operating cost reduction of 5.21%. Furthermore, the results show that the multi-stack system under the proposed AIWM-EMS operates 78.36% of the time in the high-efficiency zone, compared to 62% under the NAIWM-EMS.

In summary, the outcomes of this thesis demonstrate that a multi-stack FC system can serve as a viable replacement for a single-stack system in vehicular applications. The advantages and potential of the multi-stack system, including reduced operating cost, make it a feasible and efficient option for FC-HEVs. However, to fully leverage the advantages of a multi-stack FC system and enhance its performance, designing an advanced EMS is

essential. In other words, an EMS, as a software component, plays a key role in the development of multi-stack FC systems in vehicular applications by reducing operating cost and increasing reliability and durability. Enhancing the EMS with predictive capabilities can improve the performance of the multi-stack FC system and reduce its operating cost in vehicular applications. However, ensuring that the sub-stacks operate properly at the reference power received from the EMS commands is beyond the EMS's responsibility. Because a PEMFC is a complex system, its proper operation depends on operating parameters and their changes. One of the parameters that has a predominant effect on PEMFC performance is voltage. Reducing voltage drops and fluctuations to achieve stable voltage has a significant impact on FC performance and enables easier control of FC output power. FC voltage variations are highly dependent on the water content in the membrane, which can be controlled through effective water management. To improve the performance of the multi-stack FC system, this thesis integrates water management into the EMS, focusing on enhancing FC voltage stability.

5.1 Recommendation for Future Works

This thesis aims to enhance the performance of multi-stack FC systems in vehicular applications by developing an advanced EMS and integrating water management. However, further developments and progress are needed to enhance the performance of multi-stack FC systems and support their commercialization more effectively than before. In this regard, this section aims to propose some tips and recommendations for future work to further develop and improve the study conducted in this thesis.

5.1.1 Utilizing PEMFC Adaptive Model in EMS

This thesis employes experimental data of PEMFC to obtain polarization and hydrogen consumption curves to avoid some errors in usual numerical models and make PEMFC outputs more realistic. However, using an advanced PEMFC model that includes parameter variations can improve the EMS results. Several modeling approaches, including theoretical, empirical, and semi-empirical models, have been proposed to evaluate the characteristics of PEMFC systems [137]–[139]. Semi-empirical models, also known as grey-box models, provide a balanced compromise between complexity and simplicity. Grey-box PEMFC models have found useful applications in energy management design, thanks to advancements and developments in studies on FC-HEVs [139]–[141]. These models emphasize the fundamental electrochemical properties (polarization curve) of PEMFCs and are based on physical relationships supported by experimental data. The physical insight of the grey-box model provides valuable information about the effects on the polarization curve, such as cell reversible voltage, activation loss, ohmic loss, and concentration overvoltage. Accurate PEMFC modeling is essential for evaluating performance, optimal control, precise simulating, and maximum power and efficiency tracking [142]. However, PEMFC is a multi-physics, highly complex, and nonlinear mechanism that is challenging to model accurately. Additionally, the PEMFC's performance is affected by aging, degradation, and changes in its operating conditions [143]. Therefore, the importance of parameter estimation becomes evident as the PEMFC ages and its performance changes under different operating conditions. PEMFC behavior and parameters change depending on operating conditions, and using parameter estimation to form an adaptive model helps prevent performance drift in FC management.

Additionally, the maximum efficiency and maximum power of the PEMFC, which are considered the most important constraints when designing an EMS, can be affected by changes in operating conditions that are not accounted for in the model.

Therefore, failing to account for PEMFC parameter variation during operation will result in poor management and an unreliable EMS. Among various parameter estimation techniques, the adaptive filter-based method known as online parameter identification (OPI) is a practical option for real-time applications like EMS in FC-HEVs. An EMS that incorporates OPI has the ability to monitor the FC's actual behavior, leading to better and more reliable power distribution. Some well-known methods for OPI, frequently referenced in the literature, include recursive least square (RLS), forgetting factor recursive least square (FFRLS), Kalman filter (KF), extended Kalman filter (EKF), and square root unscented Kalman filter (SRUKF) [28], [41], [144]–[148].

5.1.2 Development of a PEMFC Degradation Model

In real-world applications like FC-HEVs, due to variable and dynamic conditions, FC degradation is an unavoidable aspect of operation. FC degradation directly affects voltage, causing the nominal voltage to gradually decrease over time. Additionally, degradation alters important operating points of the FC, such as maximum power and maximum efficiency. As a result, degradation has a significant and undeniable impact on FC performance. As discussed in this thesis, FC degradation is one of the main concerns related to FC technologies, as it can reduce FC durability and reliability while increasing the total operating cost. In this regard, one of the goals of designing an advanced EMS as a software component is to reduce FC degradation, thereby increasing its lifespan and reliability. This thesis utilizes common FC degradation models to reduce the costs

associated with PEMFC degradation [149], [150]. However, to efficiently reduce FC degradation through the EMS, a precise and comprehensive degradation model is needed to more accurately predict voltage reduction. The literature review shows that an accurate and comprehensive FC degradation model is still a limitation in current studies and requires further investigation [56]. FC degradation models are categorized into three types: physics-based models, data-driven models, and hybrid models. Physics-based models, which can be mechanistic, semi-mechanistic, or semi-empirical, rely on system-specific physical equations to simulate behavior while accounting for degradation. These models provide detailed insights into the internal state of the FC, with the key advantage of being easy to execute online and offering strong generalization. However, they require a deep understanding of degradation mechanisms and system-specific knowledge, which can be challenging [151]–[154]. Data-driven models, on the other hand, rely on experimental data and do not require knowledge of the internal system parameters, making them easier to implement. Their drawback is the need for a large amount of data to achieve accurate modeling, and they have limited generalization capabilities [155]–[159]. Hybrid models combine the strengths of both physics-based and data-driven approaches, balancing the need for data and physical understanding. While they offer a more comprehensive solution, hybrid models may also inherit the limitations of both approaches. Currently, few hybrid models are available for proton exchange membrane FCs [160]–[163].

As a future direction in developing a FC degradation model, semi-empirical models can provide reliable predictions. These models combine mathematical equations with experimental data. However, creating an accurate degradation model requires running and

sacrificing the FC under various load conditions for extended periods, allowing it to degrade until it reaches the end of its life.

5.1.3 Fault Diagnosis and Fault-Tolerant Control

Reliability and durability during operation remain the two most significant challenges preventing wider commercial adoption of PEMFC systems. Proper and healthy operation is essential, as any fault in PEMFC systems can lead to safety risks, reduced energy conversion efficiency, decreased power availability, and compromised system reliability [50], [54]. PEMFC components can experience short-term or long-term degradation and damage due to the duration of a fault, known as exposure time. Since dynamic conditions frequently occur in automotive applications, the risk of faults increases. Consequently, PEMFC systems are prone to various faults, such as cell flooding, membrane drying out, high-temperature gradients, local hot spots, fuel starvation, carbon corrosion, platinum oxidation, and CO poisoning [57], [164], [165]. Therefore, in addition to the EMS, controlling malfunctions and faults in FCs has gained increasing attention in recent years on the software side of FC management.

As mentioned earlier, one valuable advantage of the multi-stack FC system is its ability to operate in degraded mode. This feature allows the system to continue functioning even when one of the sub-stacks encounters a fault or failure. Therefore, incorporating fault-tolerant control into the EMS is essential to handle faulty situations. In other words, a modern and reliable EMS should manage power distribution among sub-stacks to prevent sub-stacks from operating for extended periods in faulty conditions. As a result, in multi-stack FC systems, the presence of several sub-stacks increases the likelihood of faults.

Monitoring the sub-stacks to diagnose faulty situations and taking remedial actions to recover them is a trending and interesting topic in current research.

PEMFC voltage serves as the system's output, and any drop in voltage indicates a fault or malfunction in the PEMFC system. In this regard, many studies investigate voltage changes to determine which type of fault they correspond to in the PEMFC, and then attempt to take remedial actions to restore PEMFC performance [50], [57], [166], [167]. The most common faults in PEMFC that affect its performance and voltage stability are related to water content, which is linked to two critical phenomena: flooding and drying out. In a DEA-PEMFC, the anode purge is the most important component for managing water content inside the PEMFC and preventing performance reduction [168]. Therefore, the proposed investigation on the purge strategy in this thesis can be further developed for use in fault-tolerant control. For fault diagnosis, the behavior of PEMFC voltage should be investigated under different load conditions. A healthy FC model is essential for comparing the voltage between healthy operation and real PEMFC performance. Determining the threshold is a critical step, as it defines the amount of voltage change that is acceptable versus what is considered a fault condition. In the final step, once a fault is identified, a fault-tolerant control system takes remedial action to restore PEMFC performance. If the fault is related to flooding, the fault-tolerant control increases the purge duration or decreases the purge interval to reduce water content and recover performance. Conversely, if the fault is due to drying out, decreasing the purge duration or increasing the purge interval helps increase water content, balance it, and restore performance.

5.1.4 Improving Water Management Strategies in Multi-stack FC System

This thesis aims to illustrate that, alongside the EMS level in a FC-HEV, the FC system management level is essential for ensuring proper performance and maintaining the FC's healthy condition. One of the main components of FC system management is the water management system, which has a significant impact on voltage, a critical parameter of FC performance. Improper water management can lead to faults such as flooding and drying out, which cause FC voltage drops and decrease its performance. In this context, as a proof of concept, this thesis integrates water management into the EMS of a multi-stack FC system to improve voltage stability and enhance the performance of the multi-stack system. For this purpose, this thesis designs an adaptive purge strategy to improve water management and maintain voltage stability. However, water management in a multi-stack FC system is a complex task due to the presence of multiple sub-stacks. The next step to improve water management in a multi-stack FC system could be the development of an efficient water management architecture. Generally, there are three methods for water management in FC systems: passive, active, and hybrid water management [20], [24].

Passive water management relies on intrinsic system properties to regulate hydration levels. A common method is self-humidification, where byproduct water generated during the FC reaction is used to maintain the membrane's humidity. This approach simplifies the system design and reduces weight, making it particularly suitable for compact applications. Additionally, internal water migration between the anode and cathode helps distribute water evenly. However, the effectiveness of passive methods depends heavily on precise temperature control, making them less adaptable to dynamic operating conditions [169], [170].

Active methods involve external components and controls to manage water levels dynamically. External humidification systems adjust the relative humidity of air and hydrogen using components like polymer wicks, which excel at absorbing and transferring water. Gas diffusion layers (GDLs), with innovative designs such as dual microporous layers or laser-perforated structures, are essential to optimizing water transport and reducing voltage losses. Electroosmotic pumps are also employed to actively remove excess water from cathode channels and GDLs, enhancing reliability. While active methods provide superior control and adaptability, they increase system complexity, cost, and energy consumption [171], [172].

Combining passive and active methods offers a balanced approach to water management. For instance, gradient pore sizes in GDLs integrated with electroosmotic pumps can enhance water transport while maintaining system simplicity. These hybrid approaches provide flexibility for varying load demands and environmental conditions but come with challenges in integration and increased design complexity [173].

In summary, water management strategy in multi-stack FC systems must be designed to meet application-specific needs, balancing simplicity, cost, and performance. Passive methods are ideal for compact, cost-sensitive applications, whereas active strategies are better suited for high-power scenarios demanding precision. Combining these approaches ensures the voltage stability and increase enhances to advance multi-stack FC technology.

References

[1] A. G. Olabi and M. A. Abdelkareem, “Renewable energy and climate change,” *Renew. Sustain. Energy Rev.*, vol. 158, no. January, p. 112111, 2022, doi: 10.1016/j.rser.2022.112111.

[2] X. Tian, C. An, and Z. Chen, “The role of clean energy in achieving decarbonization of electricity generation, transportation, and heating sectors by 2050: A meta-analysis review,” *Renew. Sustain. Energy Rev.*, vol. 182, no. January, p. 113404, 2023, doi: 10.1016/j.rser.2023.113404.

[3] S. Fujimori *et al.*, “A framework for national scenarios with varying emission reductions,” *Nat. Clim. Chang.*, vol. 11, no. 6, pp. 472–480, 2021, doi: 10.1038/s41558-021-01048-z.

[4] J. Zhan, C. Wang, H. Wang, F. Zhang, and Z. Li, “Pathways to achieve carbon emission peak and carbon neutrality by 2060: A case study in the Beijing-Tianjin-Hebei region, China,” *Renew. Sustain. Energy Rev.*, vol. 189, no. PB, p. 113955, 2024, doi: 10.1016/j.rser.2023.113955.

[5] P. Halder *et al.*, “Performance, emissions and economic analyses of hydrogen fuel cell vehicles,” *Renew. Sustain. Energy Rev.*, vol. 199, no. January, p. 114543, 2024, doi: 10.1016/j.rser.2024.114543.

[6] A. Pramuanjaroenkij and S. Kakaç, “The fuel cell electric vehicles: The highlight review,” *Int. J. Hydrogen Energy*, vol. 48, no. 25, pp. 9401–9425, 2023, doi: 10.1016/j.ijhydene.2022.11.103.

[7] A. K. Karmaker, K. Prakash, M. N. I. Siddique, M. A. Hossain, and H. Pota, “Electric vehicle hosting capacity analysis: Challenges and solutions,” *Renew. Sustain. Energy Rev.*, vol. 189, no. PA, p. 113916, 2024, doi: 10.1016/j.rser.2023.113916.

[8] A. Alyakhni, L. Boulon, J. M. Vinassa, and O. Briat, “A Comprehensive Review on Energy Management Strategies for Electric Vehicles Considering Degradation Using Aging Models,” *IEEE Access*, vol. 9, pp. 143922–143940, 2021, doi: 10.1109/ACCESS.2021.3120563.

[9] D. Kumar, R. K. Nema, and S. Gupta, “A comparative review on power conversion topologies and energy storage system for electric vehicles,” *Int. J. Energy Res.*, vol. 44, no. 10, pp. 7863–7885, 2020, doi: 10.1002/er.5353.

[10] Z. P. Cano *et al.*, “Batteries and fuel cells for emerging electric vehicle markets,” *Nat. Energy*, vol. 3, no. 4, pp. 279–289, 2018, doi: 10.1038/s41560-018-0108-1.

[11] E. B. Agyekum, F. Odoi-Yorke, A. A. Abbey, and G. K. Ayetor, “A review of the trends, evolution, and future research prospects of hydrogen fuel cells – A focus on vehicles,” *Int. J. Hydrogen Energy*, vol. 72, no. March, pp. 918–939, 2024, doi: 10.1016/j.ijhydene.2024.05.480.

[12] Y. Luo *et al.*, “Development and application of fuel cells in the automobile industry,” *J. Energy Storage*, vol. 42, no. August, p. 103124, 2021, doi: 10.1016/j.est.2021.103124.

[13] N. A. A. Qasem and G. A. Q. Abdulrahman, “A Recent Comprehensive Review of Fuel Cells: History, Types, and Applications,” *Int. J. Energy Res.*, vol. 2024, no. Figure 1, 2024, doi: 10.1155/2024/7271748.

[14] H. S. Das, C. W. Tan, and A. H. M. M. Yatim, “Fuel cell hybrid electric vehicles: A review on power conditioning units and topologies,” *Renew. Sustain. Energy Rev.*, vol. 76, no. March, pp. 268–291, 2017, doi: 10.1016/j.rser.2017.03.056.

[15] H. Togun *et al.*, “A review on recent advances on improving fuel economy and performance of a fuel cell hybrid electric vehicle,” *Int. J. Hydrogen Energy*, vol. 89, no. July, pp. 22–47, 2024, doi: 10.1016/j.ijhydene.2024.09.298.

[16] M. Waseem, M. Amir, G. S. Lakshmi, S. Harivardhagini, and M. Ahmad, “Fuel cell-based hybrid electric vehicles: An integrated review of current status, key challenges, recommended policies, and future prospects,” *Green Energy Intell. Transp.*, vol. 2, no. 6, p. 100121, 2023, doi: 10.1016/j.geits.2023.100121.

[17] M. Reveles-Miranda, V. Ramirez-Rivera, and D. Pacheco-Catalán, “Hybrid energy storage: Features, applications, and ancillary benefits,” *Renew. Sustain. Energy Rev.*, vol. 192, no. October 2023, 2024,

doi: 10.1016/j.rser.2023.114196.
[18] K. E. Mehrdad Ehsani, Yimin Gao, Stefano Longo, *Modern Electric, Hybrid Electric, and Fuel Cell Vehicles*, vol. 3, no. April. 2015.
[19] R. Ma *et al.*, "Recent progress and challenges of multi-stack fuel cell systems: Fault detection and reconfiguration, energy management strategies, and applications," *Energy Convers. Manag.*, vol. 285, no. April, 2023, doi: 10.1016/j.enconman.2023.117015.
[20] S. Zhou *et al.*, "A review on proton exchange membrane multi-stack fuel cell systems: architecture, performance, and power management," *Appl. Energy*, vol. 310, no. January, p. 118555, 2022, doi: 10.1016/j.apenergy.2022.118555.
[21] J. Wang, "System integration, durability and reliability of fuel cells: Challenges and solutions," *Appl. Energy*, vol. 189, pp. 460–479, 2017, doi: 10.1016/j.apenergy.2016.12.083.
[22] B. C. H. Steele and A. Heinzel, "Materials for fuel-cell technologies," *Nature*, vol. 414, no. 6861, pp. 345–352, 2001, doi: 10.1038/35104620.
[23] N. Marx, L. Boulon, F. Gustin, D. Hissel, and K. Agbossou, "A review of multi-stack and modular fuel cell systems: Interests, application areas and on-going research activities," *Int. J. Hydrogen Energy*, vol. 39, no. 23, pp. 12101–12111, 2014, doi: 10.1016/j.ijhydene.2014.05.187.
[24] Y. Qiu *et al.*, "Progress and challenges in multi-stack fuel cell system for high power applications: Architecture and energy management," *Green Energy Intell. Transp.*, vol. 2, no. 2, p. 100068, 2023, doi: 10.1016/j.geits.2023.100068.
[25] C. Zhang, T. Zeng, Q. Wu, C. Deng, S. H. Chan, and Z. Liu, "Improved efficiency maximization strategy for vehicular dual-stack fuel cell system considering load state of sub-stacks through predictive soft-loading," *Renew. Energy*, vol. 179, pp. 929–944, 2021, doi: 10.1016/j.renene.2021.07.090.
[26] N. Marx, D. C. T. Cárdenas, L. Boulon, F. Gustin, and D. Hissel, "Degraded mode operation of Multi-stack fuel cell systems," *IET Electr. Syst. Transp.*, vol. 6, no. 1, pp. 3–11, 2016, doi: 10.1049/iet-est.2015.0012.
[27] A. Khalatbarisoltani, M. Kandidayeni, L. Boulon, and X. Hu, "Power Allocation Strategy based on Decentralized Convex Optimization in Modular Fuel Cell Systems for Vehicular Applications," *IEEE Trans. Veh. Technol.*, vol. 9545, no. c, pp. 14563–14574, 2020, doi: 10.1109/tvt.2020.3028089.
[28] A. M. I. Fernandez *et al.*, "An Adaptive State Machine Based Energy Management Strategy for a Multi-Stack Fuel Cell Hybrid Electric Vehicle," *IEEE Trans. Veh. Technol.*, vol. 69, no. 1, pp. 220–234, 2020, doi: 10.1109/TVT.2019.2950558.
[29] R. Ghaderi, M. Kandidayeni, L. Boulon, and J. P. Trovão, "Q-learning based energy management strategy for a hybrid multi-stack fuel cell system considering degradation," *Energy Convers. Manag.*, vol. 293, no. May, p. 117524, 2023, doi: 10.1016/j.enconman.2023.117524.
[30] A. Khalatbarisoltani, M. Kandidayeni, L. Boulon, and X. Hu, "Comparison of Decentralized ADMM Optimization Algorithms for Power Allocation in Modular Fuel Cell Vehicles," *IEEE/ASME Trans. Mechatronics*, vol. 27, no. 5, pp. 1–12, 2022, doi: 10.1109/TMECH.2021.3105950.
[31] W. Shi, Y. Huangfu, L. Xu, and S. Pang, "Online energy management strategy considering fuel cell fault for multi-stack fuel cell hybrid vehicle based on multi-agent reinforcement learning," *Appl. Energy*, vol. 328, no. August, p. 120234, 2022, doi: 10.1016/j.apenergy.2022.120234.
[32] M. Bahrami *et al.*, "Multi-stack lifetime improvement through adapted power electronic architecture in a fuel cell hybrid system," *Mathematics*, vol. 8, no. 5, pp. 1–28, 2020, doi: 10.3390/MATH8050739.
[33] N. Marx, J. Cardozo, L. Boulon, F. Gustin, D. Hissel, and K. Agbossou, "Comparison of the Series and Parallel Architectures for Hybrid Multi-Stack Fuel Cell - Battery Systems," *2015 IEEE Veh. Power Propuls. Conf. VPPC 2015 - Proc.*, no. figure 2, pp. 2–7, 2015, doi: 10.1109/VPPC.2015.7352915.
[34] H. Wang and A. Gaillard, "Module Architecture Investigation," no. September, 2022.
[35] M. Kandidayeni, J. P. Trovão, M. Soleymani, and L. Boulon, "Towards health-aware energy management strategies in fuel cell hybrid electric vehicles: A review," *Int. J. Hydrogen Energy*, vol. 47, no. 17, pp. 10021–10043, 2022, doi: 10.1016/j.ijhydene.2022.01.064.
[36] D.-D. D. Tran, M. Vafaeipour, M. El Baghdadi, R. Barrero, J. Van Mierlo, and O. Hegazy, "Thorough state-of-the-art analysis of electric and hybrid vehicle powertrains: Topologies and integrated energy management strategies," *Renew. Sustain. Energy Rev.*, vol. 119, no. xxxx, p. 109596, 2020, doi: 10.1016/j.rser.2019.109596.

[37] A. Khalatbarisoltani, H. Zhou, X. Tang, M. Kandidayeni, L. Boulon, and X. Hu, "Energy Management Strategies for Fuel Cell Vehicles: A Comprehensive Review of the Latest Progress in Modeling, Strategies, and Future Prospects," *IEEE Trans. Intell. Transp. Syst.*, vol. 25, no. 1, pp. 14–32, 2024, doi: 10.1109/TITS.2023.3309052.

[38] Y. Huang *et al.*, "A review of power management strategies and component sizing methods for hybrid vehicles," *Renew. Sustain. Energy Rev.*, vol. 96, no. April, pp. 132–144, 2018, doi: 10.1016/j.rser.2018.07.020.

[39] P. Zhang, F. Yan, and C. Du, "A comprehensive analysis of energy management strategies for hybrid electric vehicles based on bibliometrics," *Renew. Sustain. Energy Rev.*, vol. 48, no. 205, pp. 88–104, 2015, doi: 10.1016/j.rser.2015.03.093.

[40] X. Zhao *et al.*, "Energy management strategies for fuel cell hybrid electric vehicles: Classification, comparison, and outlook," *Energy Convers. Manag.*, vol. 270, no. September, p. 116179, 2022, doi: 10.1016/j.enconman.2022.116179.

[41] K. Ettihir, L. Boulon, and K. Agbossou, "Energy management strategy for a fuel cell hybrid vehicle based on maximum efficiency and maximum power identification," *IET Electr. Syst. Transp.*, vol. 6, no. 4, pp. 261–268, 2016, doi: 10.1049/iet-est.2015.0023.

[42] J. A. Salva, A. Iranzo, F. Rosa, E. Tapia, E. Lopez, and F. Isorna, "Optimization of a PEM fuel cell operating conditions: Obtaining the maximum performance polarization curve," *Int. J. Hydrogen Energy*, vol. 41, no. 43, pp. 19713–19723, 2016, doi: 10.1016/j.ijhydene.2016.03.136.

[43] D. Chu and R. Jiang, "Performance of polymer electrolyte membrane fuel cell (PEMFC) stacks Part I. Evaluation and simulation of an air-breathing PEMFC stack," *J. Power Sources*, vol. 83, no. 1–2, pp. 128–133, 1999, doi: 10.1016/S0378-7753(99)00285-2.

[44] F. Barbir and T. Gómez, "Efficiency and economics of proton exchange membrane (PEM) fuels cells," *Int. J. Hydrogen Energy*, vol. 21, no. 10, pp. 891–901, 1996, doi: 10.1016/0360-3199(96)00030-4.

[45] A. S. White, E. Waddington, J. M. Merret, P. J. Ansell, E. M. Greitzer, and D. K. Hall, "System-level utilization of low-grade, mw-scale thermal loads for electric aircraft," *AIAA Aviat. 2022 Forum*, no. June, 2022, doi: 10.2514/6.2022-3291.

[46] N. Sulaiman, M. A. Hannan, A. Mohamed, P. J. Ker, E. H. Majlan, and W. R. Wan Daud, "Optimization of energy management system for fuel-cell hybrid electric vehicles: Issues and recommendations," *Appl. Energy*, vol. 228, no. May, pp. 2061–2079, 2018, doi: 10.1016/j.apenergy.2018.07.087.

[47] M. Uzunoglu, O. C. Onar, and M. S. Alam, "Dynamic behavior of PEM FCPPs under various load conditions and voltage stability analysis for stand-alone residential applications," *J. Power Sources*, vol. 168, no. 1 SPEC. ISS., pp. 240–250, 2007, doi: 10.1016/j.jpowsour.2007.02.045.

[48] Q. Zhao and F. C. Lee, "High-efficiency, high step-up dc-dc converters," *IEEE Trans. Power Electron.*, vol. 18, no. 1 I, pp. 65–73, 2003, doi: 10.1109/TPEL.2002.807188.

[49] M. Forouzesh, Y. P. Siwakoti, S. A. Gorji, F. Blaabjerg, and B. Lehman, "Step-Up DC-DC converters: A comprehensive review of voltage-boosting techniques, topologies, and applications," *IEEE Trans. Power Electron.*, vol. 32, no. 12, pp. 9143–9178, 2017, doi: 10.1109/TPEL.2017.2652318.

[50] J. Aubry, N. Y. Steiner, S. Morando, N. Zerhouni, and D. Hissel, "Fuel cell diagnosis methods for embedded automotive applications," *Energy Reports*, vol. 8, pp. 6687–6706, 2022, doi: 10.1016/j.egyr.2022.05.036.

[51] J. Hong, J. Yang, Z. Weng, F. Ma, F. Liang, and C. Zhang, "Review on proton exchange membrane fuel cells: Safety analysis and fault diagnosis," *J. Power Sources*, vol. 617, no. June, p. 235118, 2024, doi: 10.1016/j.jpowsour.2024.235118.

[52] C. Zhang, Y. Zhang, L. Wang, X. Deng, Y. Liu, and J. Zhang, "A health management review of proton exchange membrane fuel cell for electric vehicles: Failure mechanisms, diagnosis techniques and mitigation measures," *Renew. Sustain. Energy Rev.*, vol. 182, no. October 2022, p. 113369, 2023, doi: 10.1016/j.rser.2023.113369.

[53] H. Chen, R. Zhang, Z. Xia, Q. Weng, T. Zhang, and P. Pei, "Experimental investigation on PEM fuel cell flooding mitigation under heavy loading condition," *Appl. Energy*, vol. 349, no. July, p. 121632, 2023, doi: 10.1016/j.apenergy.2023.121632.

[54] J. Wang *et al.*, "Recent advances and summarization of fault diagnosis techniques for proton exchange membrane fuel cell systems: A critical overview," *J. Power Sources*, vol. 500, no. April, p.

229932, 2021, doi: 10.1016/j.jpowsour.2021.229932.
[55] L. Fan, K. Xu, Z. Jiang, C. Shen, J. Sun, and Y. Wei, “Advances of membrane electrode assembly aging research of proton exchange membrane fuel cell under variable load: degradation mechanism, aging indicators, prediction strategy, and perspectives,” *Ionics (Kiel).*, vol. 30, no. 9, pp. 5111–5140, 2024, doi: 10.1007/s11581-024-05661-8.
[56] E. Wallnöfer-Ogris, F. Poimer, R. Köll, M.-G. G. Macherhammer, and A. Trattner, “Main degradation mechanisms of polymer electrolyte membrane fuel cell stacks – Mechanisms, influencing factors, consequences, and mitigation strategies,” *Int. J. Hydrogen Energy*, vol. 50, pp. 1159–1182, 2024, doi: https://doi.org/10.1016/j.ijhydene.2023.06.215.
[57] E. Dijoux, N. Y. Steiner, M. Benne, M. C. Péra, and B. G. Pérez, “A review of fault tolerant control strategies applied to proton exchange membrane fuel cell systems,” *J. Power Sources*, vol. 359, pp. 119–133, 2017, doi: 10.1016/j.jpowsour.2017.05.058.
[58] Y. Yuan *et al.*, “Fault Diagnosis Review of Proton Exchange Membrane Fuel Cell Systems: Fault Mechanisms, Detection and Identification, and Fault Mitigation,” *Energy Technol.*, vol. 2400557, pp. 1–21, 2024, doi: 10.1002/ente.202400557.
[59] H. Pourrahmani, A. Yavarinasab, M. Siavashi, M. Matian, and J. Van herle, “Progress in the proton exchange membrane fuel cells (PEMFCs) water/thermal management: From theory to the current challenges and real-time fault diagnosis methods,” *Energy Rev.*, vol. 1, no. 1, p. 100002, 2022, doi: 10.1016/j.enrev.2022.100002.
[60] M. Pan, C. Pan, C. Li, and J. Zhao, “A review of membranes in proton exchange membrane fuel cells: Transport phenomena, performance and durability,” *Renew. Sustain. Energy Rev.*, vol. 141, no. January, p. 110771, 2021, doi: 10.1016/j.rser.2021.110771.
[61] J. Liu, Q. Li, H. Yang, Y. Han, S. Jiang, and W. Chen, “Sequence Fault Diagnosis for PEMFC Water Management Subsystem Using Deep Learning with t-SNE,” *IEEE Access*, vol. 7, pp. 92009–92019, 2019, doi: 10.1109/ACCESS.2019.2927092.
[62] R. Ma, H. Dang, R. Xie, L. Xu, and D. Zhao, “Online Fault Diagnosis for Open-Cathode PEMFC Systems Based on Output Voltage Measurements and Data-Driven Method,” *IEEE Trans. Transp. Electrif.*, vol. 8, no. 2, pp. 2050–2061, 2022, doi: 10.1109/TTE.2021.3114194.
[63] L. Yang, N. N. Nik-Ghazali, M. A. H. Ali, W. T. Chong, Z. Yang, and H. Liu, “A review on thermal management in proton exchange membrane fuel cells: Temperature distribution and control,” *Renew. Sustain. Energy Rev.*, vol. 187, no. June, p. 113737, 2023, doi: 10.1016/j.rser.2023.113737.
[64] D. Hu, Y. Wang, J. Li, Q. Yang, and J. Wang, “Investigation of optimal operating temperature for the PEMFC and its tracking control for energy saving in vehicle applications,” *Energy Convers. Manag.*, vol. 249, p. 114842, 2021, doi: 10.1016/j.enconman.2021.114842.
[65] Q. Li *et al.*, “Health Management for PEMFC System Long-Term Operation Based on Optimal Temperature Trajectory Real-Time Optimization,” *IEEE Trans. Ind. Electron.*, pp. 1–11, 2024, doi: 10.1109/tie.2024.3436539.
[66] M. Kandidayeni *et al.*, “Efficiency Enhancement of an Open Cathode Fuel Cell through a Systemic Management,” *IEEE Trans. Veh. Technol.*, vol. 68, no. 12, pp. 11462–11472, 2019, doi: 10.1109/TVT.2019.2944996.
[67] J. B. Lu, G. H. Wei, F. J. Zhu, X. H. Yan, and J. L. Zhang, “Pressure Effect on the PEMFC Performance,” *Fuel Cells*, vol. 19, no. 3, pp. 211–220, 2019, doi: 10.1002/fuce.201800135.
[68] Y. Wang and Y. Wang, “Pressure and oxygen excess ratio control of PEMFC air management system based on neural network and prescribed performance,” *Eng. Appl. Artif. Intell.*, vol. 121, no. June 2022, p. 105850, 2023, doi: 10.1016/j.engappai.2023.105850.
[69] H. Wei, C. Du, X. Li, C. Shi, and J. Zhang, “Research on anode pressure control and dynamic performance of proton-exchange membrane fuel cell system for vehicular application,” *Fuel*, vol. 358, no. PB, p. 130219, 2024, doi: 10.1016/j.fuel.2023.130219.
[70] X. Zhang, C. Zhang, Z. Zhang, S. Gao, and H. Li, “Coordinated management of oxygen excess ratio and cathode pressure for PEMFC based on synthesis variable-gain robust predictive control,” *Appl. Energy*, vol. 367, no. October 2023, 2024, doi: 10.1016/j.apenergy.2024.123415.
[71] J. Modarresi, E. Gholipour, and A. Khodabakhshian, “A comprehensive review of the voltage stability indices,” *Renew. Sustain. Energy Rev.*, vol. 63, pp. 1–12, 2016, doi: 10.1016/j.rser.2016.05.010.
[72] M. Moghadari *et al.*, “Impact of Carbon Paper Anisotropy on Water Droplet Movement through the Electrodes of Proton-Exchange Membrane Fuel Cells,” *Energy & Fuels*, vol. 34, no. 8, pp. 10039–

10049, Jun. 2020, doi: 10.1021/acs.energyfuels.0c00225.

[73] B. H. Lim, E. H. Majlan, W. R. W. Daud, T. Husaini, and M. I. Rosli, "Effects of flow field design on water management and reactant distribution in PEMFC: A review," *Ionics (Kiel).*, vol. 22, no. 3, pp. 301–316, 2016, doi: 10.1007/s11581-016-1644-y.

[74] S. G. Kandlikar, M. L. Garofalo, and Z. Lu, "Water management in a PEMFC: Water transport mechanism and material degradation in gas diffusion layers," *Fuel Cells*, vol. 11, no. 6, pp. 814–823, 2011, doi: 10.1002/fuce.201000172.

[75] H. Pourrahmani and J. Van herle, "Water management of the proton exchange membrane fuel cells: Optimizing the effect of microstructural properties on the gas diffusion layer liquid removal," *Energy*, vol. 256, p. 124712, 2022, doi: 10.1016/j.energy.2022.124712.

[76] P. C. Okonkwo and C. Otor, "A review of gas diffusion layer properties and water management in proton exchange membrane fuel cell system," *Int. J. Energy Res.*, vol. 45, no. 3, pp. 3780–3800, 2021, doi: 10.1002/er.6227.

[77] J. Yao *et al.*, "High-stability dead-end anode proton exchange membrane fuel cells by purge optimization," *J. Power Sources*, vol. 595, no. December 2023, 2024, doi: 10.1016/j.jpowsour.2024.234062.

[78] Q. Jian, L. Luo, B. Huang, J. Zhao, S. Cao, and Z. Huang, "Experimental study on the purge process of a proton exchange membrane fuel cell stack with a dead-end anode," *Appl. Therm. Eng.*, vol. 142, no. March, pp. 203–214, 2018, doi: 10.1016/j.applthermaleng.2018.07.001.

[79] B. Chen, Z. Tu, and S. H. Chan, "Performance degradation and recovery characteristics during gas purging in a proton exchange membrane fuel cell with a dead-ended anode," *Appl. Therm. Eng.*, vol. 129, pp. 968–978, 2018, doi: 10.1016/j.applthermaleng.2017.10.102.

[80] Z. Zhang *et al.*, "Research on shutdown purge characteristics of proton exchange membrane fuel cells: Purge parameters conspicuity and residual water," *Appl. Therm. Eng.*, vol. 249, no. May, p. 123437, 2024, doi: 10.1016/j.applthermaleng.2024.123437.

[81] G. Yang, K. Meng, Q. Deng, W. Chen, and B. Chen, "Numerical investigation and experimental verification of liquid water dynamic transfer characteristics in the flow field of PEMFC with dead-ended anode during gas purging," *Chem. Eng. J.*, vol. 491, no. December 2023, p. 152082, 2024, doi: 10.1016/j.cej.2024.152082.

[82] L. shi, P. Liu, M. Zheng, and S. Xu, "Numerical study on the mechanism of water and gas phase transition and water redistribution after purging based on two-dimensional multi-phase model," *Energy Convers. Manag.*, vol. 278, no. January, p. 116725, 2023, doi: 10.1016/j.enconman.2023.116725.

[83] K. Li *et al.*, "Health state monitoring and predicting of proton exchange membrane fuel cells: A review," *J. Power Sources*, vol. 612, no. May, p. 234828, 2024, doi: 10.1016/j.jpowsour.2024.234828.

[84] T. Niu *et al.*, "Purge strategy analysis of proton exchange membrane fuel cells based on experiments and comprehensive evaluation method," *Fuel*, vol. 363, no. November 2023, p. 130970, 2024, doi: 10.1016/j.fuel.2024.130970.

[85] J. Shen, Z. Tu, and S. H. Chan, "Effect of gas purging on the performance of a proton exchange membrane fuel cell with dead-ended anode and cathode," *Int. J. Energy Res.*, vol. 45, no. 10, pp. 14813–14823, 2021, doi: 10.1002/er.6757.

[86] C. Y. Hung, H. S. Huang, S. W. Tsai, and Y. S. Chen, "A purge strategy for proton exchange membrane fuel cells under varying-load operations," *Int. J. Hydrogen Energy*, vol. 41, no. 28, pp. 12369–12376, 2016, doi: 10.1016/j.ijhydene.2016.05.132.

[87] R. Omrani, S. Seif Mohammadi, Y. Mafinejad, B. Paul, R. Islam, and B. Shabani, "PEMFC purging at low operating temperatures: An experimental approach," *Int. J. Energy Res.*, vol. 43, no. 13, pp. 7496–7507, 2019, doi: 10.1002/er.4783.

[88] A. Gomez, A. P. Sasmito, and T. Shamim, "Investigation of the purging effect on a dead-end anode PEM fuel cell-powered vehicle during segments of a European driving cycle," *Energy Convers. Manag.*, vol. 106, pp. 951–957, 2015, doi: 10.1016/j.enconman.2015.10.025.

[89] J. C. Kurnia, A. P. Sasmito, and T. Shamim, "Advances in proton exchange membrane fuel cell with dead-end anode operation: A review," *Appl. Energy*, vol. 252, no. November 2018, p. 113416, 2019, doi: 10.1016/j.apenergy.2019.113416.

[90] B. Chen, H. Zhou, S. He, K. Meng, Y. Liu, and Y. Cai, "Numerical simulation on purge strategy of proton exchange membrane fuel cell with dead-ended anode," *Energy*, vol. 234, p. 121265, 2021, doi:

10.1016/j.energy.2021.121265.
[91] B. Chen, Y. Liu, W. Chen, C. Du, J. Shen, and Z. Tu, “Numerical study on purge characteristics and purge strategy for PEMFC hydrogen system based on exhaust hydrogen recirculation,” *Int. J. Energy Res.*, vol. 46, no. 8, pp. 11424–11442, 2022, doi: 10.1002/er.7939.
[92] Y. F. Lin and Y. S. Chen, “Experimental study on the optimal purge duration of a proton exchange membrane fuel cell with a dead-ended anode,” *J. Power Sources*, vol. 340, pp. 176–182, 2017, doi: 10.1016/j.jpowsour.2016.11.039.
[93] I. Dashti, S. Asghari, M. Goudarzi, Q. Meyer, A. Mehrabani-Zeinabad, and D. J. L. Brett, “Optimization of the performance, operation conditions and purge rate for a dead-ended anode proton exchange membrane fuel cell using an analytical model,” *Energy*, vol. 179, pp. 173–185, 2019, doi: 10.1016/j.energy.2019.04.118.
[94] S. W. Tsai and Y. S. Chen, “A mathematical model to study the energy efficiency of a proton exchange membrane fuel cell with a dead-ended anode,” *Appl. Energy*, vol. 188, pp. 151–159, 2017, doi: 10.1016/j.apenergy.2016.11.128.
[95] B. Jian and H. Wang, “Hardware-in-the-loop real-time validation of fuel cell electric vehicle power system based on multi-stack fuel cell construction,” *J. Clean. Prod.*, vol. 331, no. November 2021, p. 129807, 2022, doi: 10.1016/j.jclepro.2021.129807.
[96] M. M. Jahromi and H. Heidary, “Durability and economics investigations on triple stack configuration and its power management strategy for fuel cell vehicles,” *Int. J. Hydrogen Energy*, vol. 46, no. 7, pp. 5740–5755, 2021, doi: 10.1016/j.ijhydene.2020.11.103.
[97] H. B. Yamchi, M. Kandidayeni, S. Kelouwani, and L. Boulon, “Constrained exploration method for optimal energy management in hybrid multi-stack fuel cell vehicles,” *Energy Convers. Manag.*, vol. 316, no. April, p. 118841, 2024, doi: 10.1016/j.enconman.2024.118841.
[98] R. Han, H. He, Z. Zhang, S. Quan, and J. Chen, “A multi-objective hierarchical energy management strategy for a distributed fuel-cell hybrid electric tracked vehicle,” *J. Energy Storage*, vol. 76, no. November 2023, p. 109858, 2024, doi: 10.1016/j.est.2023.109858.
[99] G. Zhang, S. Zhou, Z. Xie, L. Fan, and J. Gao, “Bi-level power management strategies optimization for multi-stack fuel cell system-battery hybrid power systems,” *J. Energy Storage*, vol. 71, no. July 2022, p. 108066, 2023, doi: 10.1016/j.est.2023.108066.
[100] B. Eom, K. Eom, D. Yang, and M. Kim, “Novel Electric Vehicle Powertrain of Multi-stack Fuel Cell Using Optimal Energy Management Strategy,” *International Journal of Automotive Technology*, vol. 25, no. 2. pp. 201–211, 2024, doi: 10.1007/s12239-024-00010-0.
[101] Y. Yan, Q. Li, W. Chen, W. Huang, J. Liu, and J. Liu, “Online Control and Power Coordination Method for Multistack Fuel Cells System Based on Optimal Power Allocation,” *IEEE Trans. Ind. Electron.*, vol. 68, no. 9, pp. 8158–8168, 2021, doi: 10.1109/TIE.2020.3016240.
[102] Q. Li *et al.*, “An Energy Management Strategy Considering the Economy and Lifetime of Multi-Stack Fuel Cell Hybrid System,” *IEEE Trans. Transp. Electrif.*, vol. 9, no. 2, pp. 3498–3507, 2022, doi: 10.1109/TTE.2022.3218505.
[103] Y. F. Liang, Q. C. Liang, J. F. Zhao, and J. N. He, “Downgrade power allocation for multi-fuel cell system (MFCS) based on minimum hydrogen consumption,” *Energy Reports*, vol. 8, pp. 15574–15583, 2022, doi: 10.1016/j.egyr.2022.11.126.
[104] M. Moghadari, M. Kandidayeni, L. Boulon, and H. Chaoui, “Operating Cost Comparison of a Single-Stack and a Multi-Stack Hybrid Fuel Cell Vehicle Through an Online Hierarchical Strategy,” *IEEE Trans. Veh. Technol.*, vol. 72, no. 1, pp. 267–279, 2023, doi: 10.1109/TVT.2022.3205879.
[105] P. Xie, H. Asgharian, J. M. Guerrero, J. C. Vasquez, S. S. Araya, and V. Liso, “A two-layer energy management system for a hybrid electrical passenger ship with multi-PEM fuel cell stack,” *Int. J. Hydrogen Energy*, vol. 50, pp. 1005–1019, 2024, doi: 10.1016/j.ijhydene.2023.09.297.
[106] A. Igourzal, F. Auger, J. C. Olivier, and C. Retière, “Improving the operation of multi-stack PEM fuel cell systems to increase efficiency, durability and lifespan while reducing ageing,” *Energy Convers. Manag.*, vol. 314, no. March, 2024, doi: 10.1016/j.enconman.2024.118630.
[107] G. Zhang, S. Zhou, J. Gao, L. Fan, and Y. Lu, “Stacks multi-objective allocation optimization for multi-stack fuel cell systems,” *Appl. Energy*, vol. 331, no. September 2022, p. 120370, 2023, doi: 10.1016/j.apenergy.2022.120370.
[108] A. Khalatbarisoltani, M. Kandidayeni, L. Boulon, and X. Hu, “A Decentralized Multi-agent Energy Management Strategy Based on a Look-Ahead Reinforcement Learning Approach,” *SAE Int. J. Electrified Veh.*, vol. 11, no. 2, pp. 1–11, 2021, doi: 10.4271/14-11-02-0012.

[109] M. Kandidayeni, A. Macias, L. Boulon, and S. Kelouwani, “Investigating the impact of ageing and thermal management of a fuel cell system on energy management strategies,” *Appl. Energy*, vol. 274, no. June, p. 115293, 2020, doi: 10.1016/j.apenergy.2020.115293.

[110] M. Kandidayeni *et al.*, “Efficiency Upgrade of Hybrid Fuel Cell Vehicles’ Energy Management Strategies by Online Systemic Management of Fuel Cell,” *IEEE Trans. Ind. Electron.*, vol. 0046, no. 6, pp. 1–1, 2021, doi: 10.1109/tie.2020.2992950.

[111] K. Song, X. Huang, H. Xu, H. Sun, Y. Chen, and D. Huang, “Model predictive control energy management strategy integrating long short-term memory and dynamic programming for fuel cell vehicles,” *Int. J. Hydrogen Energy*, vol. 56, no. November 2023, pp. 1235–1248, 2024, doi: 10.1016/j.ijhydene.2023.12.245.

[112] S. Quan, Y.-X. X. Wang, X. Xiao, H. He, and F. Sun, “Real-time energy management for fuel cell electric vehicle using speed prediction-based model predictive control considering performance degradation,” *Appl. Energy*, vol. 304, no. August, p. 117845, 2021, doi: https://doi.org/10.1016/j.apenergy.2021.117845.

[113] W. Zheng, M. Ma, E. Xu, and Q. Huang, “An energy management strategy for fuel-cell hybrid electric vehicles based on model predictive control with a variable time domain,” *Energy*, vol. 312, no. March, p. 133544, 2024, doi: 10.1016/j.energy.2024.133544.

[114] C. Jia, W. Qiao, J. Cui, and L. Qu, “Adaptive Model-Predictive-Control-Based Real-Time Energy Management of Fuel Cell Hybrid Electric Vehicles,” *IEEE Trans. Power Electron.*, vol. 38, no. 2, pp. 2681–2694, 2023, doi: 10.1109/TPEL.2022.3214782.

[115] Y. Zhou, A. Ravey, and M.-C. C. Péra, “Real-time cost-minimization power-allocating strategy via model predictive control for fuel cell hybrid electric vehicles,” *Energy Convers. Manag.*, vol. 229, no. September 2020, p. 113721, 2021, doi: 10.1016/j.enconman.2020.113721.

[116] X. Hu, C. Zou, X. Tang, T. Liu, and L. Hu, “Cost-optimal energy management of hybrid electric vehicles using fuel cell/battery health-aware predictive control,” *IEEE Trans. Power Electron.*, vol. 35, no. 1, pp. 382–392, 2020, doi: 10.1109/TPEL.2019.2915675.

[117] X. Li, Z. Shang, F. Peng, L. Li, Y. Zhao, and Z. Liu, “Increment-oriented online power distribution strategy for multi-stack proton exchange membrane fuel cell systems aimed at collaborative performance enhancement,” *J. Power Sources*, vol. 512, no. May, p. 230512, 2021, doi: 10.1016/j.jpowsour.2021.230512.

[118] J. Zuo, C. Cadet, Z. Li, C. Berenguer, and R. Outbib, “Post-prognostics decision-making strategy for load allocation on a stochastically deteriorating multi-stack fuel cell system,” *Proc. Inst. Mech. Eng. Part O J. Risk Reliab.*, vol. 237, no. 1, pp. 40–57, 2022, doi: 10.1177/1748006X221086381.

[119] T. Wang, Q. Li, L. Yin, W. Chen, E. Breaz, and F. Gao, “Hierarchical Power Allocation Method Based on Online Extremum Seeking Algorithm for Dual-PEMFC/Battery Hybrid Locomotive,” *IEEE Trans. Veh. Technol.*, vol. 70, no. 6, pp. 5679–5692, 2021, doi: 10.1109/TVT.2021.3078752.

[120] Y. Yan, Q. Li, W. Chen, W. Huang, and J. Liu, “Hierarchical management control based on equivalent fitting circle and equivalent energy consumption method for multiple fuel cells hybrid power system,” *IEEE Trans. Ind. Electron.*, vol. 67, no. 4, pp. 2786–2797, 2020, doi: 10.1109/TIE.2019.2908615.

[121] D. Jiang, Y. Long, P. Fu, C. Guo, Y. Tang, and H. Huang, “A novel multi-stack fuel cell hybrid system energy management strategy for improving the fuel cell durability of the hydrogen electric Multiple Units,” *Int. J. Green Energy*, vol. 21, no. 8, pp. 1766–1775, 2024, doi: 10.1080/15435075.2023.2266724.

[122] S. Zhou, G. Zhang, L. Fan, J. Gao, and F. Pei, “Scenario-oriented stacks allocation optimization for multi-stack fuel cell systems,” *Appl. Energy*, vol. 308, no. April 2021, p. 118328, 2022, doi: 10.1016/j.apenergy.2021.118328.

[123] R. Ghaderi, M. Kandidayeni, M. Soleymani, L. Boulon, and J. P. F. Trovao, “Online Health-Conscious Energy Management Strategy for a Hybrid Multi-Stack Fuel Cell Vehicle Based on Game Theory,” *IEEE Trans. Veh. Technol.*, vol. 71, no. 6, pp. 5704–5714, 2022, doi: 10.1109/TVT.2022.3167319.

[124] T. Wang, Q. Li, L. Yin, and W. Chen, “Hydrogen consumption minimization method based on the online identification for multi-stack PEMFCs system,” *Int. J. Hydrogen Energy*, vol. 4, pp. 5074–5081, 2019, doi: 10.1016/j.ijhydene.2018.09.181.

[125] H. Zhang, X. Li, X. Liu, and J. Yan, “Enhancing fuel cell durability for fuel cell plug-in hybrid electric vehicles through strategic power management,” *Appl. Energy*, vol. 241, no. August 2017, pp.

483–490, 2019, doi: 10.1016/j.apenergy.2019.02.040.
[126] X. Han, F. Li, T. T. Zhang, T. T. Zhang, and K. Song, “Economic energy management strategy design and simulation for a dual-stack fuel cell electric vehicle,” *Int. J. Hydrogen Energy*, vol. 42, no. 16, pp. 11584–11595, 2017, doi: 10.1016/j.ijhydene.2017.01.085.
[127] B. Chen *et al.*, “Operation characteristics and carbon corrosion of PEMFC (Proton exchange membrane fuel cell) with dead-ended anode for high hydrogen utilization,” *Energy*, vol. 91, pp. 799–806, 2015, doi: https://doi.org/10.1016/j.energy.2015.08.083.
[128] J. H. Jang, W. M. Yan, H. C. Chiu, and J. Y. Lui, “Dynamic cell performance of kW-grade proton exchange membrane fuel cell stack with dead-ended anode,” *Appl. Energy*, vol. 142, pp. 108–114, 2015, doi: 10.1016/j.apenergy.2014.12.073.
[129] A. Manokaran, S. Pushpavanam, P. Sridhar, and S. Pitchumani, “Experimental analysis of spatio-temporal behavior of anodic dead-end mode operated polymer electrolyte fuel cell,” *J. Power Sources*, vol. 196, no. 23, pp. 9931–9938, 2011, doi: 10.1016/j.jpowsour.2011.06.103.
[130] J. Zhao, Q. Jian, L. Luo, B. Huang, S. Cao, and Z. Huang, “Dynamic behavior study on voltage and temperature of proton exchange membrane fuel cells,” *Appl. Therm. Eng.*, vol. 145, no. August, pp. 343–351, 2018, doi: 10.1016/j.applthermaleng.2018.09.030.
[131] S. Xu, B. Yin, Z. Li, and F. Dong, “A review on gas purge of proton exchange membrane fuel cells: Mechanisms, experimental approaches, numerical approaches, and optimization,” *Renew. Sustain. Energy Rev.*, vol. 172, no. June 2022, p. 113071, 2023, doi: 10.1016/j.rser.2022.113071.
[132] S. Liu *et al.*, “Study on the effect of purging time on the performance of PEMFC with dead-ended anode under gravity,” *Renew. Energy*, vol. 200, no. October, pp. 1141–1151, 2022, doi: 10.1016/j.renene.2022.10.065.
[133] L. Grüne and J. Pannek, “Nonlinear Model Predictive Control,” in *Nonlinear Model Predictive Control: Theory and Algorithms*, Cham: Springer International Publishing, 2017, pp. 45–69.
[134] Z. Zhao, W. Chen, X. Wu, P. C. Y. Chen, and J. Liu, “LSTM network: A deep learning approach for Short-term traffic forecast,” *IET Intell. Transp. Syst.*, vol. 11, no. 2, pp. 68–75, 2017, doi: 10.1049/iet-its.2016.0208.
[135] J. T. Pukrushpan, A. G. Stefanopoulou, and H. Peng, *Fuel Cell System Model: Fuel Cell Stack*. 2004.
[136] M. Kandidayeni *et al.*, “An Online Energy Management Strategy for a Fuel Cell/Battery Vehicle Considering the Driving Pattern and Performance Drift Impacts,” *IEEE Trans. Veh. Technol.*, vol. 68, no. 12, pp. 11427–11438, 2019, doi: 10.1109/TVT.2019.2936713.
[137] J. J. Giner-Sanz, E. M. Ortega, and V. Pérez-Herranz, “Mechanistic equivalent circuit modelling of a commercial polymer electrolyte membrane fuel cell,” *J. Power Sources*, vol. 379, no. January, pp. 328–337, 2018, doi: 10.1016/j.jpowsour.2018.01.066.
[138] S. Busquet, C. E. Hubert, J. Labbé, D. Mayer, and R. Metkemeijer, “A new approach to empirical electrical modelling of a fuel cell, an electrolyser or a regenerative fuel cell,” *J. Power Sources*, vol. 134, no. 1, pp. 41–48, 2004, doi: 10.1016/j.jpowsour.2004.02.018.
[139] J. C. Amphlett, R. M. Baumert, R. F. Mann, B. A. Peppley, P. R. Roberge, and T. J. Harris, “Performance Modeling of the Ballard Mark IV Solid Polymer Electrolyte Fuel Cell: II . Empirical Model Development,” *J. Electrochem. Soc.*, vol. 142, no. 1, pp. 9–15, Jan. 1995, doi: 10.1149/1.2043959.
[140] M. A. R. S. Al-Baghdadi, “Modelling of proton exchange membrane fuel cell performance based on semi-empirical equations,” *Renew. Energy*, vol. 30, no. 10, pp. 1587–1599, 2005, doi: 10.1016/j.renene.2004.11.015.
[141] R. F. Mann, J. C. Amphlett, M. A. I. Hooper, H. M. Jensen, B. A. Peppley, and P. R. Roberge, “Development and application of a generalized steady-state electrochemical model for a PEM fuel cell,” *J. Power Sources*, vol. 86, no. 1, pp. 173–180, 2000, doi: 10.1016/S0378-7753(99)00484-X.
[142] H. Ashraf, S. O. Abdellatif, M. M. Elkholy, and A. A. El-Fergany, “Computational Techniques Based on Artificial Intelligence for Extracting Optimal Parameters of PEMFCs: Survey and Insights,” *Arch. Comput. Methods Eng.*, vol. 29, no. 6, pp. 3943–3972, 2022, doi: 10.1007/s11831-022-09721-y.
[143] M. Kandidayeni, A. Macias, A. A. Amamou, L. Boulon, S. Kelouwani, and H. Chaoui, “Overview and benchmark analysis of fuel cell parameters estimation for energy management purposes,” *J. Power Sources*, vol. 380, no. January, pp. 92–104, 2018, doi: 10.1016/j.jpowsour.2018.01.075.
[144] K. Ettihir, L. Boulon, and K. Agbossou, “Optimization-based energy management strategy for a fuel cell/battery hybrid power system,” *Appl. Energy*, vol. 163, pp. 142–153, 2016, doi: 10.1016/j.apenergy.2015.10.176.

[145] K. Ettihir, L. Boulon, M. Becherif, K. Agbossou, and H. S. Ramadan, "Online identification of semi-empirical model parameters for PEMFCs," *Int. J. Hydrogen Energy*, vol. 39, no. 36, pp. 21165–21176, 2014, doi: 10.1016/j.ijhydene.2014.10.045.

[146] K. Ettihir, M. Higuita Cano, L. Boulon, and K. Agbossou, "Design of an adaptive EMS for fuel cell vehicles," *Int. J. Hydrogen Energy*, vol. 42, no. 2, pp. 1481–1489, 2017, doi: 10.1016/j.ijhydene.2016.07.211.

[147] M. Kandidayeni, H. Chaoui, L. Boulon, and J. P. F. Trovao, "Adaptive Parameter Identification of a Fuel Cell System for Health-Conscious Energy Management Applications," *IEEE Trans. Intell. Transp. Syst.*, vol. 23, no. 7, pp. 7963–7973, 2022, doi: 10.1109/TITS.2021.3074903.

[148] M. Kandidayeni, A. Macias, L. Boulon, and J. P. F. Trovão, "Online modeling of a fuel cell system for an energy management strategy design," *Energies*, vol. 13, no. 14, pp. 1–17, 2020, doi: 10.3390/en13143713.

[149] H. Chen, P. Pei, and M. Song, "Lifetime prediction and the economic lifetime of Proton Exchange Membrane fuel cells," *Appl. Energy*, vol. 142, pp. 154–163, 2015, doi: https://doi.org/10.1016/j.apenergy.2014.12.062.

[150] P. Pei, Q. Chang, and T. Tang, "A quick evaluating method for automotive fuel cell lifetime," *Int. J. Hydrogen Energy*, vol. 33, no. 14, pp. 3829–3836, 2008, doi: https://doi.org/10.1016/j.ijhydene.2008.04.048.

[151] A. Kneer and N. Wagner, "A Semi-Empirical Catalyst Degradation Model Based on Voltage Cycling under Automotive Operating Conditions in PEM Fuel Cells," *J. Electrochem. Soc.*, vol. 166, no. 2, pp. F120–F127, 2019, doi: 10.1149/2.0641902jes.

[152] D. Bernhard, T. Kadyk, S. Kirsch, H. Scholz, and U. Krewer, "Model-assisted analysis and prediction of activity degradation in PEM-fuel cell cathodes," *J. Power Sources*, vol. 562, no. November 2022, p. 232771, 2023, doi: 10.1016/j.jpowsour.2023.232771.

[153] M. Zhou *et al.*, "Modeling the Performance Degradation of a High-Temperature PEM Fuel Cell," *Energies*, vol. 15, no. 15, pp. 1–21, 2022, doi: 10.3390/en15155651.

[154] Y. Ao, K. Chen, S. Laghrouche, and D. Depernet, "Proton exchange membrane fuel cell degradation model based on catalyst transformation theory," *Fuel Cells*, vol. 21, no. 3, pp. 254–268, 2021, doi: 10.1002/fuce.202100002.

[155] L. Hongwei, Q. Binxin, H. Zhicheng, L. Junnan, Y. Yue, and L. Guolong, "An interpretable data-driven method for degradation prediction of proton exchange membrane fuel cells based on temporal fusion transformer and covariates," *Int. J. Hydrogen Energy*, vol. 48, no. 66, pp. 25958–25971, 2023, doi: 10.1016/j.ijhydene.2023.03.316.

[156] H. Deng *et al.*, "Degradation trajectories prognosis for PEM fuel cell systems based on Gaussian process regression," *Energy*, vol. 244, p. 122569, 2022, doi: 10.1016/j.energy.2021.122569.

[157] V. M. Nagulapati, S. S. Kumar, V. Annadurai, and H. Lim, "Machine learning based fault detection and state of health estimation of proton exchange membrane fuel cells," *Energy AI*, vol. 12, no. November 2022, p. 100237, 2023, doi: 10.1016/j.egyai.2023.100237.

[158] M. Shateri and F. Torabi, "Influence of liquid water accumulation on the impedance of a PEM fuel cell operating in dead end mode: Physical modeling and experimental validation," *Electrochim. Acta*, vol. 443, no. January, p. 141940, 2023, doi: 10.1016/j.electacta.2023.141940.

[159] L. Baum, M. Schumann, F. Grumm, and D. Schulz, "Large-signal time-domain equivalent circuit model for PEM fuel cell stacks," *Int. J. Hydrogen Energy*, no. xxxx, 2023, doi: 10.1016/j.ijhydene.2023.07.240.

[160] R. Ma, R. Xie, L. Xu, Y. Huangfu, and Y. Li, "A Hybrid Prognostic Method for PEMFC with Aging Parameter Prediction," *IEEE Trans. Transp. Electrif.*, vol. 7, no. 4, pp. 2318–2331, 2021, doi: 10.1109/TTE.2021.3075531.

[161] Y. Cheng, N. Zerhouni, and C. Lu, "A hybrid remaining useful life prognostic method for proton exchange membrane fuel cell," *Int. J. Hydrogen Energy*, vol. 43, no. 27, pp. 12314–12327, 2018, doi: 10.1016/j.ijhydene.2018.04.160.

[162] D. Zhang, P. Baraldi, C. Cadet, N. Yousfi-Steiner, C. Bérenguer, and E. Zio, "An ensemble of models for integrating dependent sources of information for the prognosis of the remaining useful life of Proton Exchange Membrane Fuel Cells," *Mech. Syst. Signal Process.*, vol. 124, pp. 479–501, 2019, doi: 10.1016/j.ymssp.2019.01.060.

[163] T. Lan and K. Strunz, "Modeling of multi-physics transients in PEM fuel cells using equivalent circuits for consistent representation of electric, pneumatic, and thermal quantities," *Int. J. Electr.*

Power Energy Syst., vol. 119, no. February, p. 105803, 2020, doi: 10.1016/j.ijepes.2019.105803.

[164] J. M. Andújar, F. Segura, F. Isorna, and A. J. Calderón, "Comprehensive diagnosis methodology for faults detection and identification, and performance improvement of Air-Cooled Polymer Electrolyte Fuel Cells," *Renew. Sustain. Energy Rev.*, vol. 88, no. December 2017, pp. 193–207, 2018, doi: 10.1016/j.rser.2018.02.038.

[165] Z. Li, Z. Zheng, and F. Gao, "Diagnosis and Prognosis of Proton Exchange Membrane Fuel Cells," *Electr. Syst. 2*, pp. 153–198, 2020, doi: 10.1002/9781119720584.ch5.

[166] Y. Akimoto and K. Okajima, "Simple on-board fault-detection method for proton exchange membrane fuel cell stacks using by semi-empirical curve fitting," *Appl. Energy*, vol. 303, no. August, p. 117654, 2021, doi: 10.1016/j.apenergy.2021.117654.

[167] X. Gu, Z. Hou, and J. Cai, "Data-based flooding fault diagnosis of proton exchange membrane fuel cell systems using LSTM networks," *Energy AI*, vol. 4, p. 100056, 2021, doi: 10.1016/j.egyai.2021.100056.

[168] N. Yousfi Steiner, D. Hissel, P. Moçtéguy, and D. Candusso, "Diagnosis of polymer electrolyte fuel cells failure modes (flooding & drying out) by neural networks modeling," *Int. J. Hydrogen Energy*, vol. 36, no. 4, pp. 3067–3075, 2011, doi: 10.1016/j.ijhydene.2010.10.077.

[169] I. Tolj, D. Bezmalinovic, and F. Barbir, "Maintaining desired level of relative humidity throughout a fuel cell with spatially variable heat removal rates," *Int. J. Hydrogen Energy*, vol. 36, no. 20, pp. 13105–13113, 2011, doi: 10.1016/j.ijhydene.2011.07.078.

[170] D. G. Strickland and J. G. Santiago, "In situ-polymerized wicks for passive water management in proton exchange membrane fuel cells," *J. Power Sources*, vol. 195, no. 6, pp. 1667–1675, 2010, doi: 10.1016/j.jpowsour.2009.09.034.

[171] S. Litster, C. R. Buie, T. Fabian, J. K. Eaton, and J. G. Santiago, "Active Water Management for PEM Fuel Cells," *J. Electrochem. Soc.*, vol. 154, no. 10, p. B1049, Aug. 2007, doi: 10.1149/1.2766650.

[172] T. Li *et al.*, "Optimization of GDL to improve water transferability," *Renew. Energy*, vol. 179, pp. 2086–2093, 2021, doi: 10.1016/j.renene.2021.08.026.

[173] I. Vincent, E. C. Lee, and H. M. Kim, "Solutions to the water flooding problem for unitized regenerative fuel cells: status and perspectives," *RSC Adv.*, vol. 10, no. 29, pp. 16844–16860, 2020, doi: 10.1039/d0ra00434k.

Publications

- **Journal Articles**

1) **M. Moghadari**, M. Kandidayeni, L. Boulon, and H. Chaoui, "Predictive Health-Conscious Energy Management Strategy of a Hybrid Multi-Stack Fuel Cell Vehicle," IEEE Trans. Veh. Technol., vol. PP, pp. 1–16, 2024, doi: 10.1109/TVT.2024.3512204.

2) **M. Moghadari**, M. Kandidayeni, L. Boulon, and H. Chaoui, "Operating Cost Comparison of a Single-Stack and a Multi-Stack Hybrid Fuel Cell Vehicle Through an Online Hierarchical Strategy," IEEE Trans. Veh. Technol., vol. 72, no. 1, pp. 267–279, 2023, doi: 10.1109/TVT.2022.3205879.

3) **M. Moghadari**, M. Kandidayeni, L. Boulon, and H. Chaoui, "Integration of Water Management into the Energy Management Strategy for a Fuel Cell Vehicle," IEEE Transactions on Industrial Electronic., 2025 (Under review with comments received).

- **Conference Articles**

1) **M. Moghadari**, M. Kandidayeni, L. Boulon, and H. Chaoui, "Minimizing the Operating Cost of a Hybrid Multi-Stack Fuel Cell Vehicle Based on a Predictive Hierarchical Strategy," 2023 IEEE Veh. Power Propuls. Conf. VPPC 2023 - Proc., pp. 1–5, 2023, doi: 10.1109/VPPC60535.2023.10403199.

2) **M. Moghadari**, M. Kandidayeni, L. Boulon, and H. Chaoui, "Hydrogen Minimization of a Hybrid Multi-Stack Fuel Cell Vehicle Using an Optimization-Based Strategy," 2021 IEEE Veh. Power Propuls. Conf. VPPC 2021 - Proc., pp. 1–5, 2021, doi: 10.1109/VPPC53923.2021.9699262.